483-E-1 EP 4.2:Ur 1/3

United States
Environmental Protection
Agency

Office of Air Quality
Planning and Standards
Research Triangle Park NC 27711

EPA-450/4-85-003
June 1985

Air

EPA

Evaluation And Application Of The Urban Airshed Model In The Philadelphia Air Quality Control Region

260

ORDERED

BEST COPY AVAILABLE

EPA-450/4-85-003

Evaluation And Application Of The Urban Airshed Model In The Philadelphia Air Quality Control Region

Prepared By

Jay L. Haney
Systems Applications, Inc.
101 Lucas Valley Road
San Rafael, California 94903

and

Thomas N. Braverman
U.S. Environmental Protection Agency
Office of Air Quality Planning and Standards
Office of Air and Radiation
Research Triangle Park, North Carolina 27711

Prepared For

U.S. ENVIRONMENTAL PROTECTION AGENCY
Office Of Air And Radiation
Office Of Air Quality Planning And Standards
Research Triangle Park, NC 27711

June 1985

BEST COPY AVAILABLE

This report has been reviewed by The Office Of Air Quality Planning And Standards, U.S. Environmental Protection Agency, and has been approved for publication. Mention of trade names or commercial products is not intended to constitute endorsement or recommendation for use.

EPA-450/4-85-003

BEST COPY AVAILABLE

ACKNOWLEDGMENTS

A number of people made significant contributions to the work reported herein. The authors thank the many individuals at Systems Applications and EPA-OAQPS who participated in the various technical tasks associated with these modeling efforts. Particular recognition is due Drs. Tom Tesche and Christian Seigneur and Mr. James Killus of Systems Applications, and Messrs. Norman Posseil and David Layland of EPA-OAQPS. Special thanks are also extended to the Systems Applications' production staff and to the project editor, Ms. Carol Wade.

BEST COPY AVAILABLE

BLANK PAGE

TJ

CONTENTS

Notice ii

Acknowledgements iii

Figures vii

Tables xiii

1 INTRODUCTION 1

Overview of Study 1
Technical Approach 2

2 CHARACTERIZATION OF THE 13 JULY 1979 OZONE EPISODE 7

3 DESCRIPTION OF MODEL INPUTS FOR 13 JULY 1979 11

Modeling Region Specifications 11
Mixing Heights 12
Wind Field 17
Background Concentrations 37
Initial Conditions 37
Boundary Conditions 40
Emission Inventory 42
Metscalars 49
Terrain 52

4 CHARACTERIZATION OF THE 19 JULY 1979 EPISODE 55

5 DESCRIPTION OF MODEL INPUTS FOR 19 JULY 1979 57

Mixing Heights 57
Wind Field 59
Background Concentrations 69
Initial Conditions 75
Boundary Conditions 75
Metscalars 78

6 ANALYSIS OF URBAN AIRSHED MODEL PERFORMANCE FOR THE PHILADELPHIA SIMULATIONS OF 13 AND 19 July 1979 81

Model Performance Evaluation Measures 81
Model Evaluation Results for the 13 July 1979 Simulation 87
Model Evaluation Results for the 19 July 1979 Simulation 96
Comparison of Philadelphia Results with UAM Performance in Other Cities 107

BEST COPY AVAILABLE

7 OZONE SENSITIVITY ANALYSIS..... 111

Methodology..... 111
Results of Ozone Sensitivity Simulations for 13 July..... 116
Results of Ozone Sensitivity Simulations for 19 July..... 130

8 SUMMARY AND CONCLUSIONS..... 175

References..... 183

Appendix A: COMPILATION OF AIRSHED RESULTS FOR 13 JULY 1979

Appendix B: COMPILATION OF AIRSHED RESULTS FOR 19 JULY 1979

BEST COPY AVAILABLE

LIST OF FIGURES

1-1	Geographical location of the Philadelphia airshed modeling region	4
1-2	Philadelphia airshed modeling region	5
2-1	Synoptic situation, 0700 EST, 13 July 1979	8
3-1	Temperature sounding for JFK Airport on 13 July 1979--0700 EST	13
3-2	Temperature sounding for JFK Airport on 13 July--1900 EST	14
3-3	Temperature sounding for Dulles airport on 13 July 1979--0700 EST	15
3-4	Temperature sounding for Dulles Airport on 13 July 1979--1900 EST	16
3-5	Mixing height profile for urban and rural cells for the 13 July 1979 simulation	19
3-6	Observed surface wind vectors and wind vectors used in preparing the interpolated surface wind field for 13 July 1979	20
3-7	Upper level winds aloft at JFK Airport on 13 July 1979--0700 EST	27
3-8	Upper level winds at JFK Airport on 13 July 1979--1900 EST	28
3-9	Upper level winds at Dulles Airport on 13 July 1979--0700 EST	29
3-10	Upper level winds at Dulles Airport on 13 July 1979--1900 EST	30

BEST COPY AVAILABLE

3-11	Airshed Model surface winds for 13 July 1979	33
3-12	Physical boundaries used in the 13 July 1979 Airshed Model simulation	41
3-13	Surface layer total hydrocarbon emissions for the Philadelphia airshed region for 1979	47
3-14	Surface layer total NO_x emissions for the Philadelphia airshed region for 1979	48
3-15	Land use classification for the Philadelphia airshed modeling region	54
4-1	Synoptic situation, 0700 EST, 19 July 1979	56
5-1	Temperature sounding for Philadelphia, 0410 EST, 19 July 1979	58
5-2	Mixing height profiles for urban and rural cells on 19 July 1979	61
5-3	Observed surface wind vectors and vectors used in preparing the interpolated surface wind field for three time periods for 19 July 1979	62
5-4	Pibal sounding at Wilmington, Delaware on 19 July 1979, 1200 EST	66
5-5	Pibal sounding at Philadelphia on 19 July, 1979, 1150 EST	67
5-6	Pibal sounding at Trenton, New Jersey on 19 July 1979, 1200 EST	68
5-7	Airshed Model surface winds for 19 July 1979	71
5-8	Boundary specifications for 19 July 1979 simulations	77
6-1	Scatter plot of predicted and observed station peak ozone concentrations for 13 July 1979	91
6-2	Mean normalized bias, mean normalized error as function of measured O_3 concentrations and distribution of residuals for 13 July 1979	93

BEST COPY AVAILABLE

6-3 Time series (24 hours) of predicted versus observed ozone, and spatially predicted ozone (ppmm), for the 13 July 1979 simulation, 1600-1700 EST 94

6-4 Scatter plot of predicted and observed ozone concentrations for 13 July 1979 97

6-5 Scatter plot of predicted and observed station peak ozone concentrations for 19 July 1979 102

6-6 Mean normalized bias, mean normalized error as function of measured O_3 concentrations and distributions of residuals for 19 July 1979 104

6-7 Time series (24 hours) of predicted versus observed ozone and spatially predicted ozone for the simulation of 19 July 1979, 1400-1500 EST 105

6-8 Scatter plot of predicted and observed ozone concentrations for 19 July 1979 108

7-1 Predicted ozone response to hydrocarbon emission reductions for peak regional ozone in the Philadelphia urban plume for 13 July 119

7-2 Predicted ozone response to hydrocarbon emission reductions for 13 July at the Roxy Water, PA monitor 121

7-3 Predicted ozone response to hydrocarbon emission reductions for 13 July at the Norristown, PA monitor 122

7-4 Relative ozone reduction (%) versus percent hydrocarbon emission reduction for peak regional ozone in the Philadelphia urban plume for 13 July 123

7-5 Relative ozone reduction (%) versus percent hydrocarbon emission reduction for 13 July at the Roxy Water, PA monitor 124

7-6 Relative ozone reduction (%) versus percent hydrocarbon emission reduction for 13 July at the Norristown, PA monitor 125

7-7 Total ozone reduction (%) versus percent hydrocarbon emission reduction for peak regional ozone in the Philadelphia urban plume for 13 July 126

BEST COPY AVAILABLE

7-8 Total ozone reduction (%) versus percent hydrocarbon emission reduction for 13 July at the Roxy Water, PA monitor 127

7-9 Total ozone reduction (%) versus percent hydrocarbon emission reduction for 13 July at the Norristown, PA monitor 128

7-10 Maximum deficit/enhancement for ozone (pphm) for all hours for 13 July (D.25HC minus D.BASE) 132

7-11 Maximum deficit/enhancement for ozone (pphm) for all hours for 13 July (D.50HC minus D.BASE) 133

7-12 Maximum deficit/enhancement for ozone (pphm) for all hours for 13 July (D.75HC minus D.BASE) 134

7-13 Maximum deficit/enhancement for ozone (pphm) for all hours for 13 July (D.BK03 minus D.BASE) 135

7-14 Maximum deficit/enhancement for ozone (pphm) for all hours for 13 July (D.BKHC minus D.BASE) 136

7-15 Maximum deficit/enhancement for ozone (pphm) for all hours for 13 July (D.BKHC.03 minus D.BASE) 137

7-16 Maximum deficit/enhancement for ozone (pphm) for all hours for 13 July (D.50HC.BK03 minus D.BASE) 138

7-17 Maximum deficit/enhancement for ozone (pphm) for all hours for 13 July (D.50HC.BKHC minus D.BASE) 139

7-18 Maximum deficit/enhancement for ozone (pphm) for all hours for 13 July (D.50HC.BKHC.03 minus D.BASE) 140

7-19 Maximum deficit/enhancement for ozone (pphm) for all hours for 13 July (D.50HC.BK03 minus D.BK03) 141

7-20 Maximum deficit/enhancement for ozone (pphm) for all hours for 13 July (D.50HC.BKHC minus D.BKHC) 142

7-21 Maximum deficit/enhancement for ozone (pphm) for all hours for 13 July (D.50HC.BKHC.03 minus D.BKHC.03) 143

BEST COPY AVAILABLE

7-22 Predicted ozone response to hydrocarbon emission reductions for peak regional ozone in the Philadelphia urban plume for 19 July 146

7-23 Predicted ozone response to hydrocarbon emission reductions for 19 July at the Downington, PA monitor 147

7-24 Predicted ozone response to hydrocarbon emission reductions for 19 July at the Roxy Water, PA monitor 148

7-25 Relative ozone reduction (%) versus percent hydrocarbon emission reduction for peak regional ozone in the Philadelphia urban plume for 19 July 149

7-26 Relative ozone reduction (%) versus percent hydrocarbon emission reduction for 19 July at the Downington, PA monitor 150

7-27 Relative ozone reduction (%) versus percent hydrocarbon emission reduction for 19 July at the Roxy Water, PA monitor 151

7-28 Total ozone reduction (%) versus percent hydrocarbon emission reduction of peak regional ozone in the Philadelphia urban plume for 19 July 152

7-29 Total ozone reduction (%) versus percent hydrocarbon emission reduction for 19 July at the Downington, PA monitor 153

7-30 Total ozone reduction (%) versus percent hydrocarbon emission reduction for 19 July at the Roxy Water, PA monitor 154

7-31 Maximum deficit/enhancement for ozone (pphm) for all hours on 19 July (6.25HC minus 6.BASE) 158

7-32 Maximum deficit/enhancement for ozone (pphm) for all hours on 19 July (6.50HC minus 6.BASE) 159

7-33 Maximum deficit/enhancement for ozone (pphm) for all hours on 19 July (6.75HC minus 6.BASE) 160

7-34 Maximum deficit/enhancement for ozone (pphm) for all hours on 19 July (6.B25HC minus 6.BASE) 162

7-35 Maximum deficit/enhancement for ozone (pphm) for all hours on 19 July (6.B50HC minus 6.BASE) 163

BEST COPY AVAILABLE

7-36 Maximum deficit/ennancement for ozone (pphm) for all nours on 19 July (6.B75HC minus 6.BASE) 164

7-37 Maximum deficit/ennancement for ozone (pphm) for all nours on 19 July (6.BK03 minus 6.BASE) 165

7-38 Maximum deficit/ennancement for ozone (pphm) for all nours on 19 July (6.BKHC minus 6.BASE) 166

7-39 Maximum deficit/ennancement for ozone (pphm) for all nours on 19 July (6.BKHC.03 minus 6.BASE) 167

7-40 Maximum deficit/ennancement for ozone (pphm) for all nours on 19 July (6.B50HC.BK03 minus 6.BASE) 168

7-41 Maximum deficit/ennancement for ozone (pphm) for all nours on 19 July (6.B50HC.BKHC minus 6 BASE) 169

7-42 Maximum deficit/ennancement for ozone (pphm) for all nours on 19 July (6.B50HC.BKHC.03 minus 6.BASE) 170

7-43 Maximum deficit/ennancement for ozone (pphm) for all nours on 19 July (6.B50HC.BK03 minus 6.BK03) 171

7-44 Maximum deficit/ennancement for ozone (pphm) for all nours on 19 July (6.B50HC.BKHC minus 6.BKHC) 172

7-45 Maximum deficit/ennancement for ozone (pphm) for all nours on 19 July (6.B50HC.BKHC.03 minus 6.BKHC.03) 173

BEST COPY AVAILABLE

LIST OF TABLES

3-1	Urban and rural mixing height values used in the DIFFBREAK file for 13 July 1979	18
3-2	Spatially constant wind vectors for level 4 winds for 13 July 1979	31
3-3	Background concentration values for 13 July at the top of the modeling region (TOPCONC), as initial concentrations above the mixing height, and for all levels of all boundaries except the levels below the mixing height on the Southeast boundary	38
3-4	Initial conditions for 13 July 1979	39
3-5	Southeast boundary conditions for cells below the mixing height for the simulation of 13 July 1979	43
3-6	Hourly emissions of NO_x and hydrocarbon (tons/hr) used for the 1979 Philadelphia emission inventory	45
3-7	Total daily emissions by source type (g-mole) in the 1979 Philadelphia inventory	46
3-8	METSCALAR file for the 13 July 1979 airshed simulation	51
3-9	Surface roughness and vegetation factor values	53
5-1	Urban and rural mixing height values used in the DIFFBREAK file for 19 July 1979	60
5-2	Estimated spatially constant, temporally varying wind input for levels 2, 3, and 4 for the 19 July 1979 wind file	70
5-3	Background concentration values for 19 July at the top of the modeling region (TOPCONC), as initial concentrations above the mixing height, and for all levels of all boundaries except the levels below the mixing height on the Northeast and East boundaries	74

BEST COPY AVAILABLE

5-4	Initial conditions at station monitors for 19 July	76
5-5	Boundary conditions for the Northeast and East boundaries below the mixing height estimated from data collected at the Van Hiseville, New Jersey monitor	79
5-6	METSCALAR inputs for the 19 July 1979 simulation	80
6-1	Maximum predictions/observations for 13 July 1979 for ozone	88
6-2	Performance measures for the UAM simulation of the 13 July 1979 episode in Philadelphia (for peak station predictions/observations and ozone measurements above 5 pphm)	89
6-3	Maximum predictions/observations for 19 July 1979 for ozone (pphm)	99
6-4	Performance measures for the UAM simulation of the 19 July 1979 episode in Philadelphia	100
6-5	Comparison of UAM performance evaluation for ozone in Los Angeles, Tulsa, Sacramento, Denver, and Philadelphia	109
7-1	Simulation designations for Philadelphia Airshed sensitivity analysis for 13 and 19 July 1979	112
7-2	Total RHC concentrations used as initial conditions for base case and hydrocarbon reduction simulations for 13 July	113
7-3	Total RHC concentrations used as initial conditions for base case and hydrocarbon reduction simulations for 19 July	115
7-4	Reduced background concentrations used in the ozone sensitivity simulations of 13 and 19 July	117
7-5	Hourly predicted maximum ozone (pphm) and ozone reductions for the ozone sensitivity simulations of 13 July	118
7-6	Hydrocarbon emission reductions required to meet the NAAQS for ozone from the sensitivity simulations of 13 July	129

BEST COPY AVAILABLE

7-7 Deficit/enhancement figures for ozone for the 13 July sensitivity simulations 131

7-8 Hourly predicted maximum ozone (pphm) and ozone reductions for the ozone sensitivity simulations of 19 July 145

7-9 Hydrocarbon emission reductions required to meet the NAAQS for ozone from the sensitivity simulations of 19 July 156

7-10 Deficit/enhancement figures for ozone for the 19 July sensitivity simulations 157

BEST COPY AVAILABLE

1 INTRODUCTION

OVERVIEW OF STUDY

The U.S. Environmental Protection Agency's (EPA) Office of Air Quality Planning and Standards (OAQPS) contracted with Systems Applications, Inc. to carry out a photochemical air quality modeling evaluation study in the Philadelphia Air Quality Control Region (AQCR). The goal of the study was to assess the potential utility of the Urban Airshed Model (UAM) as an air quality planning tool in a large metropolitan area that often receives a considerable influx of ozone and precursors from other parts of the Northeast urban corridor. To achieve this goal, it was necessary to evaluate the model's performance to ensure that it provides an adequate representation of the physical and chemical processes that influence ozone formation in the Philadelphia atmosphere. Model performance evaluation is typically carried out through comparison of predictions of hourly averaged ozone concentrations with corresponding ozone measurements on one or more historical episode days. This report discusses the results of simulations of two summer ozone episodes--13 and 19 July 1979--in Philadelphia. The 13 July episode is characterized as a stagnation period, whereas the 19 July episode resulted in part from the transport of regional precursor emissions from the New Jersey/New York urban area located northeast of Philadelphia.

The requirements for the evaluation study were to

Acquire, format, and install on computer the 1979 Philadelphia air quality, emissions, and meteorological data base;

Prepare UAM input files for the 13 and 19 July 1979 ozone episodes;

Evaluate the model's performance in estimating the magnitude of ozone concentrations and temporal and spatial distributions;

Using base cases for both days, carry out a number of ozone sensitivity simulations; and

Prepare a final report describing model inputs, model base-case results, performance evaluation findings, and results of the ozone sensitivity simulations

BEST COPY AVAILABLE

This report is organized as follows: Section 2 provides a brief overview of the characteristics of the 13 July 1979 ozone episode in Philadelphia; Section 3 describes the procedures used to prepare each of the model input files for this day. The characteristics of the 19 July 1979 episode are described in Section 4; a description of the model input preparation for this day is presented in Section 5. Section 6 contains an analysis of model performance on 13 and 19 July 1979. Section 7 discusses several hydrocarbon emission reduction scenarios and input sensitivity simulations. Summary and conclusions are presented in Section 8.

Two appendixes are included with this report. Appendixes A and B present predicted hourly average ozone isopleths and time series plots of ozone predictions and observations at monitoring stations for the 13 and 19 July 1979 simulations, respectively.

TECHNICAL APPROACH

The photochemical modeling approach adopted in the Philadelphia study is similar to, and draws heavily from, past UAM application studies in other urban areas in the United States and abroad, including Los Angeles (Tesche et al., 1982a,b), St. Louis (EPA, 1983a), Denver (EPA, 1983b), and Tulsa (Reynolds, 1982). Although the Philadelphia application can be considered straightforward in many respects, certain unique characteristics of the region require special consideration (e.g., treatment of upwind boundary conditions to reflect precursor emissions transported from the New Jersey/New York urban area). The steps followed in the Philadelphia study are summarized next.

The evaluation of the UAM in the Philadelphia metropolitan area comprised the following technical steps:

(1) Selection, through consultation with the EPA project officer, of the ozone modeling episodes to be simulated;

(2) Identification, receipt, and installation of meteorological, air quality, emissions, and other geographic data;

(3) Performance of a quality assurance audit of the data base to identify and subsequently correct errors and biases found in the meteorological and air quality data bases;

(4) Specification of the modeling region;

(5) Preparation and review of UAM input files;

BEST COPY AVAILABLE

(6) Initial UAM simulations and evaluations;

(7) Diagnostic analyses of simulation results in order to identify and subsequently remove biases or errors in the model input files;

(8) Final simulation of the ozone episodes to obtain suitable base cases; and

(9) Evaluation of UAM performance following prescribed statistical procedures.

After preparation and evaluation of the base-case simulations, a series of hydrocarbon emission reduction simulations involving various assumptions of background concentration for hydrocarbons and ozone were performed to (1) assess the sensitivity of predicted ozone concentrations, and (2) demonstrate the value of using the UAM in the formulation of emission control requirements for improving air quality in large metropolitan areas such as Philadelphia.

Figure 1-1 presents the general geographical setting of the Philadelphia airshed modeling region. Figure 1-2 shows a more resolved view of this region. (Further details of the modeling region are given in Section 3.)

BEST COPY AVAILABLE

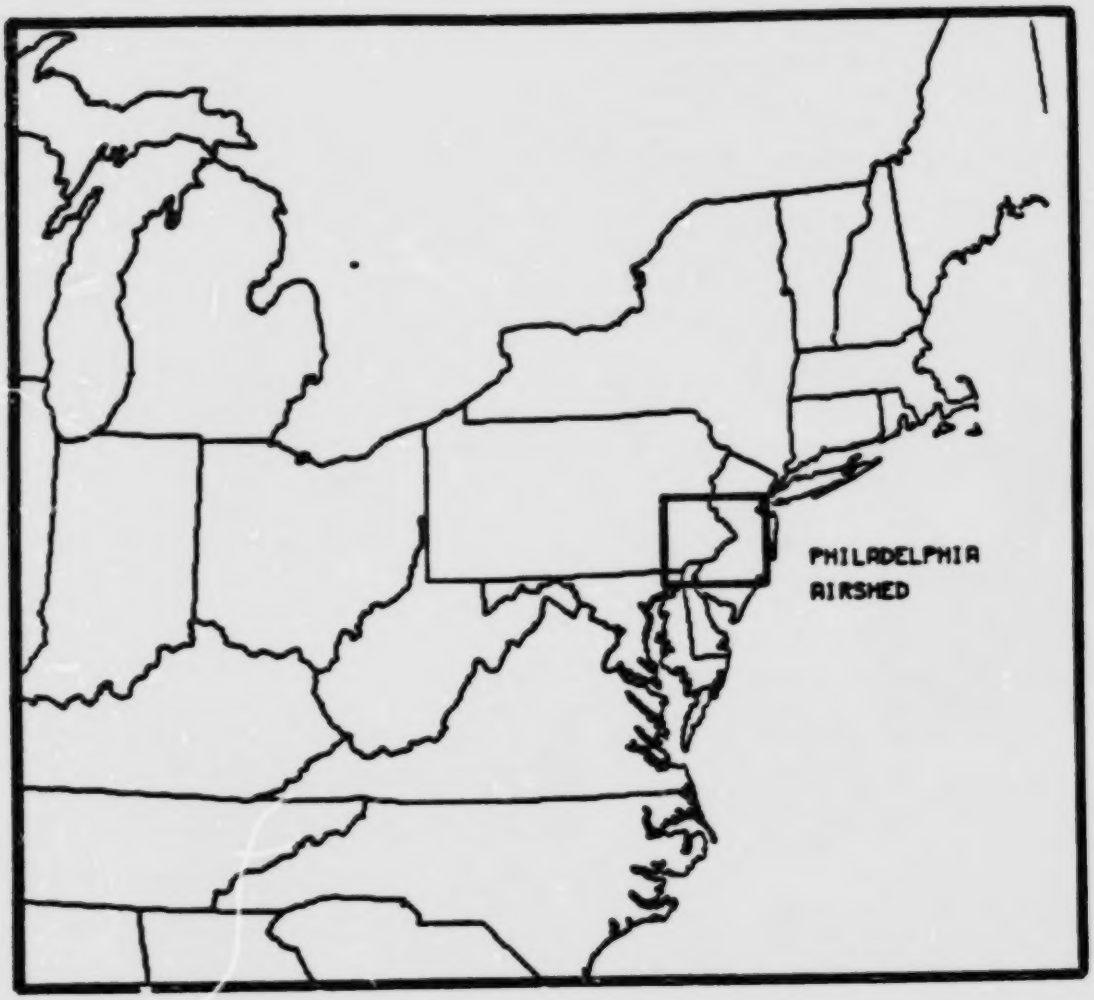

FIGURE 1-1. Geographical location of the Philadelphia airshed modeling region.

BEST COPY AVAILABLE

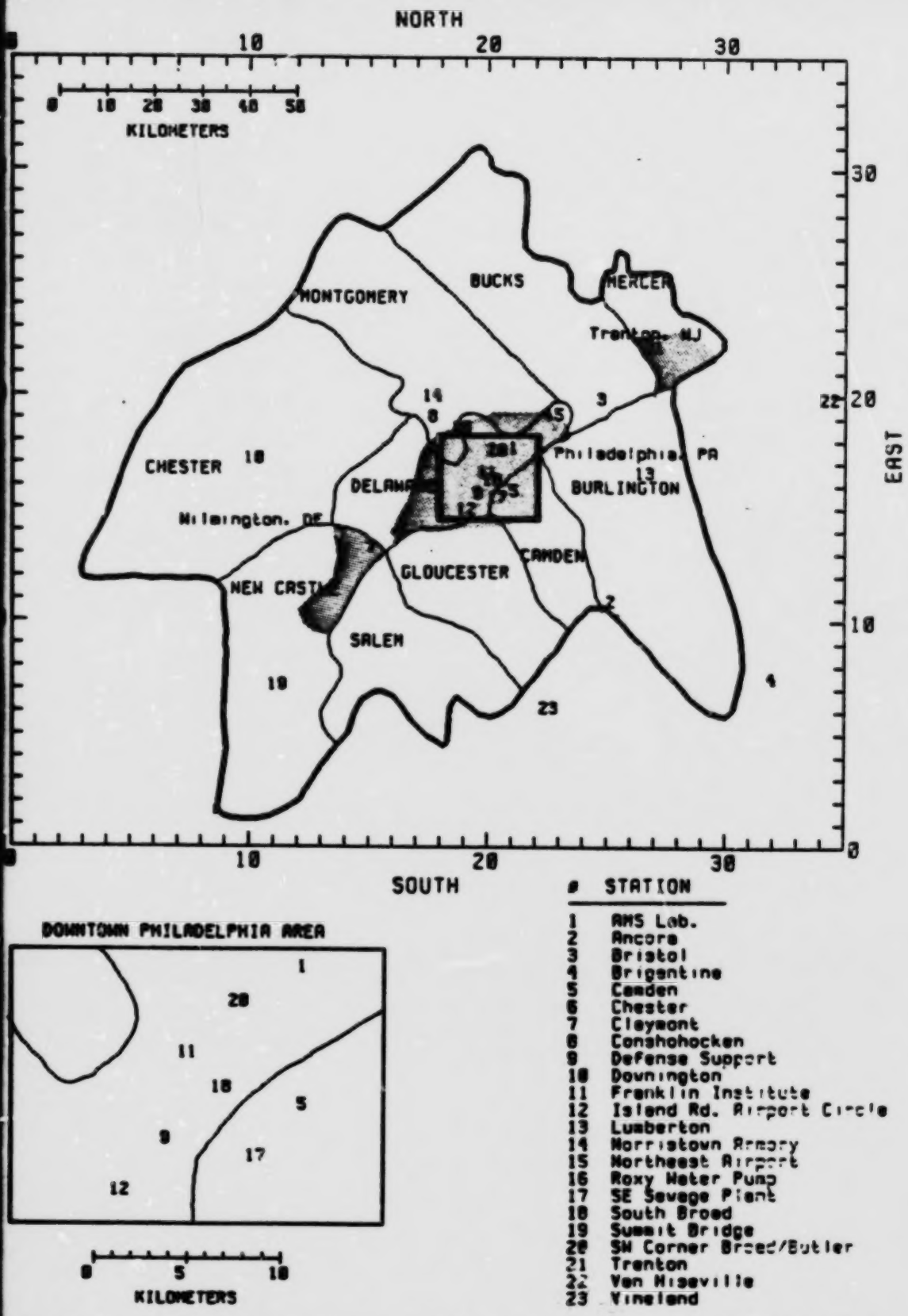

#	STATION
1	AMS Lab.
2	Ancora
3	Bristol
4	Brigantine
5	Camden
6	Chester
7	Claymont
8	Conshohocken
9	Defense Support
10	Downington
11	Franklin Institute
12	Island Rd. Airport Circle
13	Lumberton
14	Norristown Armory
15	Northeast Airport
16	Roxy Water Pump
17	SE Sewage Plant
18	South Broad
19	Summit Bridge
20	SW Corner Broad/Butler
21	Trenton
22	Van Hiseville
23	Vineland

FIGURE 1-2. Philadelphia airshed modeling region. Philadelphia AQCR for which emissions are available is shown by bold lines. Lighter lines denote county boundaries. Stippling represents urban areas.

BEST COPY AVAILABLE

BLANK PAGE

2 CHARACTERIZATION OF THE 13 JULY 1979 OZONE EPISODE

The highest and most widespread ozone concentrations measured during the summer of 1979 occurred on Friday, 13 July. These high concentrations were the result of a buildup of precursors from near-stagnant conditions on the previous day (12 July), and generally weak and variable winds prevailing until noon of the 13th, when a stronger southerly flow was established. The synoptic pattern showed high pressure throughout the day dominating the surface and upper-level (2000 m) flow fields (see Figure 2-1). This high pressure was part of the seasonally semipermanent Bermuda high-pressure cell centered east of Florida. The high pressure weakened through the course of the day as a trough (the remnants of Hurricane Bob) over the Ohio Valley moved slowly eastward bringing precipitation to western Pennsylvania.

Light west-northwesterly surface winds were present throughout the region from noon on 12 July until the early morning hours of 13 July when the winds became calm or very light with a northerly direction. This wind flow pattern was responsible for transporting ozone and precursors to the southeast of the region during this period. Surface wind measurements showed these calm-to-very-light winds during the early morning hours of 13 July, with northerly directions increasing slightly in speed and shifting to a general southerly direction by late morning (1000 EST). This shift in surface wind direction resulted in a recirculation of material that had been transported to the southeast during the previous 24 hours. Influx of ozone and precursor from the southeast, a buildup of regional ozone and precursors from near-stagnant conditions on the previous day (12 July), the day's emissions, generally light winds, high region-wide temperatures, and mostly clear skies were the primary conditions leading to high ozone concentrations.

Evidence of this recirculation of ozone and precursor material and the possible existence of a reservoir of ozone aloft from the previous day is shown in the observed ozone concentration data at upwind monitors. For the morning of 13 July, stations to the south and east were upwind. Examination of the ozone concentration during the initial onset of mixing is one way of providing information on ozone levels aloft. At 1000 EST, observed ozone concentrations were 8.4 pphm at Brigantine, New Jersey; 9.7

BEST COPY AVAILABLE

FIGURE 2-1. Synoptic situation, 0700 EST, July 13, 1979. (Source: Allard et al., 1981)

BEST COPY AVAILABLE

pphm at Lumberton, New Jersey; and 12.3 pphm at Ancora, New Jersey. At another upwind monitor (Vineland, New Jersey), ozone data were missing for 1000 EST; however, an hour earlier (900 EST) this monitor recorded an ozone concentration of 10.2 pphm. For this time period (onset of mixing), these ozone concentrations were among the highest observed during the summer of 1979. This indicates that a large reservoir of ozone existed aloft and was available for mixing down to the surface.

No upper-air measurements were available in Philadelphia on this day; however, radiosonde data from New York City (JFK) and Washington D.C. (Dulles International Airport) showed very light westerly winds at 2000 m throughout the day.

Because surface wind flow patterns established a southerly direction by late morning, peak ozone concentrations occurred north of the high urban emission source region. The highest ozone concentration recorded on this day was a value of 20.5 pphm at Conshohocken at 1600 EST. The second highest value of 20 pphm occurred earlier in the afternoon at the Roxy Water Pump monitor at 1400 EST. Thirteen monitors recorded ozone concentrations greater than 12 pphm.

BEST COPY AVAILABLE

BLANK PAGE

3 DESCRIPTION OF MODEL INPUTS FOR 13 JULY 1979

This section describes the preparation of the UAM input files for the 13 July 1979 episode. The majority of the files were prepared after examination of the air quality and meteorological data from the Philadelphia Oxidant Data Enhancement Study carried out during the summer of 1979 (Allard et al., 1981). The emissions and terrain files (estimates of surface roughness and uptake) were prepared after examination of the study detailing the preparation of the emission inventory for the Philadelphia AQCR (EPA, 1982). All input files times were set to Eastern Standard Time (EST). Input specifications for some of the files were prepared either wholly or in part by members of the EPA project team at OAQPS, whereas the computer simulations were all performed at Systems Applications, Inc.

MODELING REGION SPECIFICATIONS

The modeling region of the Philadelphia airshed specified in this study is 180 x 170 km, or a total area of 30,600 km^2. This region covers parts of Pennsylvania, Delaware, Maryland, and New Jersey, and includes the metropolitan areas of Philadelphia, Pennsylvania; Wilmington, Delaware; and Trenton, New Jersey (see Figures 1-1 and 1-2).

The modeling region specifications (e.g., grid origin, grid size, number of horizontal cells, etc.) are contained in what is known as the REGION packet. For the Philadelphia application, the modeling grid contains 36 by 34 horizontal cells that are fixed at 5000 m by 5000 m, along with 4 vertical cells (layers) that vary in thickness depending on the hourly mixing height and the height of the top of the modeling region. Two vertical cells are specified below the mixing height, with two cells above. In the simulations, the cells, or layers, below the mixing height may attain the minimum cell thickness specified (for this application, 50 m) during the night when the mixing height is at a minimum. As the mixed layer thickens during the day, the vertical thickness of layers 1 and 2 grows, while the thickness of the upper layers (3 and 4) decreases. The specified height for the top of the modeling region was fixed for each hour and was used in preparing the REGIONTOP file. The Airshed Model REGION packet in all input files was specified as follows:

BEST COPY AVAILABLE

UTM ZONE: 18
X ORIGIN: 387000. m EASTING
Y ORIGIN: 4340000. m NORTHING
GRID SIZE: 5000.0 m
TOP OF REGION: 1630.0 m
NX: 36 cells
NY: 34 cells
NZ: 4 cells
MINIMUM CELL THICKNESS-LOWER LAYERS: 50 m
MINIMUM CELL THICKNESS-UPPER LAYERS: 50 m

MIXING HEIGHTS

Mixing heights for 13 July 1979 were estimated every half hour for urban and rural areas for daytime, transitional, and nighttime regimes. Urban and rural mixing height cell designations are included in the discussion of the terrain file. Since no soundings were available for Philadelphia on this day, the daytime mixing heights between 0600 and 1400 EST were estimated using the available morning (0700 EST) and evening (1900 EST) radiosonde soundings in New York (JFK) and Washington, DC (IAD). These temperature soundings are shown in Figures 3-1 through 3-4. The procedure used to estimate daytime mixing heights is similar to the methodology used by Holzworth (1972). First, spatially averaged surface temperatures for the Philadelphia region were computed for each hour using all available meteorological measurement sites. The resultant average hourly surface temperatures were plotted on temperature-versus-height graphs of each sounding. The height of the intersection between the dry adiabat of the surface temperature and the temperature sounding was then taken as an estimate of the mixing height.

Between 0600 and 1200 EST, the mixing height was computed as the average of the values estimated from the JFK and Dulles airport morning soundings. An average of the JFK and Dulles morning and afternoon soundings was used to compute mixing heights between 1200 and 1400 EST. An exception to this procedure was made for estimating rural mixing heights between 0600 and 0900 EST, before the dissipation of the rural surface stable layer. During this period rural mixing heights were subjectively estimated to increase from the overnight value of 100 m to the 0900 EST value. Because of the general nature of the "adiabatic" procedure used for estimating daytime mixing heights, no other distinction was made between urban and rural mixing heights during the 0600-1400 EST time period.

BEST COPY AVAILABLE

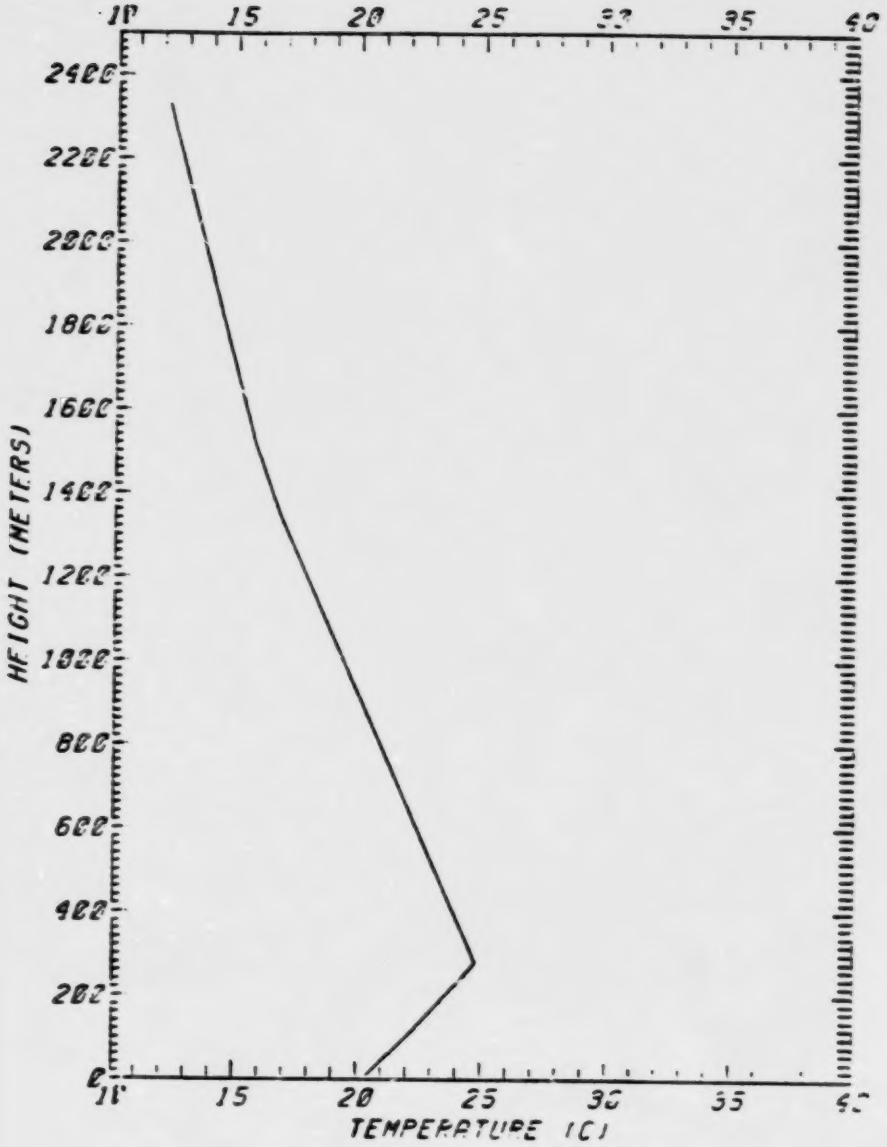

Figure 3-1. Temperature sounding for JFK airport on 13 July 1979 -- 0700 EST.

BEST COPY AVAILABLE

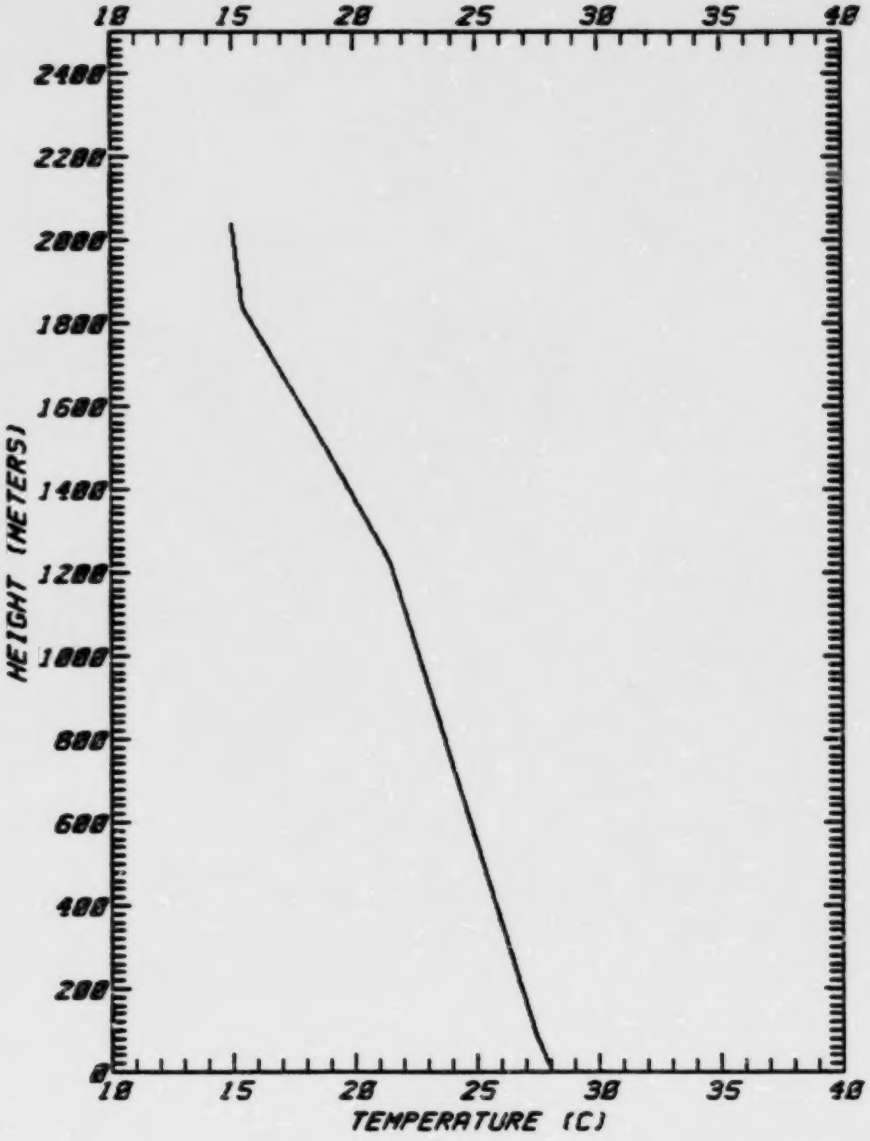

Figure 3-2. Temperature sounding for JFK airport on 13 July 1979 -- 1900 EST.

BEST COPY AVAILABLE

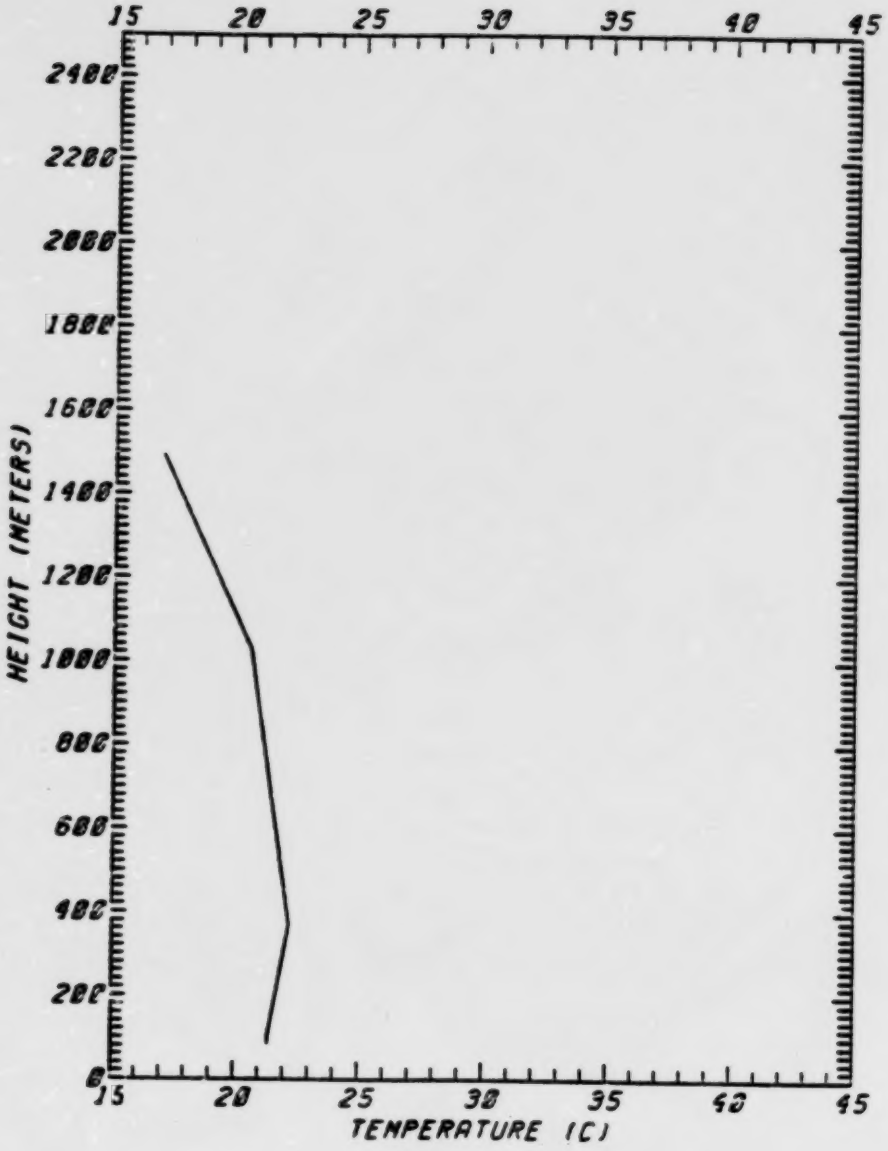

Figure 3-3. Temperature sounding for Dulles airport on 13 July 1979 -- 0700 EST.

BEST COPY AVAILABLE

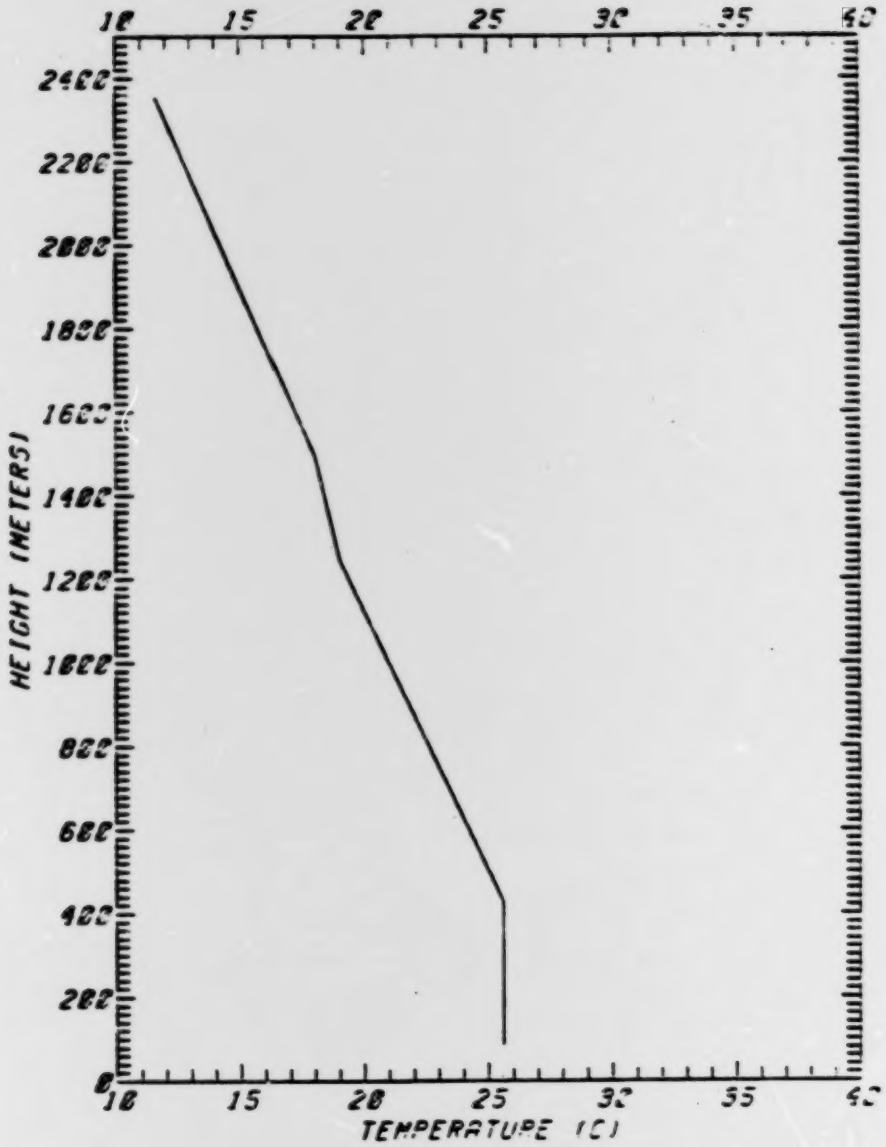

Figure 3-4. Temperature sounding for Dulles airport on 13 July 1979 -- 1900 EST.

BEST COPY AVAILABLE

The overnight (0000 through 0600 EST) mechanically dominated mixing heights were set to a constant value of 250 m in urban areas and 100 m in rural areas. These "default" values were obtained from analyses of overnight mixing heights in Philadelphia, St. Louis, and other cities (Godowitch, 1984; Godowitch, et al., 1984b; Bornstein, 1968; Clarke, 1969).

Mixing heights during the evening transition between convectively dominated and mechanically dominated mixing are difficult to estimate, particularly in the absence of local measurements. To approximate this transition in a manner consistent with the capabilities of the Airshed Model (and at the same time avoid sharp discontinuities in mixing height), mixing heights were decreased at a rate of ~2-3 m/min after the time of maximum average surface temperature at 1400 EST (Noonkester, 1976; Kaimal, et al., 1982). This rate was used for urban mixing heights until 2300 EST when the overnight value of 250 m was assumed to be applicable. In rural areas, this rate was applied until 1800 EST, at which time the mixing height was decreased more rapidly to reach the overnight value of 100 m by 2000 EST (Godowitch, 1984b). The resulting half-hour mixing height values for urban and rural grid cells are presented in Table 3-1 and graphically illustrated in Figure 3-5.

WIND FIELD

Preparation of the wind field for a specified simulation day is one of the more critical inputs in achieving acceptable model performance. There is no "correct" way of specifying a three-dimensional flow field using only a limited number of surface observations and even fewer upper air observations covering an area as large as the Philadelphia airshed region. Yet the "modeled" flow field is the crucial element in the final spatial alignment of the urban plume. In any Urban Airshed Model application, certain areas of the airshed grid will lack surface data. These data "gaps" must be filled in with realistic estimates so that a smooth continuity is maintained for the mass flow both in time and space. Because of the light and variable nature of the observed surface winds on 13 July, it was apparent that it might be difficult to prescribe a three-dimensional flow field free from directional and speed biases. The following procedure was used in preparing the hourly flow fields for the 13 July 1979 simulation.

Surface wind data collected during the 1979 Philadelphia Oxidant Data Enhancement Study (Allard et al., 1981) were available for 16 stations for 13 July. The first step in the preparation of the wind field was to graphically plot the surface vectors on the airshed grid. Figure 3-6 depicts these plotted vectors for four separate hours of the day. This

BEST COPY AVAILABLE

TABLE 3-1. Urban and rural mixing height values used in the DIFFBREAK file for 13 July 1979.

Time (EST)	Urban (m)	Rural (m)
0000	250	100
0030	250	100
0100	250	100
0130	250	100
0200	250	100
0230	250	100
0300	250	100
0330	250	100
0400	250	100
0430	250	100
0500	250	100
0530	250	100
0600	250	100
0630	270	135
0700	295	150
0730	375	250
0800	450	350
0830	680	620
0900	925	925
0930	1160	1160
1000	1200	1200
1030	1330	1330
1100	1480	1480
1130	1480	1480
1200	1480	1480
1230	1500	1500
1300	1530	1530
1330	1530	1530
1400	1530	1530
1430	1475	1475
1500	1420	1420
1530	1365	1365
1600	1310	1310
1630	1220	1220
1700	1130	1130
1730	1035	1035
1800	950	950
1830	855	730
1900	770	525
1930	675	320
2000	590	100
2030	500	100
2100	410	100
2130	370	100
2200	330	100
2230	290	100
2300	250	100
2330	250	100
2400	250	100

BEST COPY AVAILABLE

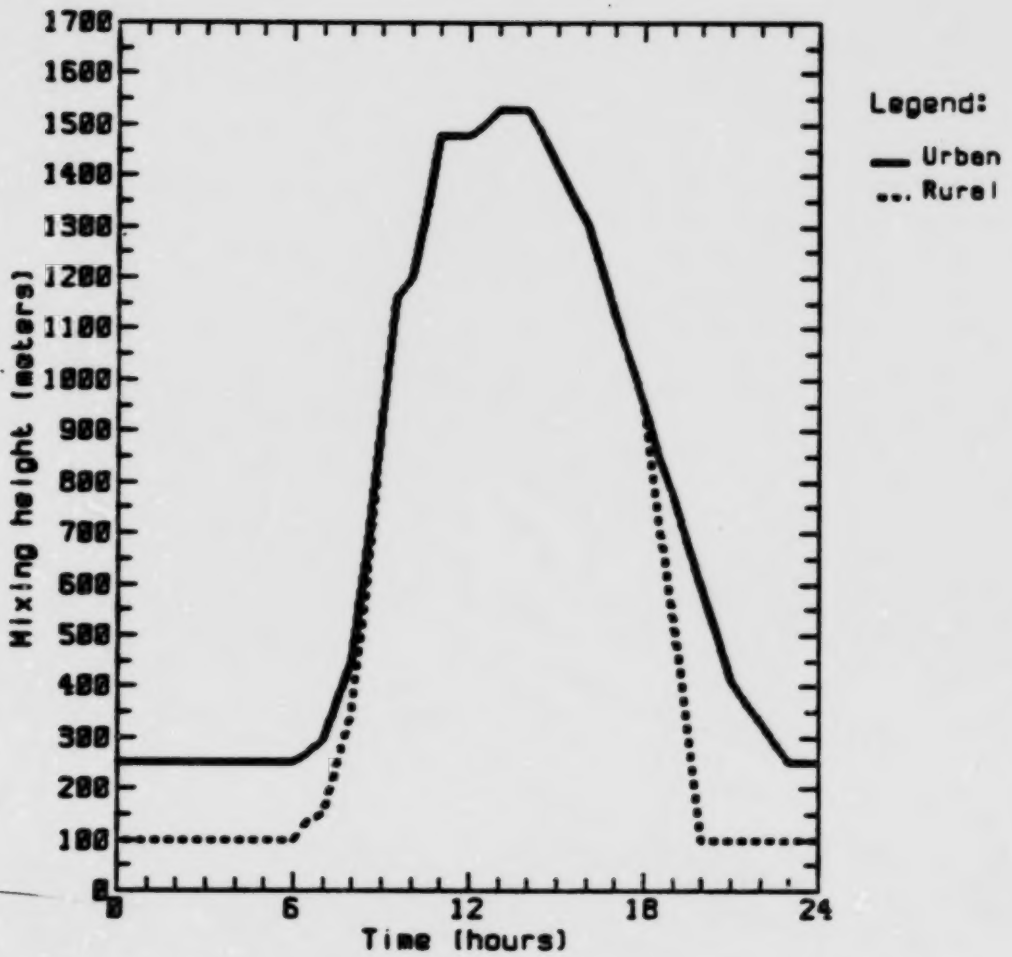

FIGURE 3-5. Mixing height profile for urban and rural cells for the 13 July 1979 simulation.

BEST COPY AVAILABLE

FIGURE 3-6. Observed surface wind vectors and wind vectors used in preparing the interpolated surface wind field for 13 July 1979.

BEST COPY AVAILABLE

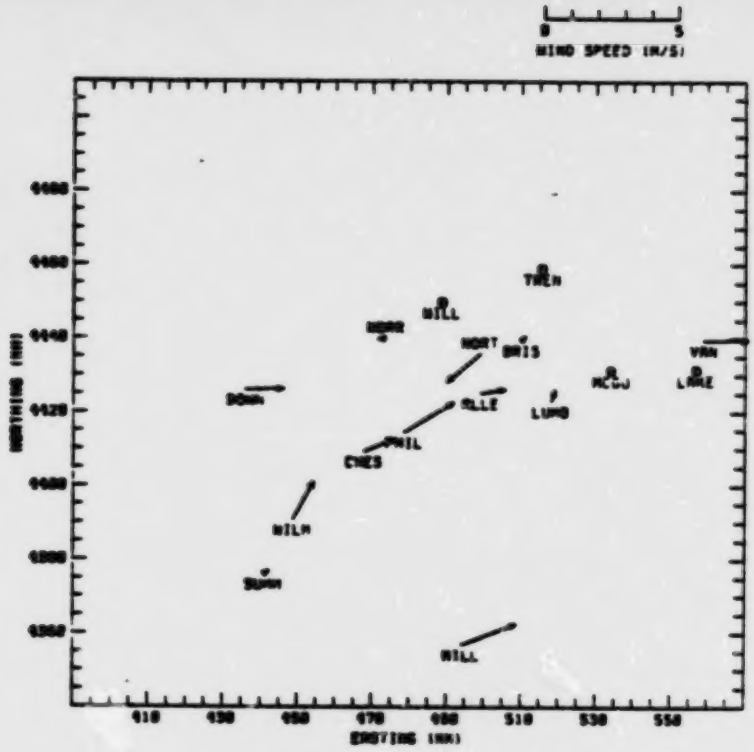

Observed wind vectors

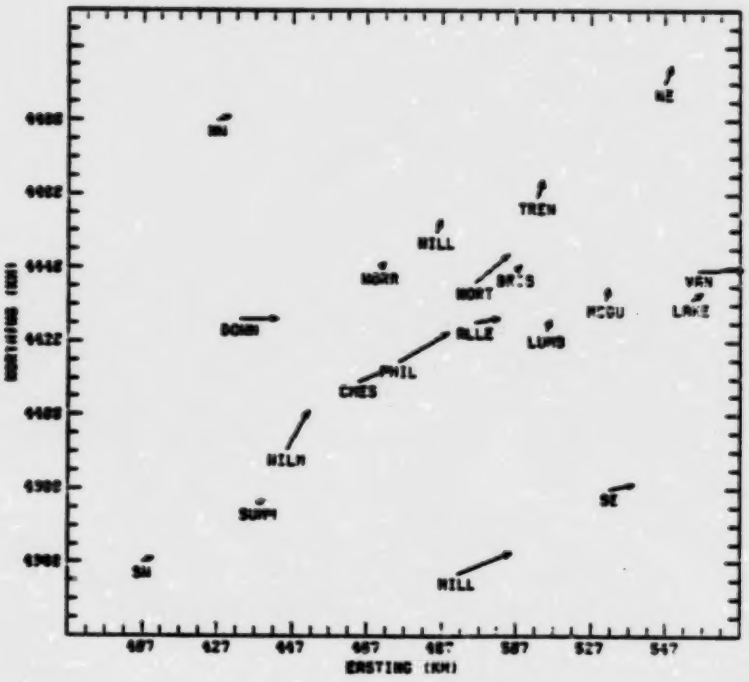

Wind vectors used in preparing model input wind fields for surface layer.

FIGURE 3-6a. 0000-0100 EST

BEST COPY AVAILABLE

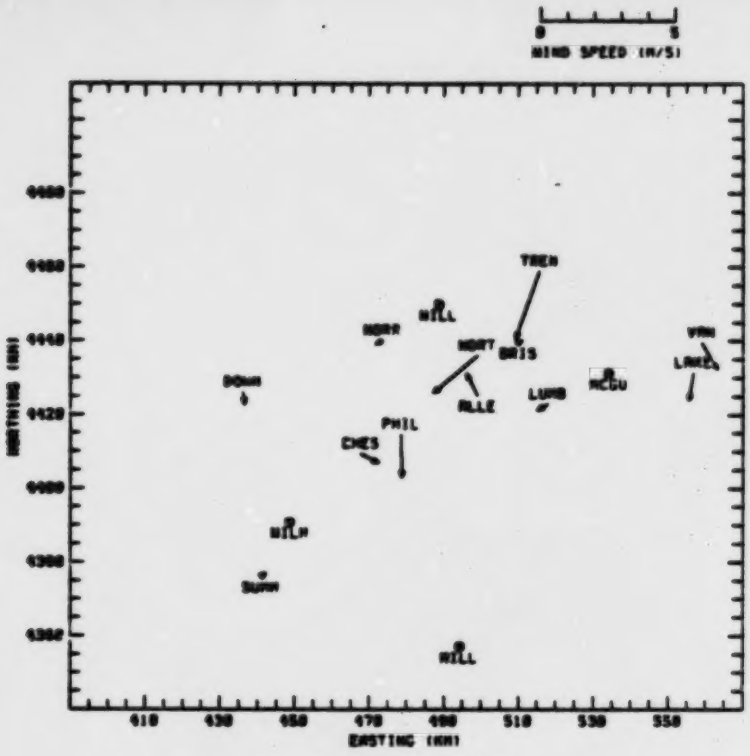

Observed wind vectors

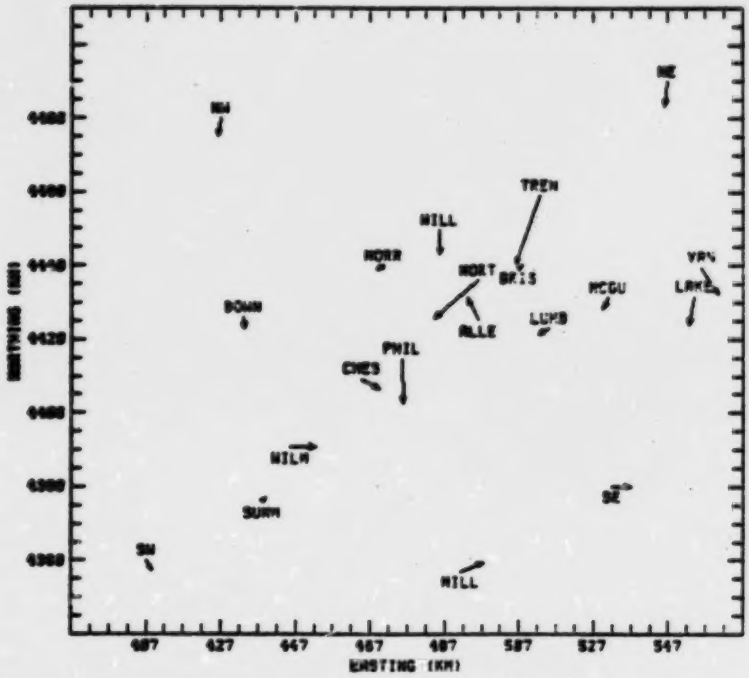

Wind vectors used in preparing model input wind fields for surface layer.

FIGURE 3-6b. 0600-0700 EST

BEST COPY AVAILABLE

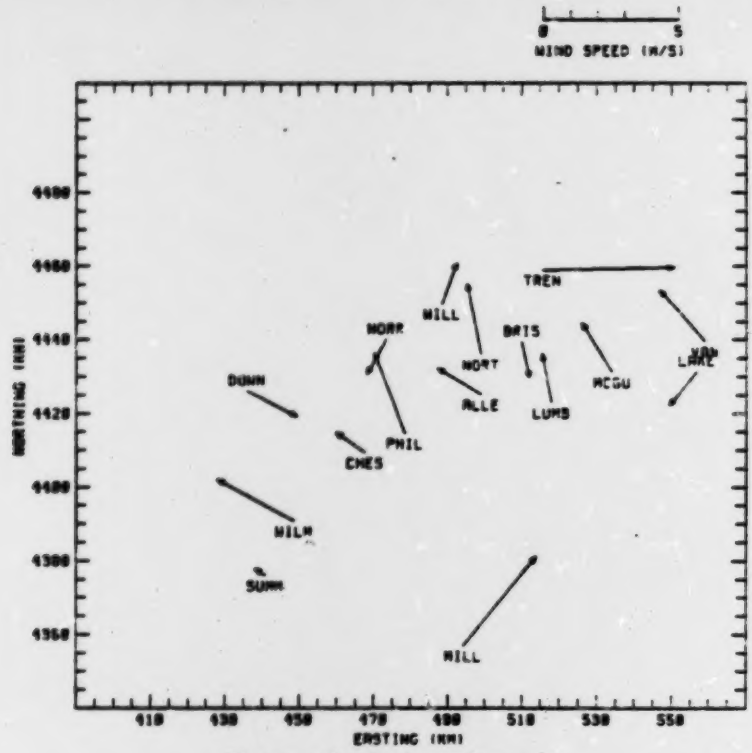

Observed wind vectors

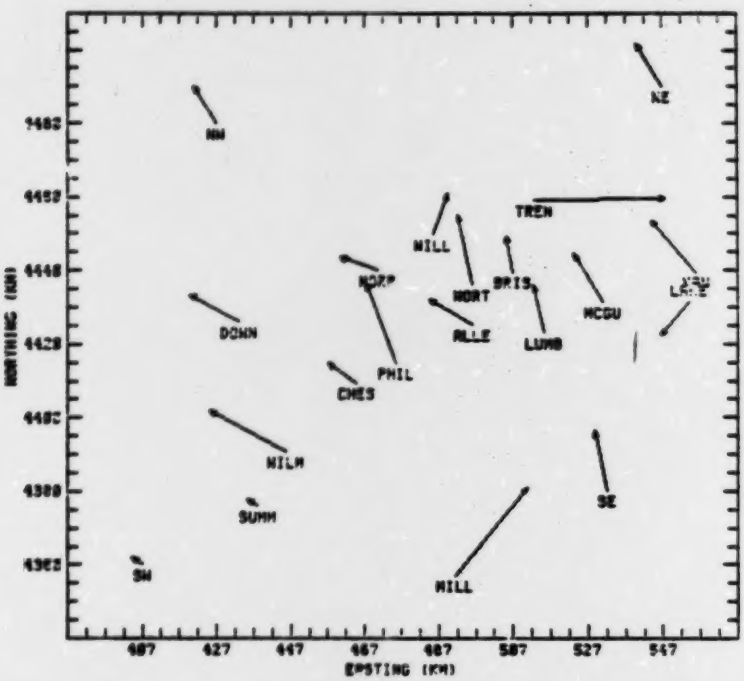

Wind vectors used in preparing model input wind fields for surface layer.

FIGURE 3-6c. 1200-1300 EST

BEST COPY AVAILABLE

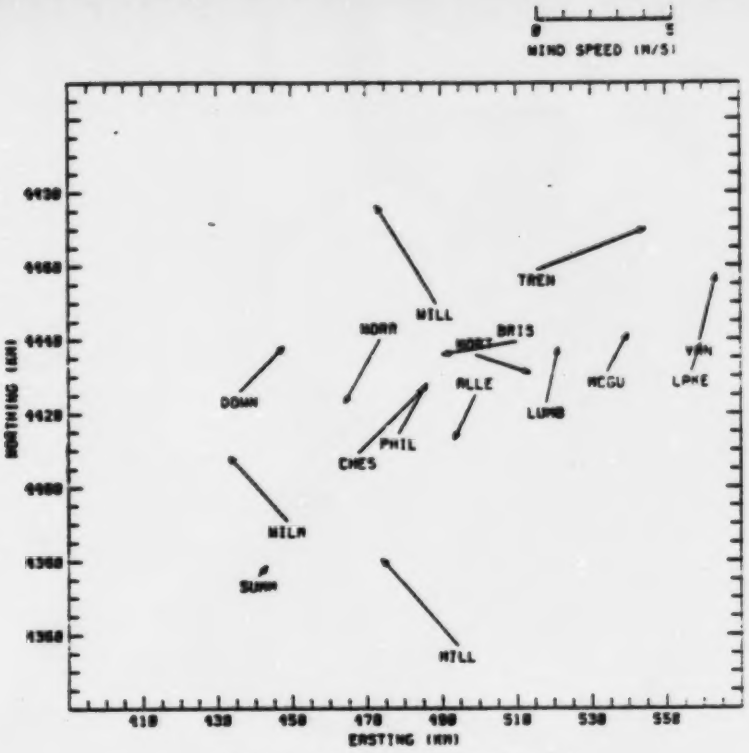

Observed wind vectors

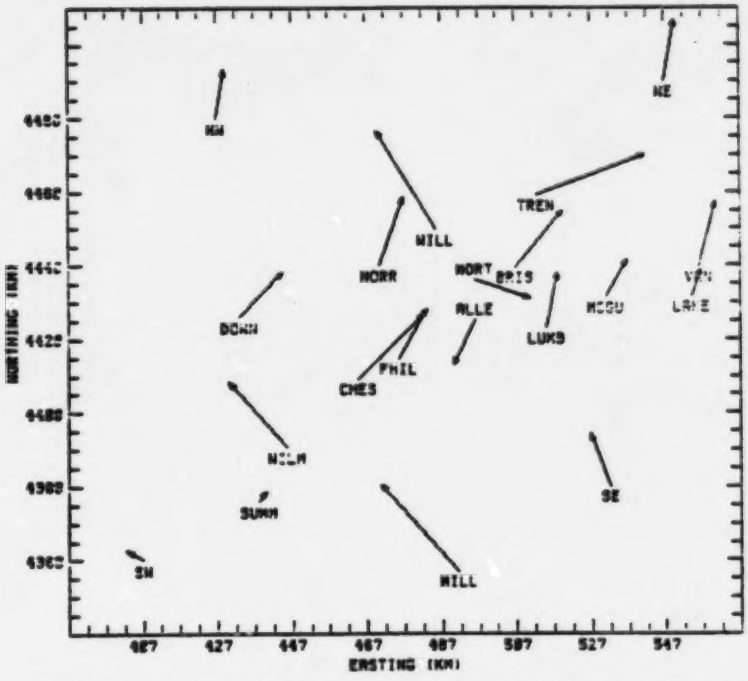

Wind vectors used in preparing model input wind fields for surface layer.

FIGURE 3-6d. 1800-1900 EST

BEST COPY AVAILABLE

graphical plotting is performed as a data screening procedure. By examining the hourly observed vectors plotted on the airshed grid, it is possible to gain insight into the actual flow field one is attempting to model.

The plotting of surface vectors can uncover questionable data (e.g., a surface vector that is 180° out of phase with the other nearby stations). It can also be used to identify areas of the airshed grid for which observational data are sparse; these areas may need to be supplemented with estimated data to complete the spatial coverage of the mass flow field.

Observed surface wind data were available at the following locations:

Station	UTM Easting (km)	UTM Northing (km)
Northeast Philadelphia Airport, Pennsylvania	499.0	4436.0
Philadelphia International Airport, Pennsylvania	478.6	4414.6
McGuire Air Force Base, New Jersey	534.1	4431.3
Willow Grove Naval Air Station, Pennsylvania	488.7	4449.8
Lakehurst Naval Air Station, New Jersey	556.9	4431.5
Trenton-Mercer County Airport, New Jersey	515.6	4459.0
Millville Airport, New Jersey	494.3	4357.0
Greater Wilmington Airport, Delaware	448.6	4390.7
Chester, Pennsylvania	467.8	4409.3
Bristol, Pennsylvania	510.0	4439.5
Allegheny-Philadelphia, Pennsylvania	491.7	4425.2
Summit Bridge, Delaware	441.0	4376.0
Downington, Pennsylvania	436.0	4426.0
Lumberton, New Jersey	518.0	4423.0
Van Hiseville, New Jersey	559.0	4439.5
Norristown, Pennsylvania	473.5	4440.0
NW	430.0	4480.0
NE	550.0	4490.0
SE	535.0	4380.0
SW	410.0	4360.0

The last four stations in this list were the designated "pseudo" stations used to fill the gaps in the observed surface field before the interpolation procedure. Each hourly plot of observed vectors was subjectively reviewed, and certain inconsistent or questionable data points were removed from the data file before proceeding. Overall, the wind data collected during the field program (for those days reviewed) looked

BEST COPY AVAILABLE

reasonable, and only minor corrections or deletions were needed before wind field preparation could commence. Figure 3-6 presents observed wind vectors for 13 July and the set of vectors used in the wind interpolation scheme for the corresponding time period. Comparison of the sets of vectors indicates those vectors deemed unreasonable and data used to fill the gaps in the interpolation.

The next step in the wind field preparation involved an interpolation program to obtain a complete surface wind field. The program WINTER employed a $1/R^2$ interpolation scheme and used the screened observation file to create a gridded surface wind field. Preparation of the winds in the upper layers was the next step in the process.

Although they were performed on other days during the 1979 Philadelphia Oxidant Study, upper-level atmospheric measurements were not performed on 13 July in central Philadelphia. Consequently, the nearest upper-level radiosonde data for this day correspond to the twice-daily releases at JFK and Dulles airports. These data were carefully analyzed to establish their utility for prescribing upper-level wind and temperature fields over Philadelphia. Figures 3-7 through 3-10 present vector plots of the morning and afternoon radiosonde wind profiles at JFK and Dulles airports, respectively. These data confirm the existence of a southwesterly through northwesterly synoptic flow, which is apparent from an examination of the NWS daily weather map for this day (see Figure 2-1). On the basis of these four soundings, the 1900 EST sounding of 12 July, and the 0700 EST sounding of 14 July, an attempt was made to estimate average synoptic-level (i.e., ≈1500 m) wind velocities at JFK and Dulles for the entire day. This was achieved by averaging the radiosonde values over a range of 1200 to 1800 m for each sounding. Hourly estimates of winds aloft were derived using vector interpolation between soundings. This review of both sets of soundings resulted in the selection of a constant vector to be used for each hour to describe the level-4 winds. The spatially constant, temporally varying wind vectors used for level 4 are presented in Table 3-2.

To obtain wind vectors for levels 2 and 3, the program WINDCHANG was used. This program performed a linear vector interpolation to obtain the vectors for levels 2 and 3 using the surface vector and the level-4 vector for each grid cell. The program read the REGIONTOP and DIFFBREAK mixing height files to determine the height of the node for each level for each hour. These files were read because the mixing height changes hourly and determines the thickness of each vertical cell. After the node heights were determined for levels 2 and 3, a linear interpolation was performed to compute the mid-level direction. The speed of the level 2 or level 3 vector was then increased by employing a power law equation as follows:

BEST COPY AVAILABLE

Delta H = 250 Meters
Delta S = 2 M/S

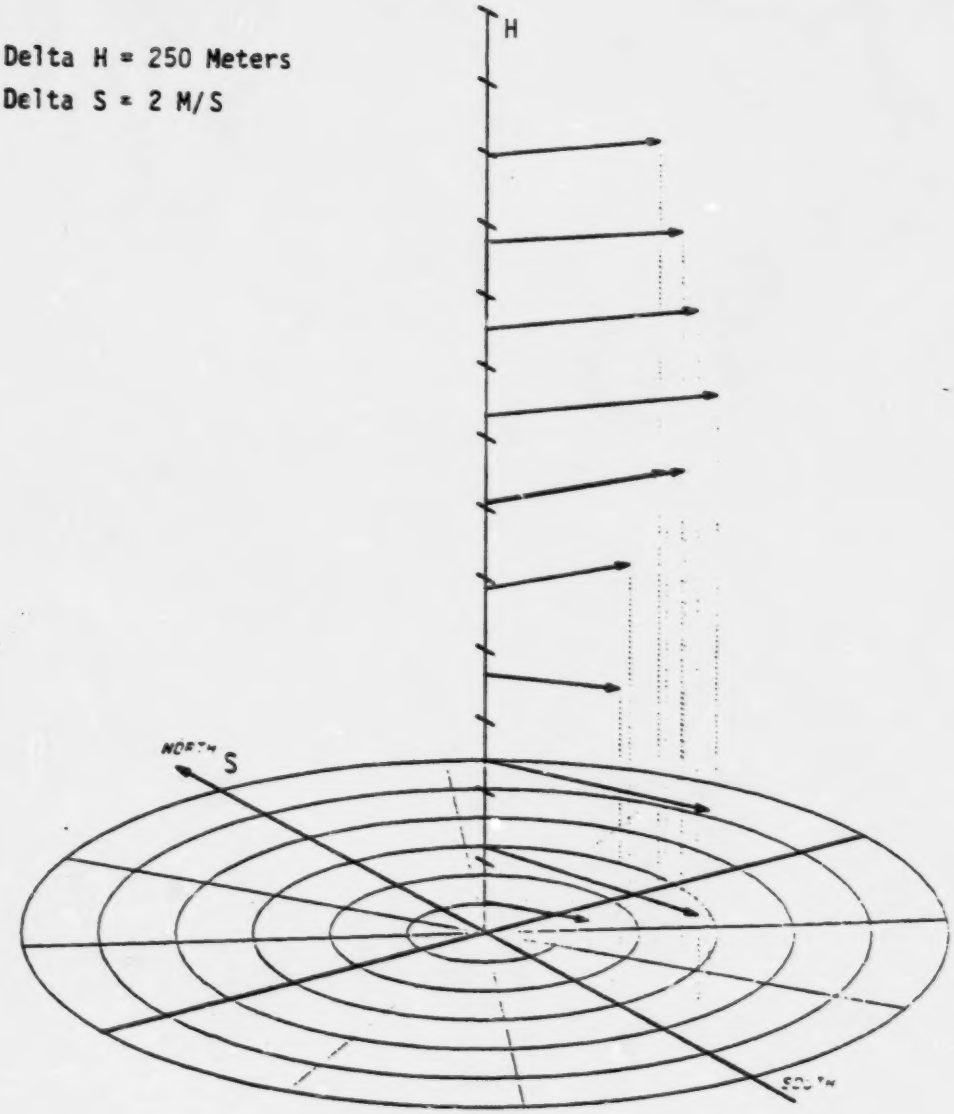

Figure 3-7. Upper-level winds at JFK airport on 13 July 1979 -- 0700 EST.

BEST COPY AVAILABLE

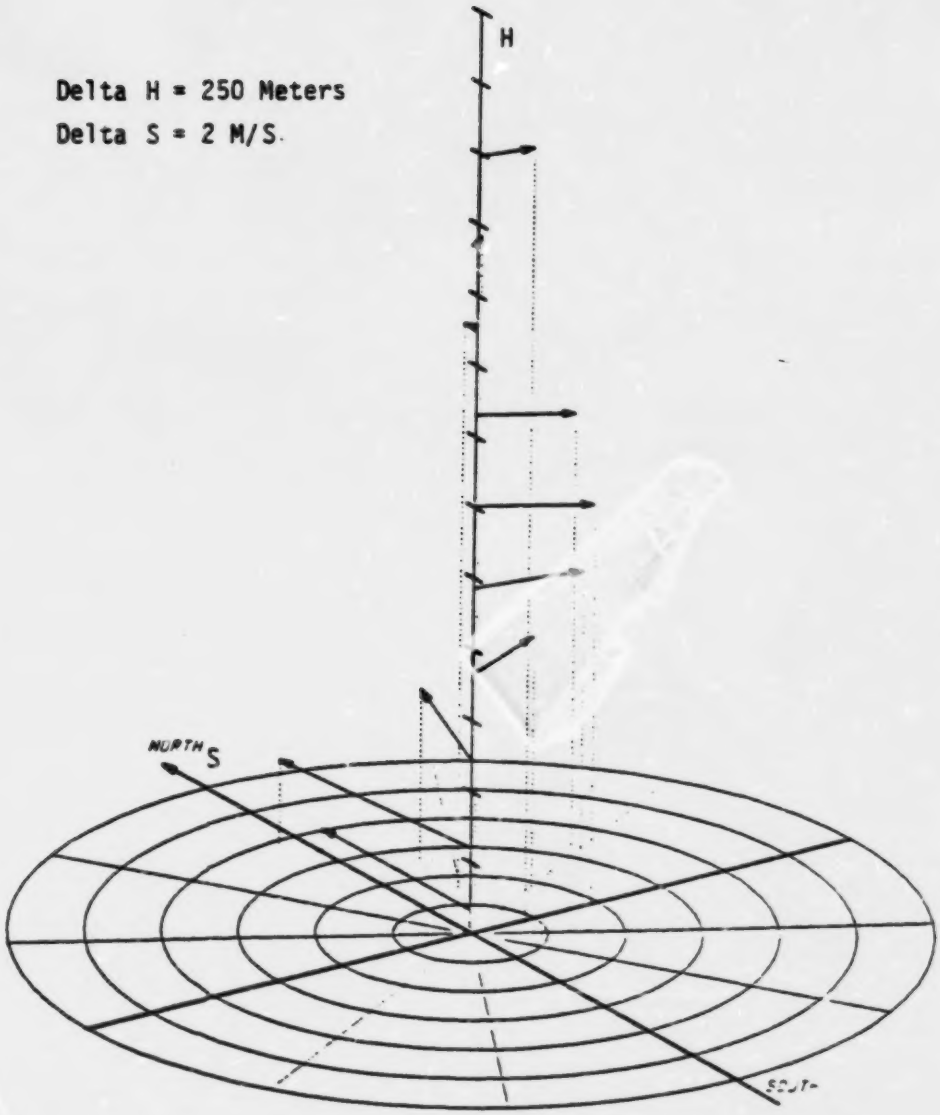

Figure 3-8. Upper-level winds at JFK airport on 13 July 1979 -- 1900 EST.

BEST COPY AVAILABLE

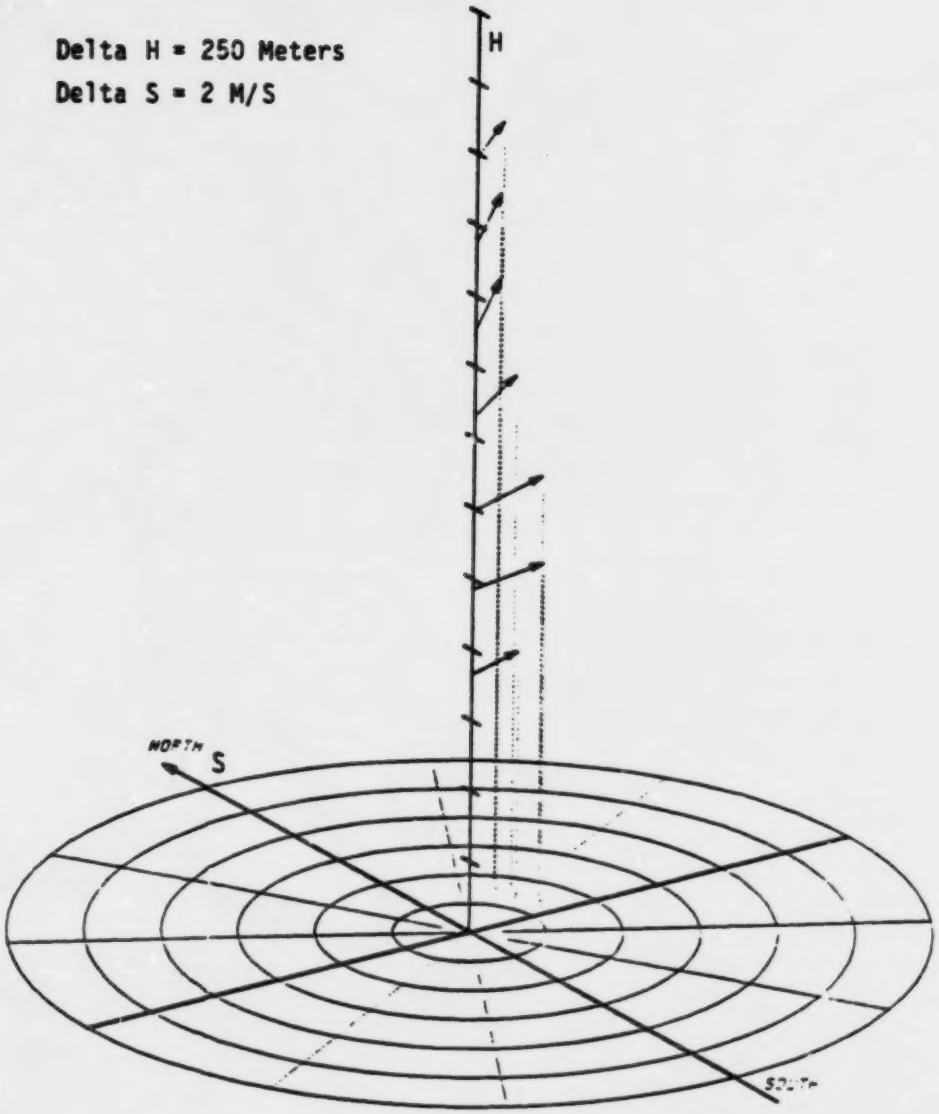

Figure 3-9. Upper-level winds at Dulles airport on 13 July 1979 -- 0700 EST.

BEST COPY AVAILABLE

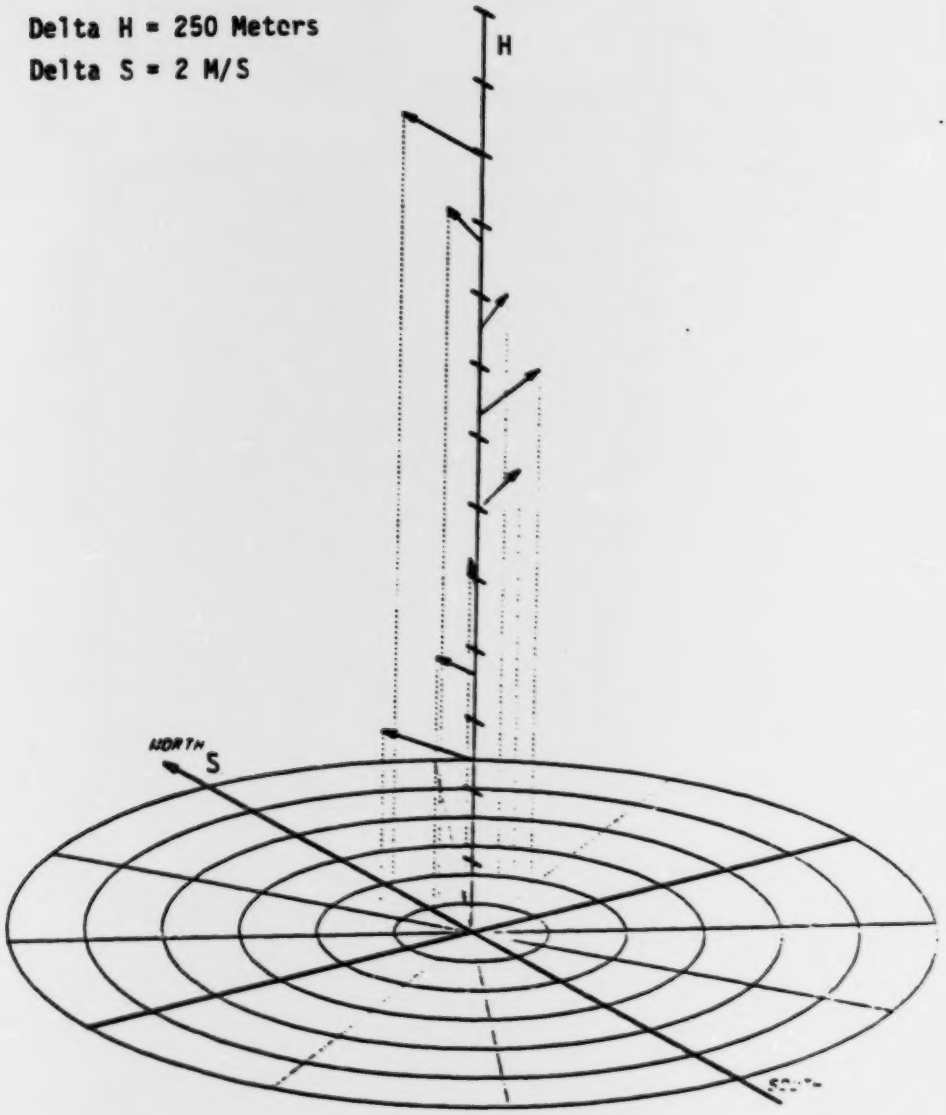

Figure 3-10. Upper-level winds at Dulles airport on 13 July 1979 -- 1900 EST.

BEST COPY AVAILABLE

TABLE 3-2. Spatially constant wind vectors for level 4 winds for 13 July 1979.

Hour (EST)	Direction (Degrees)	Speed (m/s)
0000-0100	284	5.5
0100-0200	282	5.5
0200-0300	280	5.2
0300-0400	278	5.0
0400-0500	276	4.8
0500-0600	274	4.4
0600-0700	272	4.2
0700-0800	270	4.0
0800-0900	270	4.0
0900-1000	270	4.0
1000-1100	270	4.0
1100-1200	268	4.0
1200-1300	268	4.0
1300-1400	268	3.5
1400-1500	268	3.5
1500-1600	268	3.0
1600-1700	265	3.0
1700-1800	265	3.0
1800-1900	265	3.0
1900-2000	250	4.0
2000-2100	250	4.0
2100-2200	240	4.0
2200-2300	240	4.0
2300-2400	240	4.0

BEST COPY AVAILABLE

$$V_2 = (V_4 - V_1)*(NODE_2/1500)^{\alpha} + V_1$$

$$V_3 = (V_4 - V_1)*(NODE_3/1500)^{\alpha} + V_1$$

where

$NODE_2$ = the height of the node of level 2,

$NODE_3$ = the height of the node of level 3,

V_4 = the speed of the vector for level 4,

V_1 = the speed of the vector of the surface wind, and

α = 0.2

This method is only one means of interpolating for the winds in levels 2 and 3. In the equation, α is the surface friction coefficient that varies as underlying features on the surface vary. If the α coefficient had been dropped, a straightforward linear interpolation would have resulted from the equation; however, the magnitude of the winds in levels 2 and 3 would have been underestimated with this procedure. Only one value of α was used in this application to reflect an average value of surface friction throughout the region.

A full three-dimensional flow field is thus created for each hour. Either because of noise in the wind sampling network, or because of the nature of the vectors sampled at two distinct points, the resulting flow field will contain a great deal of divergence. If the field is employed by the Urban Airshed Model with the divergence left in, spurious artificial vertical motions will result in unrealistic vertical transport. The last phase of the wind field preparation involves the elimination of nearly all divergence.

The program DIVFREE was written to read the three-dimensional file and eliminate most of the divergence in the flow field. This program was adopted from an EPA algorithm developed by Clark and Eskridge (1977) and is the final step in the creation of the wind field. As a quality control check, the wind vectors are then plotted on the airshed grid and examined for reasonableness before use in the UAM simulation. Trajectory analysis can be performed using this final file to determine, for example, the origin both in space and time of the parcels affecting the peak ozone concentrations. Figure 3-11 presents the gridded, smoothed surface vectors for the same hours presented in Figure 3-6. The gridded plots of the

BEST COPY AVAILABLE

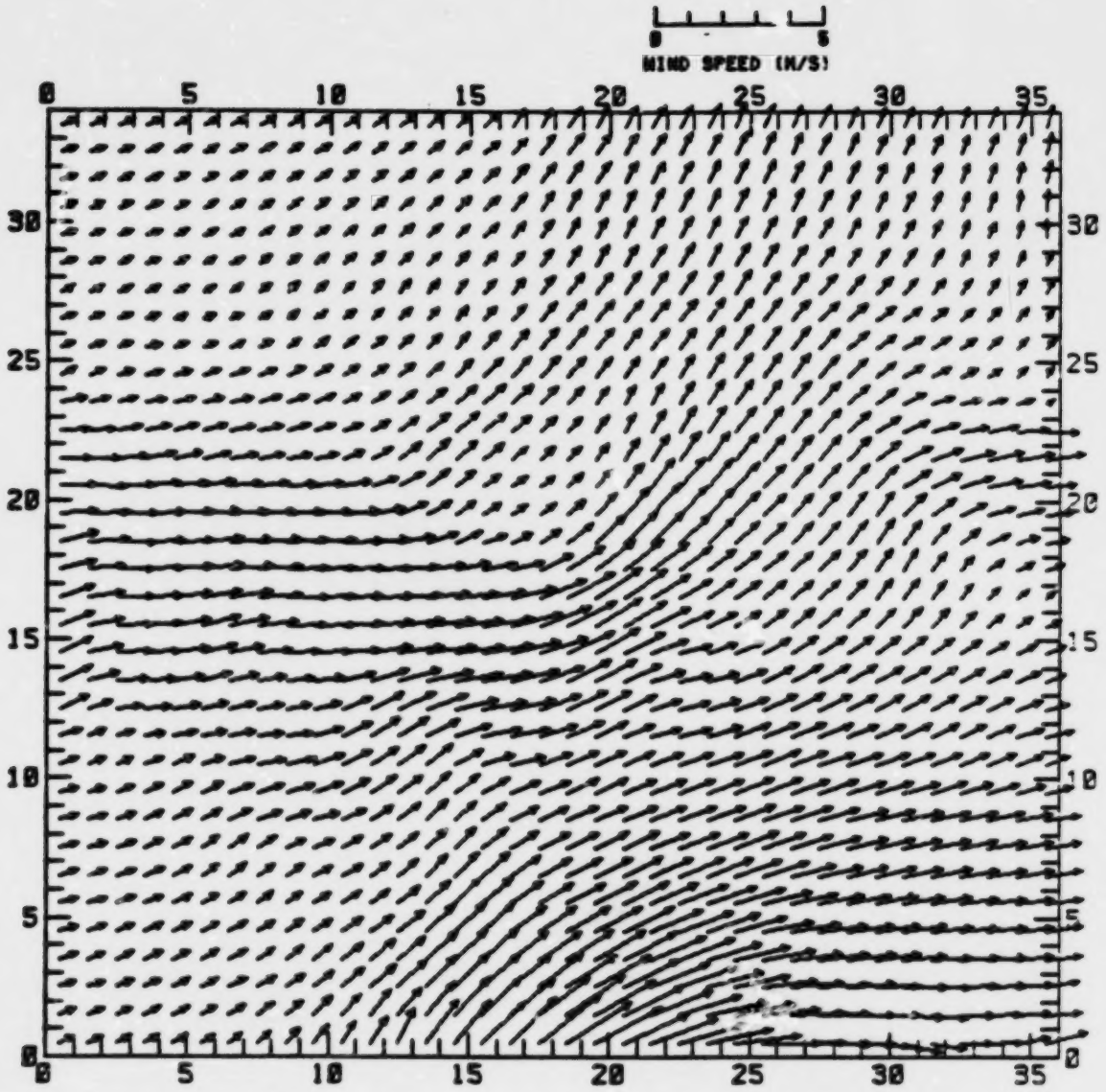

(a) 0 - 100 EST

FIGURE 3-11. Airshed model surface winds for 13 July 1979.

BEST COPY AVAILABLE

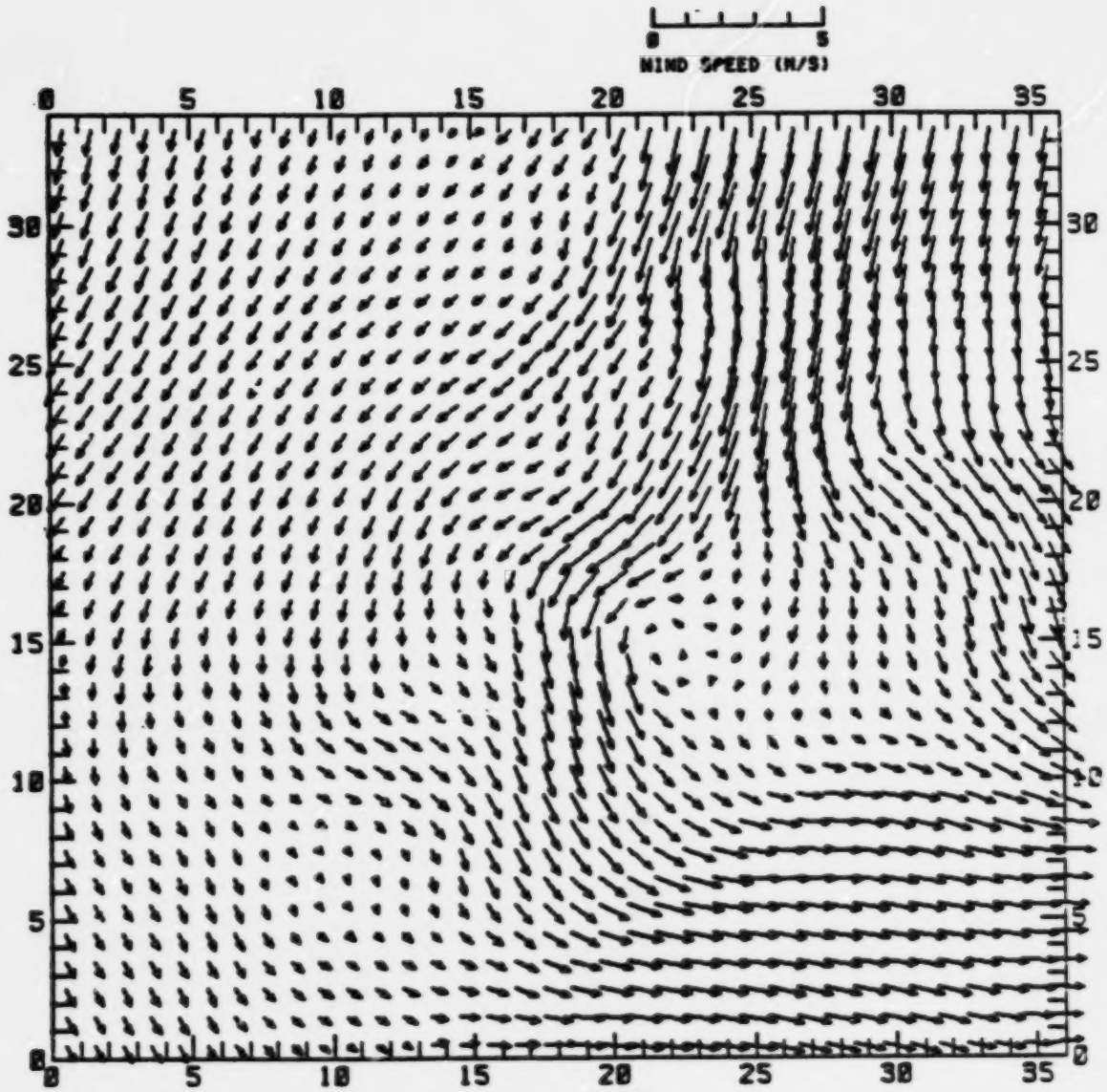

(b) 600 - 700 EST

FIGURE 3-11(continued)

BEST COPY AVAILABLE

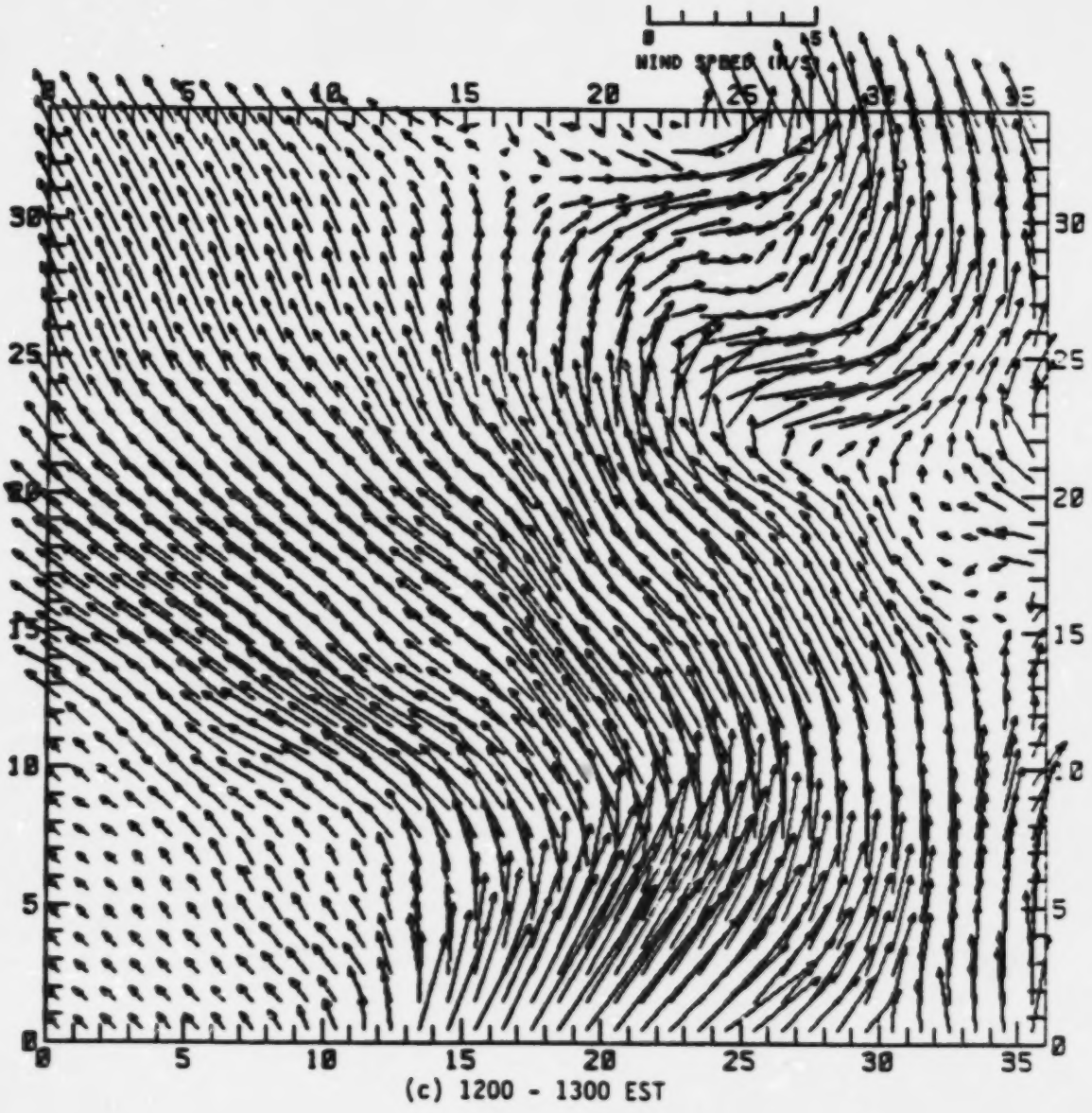

(c) 1200 - 1300 EST

FIGURE 3-11(continued)

BEST COPY AVAILABLE

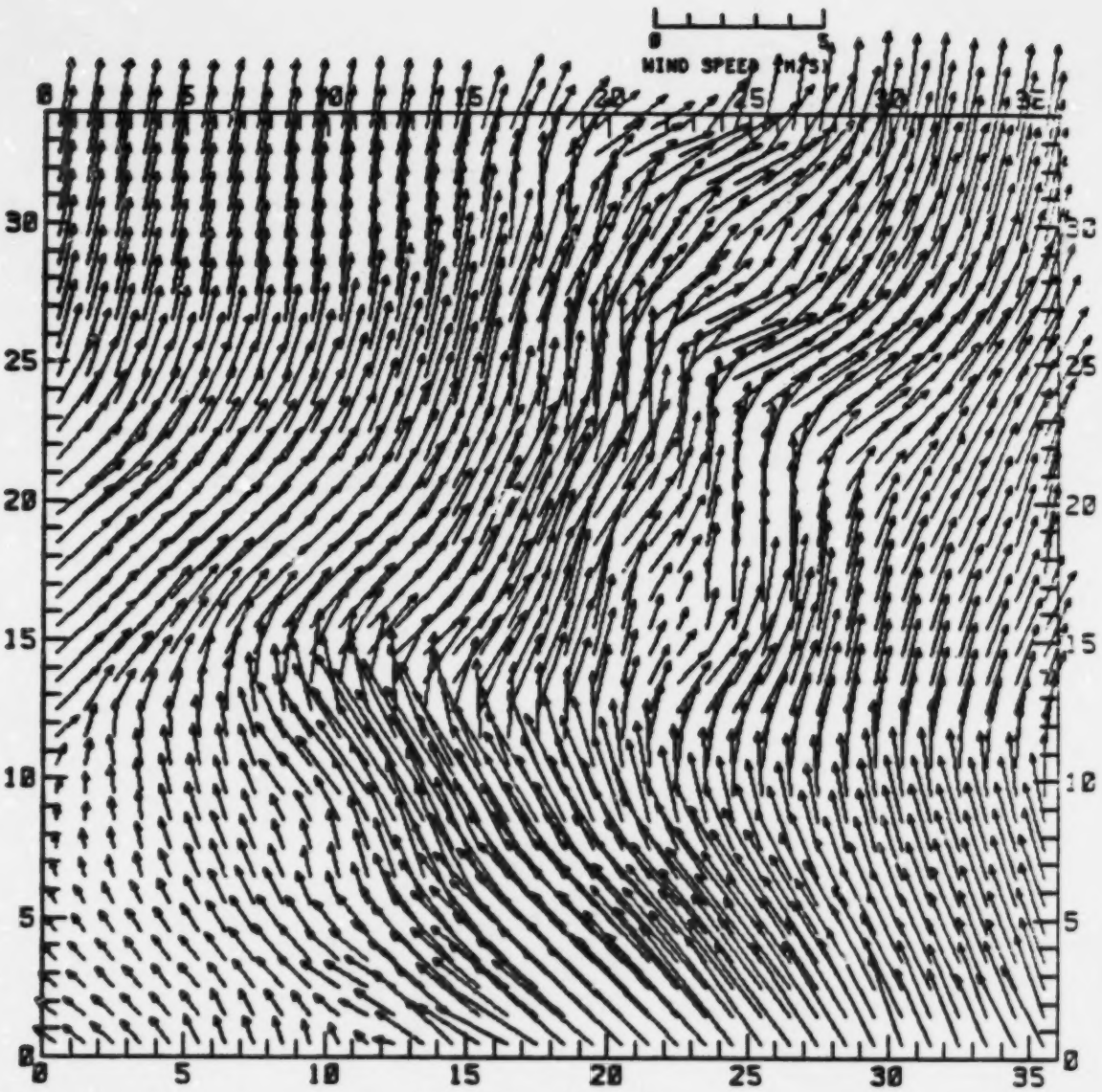

(d) 1800 - 1900 EST

FIGURE 3-11(concluded)

BEST COPY AVAILABLE

upper-level winds are not presented here, but are routinely examined for consistency before a UAM simulation is carried out.

BACKGROUND CONCENTRATIONS

Estimates of background concentrations at the top of the modeling region (for TOPCONC file), initial concentrations aloft (above mixing height-levels 3 and 4), and concentrations for all boundaries except those below the mixing height (levels 1 and 2 along the Southeast boundary) are presented in Table 3-3. Concentration values of NO, NO_2, CO, and hydrocarbons were specified on the basis of work by Killus (1982) to reflect concentrations of a typical urban atmosphere. Hydrocarbon speciation is that used in the Carbon-Bond Mechanism (Killus and Whitten, 1981). To represent an aged polluted atmosphere with a reservoir of ozone aloft, a value of 0.08 ppm for ozone was specified. This value was obtained from the ozone measurement at upwind monitoring sites during mid-morning when the surface-based inversion was dissipating. These stations included Brigantine, Lumberton, and Ancora, New Jersey. A background concentration of 0.000025 ppm peroxyacetylnitrate (PAN) was specified following the work performed by Singh and Hanst (1981).

INITIAL CONDITIONS

Initial conditions for all species were specified using all available monitoring data in the Philadelphia region. The simulation of 13 July commenced at midnight, requiring concentration values corresponding to this time. Rather than using the hourly averaged observed value for each species for the midnight hour, initial condition concentrations were calculated for each monitor by averaging the observed hourly average pollutant concentrations from 2300-2400 EST on 12 July with the 0000-0100 EST concentration on 13 July to obtain a two-hour average value for midnight. Initial condition concentrations used in the preparation of the AIRQUALITY file for 13 July are presented in Table 3-4 for 23 monitoring sites.

Because no carbon monoxide (CO) data were available at rural monitors on 13 July, background CO concentrations of 0.20 ppm were input at the Downington, Summit Bridge, and Van Hiseville monitors. Also, a CO concentration of 1.6 ppm at Ancora was eliminated because it was not considered representative of an outlying rural area, having possibly been the result of some local pollutant source. Also included in the table are the emission inventory reactive hydrocarbon (RHC) split factors used to compute initial concentrations of single-bond carbons (PAR), double-bond carbon groups (OLE), ethylene (ETH), aromatic rings (ARO), and carbonyl groups

BEST COPY AVAILABLE

TABLE 3-3. Background concentration values for 13 July at the top of the modeling region (TOPCONC), as initial concentrations above the mixing height, and for all levels of all boundaries except the levels below the mixing height on the Southeast boundary.

Species	Concentration (ppm)
NO	0.001
NO_2	0.002
O_3	0.08
CO	0.2
ETH	0.001
OLE	0.0004
PAR	0.040
CARB	0.010
ARO	0.0008
PAN	0.000025
BZA	0.00001

BEST COPY AVAILABLE

TABLE 3-4. Initial conditions for 13 July 1979 (concentrations in ppm).

Station	Easting (m)	Northing (m)	NO	NO_2	CO	O_3	RHC
AMS Lab.	491600	4428500	0.005	0.075	1.5	0.035	1.05
Ancora	511800	4392400	--	--	--	0.051	--
Brigantine	546000	4377506	--	--	--	0.037	--
Bristol	511000	4440000	--	--	--	0.000	--
Camden	491700	4419000	0.022	0.105	2.4	0.004	--
Chester	469000	4410000	--	0.030	--	0.058	2.10
Claymont	461500	4406400	--	0.045	--	--	--
Conshohocken	474500	4435600	--	--	--	0.000	--
Defense Support	483800	4418300	--	--	--	0.020	--
Downington	436000	4426000	0.002	0.012	0.2	0.073	0.00
Franklin Inst.	485200	4422800	0.010	0.065	--	0.035	--
Island Rd. Airp. Cir.	480300	4414800	--	--	--	0.010	--
Lumberton	518000	4423000	0.006	0.031	1.2	0.010	0.20
Norristown Armory	473500	4440000	--	0.075	--	0.000	0.39
Northeast Airp.	499000	4436000	0.035	0.060	--	0.000	--
Roxy Water Pump	479500	4433100	--	--	--	0.045	--
SE Sewage Plant	487200	4417300	--	--	--	0.010	--
South Broad	486100	4421600	0.020	0.080	3.5	0.035	0.30
Summit Bridge	441000	4376000	0.000	0.003	0.2	0.046	0.05
SW Corner Broad/Butler	487000	4428000	--	--	--	0.035	--
Trenton	520000	4452000	--	--	--	0.009	--
Van Hiseville	559000	4439500	0.001	0.006	0.2	0.005	--
Vineland	498200	4371200	--	0.024	--	0.054	--

RHC Component	Carbon-Bond Fraction (% as Carbon)
PAR	74.0
OLE	2.8
ETH	4.1
ARO	13.2
CARB	5.9

BEST COPY AVAILABLE

(CARB) as ppmC according to the Carbon-Bond Mechanism formulation. The observed total RHC observation value for each hour is multiplied by each splitting factor to obtain the speciated reactive hydrocarbon component as ppmC.

Initial conditions in surface grid cells without monitors were obtained by employing a Poisson interpolation. After this surface field was computed, a vertical interpolation method was chosen such that the background concentration at the top of the modeling region (TOPCONC) was used in levels 3 and 4, and the level 2 value was obtained by a linear interpolation between the surface (level 1) value and the level-3 value. Using this method, all grid cells in all levels were initialized with appropriate concentrations for all species before commencement of the simulation.

BOUNDARY CONDITIONS

The physical boundaries used in the 13 July simulation are presented in Figure 3-12. Because of the stagnation characteristics of this episode, much of the large airshed region was "blocked off" and not included in the simulation. No grid cells containing major emissions sources were excluded by this procedure. The winds were light and variable throughout much of the simulation day, so it was determined that a large portion of the grid need not be modeled. This procedure cut simulation costs, but did not hinder the analysis of the core of the urban ozone plume located to the north of the urban center.

Background values for all species were designated for all boundaries except the Southeast boundary below the mixing height. Because the Philadelphia region was dominated by a large, slow-moving high-pressure system on the days preceding the 13 July episode, stagnation and recirculation of urban oxidant precursors occurred. The wind flow on 12 July was light and westerly, with northerly flow established early on the 13th. By mid-morning (1000 EST), the flow had veered from a northerly to southeasterly direction, and continued south-southeasterly throughout the rest of the day. It is believed that the urban plume from Philadelphia was transported to the east late on 12 July and recirculated back toward the Philadelphia area by the moderate southeasterly flow on the 13th. This hypothesis is substantiated by an unusally high ozone reading of 13.9 pphm at 1200 EST at the Vineland monitor located 50 km to the southeast of Philadelphia. This advection of oxidant precursors from the previous day's emissions, along with the daily emissions and meteorological conditions conducive to ozone formation (e.g., lack of ventilation), led to high ozone levels on 13 July. Because the flow field for most of the daylight hours exhibited a southerly component, a different set of concentrations for the Southeast boundary grid cells below the mixing height was

BEST COPY AVAILABLE

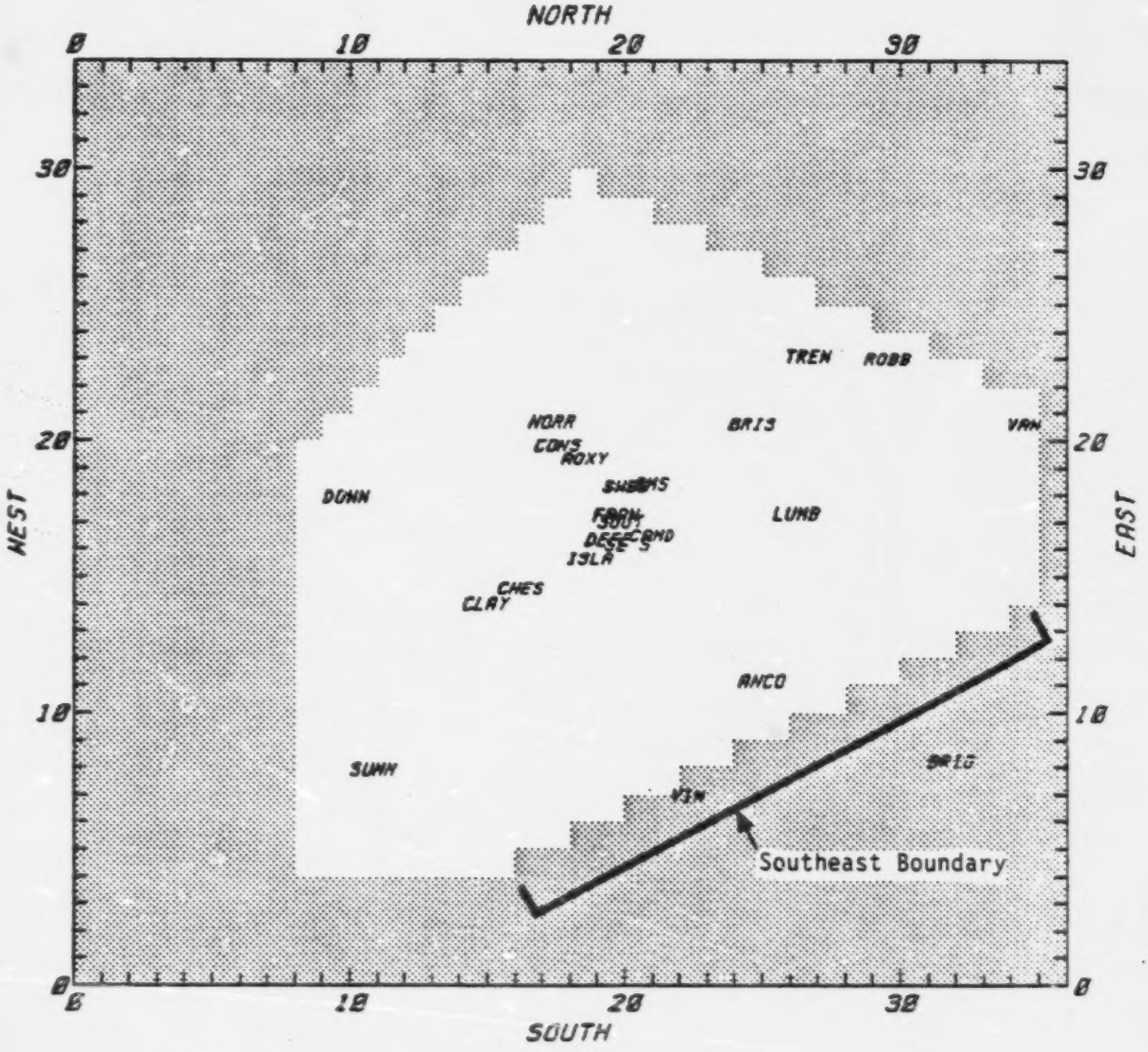

FIGURE 3-12. Physical boundaries used in the 13 July 1979 Airshed Model simulation (shaded area is not included in the simulation).

BEST COPY AVAILABLE

made to duplicate the inflow of aged air parcels containing ozone and precursors from the previous day's emissions.

For the Southeast boundary, the ozone concentrations on 13 July at the Vineland monitor, located on the designated Southeast boundary of the modeling region (see Figure 3-12), were used to obtain temporally varying ozone concentrations for the two vertical cells below the mixing height. Because of recirculation through the Southeast boundary, early morning (0000-0700 EST) NO, NO_2, and PAN concentrations for grid cells below the mixing height were obtained from late-afternoon measurements of these species at the Downington, Pennsylvania and Van Hiseville, New Jersey monitors when these sites were being influenced by the urban plumes. An early morning (0000-0700 EST) nonmethane hydrocarbon (NMHC) concentration of 0.15 ppmC was specified for cells below the mixing height, based on an analysis of data from other Northeast urban corridor cities under similar meteorological conditions (stagnation and carryover). The hydrocarbon species split of NMHC was chosen to represent an aged urban air mass as recommended by Killus (1982.).

The early morning (0000-0700) NO, NO_2, PAN, and other speciated NMHC concentrations were input to the CBM-III mechanism of the EKMA trajectory model, OZIPM (Whitten and Hogo, 1978) to simulate daytime (0700-1700) variation in these pollutant species due to chemistry. The resultant values of these pollutant species were used for temporally varying NO, NO_2, PAN, and other NMHC species concentrations for grid cells below the mixing height along the Southeast boundary, except that background concentrations were substituted for resultant concentrations below background values. The OZIPM kinetics model simulation produced a similar amount of ozone as recorded at the Vineland monitor, thus giving credence to these boundary condition species. The 1700 EST pollutant species concentrations were extended until 2400 EST. The concentration values used for the Southeast boundary below the mixing height for all species are given in Table 3-5.

EMISSION INVENTORY

The gridded minor point, area source, mobile source, and elevated point source emission inventory was prepared for the EPA in 1981 by Engineering Science, Inc. (EPA, 1982). (The boundary of the gridded inventory is shown in Figure 1-2.) Hourly (local daylight time) emission values for total NO_x and total hydrocarbon are presented in Table 3-6. Total daily emissions by source type are presented in Table 3-7 for NO, NO_2, and hydrocarbons. This table also gives the average hydrocarbon split for the entire emission inventory. The gridded spatial distribution of surface-layer hydrocarbon emissions is presented in Figure 3-13. The gridded spatial distribution of surface-layer NO_x emissions is presented in Figure 3-14; the bold line defines the area for which gridded emission estimates

BEST COPY AVAILABLE

TABLE 3-5. Southeast boundary conditions for cells below the mixing height for the simulation of 13 July 1979 (concentrations in ppm).

Time interval	NO	NO_2	O_3	PAR	OLE	ETH	ARO	CARB	PAN
0000-0100	0.001	0.009	0.053	0.1041	0.00105	0.0026	0.0021	0.0261	0.0040
0100-0200	0.001	0.009	0.041	0.1041	0.00105	0.0026	0.0021	0.0261	0.0040
0200-0300	0.001	0.009	0.037	0.1041	0.00105	0.0026	0.0021	0.0261	0.0040
0300-0400	0.001	0.009	0.036	0.1041	0.00105	0.0026	0.0021	0.0261	0.0040
0400-0500	0.001	0.009	0.028	0.1041	0.00105	0.0026	0.0021	0.0261	0.0040
0500-0600	0.001	0.009	0.010	0.1041	0.00105	0.0026	0.0021	0.0261	0.0040
0600-0700	0.001	0.009	0.021	0.1041	0.00105	0.0026	0.0021	0.0261	0.0040
0700-0800	0.001	0.007	0.035	0.0983	0.00065	0.0022	0.0017	0.0259	0.0044
0800-0900	0.001	0.004	0.072	0.0904	0.00040	0.0018	0.0012	0.0244	0.0054
0900-1000	0.001	0.002	0.102	0.0825	0.00040	0.0015	0.0008	0.0218	0.0062
1000-1100	0.001	0.002	0.111	0.0758	0.00040	0.0012	0.0008	0.0188	0.0062
1100-1200	0.001	0.002	0.121	0.0698	0.00040	0.0010	0.0008	0.0157	0.0058
1200-1300	0.001	0.002	0.139	0.0644	0.00040	0.0010	0.0008	0.0129	0.0052
1300-1400	0.001	0.002	0.113	0.0596	0.00040	0.0010	0.0008	0.0107	0.0047
1400-1500	0.001	0.002	0.105	0.0546	0.00040	0.0010	0.0008	0.0100	0.0040
1500-1600	0.001	0.002	0.093	0.0525	0.00040	0.0010	0.0008	0.0100	0.0037
1600-1700	0.001	0.002	0.069	0.0506	0.00040	0.0010	0.0008	0.0100	0.0032
1700-1800	0.001	0.002	0.068	0.0506	0.00040	0.0010	0.0008	0.0100	0.0032

BEST COPY AVAILABLE

TABLE 3-5 (Concluded).

Time interval	NO	NO_2	O_3	PAR	OLE	ETH	ARO	CARB	PAN
1800-1900	0.001	0.002	0.058	0.0506	0.0004	0.001	0.0008	0.010	0.0032
1900-2000	0.001	0.002	0.065	0.0506	0.0004	0.001	0.0008	0.010	0.0032
2000-2100	0.001	0.002	0.059	0.0506	0.0004	0.001	0.0008	0.010	0.0032
2100-2200	0.001	0.002	0.056	0.0506	0.0004	0.001	0.0008	0.010	0.0032
2200-2300	0.001	0.002	0.051	0.0506	0.0004	0.001	0.0008	0.010	0.0032
2300-2400	0.001	0.002	0.050	0.0506	0.0004	0.001	0.0008	0.010	0.0032

BEST COPY AVAILABLE

TABLE 3-6. Hourly emissions of NO_x and hydrocarbon (tons/hr) used in the 1979 Philadelphia emission inventory.

Hour (LDT)	Total NO_x	%	Total HC	%
0000 - 0100	23.413	2.50	17.255	1.42
0100 - 0200	21.070	2.25	15.090	1.24
0200 - 0300	19.886	2.13	12.413	1.02
0300 - 0400	19.712	2.11	11.777	0.97
0400 - 0500	20.461	2.19	11.444	0.94
0500 - 0600	24.625	2.63	14.422	1.18
0600 - 0700	33.658	3.60	25.677	2.11
0700 - 0800	53.234	5.70	81.214	6.67
0800 - 0900	53.623	5.74	94.468	7.76
0900 - 1000	49.794	5.33	89.978	7.39
1000 - 1100	50.629	5.42	89.809	7.37
1100 - 1200	51.720	5.53	84.016	6.90
1200 - 1300	46.660	4.99	77.34	6.35
1300 - 1400	50.451	5.40	75.132	6.17
1400 - 1500	51.662	5.53	75.917	6.23
1500 - 1600	54.883	5.87	81.869	6.72
1600 - 1700	58.815	6.29	74.434	6.11
1700 - 1800	52.584	5.63	67.097	5.51
1800 - 1900	42.650	4.56	56.362	4.63
1900 - 2000	35.866	3.84	39.228	3.22
2000 - 2100	32.448	3.47	35.537	2.92
2100 - 2200	30.728	3.29	33.102	2.72
2200 - 2300	29.480	3.15	31.363	2.58
2300 - 2400	26.664	2.85	22.956	1.88
Total (tons/day)	934.718	100.0	1217.897	100.0
Total (tons/year)	341,172.000		444,532.000	

BEST COPY AVAILABLE

TABLE 3-7. Total daily emissions by source type (g-mole) in the 1979 Philadelphia inventory.

Source	NO	NO_2	ETH	OLE	PAR	CARB	ARO
Elevated Point	5,738,955	257,086	12,144	7,792	901,823	570,765	139,960
Minor Point	2,041,679	114,837	385,284	183,632	15,846,729	818,880	510,799
Area Source	2,705,097	207,808	295,258	194,471	26,841,693	1,669,555	491,833
Mobile Source	6,646,688	738,496	827,355	664,553	11,635,952	1,337,697	495,926
Total	17,132,419	1,318,227	1,520,041	1,050,448	55,226,197	4,396,897	1,638,518

Total HC = 63,832,101 Total NO_x = 18,450,646

Philadelphia Hydrocarbon Splits

Species	Carbon-Bond Fraction (% as Carbon)
PAR	74.0
OLE	2.8
ETH	4.1
ARO	13.2
CARB	5.9

BEST COPY AVAILABLE

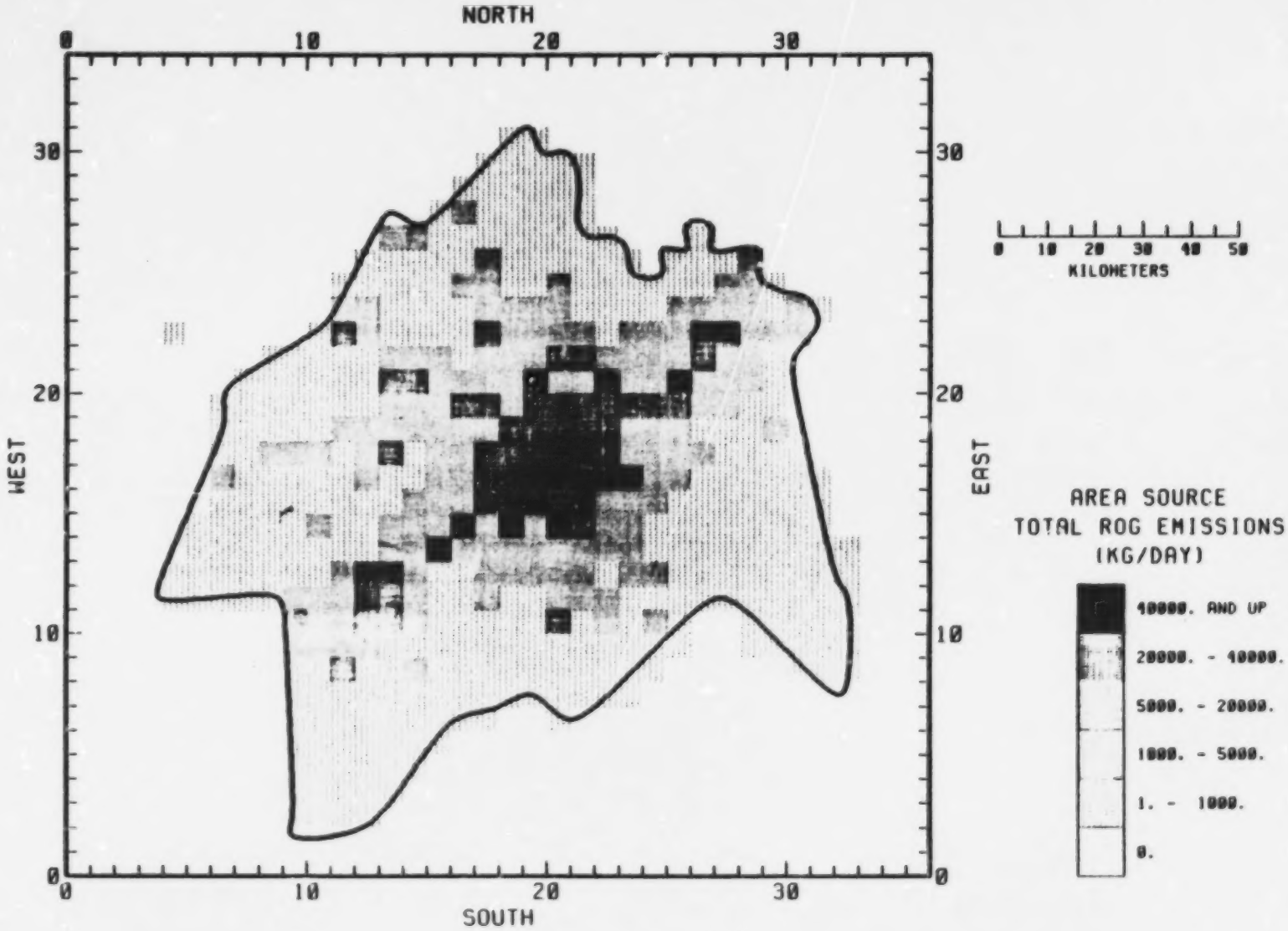

FIGURE 3-13. Surface layer total hydrocarbon emissions for the Philadelphia airshed region for 1979.

BEST COPY AVAILABLE

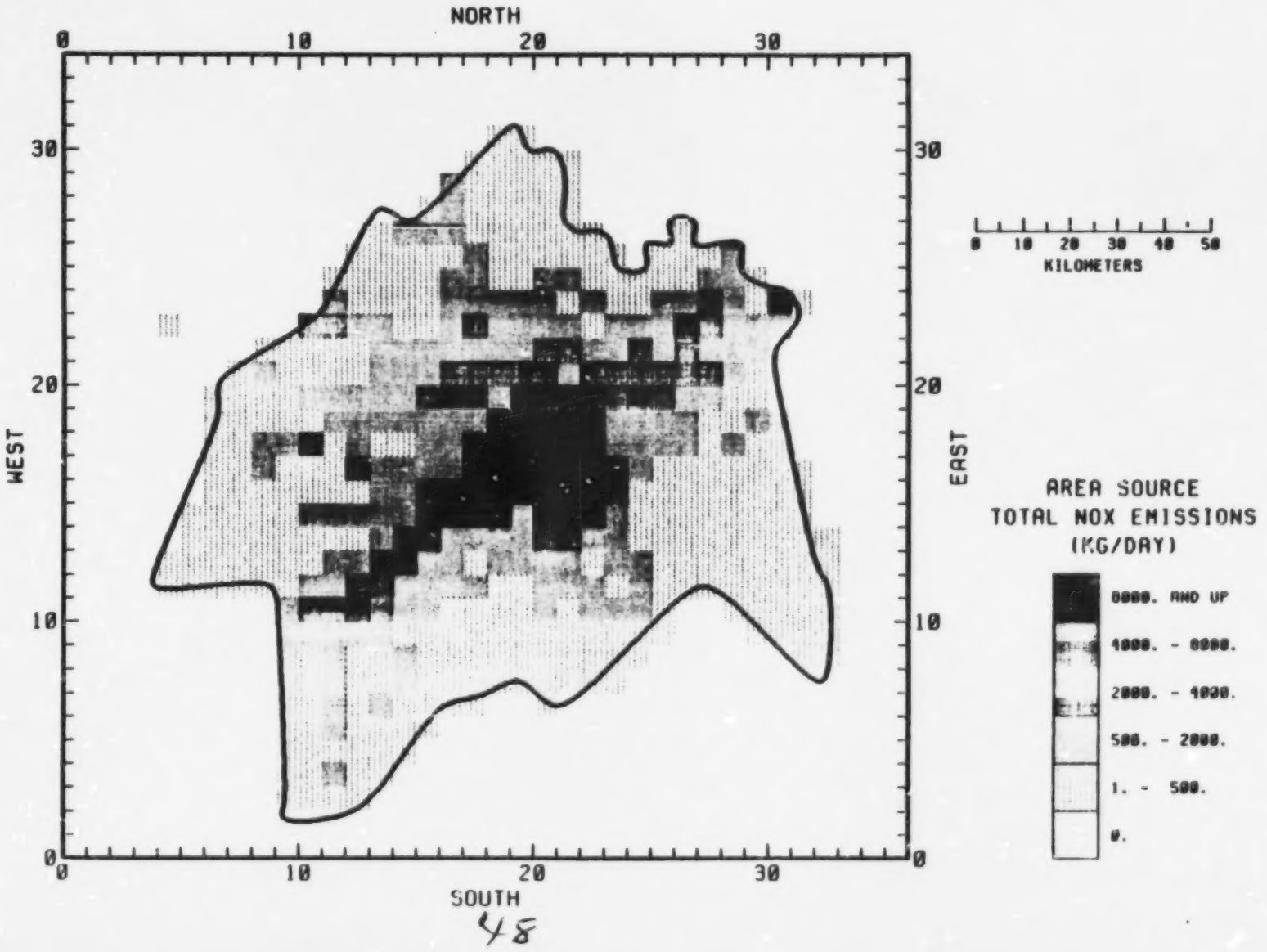

BEST COPY AVAILABLE

48

FIGURE 3-14. Surface layer total NO_x emissions for the Philadelphia airshed region for 1979.

were available for the 1979 inventory (the Philadelphia AQCR). Emission estimates contained in the inventory and used in the simulation represent a typical summer weekday in 1979.

METSCALARS

The term "metscalars" refers to those model inputs that are considered spatially invariant across the modeling region. Metscalars include the region-wide average temperature gradient below the mixing height, the average temperature gradient above the mixing height, the exposure class (related to the degree of boundary-layer thermal stratification), and the radiation factor (related to the NO_2 photolysis rate).

The hourly temperature gradient above and below the inversion was specified after examining the available temperature soundings for 13 July 1979. Radiosonde data from JFK and Dulles airports at 1900 EST, 12 July; 0700 and 1900 EST, 13 July; and 0700, 14 July were used. To obtain the temperature gradients, a simple procedure was followed. The vertical temperature profile was plotted graphically (temperature versus height) for each sounding. Using the hourly specified mixing height, an average temperature gradient was subjectively drawn from the surface to the top of the mixed layer. This average temperature gradient was also obtained for the layer above the mixing height to the top of the modeling region using the same procedure. The temperature gradients thus obtained were the result of examining data from multiple soundings near the region. Specific hourly values for the temperature gradients above and below the mixing height were obtained by averaging the two sets of sounding data. For the temperature gradient above, the data showed a nearly neutral atmosphere for the entire day with a value of -0.006°K/m specified for all hours. The data showed a nearly adiabatic atmosphere below the mixing height for the entire day, with a temperature gradient of -0.01°K/m specified for the daylight hours. For nighttime hours, a value of 0.0°K/m was specified to reflect a slightly stable rather than adiabatic atmosphere.

As detailed in Ames et al. (1978), the exposure class is a measure of near ground-level stability due to surface heating or cooling and can be estimated from insolation as follows:

$$\text{exposure class} = \begin{cases} 3, \text{strong} \\ 2, \text{moderate} \\ 1, \text{slight} \end{cases} \text{daytime insolation}, \quad \begin{cases} 0, \text{heavy overcast} \end{cases} \text{day or night}, \quad \begin{cases} -1, \geq \frac{4}{8} \text{ cloud cover} \\ -2, \leq \frac{3}{8} \text{ cloud cover} \end{cases} \text{nighttime cloudiness.}$$

BEST COPY AVAILABLE

The exposure class categories chosen for each hour were specified after reviewing the available meteorological data including surface temperatures, solar radiation data, and synoptic weather summaries for 13 July.

A computer program developed by Schere and Demerjian (1977) was used to calculate layer-averaged NO_2 photolysis rate constants based on month, day, year, latitude, longitude, time zone, time of day, mixing height, and measured solar radiation data. The first seven parameters were used to calculate zenith angles and corresponding clear sky theoretical surface NO_2 photolysis rate constants. The mixing heights, along with the parameters used to calculate clear sky theoretical surface NO_2 pnotolysis rate constants, were used in the calculation of clear sky theoretical layer-averaged NO_2 photolysis rate constants. The methodology used to determine the clear sky theoretical surface and layer-averaged NO_2 photolysis rate constants is described by Demerjian et al. (1980). The total measured solar radiation data in langley/min was multiplied by the constant 0.40 min^{-1} min/langley derived by Jeffries et al. (1982) to convert the solar radiation data to empirical surface NO_2 photolysis rate constants (min^{-1}). The empirical layer-averaged NO_2 photolysis rate constant was calculated by the following equation:

$$\text{Empirical layer-averaged } NO_2 \text{ photolysis rate constant} = \frac{\text{Empirical surface } NO_2 \text{ photolysis rate constant}}{\text{Clear sky theoretical surface } NO_2 \text{ photolysis rate constant}} \times \text{Clear sky theoretical layer-averaged } NO_2 \text{ photolysis rate constant}$$

Because dewpoint values were in tne upper 60s to lower 70s throughout the region for the entire day, a constant of 24000 ppm was designated for the concentration of water. Atmospheric pressure throughout the region ranged from 1010 to 1013 mb as measured by the surface stations of Philadelphia (PHL) and radiosonde data from JFK and Dulles airports. On the basis of these measurements, a constant value of 1.0 atm was specified for atmospheric pressure for all hours of the simulation day. The complete set of inputs used in the METSCALARS file for 13 July 1979 is contained in Table 3-8.

BEST COPY AVAILABLE

TABLE 3-8. METSCALAR file for the 13 July 1979 airshed simulation.

Hour (EST)	Temp. Gradient (°K/m) Above	Below	Exposure Class	NO_2 Photolysis Rate (RADFACTOR)	Water Concentration (ppm)	Atmospheric Pressure (atm)
0000-0100	-0.006	-0.000	0	--	24,000	1.0
0100-0200	-0.006	-0.000	0	--	24,000	1.0
0200-0300	-0.006	-0.000	0	--	24,000	1.0
0300-0400	-0.006	-0.000	0	--	24,000	1.0
0400-0500	-0.006	-0.000	0	0.005	24,000	1.0
0500-0600	-0.006	-0.010	1	0.067	24,000	1.0
0600-0700	-0.006	-0.010	1	0.150	24,000	1.0
0700-0800	-0.006	-0.010	1	0.264	24,000	1.0
0800-0900	-0.006	-0.010	2	0.404	24,000	1.0
0900-1000	-0.006	-0.010	2	0.512	24,000	1.0
1000-1100	-0.006	-0.010	2	0.543	24,000	1.0
1100-1200	-0.006	-0.010	3	0.550	24,000	1.0
1200-1300	-0.006	-0.010	3	0.547	24,000	1.0
1300-1400	-0.006	-0.010	3	0.479	24,000	1.0
1400-1500	-0.006	-0.010	3	0.393	24,000	1.0
1500-1600	-0.006	-0.010	3	0.263	24,000	1.0
1600-1700	-0.006	-0.010	2	0.095	24,000	1.0
1700-1800	-0.006	-0.010	2	0.027	24,000	1.0
1800-1900	-0.006	-0.000	1	0.015	24,000	1.0
1900-2000	-0.006	-0.000	1	--	24,000	1.0
2000-2100	-0.006	-0.000	0	--	24,000	1.0
2200-2300	-0.006	-0.000	0	--	24,000	1.0
2300-2400	-0.006	-0.000	0	--	24,000	1.0

BEST COPY AVAILABLE

TERRAIN

The terrain of the modeling region was classified according to land-use values estimated while compiling the emission inventory (EPA, 1982). For grid squares not contained in the emission inventory region, land-use classifications were obtained from a United States Geological Survey (USGS) map with a 1:250,000 scale. Each land-use category was assigned a surface roughness value and an estimate of surface uptake velocity (vegetation factor) according to Wesely (1983) (Table 3-9). Land-use classification by grid cells for the Philadelphia modeling region is presented in Figure 3-15.

BEST COPY AVAILABLE

TABLE 3-9. Surface roughness and vegetation factor values.

Land-Use Category	Surface Roughness (m)	Surface Resistance (s/cm)	Uptake Velocity (cm/s)	Vegetation Factor
Mixed Grassland and Cropland	0.10	1.0	1.0	1.0
Deciduous Forest	1.0	0.6	1.7	1.7
Coniferous Forest	1.0	1.5	0.7	0.7
Urban Area	1.0	3.0	0.3	0.3
Ocean Water	0.001	20	0.05	0.05

BEST COPY AVAILABLE

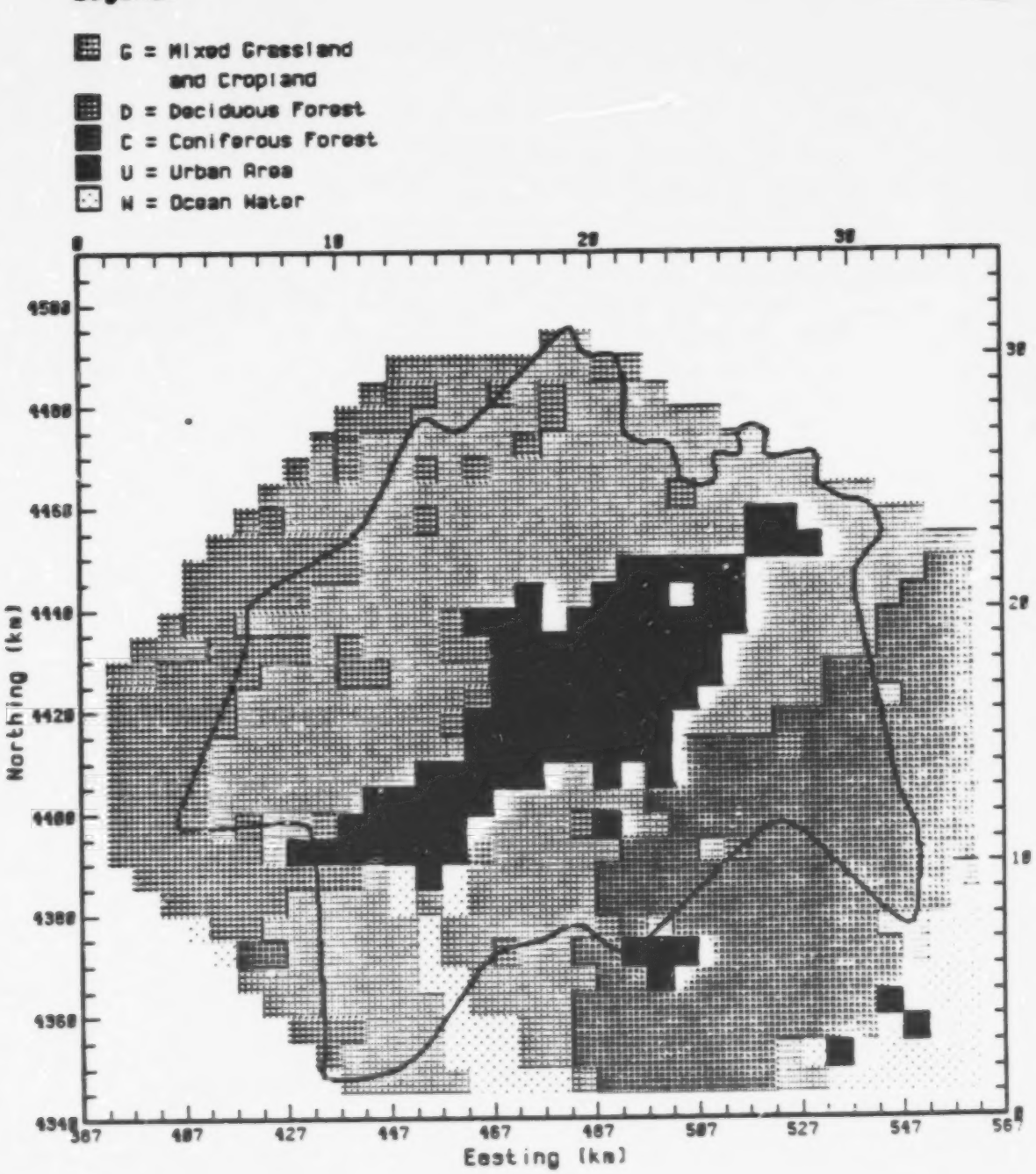

FIGURE 3-15. Land-use classifications for the Philadelphia airshed modeling region.

BEST COPY AVAILABLE

4 CHARACTERIZATION OF THE 19 JULY 1979 OZONE EPISODE

The second-highest peak ozone readings in the Philadelphia AQCR during the 1979 summer oxidant data enhancement study occurred on Thursday, 19 July (Allard et al., 1981). On this day, the Philadelphia urban plume was transported to the west of the central city and precursor transport from the New York/New Jersey urban area was the apparent cause of a substantial portion of the ozone concentrations measured in the Philadelphia area.

A broad high-pressure area extending from the midwest through the northeast to Nova Scotia influenced surface wind patterns. The eastern core of this high-pressure area was situated to the north of Philadelphia in the early morning hours, bringing light northerly winds through the airshed (see Figure 4-1). This high-pressure ridge moved eastward throughout the day. As a result, the surface winds veered to an easterly direction around noon and then to a southeasterly flow that persisted the rest of the day. Winds aloft showed a persistent west-southwesterly flow during the entire day. Surface trajectory analysis indicated that air parcels arriving in the urban center of Philadelphia at 1200 EST originated to the northeast in the New Jersey/New York urban area.

The peak ozone concentration recorded on 19 July 1979 was 17.0 pphm at the Roxy Water Pump monitoring station, 10 km northeast of central Philadelphia. An ozone reading of 16.0 pphm was also recorded at Downington, 45 km due west of downtown Philadelphia. Six monitors recorded ozone concentrations equal to, or greater than, 12 pphm; an additional four monitors recorded ozone concentrations greater than, or equal to, 10 pphm.

BEST COPY AVAILABLE

FIGURE 4-1. Synoptic situation, 0700 EST, 19 July 1979. (Source: Allard et al., 1981).

BEST COPY AVAILABLE

5 DESCRIPTION OF MODEL INPUTS FOR 19 JULY 1979

This section describes the preparation of the UAM input files for the 19 July 1979 episode. The area source emissions, elevated point source, top of region, and terrain files prepared for the 13 July 1979 simulation were not day-specific. Only the internal date was changed in these files before they were used in the UAM simulation for 19 July; therefore, they are not described in this section. The modeling region specified for 19 July 1979 was that used in the 13 July 1979 simulation (see Section 3). However, different boundaries were defined for the 19 July 1979 simulation (see Figure 5-8).

MIXING HEIGHTS

The hourly averaged mixing height values were estimated using available radiosonde observations and sodar data for the Philadelphia area. The radiosondes were released in downtown Philadelphia; the sodar was located at Summit Bridge, Delaware. An example of temperature sounding data for 19 July 1979 is given in Figure 5-1. Both urban and rural mixing heights were specified on the half hour beginning at midnight. The following procedures were used in specifying the mixing heights used in the simulation:

Urban mixing heights from 0500 through 1500 EST were estimated using vertical potential temperature profiles obtained from Philadelphia upper-air soundings. For each hour, the mixing height was considered to be at the base of the layer in which the potential temperature increased rapidly with height. Upper-air sounding data were available from the urban site for 0500, 0714, 0937, 1150, and 1500 EST. For hours between soundings, potential temperature profiles were obtained by interpolation;

Urban mixing heights between 0000 and 0500 EST were set at the value estimated from the 0500 EST sounding;

The data indicate that the maximum mixing height was reached at 1200 EST. Urban mixing heights following the time of the 1500 EST sounding were determined by decreasing the mixing height at a rate of ~2-3 m/min (Noonkester, 1976; Kaimal, et al., 1982) to reach the 250-m overnight default value by 2100 EST.

BEST COPY AVAILABLE

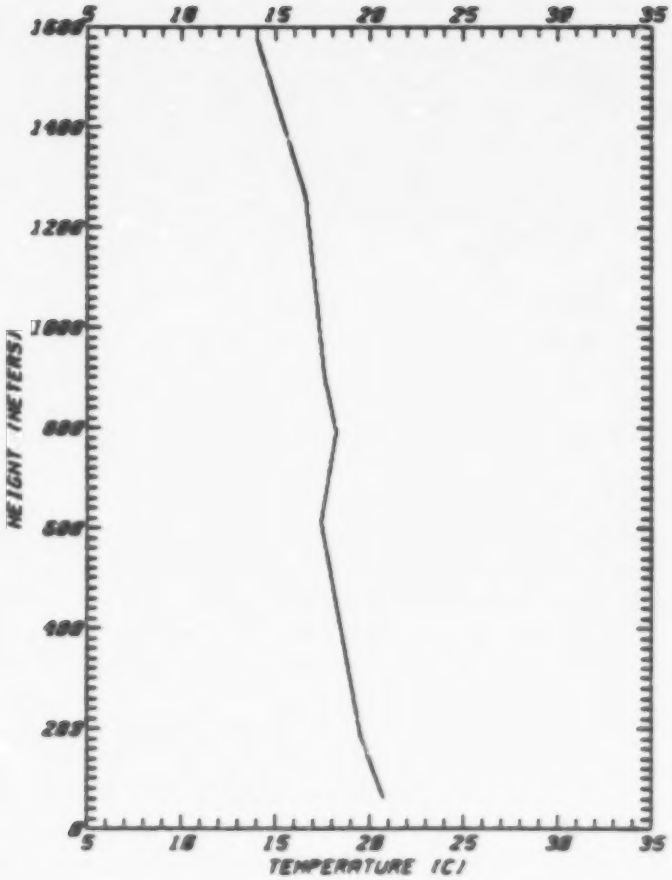

FIGURE 5-1. Temperature sounding for Philadelphia, 0410 EST, 19 July 1979.

BEST COPY AVAILABLE

Rural mixing heights between 0700 and 1100 EST were estimated from sodar data measured at Summit Bridge, Delaware. Until 0700 and after 1800 EST, the rural mixing heights were held at the 100-m overnight default value used for 13 July. Between 1100 and 1700 EST, when the mixing height exceeded the vertical range of the sodar, rural mixing heights were set at 100 m below the mixing heights estimated from urban soundings (Spangler et al., 1974).

The resulting mixing height values for both urban and rural grid cells for 19 July are presented in Table 5-1. A graphical representation of the temporal increase and subsequent decrease in the mixing depth layer for both urban and rural cells is presented in Figure 5-2.

WIND FIELD

For the 19 July 1979 episode, surface wind measurements were available for 16 stations. Gridded surface wind fields used with the Urban Airshed Model were prepared following the same procedure as that for the 13 July 1979 simulation day (see Section 3). The observed surface wind pattern for three hours during the day is presented in Figure 5-3. Pseudostations were placed in the same locations as for the 13 July application, and data were specified to make the interpolation produce a spatially and temporally consistent flow field. The surface winds veered from a light northeasterly direction in the morning to a consistent southeasterly direction with moderate speeds by late afternoon. Also included in Figure 5-3 are the actual vectors used in the interpolation of the surface wind field. This figure shows those vectors that were changed and also data ed to fill gaps for the interpolated field.

Because of the availability of upper-air data within the airshed region on this day, the procedure used for specifying winds in levels 2, 3, and 4 differed from that used for the upper-level winds for 13 July. Radiosonde or pibal wind measurements were available for three sites: Wilmington, Delaware, Downtown Philadelphia, and Trenton, New Jersey. These data were plotted graphically for review purposes. Figures 5-4, 5-5, and 5-6 present measured winds aloft up to 3250 m above Wilmington, Downtown Philadelphia, and Trenton, respectively for 1200 EST on 19 July. The data plotted in these figures show a light surface flow (2 to 4 m/s) in a general southeasterly direction, while the wind speeds aloft (1250 to 3000 m) were moderate with a general westerly direction. All available upper-level wind data were plotted in this manner and utilized to estimate specific hourly inputs for each level. After the data were examined, a constant average wind vector was obtained for each hour for levels 2, 3, and 4.

BEST COPY AVAILABLE

TABLE 5-1. Urban and rural mixing height values used in the DIFFBREAK file for 19 July 1979.

Time (EST)	Urban (m)	Rural (m)
0000	190	100
0030	190	100
0100	190	100
0130	190	100
0200	190	100
0230	190	100
0300	190	100
0330	190	100
0400	190	100
0430	190	100
0500	190	100
0530	190	100
0600	190	100
0630	190	100
0700	190	100
0730	240	260
0800	350	440
0830	460	490
0900	600	540
0930	740	560
1000	890	580
1030	1060	630
1100	1240	880
1130	1420	1320
1200	1530	1430
1230	1530	1430
1300	1480	1380
1330	1410	1310
1400	1340	1240
1430	1270	1170
1500	1200	1100
1530	1120	1020
1600	1020	920
1630	940	840
1700	850	750
1730	750	480
1800	660	160
1830	570	100
1900	480	100
1930	410	100
2000	340	100
2030	300	100
2100	250	100
2130	250	100
2200	250	100
2230	250	100
2300	250	100
2330	250	100
2400	250	100

BEST COPY AVAILABLE

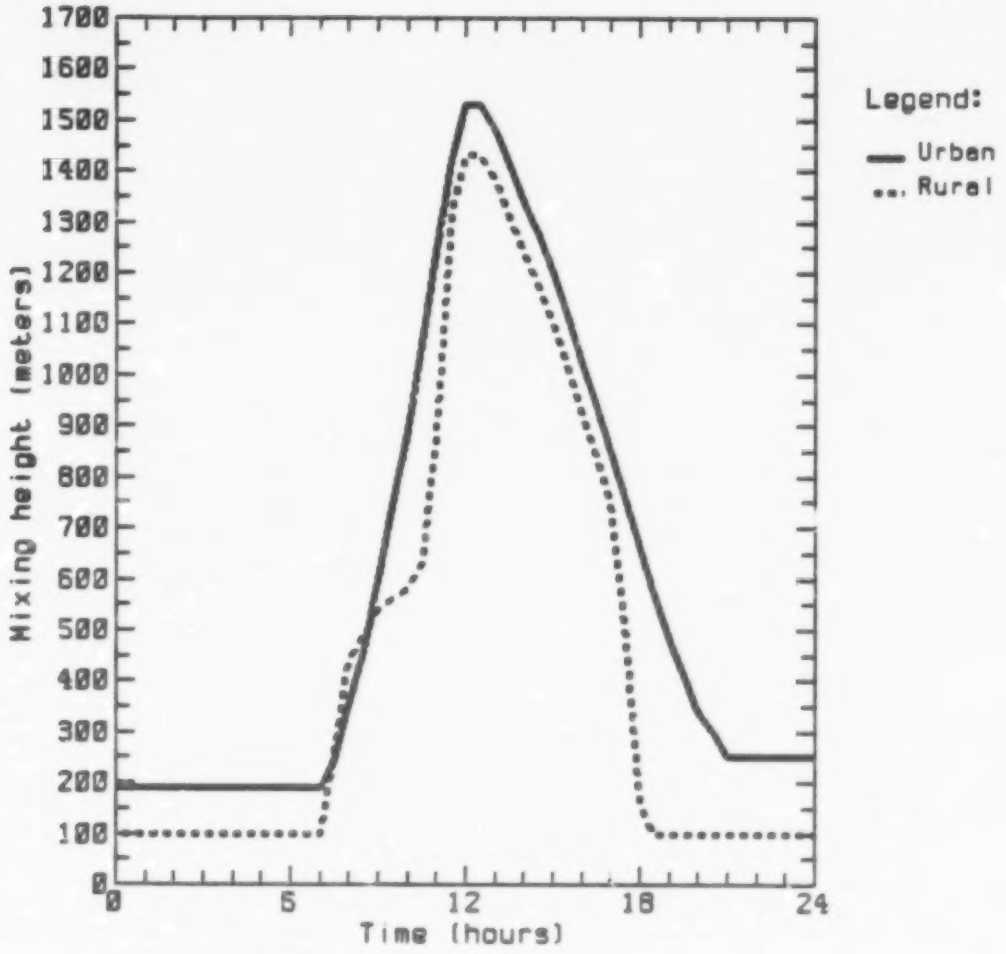

FIGURE 5-2. Mixing height profiles for urban and rural cells on 19 July 1979.

BEST COPY AVAILABLE

FIGURE 5-3. Observed surface wind vectors and wind vectors used in preparing the interpolated surface wind field for 19 July 1979.

BEST COPY AVAILABLE

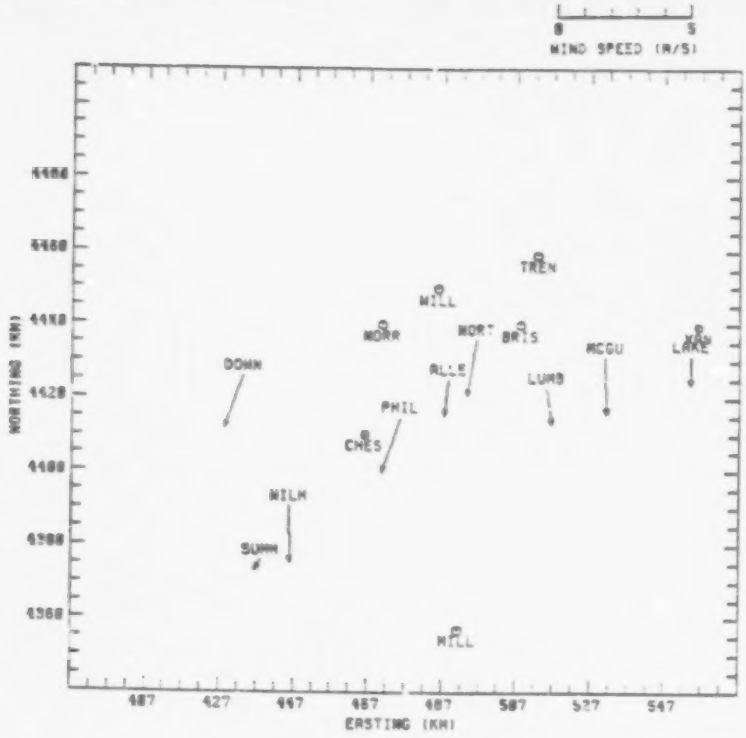

Observed wind vectors

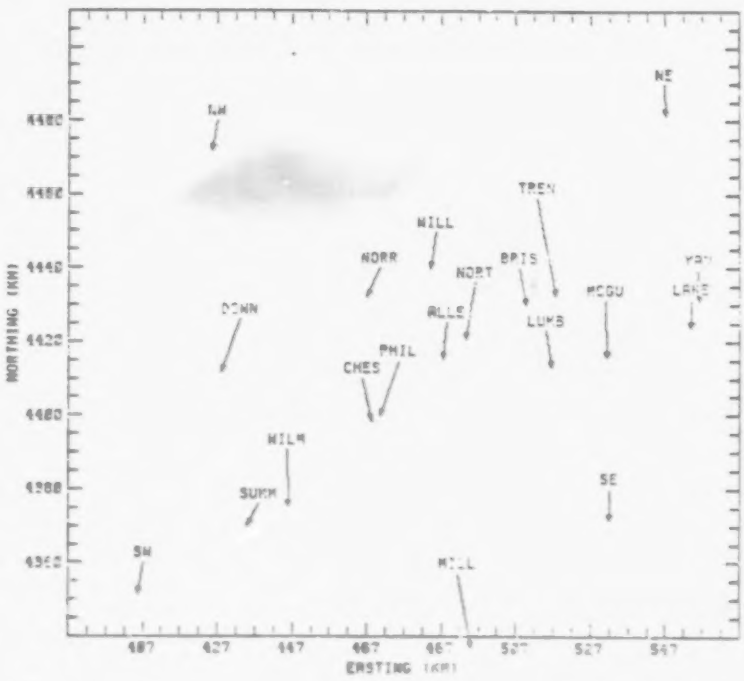

Wind vectors used in preparing model input wind fields for surface layer.

FIGURE 5-3a. 0400-0500 EST

BEST COPY AVAILABLE

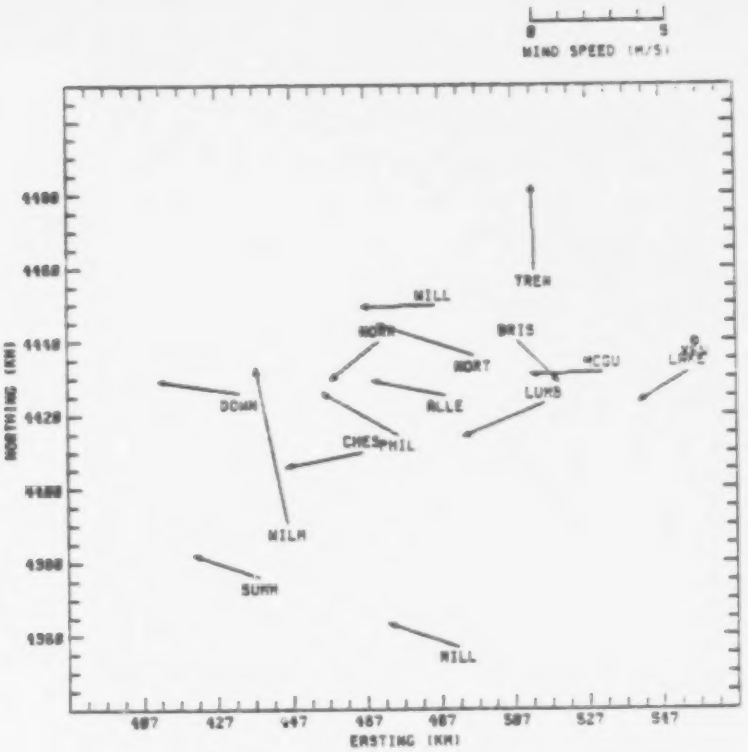

Observed wind vectors

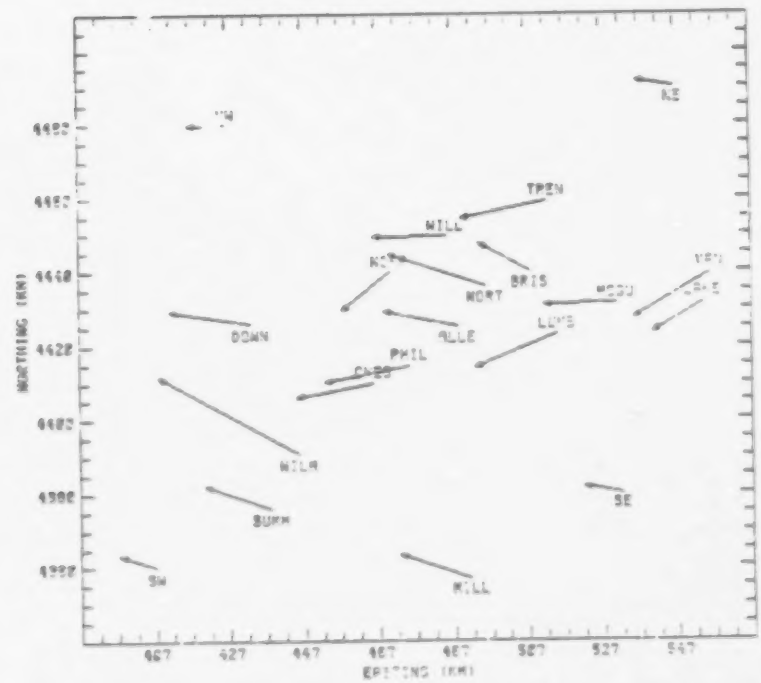

Wind vectors used in preparing model input wind fields for surface layer.

FIGURE 5-3b. 1200-1300 EST

BEST COPY AVAILABLE

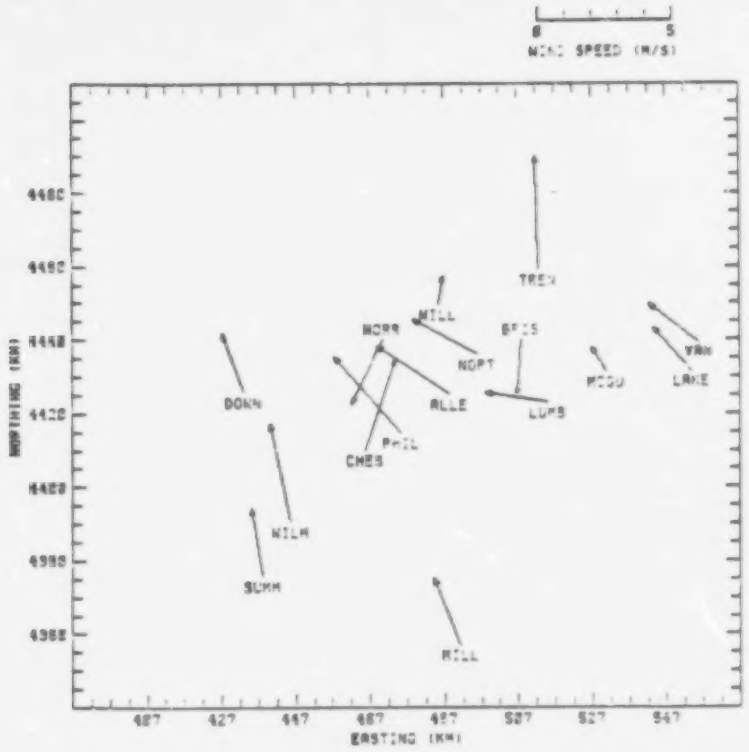

Observed wind vectors

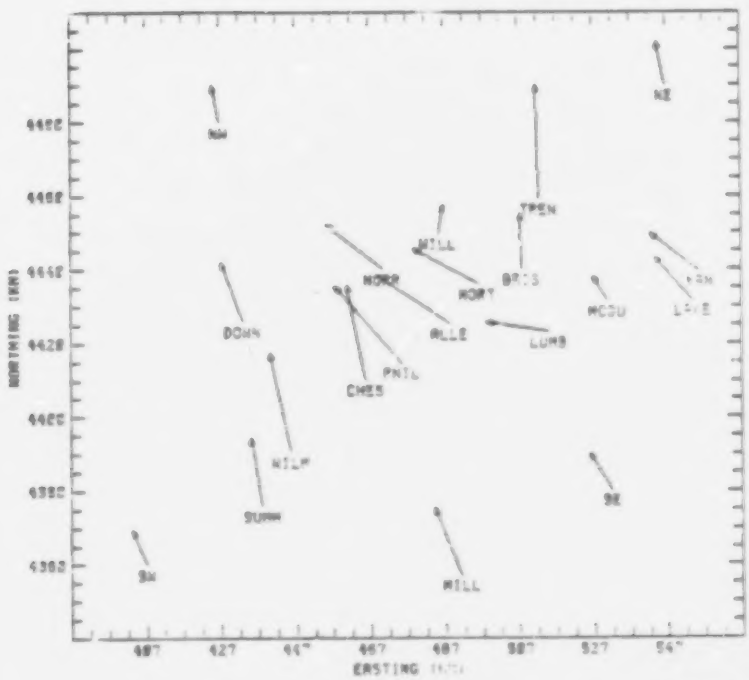

Wind vectors used in preparing model input wind fields for surface layer.

FIGURE 5-3c. 1800-1900 EST

BEST COPY AVAILABLE

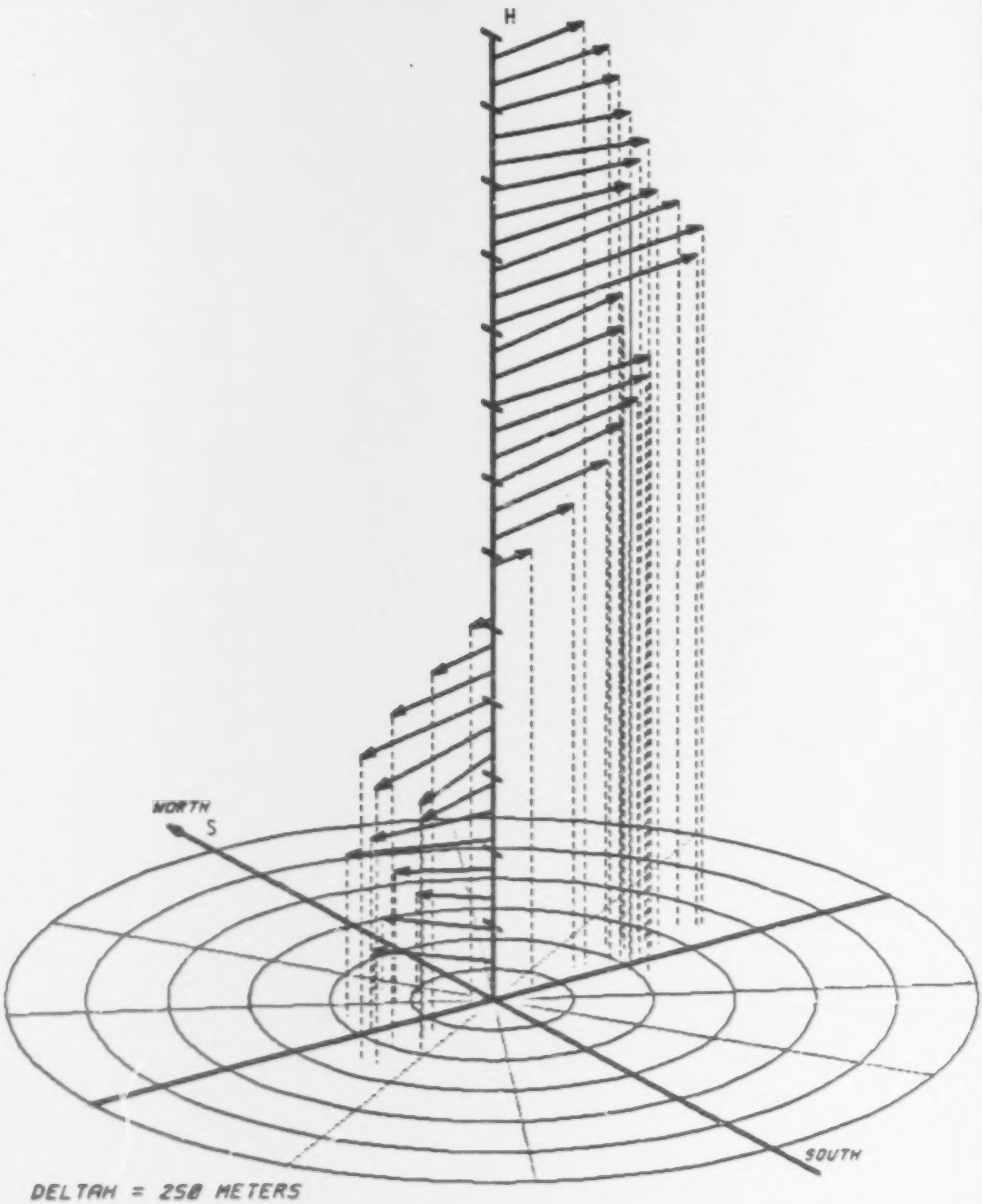

FIGURE 5-4. Pibal sounding at Wilmington, Delaware on 19 July 1979, 1200 EST.

BEST COPY AVAILABLE

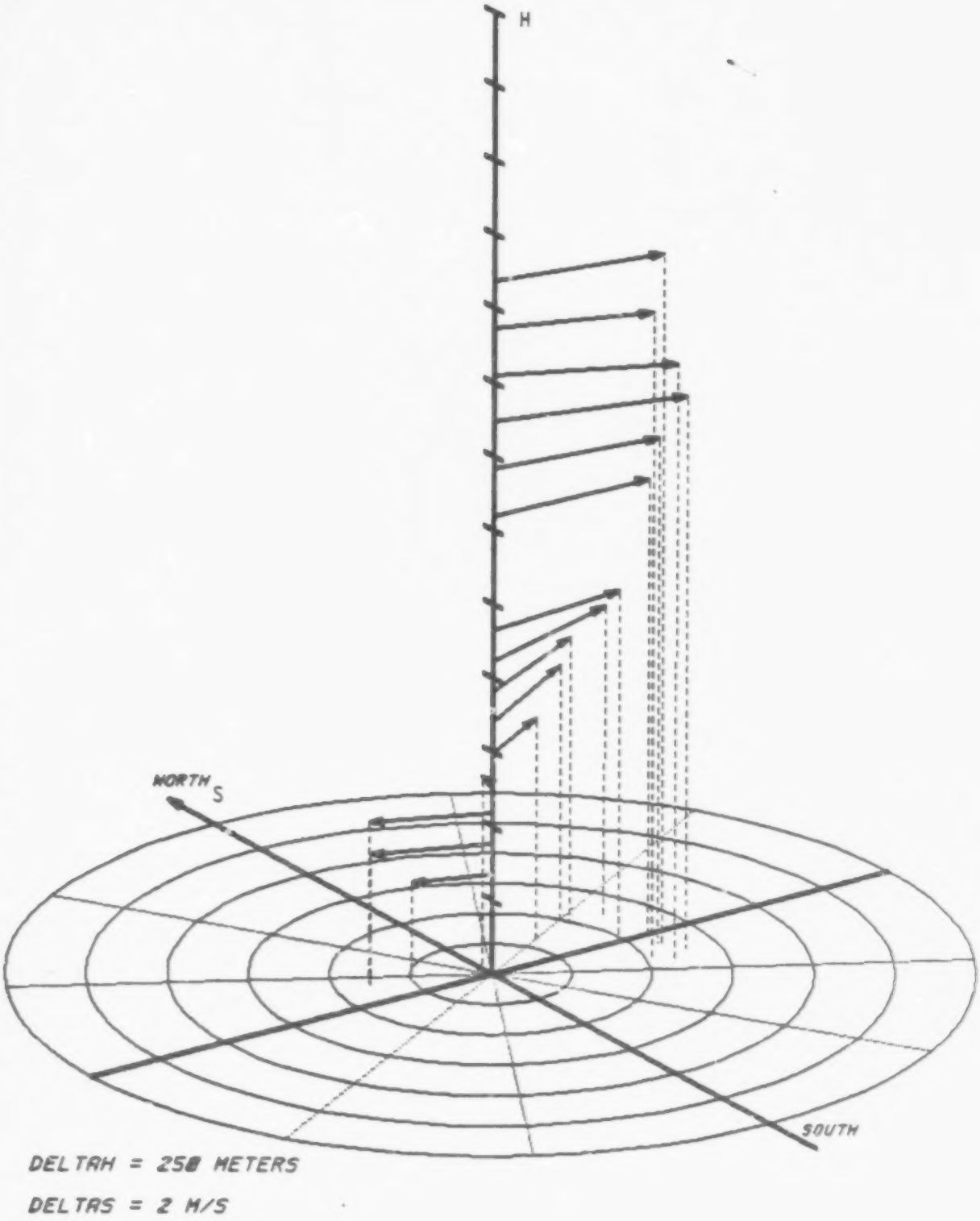

FIGURE 5-5. Pibal sounding at Philadelphia, Pennsylvania on 19 July 1979, 1150 EST.

BEST COPY AVAILABLE

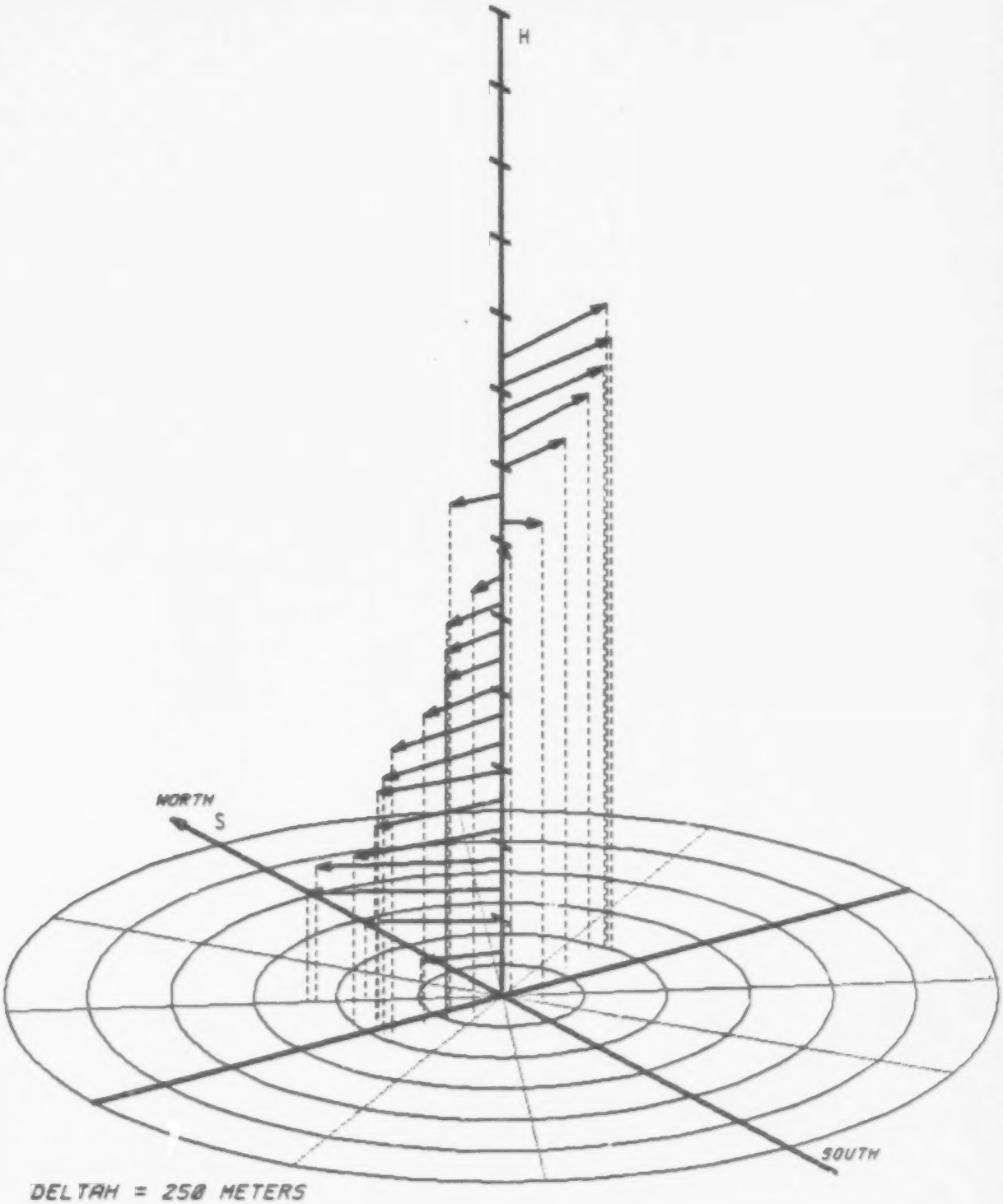

FIGURE 5-6. Pibal sounding at Trenton, New Jersey on 19 July 1979, 1200 EST.

BEST COPY AVAILABLE

The preparation of inputs for upper-level winds involved the following steps:

For the hours of 0500 through 1600 EST, layer-average wind speed (arithmetic average) and wind direction (predominant direction) values were obtained for each of the three layers from the rawinsonde sounding and pibal observations. Linear interpolation was used for estimating winds for hours without upper-air measurements during this period.

For the hours of 0000 through 0400 EST, layer-average wind speeds and wind directions were obtained by interpolation between upper-air winds from the Washington, D.C. NWS sounding at 1900 EST on July 18 and the Philadelphia sounding at 0500 EST on July 19.

For hours after 1600 EST, winds in layers 3 and 4 were held constant using the 1600 EST values. In layer 2, winds were held constant through 1800 EST using the 1600 EST values. After 1800 EST, layer 1 winds were used for layer 2.

A complete list of spatially constant, temporally varying wind inputs for layers 2, 3, and 4 is presented in Table 5-2. The intermediate step for completing the three-dimensional wind field involved the use of the interpolated surface field, and the program WINDCHANG. This program reads the gridded surface field and input data presented in Table 5-2 to create the three-dimensional wind file. As was done for the 13 July wind file, this three-dimensional field was rendered nearly free of divergence by running it through the DIVFREE program. The completed, divergence-free wind file was then plotted on the airshed grid and inspected for consistency. The surface flow field used in the simulation is plotted for three hours in Figure 5-7, and clearly depicts the northeasterly-to-southeasterly shift in wind direction through the day.

BACKGROUND CONCENTRATIONS

Values used for 19 July background concentrations are the same as those used in the 13 July simulation except for the ozone background value. On the basis of examination of upwind monitoring data at the time of mixing, the value specified for ozone above the mixing height was 0.06 ppm. This represents a decrease from the 0.08 ppm used in the 13 July stagnation simulation. Table 5-3 lists the background concentrations used at the top of the modeling region, as initial concentrations above the mixing height and for all boundaries above the mixing height. Below the mixing height, for all boundaries except the Northeast and East boundaries, an ozone

BEST COPY AVAILABLE

TABLE 5-2. Estimated spatially constant, temporally varying wind input for levels 2, 3, and 4 for the 19 July 1979 wind file.

	Level 2		Level 3		Level 4	
Hour (EST)	Wind Speed (m/s)	Wind Direction (Degrees)	Wind Speed (m/s)	Wind Direction (Degrees)	Wind Speed (m/s)	Wind Direction (Degrees)
0000-0100	2.0	30	5.5	30	5.0	350
0100-0200	2.0	40	5.5	40	4.5	350
0200-0300	2.0	50	5.5	50	4.5	345
0300-0400	2.5	50	5.5	50	4.0	345
0400-0500	3.0	55	5.5	50	4.0	345
0500-0600	3.0	55	5.5	50	4.0	345
0600-0700	2.5	50	6.0	55	4.5	10
0700-0800	2.5	40	6.0	55	5.0	30
0800-0900	5.0	55	7.4	60	6.0	30
0900-1000	4.5	75	6.0	75	4.0	35
1000-1100	4.0	90	5.5	85	3.0	25
1100-1200	3.5	85	4.5	70	2.0	150
1200-1300	3.0	75	4.5	70	4.0	265
1300-1400	4.0	90	2.5	95	6.0	250
1400-1500	3.0	105	1.5	50	6.0	275
1500-1600	3.0	120	2.0	155	4.5	240
1600-1700	3.0	165	2.0	155	3.5	280
1700-1800	3.0	165	2.0	155	3.5	280
1800-1900	3.0	165	2.0	155	3.5	280
1900-2000	Surface Winds Used		2.0	155	3.5	280
2000-2100	"	" "	2.0	155	3.5	280
2100-2200	"	" "	2.0	155	3.5	280
2200-2300	"	" "	2.0	155	3.5	280
2300-2400	"	" "	2.0	155	3.5	280

BEST COPY AVAILABLE

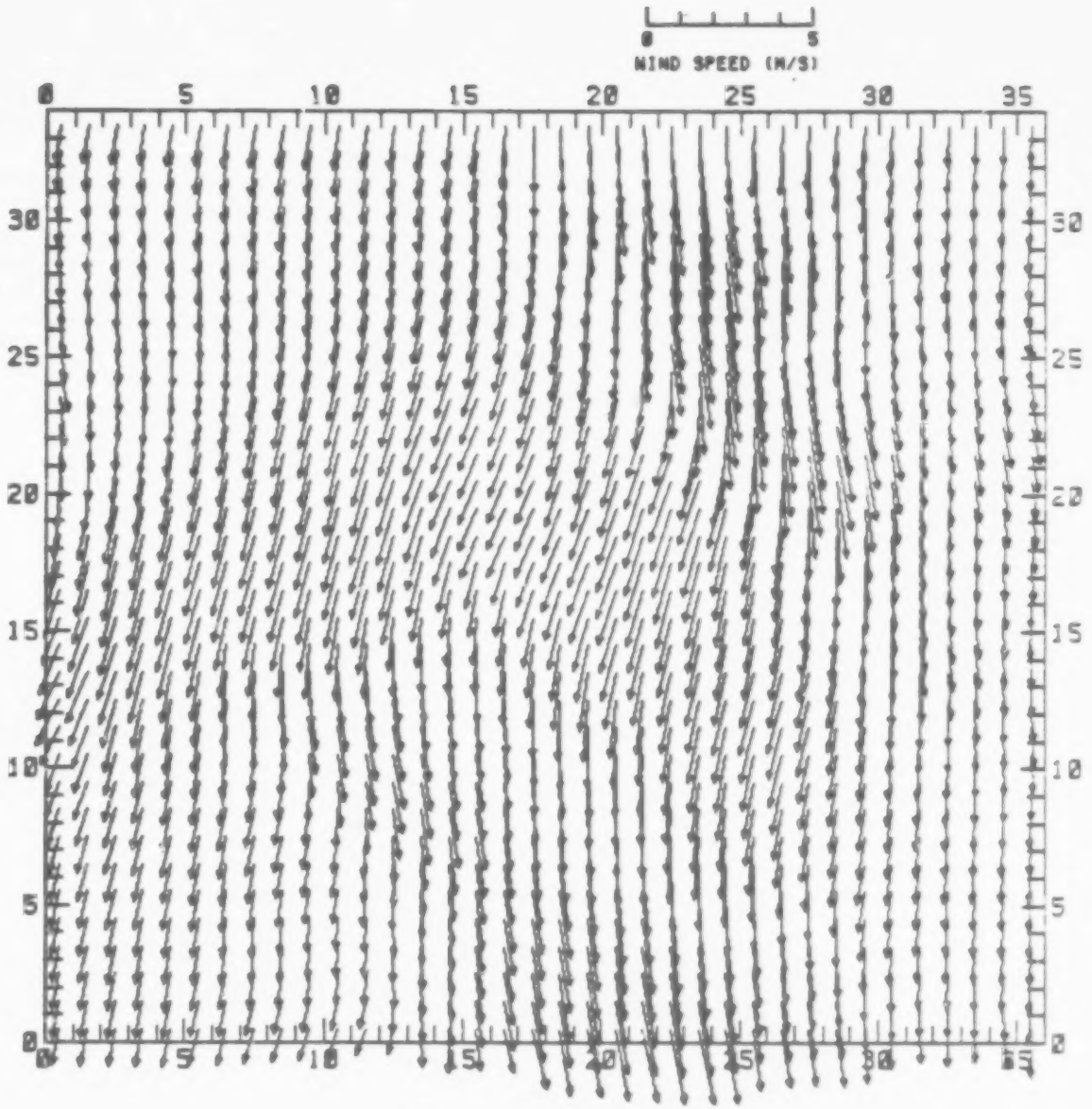

(a) 400 - 500 EST

FIGURE 5-7. Airshed model surface winds for 19 July 1979.

BEST COPY AVAILABLE

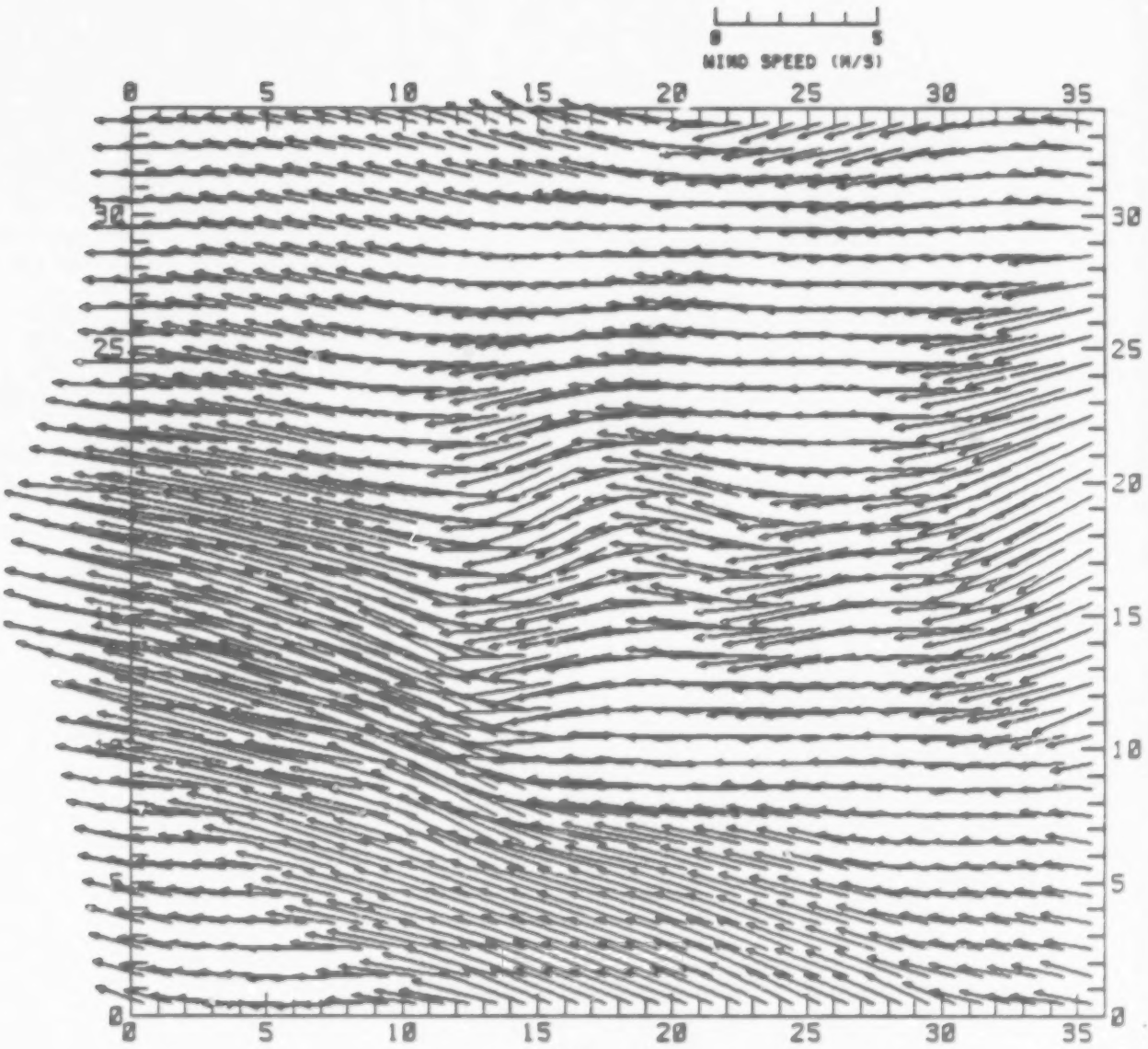

(b) 1200 - 1300 EST

FIGURE 5-7 (continued).

BEST COPY AVAILABLE

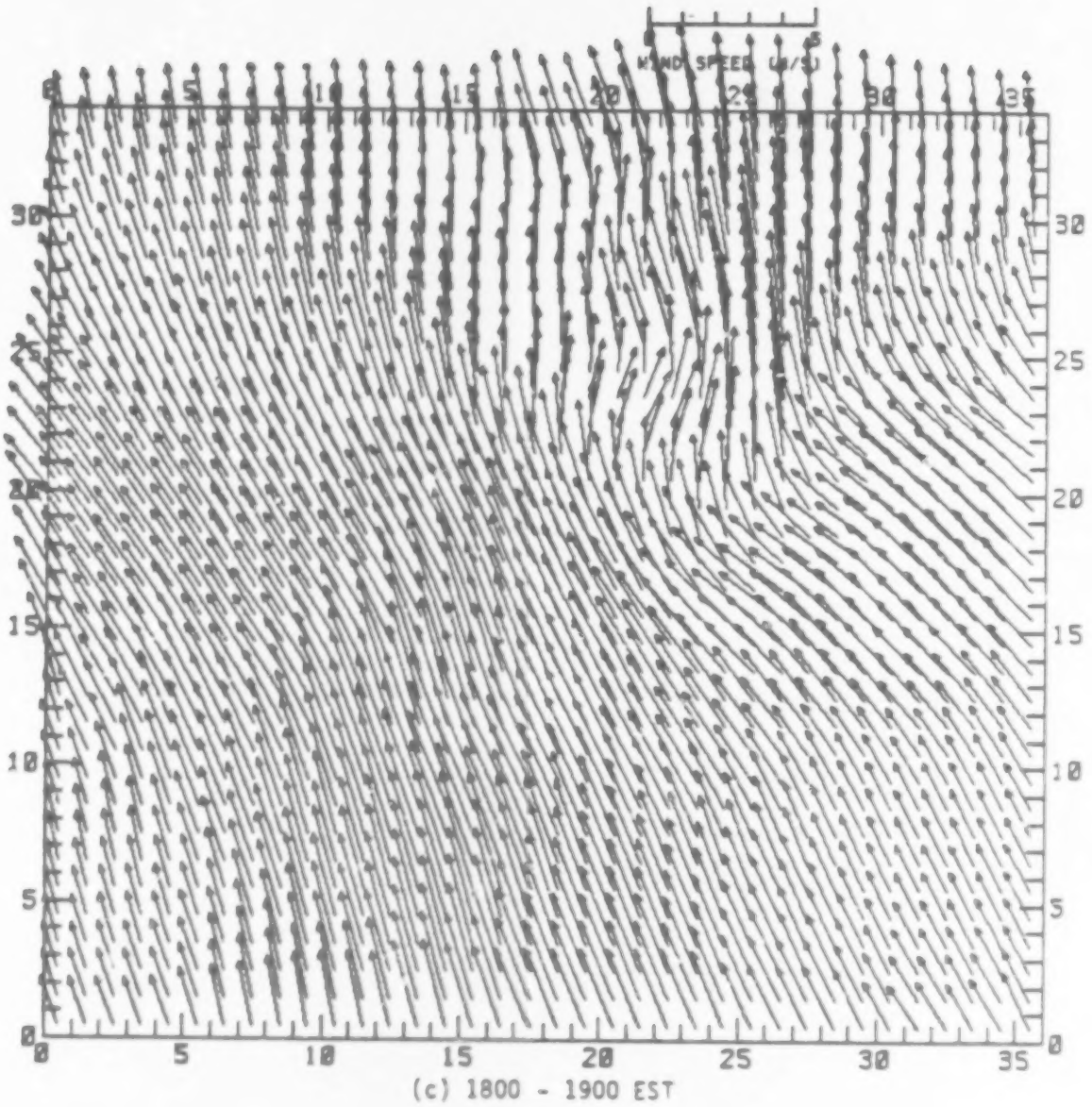

(c) 1800 - 1900 EST

FIGURE 5-7 (concluded).

BEST COPY AVAILABLE

TABLE 5-3. Background concentration values for 19 July at the top of the modeling region (TOPCONC), as initial concentrations above the mixing height, and for all levels of all boundaries except the levels below the mixing height on the Northeast and East boundaries.

Species	Concentration (ppm)
NO	0.001
NO_2	0.002
O_3	0.06*
CO	0.2
ETH	0.001
OLE	0.0004
PAR	0.040
CARB	0.010
ARO	0.0008
PAN	0.000025
BZA	0.00001

* A value of 0.05 ppm was used below the mixing height for all boundaries except the Northeast and East boundaries.

BEST COPY AVAILABLE

value of 0.05 ppm was specified. The value should have been 0.06 ppm; however, the difference is not significant because these are outflow boundaries.

INITIAL CONDITIONS

The initial-condition field for 19 July was created following the same procedure as that used for 13 July 1979 (see Section 3). Because the simulation began at midnight, the initial-condition values were obtained by computing a two-hour average starting at 2300 on 18 July. Stations without data for a particular species were left out of the Poisson interpolation scheme. Background concentrations for all species were used in levels 3 and 4 above the mixing height, and a linear interpolation was used between the background values aloft and the surface (layer 1) value for each cell to obtain the concentration value in level 2. The initial-condition input values used in the preparation of the AIRQUALITY file for 19 July are presented in Table 5-4.

BOUNDARY CONDITIONS

Boundary conditions were specified after examination of all air quality and meteorological data collected during this episode. Because of wind flow through the airshed on this day and the need to limit simulation costs, certain unnecessary grid cells were eliminated from the simulation by the boundary specifications. No grid cells containing major emissions sources were excluded by this procedure. The boundaries used in the simulation are shown in Figure 5-8. After the hourly three-dimensional wind fields were prepared, a number of parcel trajectories were released at various locations within the grid. The trajectory analysis revealed that air parcels arriving in central downtown Philadelphia near noontime orginated in the New Jersey/New York urban area directly to the northeast in the early morning hours. Because of this inflow from an adjacent airshed region, it was important to estimate the levels of migratory regional pollutants being advected from the neighboring "dirty" air mass. Therefore, two sets of boundary conditions were specified: one set of conditions for the East and Northeast boundaries below the mixing height to estimate the inflow of pollutants from the New Jersey/New York urban area, and another set for all other boundary conditions as an estimate of background conditions presented earlier (see Table 5-3). The estimates of the Northeast and East boundaries below the mixing height were the result of further analysis.

Precursor transport from the New Jersey/New York urban area into the Philadelphia AQCR occurred on 19 July 1979. This occurrence is supported

BEST COPY AVAILABLE

TABLE 5-4. Initial conditions for 19 July 1979 (concentrations in ppm).

Station	Easting (m)	Northing (m)	NO	NO_2	CO	O_3	RHC
AMS Lab.	491600	4428500	0.000	0.025	0.5	0.015	0.35
Ancora	511800	4392400	--	--	--	0.015	--
Brigantine	546000	4337506	--	--	--	0.017	--
Bristol	511000	4440000	--	0.039	--	0.012	--
Camden	491700	4419000	0.011	0.051	2.5	0.004	--
Chester	469000	4410000	--	0.024	--	0.026	0.95
Claymont	461500	4406400	--	0.045	--	0.020	--
Conshohocken	474500	4435600	--	--	--	0.000	--
Defense Support	483800	4418300	--	--	--	0.000	--
Downington	436000	4426000	0.006	0.015	0.2	0.024	0.05
Franklin Inst.	485200	4422800	0.030	0.050	0.5	0.010	--
Island Rd. Airp. Cir.	480300	4414800	--	--	--	0.015	--
Lumberton	518000	4423000	0.000	0.028	0.0	0.008	0.40
Norristown Armory	473500	4440000	--	--	--	0.030	0.29
Northeast Airp.	499000	4436000	0.000	0.015	--	--	--
Roxy Water Pump	479500	4433100	--	--	--	0.010	--
SE Sewage Plant	487200	4417300	--	--	--	0.005	--
South Broad	486100	4421600	0.020	0.045	1.5	0.010	0.25
Summit Bridge	441000	4376000	0.000	0.009	0.2	0.009	0.10
SW Corner Broad/Butler	487000	4418000	--	--	--	--	--
Trenton	520000	4452000	--	--	--	0.002	--
Van Hiseville	559000	4439500	0.000	0.006	0.2	0.021	--
Vineland	498200	4371200	--	0.025	--	0.010	--

RHC Component	Carbon-Bond Fraction (% as Carbon)
PAR	74.0
OLE	2.8
ETH	4.1
ARO	13.2
CARB	5.9

BEST COPY AVAILABLE

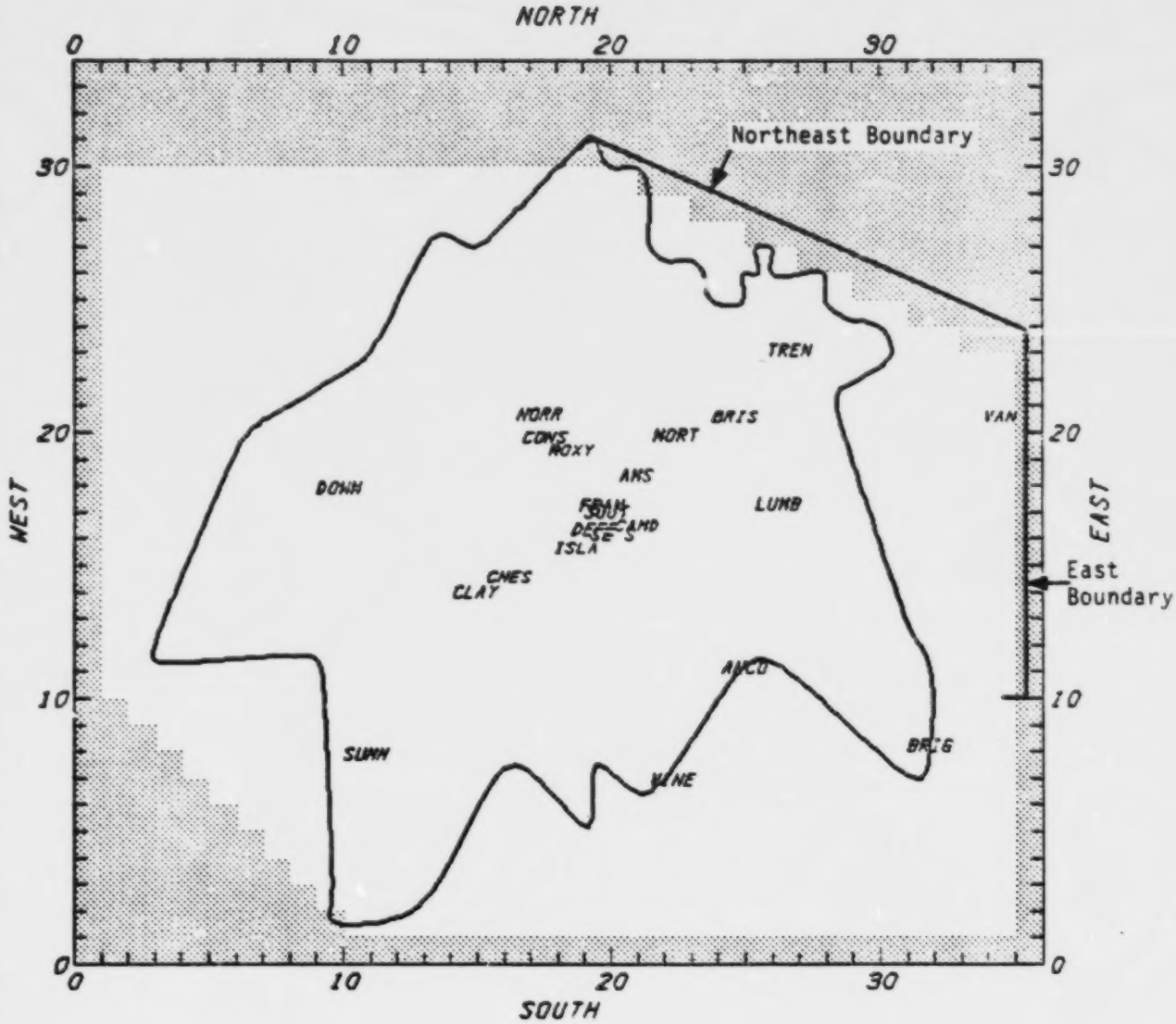

FIGURE 5-8. Boundary specifications for 19 July 1979 simulation. (Bold line is emissions region.)

BEST COPY AVAILABLE

by the following observations: (1) overnight winds were northerly in the New York and Philadelphia areas, (2) high NO_x concentrations were recorded in the early morning hours upwind of Philadelphia at the Van Hiseville, New Jersey monitor, and (3) a surface layer back trajectory from the high ozone concentration of 16.0 pphm recorded at Claymont, Delaware, using interpolated surface wind fields generated from observed data, indicates a pathway back towards the New Jersey/New York metropolitan area that does not traverse the high-emission-density area of Philadelphia. Therefore, for the East and Northeast boundaries, the Van Hiseville monitor, which is located near the intersection of these two boundaries, was used to define boundary conditions. On the basis of the expected behavior of the New York plume derived from field studies in New York and several other cities, overnight precursor transport is likely to have occurred just above the surface (Alkezweeny et al., 1981; Clarke, 1969; Godowitch et al., 1984b, Possiel et al., 1984). Thus, the Van Hiseville monitor is likely to have been just below the urban precursors transported throughout the night. Therefore, the 0500-0600 EST surface NO_x measurements at Van Hiseville were extrapolated back in time to midnight to account for overnight transport of precursors just above the surface monitor at Van Hiseville, but within the mixed layer.

Estimates of boundary conditions for the Northeast and East boundaries below the mixing height are presented in Table 5-5. Observed NO and NO_2 data for the hour of 0500-0600 EST were used as input boundary values for the hours of 0000-0600. Since hydrocarbons were not measured at the Van Hiseville monitor, estimates of the influx of total reactive hydrocarbons across the Northeast and East boundaries below the mixing height were specified by multiplying the hourly NO_x concentrations at the Van Hiseville monitor by the Philadelphia surface layer emission inventory hydrocarbon/NO_x ratio of 6. The total reactive hydrocarbon value was then speciated into carbon-bond components using the carbon-bond fractions of the emission inventory.

METSCALARS

The inputs for the METSCALARS file were obtained for 19 July using the same procedures as those employed for the 13 July simulation (see Section 3). Radiosonde data from central Philadelphia were used to specify the temperature gradients above and below the mixing height. A value of 24000 ppm for the concentration of water vapor was specified because dewpoints for a number of stations in the region were in the upper 60s and low 70s. Surface pressure at 0700 EST was 1021.7 mb, so a value of 1.0 atm was specified for the atmospheric pressure model input. The NO_2 photolysis rate constants were obtained by the procedure used in the 13 July simulation. The values used for all parameters in the METSCALARS file for 19 July are presented in Table 5-6.

BEST COPY AVAILABLE

TABLE 5-5. Boundary conditions used for the Northeast and East boundaries below the mixing height estimated from data collected at the Van Hiseville, New Jersey monitor (concentrations in ppm).

Hour (EST)	NO	NO_2	O_3	PAR	OLE	ETH	ARO	CARB	PAN
0000-0100	0.044	0.036	0.018	0.3552	0.00672	0.00985	0.01056	0.02832	0.0002
0100-0200	0.044	0.036	0.009	0.3552	0.00672	0.00985	0.01056	0.02832	0.0001
0200-0300	0.044	0.036	0.000	0.3552	0.00672	0.00985	0.01056	0.02832	0.0000
0300-0400	0.044	0.036	0.000	0.3552	0.00672	0.00985	0.01056	0.02832	0.0000
0400-0500	0.044	0.036	0.000	0.3552	0.00672	0.00985	0.01056	0.02832	0.0000
0500-0600	0.044	0.036	0.000	0.3552	0.00672	0.00985	0.01056	0.02832	0.0000
0600-0700	0.047	0.041	0.000	0.39072	0.00739	0.010825	0.01162	0.03115	0.0000
0700-0800	0.043	0.0494	0.004	0.40996	0.007755	0.01135	0.01218	0.03269	0.0004
0800-0900	0.026	0.0478	0.015	0.32782	0.0062	0.00908	0.00975	0.02614	0.0008
0900-1000	0.009	0.0273	0.051	0.16132	0.00305	0.00447	0.0048	0.01286	0.0013
1000-1100	0.001	0.0099	0.083	0.04839	0.000915	0.00134	0.00143	0.00386	0.0019
1100-1200	0.000	0.0058	0.078	0.02575	0.000487	0.000716	0.000767	0.00205	0.0018
1200-1300	0.000	0.0054	0.075	0.02397	0.0004535	0.000665	0.000717	0.00191	0.0014
1300-1400	0.000	0.0072	0.072	0.03196	0.000605	0.000885	0.00095	0.00255	0.0012
1400-1500	0.000	0.0047	0.072	0.02087	0.0003945	0.000578	0.00062	0.00166	0.0007
1500-1600	0.000	0.0035	0.062	0.01554	0.000294	0.0004305	0.000462	0.00124	0.0005
1600-1700	0.000	0.0043	0.059	0.01909	0.000361	0.000529	0.000568	0.00152	0.0003
1700-1800	0.000	0.0053	0.052	0.0235	0.000445	0.000652	0.0007	0.001876	0.0003
1800-1900	0.000	0.0072	0.044	0.03197	0.000605	0.000885	0.00095	0.00255	0.0002
1900-2000	0.000	0.0071	0.036	0.03152	0.0005965	0.000875	0.000937	0.00251	0.0001
2000-2100	0.000	0.0041	0.020	0.0182	0.0003445	0.000505	0.000542	0.00145	0.0001
2100-2200	0.002	0.0030	0.010	0.0222	0.00042	0.000615	0.00066	0.00177	0.0000
2200-2300	0.005	0.0060	0.000	0.04884	0.000925	0.001355	0.00145	0.00389	0.0000
2300-2400	0.008	0.0030	0.001	0.04884	0.000925	0.001355	0.00145	0.00389	0.0000

Philadelphia Inventory Split

Species	Carbon-Bond Fraction (% as Carbon)
PAR	74.
OLE	2.8
ETH	4.1
ARO	13.2
CARB	5.9

BEST COPY AVAILABLE

TABLE 5-6. METSCALAR inputs for the 19 July 1979 simulation.

Hour (EST)	Temp. Gradient (°K/m) Above	Below	Exposure Class	NO_2 Photolysis Rate (RADFACTOR)	Water Concentration (ppm)	Atmospheric Pressure (atm)
0000-0100	+0.004	-0.005	0.0	0.000	24,000	1.0
0100-0200	+0.004	-0.005	0.0	0.000	24,000	1.0
0200-0300	+0.004	-0.005	0.0	0.000	24,000	1.0
0300-0400	+0.004	-0.005	0.0	0.000	24,000	1.0
0400-0500	+0.004	-0.005	0.0	0.000	24,000	1.0
0500-0600	+0.004	-0.009	1.0	0.050	24,000	1.0
0600-0700	+0.040	-0.009	1.0	0.147	24,000	1.0
0700-0800	-0.005	-0.009	1.0	0.290	24,000	1.0
0800-0900	-0.005	-0.009	2.0	0.410	24,000	1.0
0900-1000	-0.005	-0.011	2.0	0.483	24,000	1.0
1000-1100	-0.005	-0.011	2.0	0.499	24,000	1.0
1100-1200	-0.007	-0.011	3.0	0.497	24,000	1.0
1200-1300	-0.007	-0.011	3.0	0.487	24,000	1.0
1300-1400	-0.007	-0.011	3.0	0.453	24,000	1.0
1400-1500	-0.007	-0.011	3.0	0.387	24,000	1.0
1500-1600	-0.008	-0.011	3.0	0.279	24,000	1.0
1600-1700	-0.008	-0.011	2.0	0.192	24,000	1.0
1700-1800	-0.005	-0.009	2.0	0.109	24,000	1.0
1800-1900	-0.005	-0.009	1.0	0.019	24,000	1.0
1900-2000	-0.005	-0.009	1.0	0.000	24,000	1.0
2000-2100	-0.005	-0.009	0.0	0.000	24,000	1.0
2100-2200	+0.004	-0.005	0.0	0.000	24,000	1.0
2200-2300	+0.004	-0.005	0.0	0.000	24,000	1.0
2300-2400	+0.004	-0.005	0.0	0.000	24,000	1.0

BEST COPY AVAILABLE

6 ANALYSIS OF URBAN AIRSHED MODEL PERFORMANCE FOR THE PHILADELPHIA SIMULATIONS OF 13 and 19 JULY 1979

This section presents a brief overview of the results and the analysis of model performance for the UAM simulations conducted for the Philadelphia region for 13 and 19 July 1979. These simulations originated at midnight and continued for 24 hours. For a more complete presentation of the results of the 13 and 19 July 1979 simulations, refer to Appendixes A and B. The statistical measures used in the analysis of model performance are first defined; then the simulation results and the performance evaluations for 13 and 19 July 1979 are presented.

MODEL PERFORMANCE EVALUATION MEASURES

The primary objective of the model performance evaluation effort is to ascertain how well the UAM computes the peak concentrations and spatial and temporal distribution of O_3 throughout the Philadelphia study area. This computation can be accomplished by comparison of available hourly averaged measurements of O_3 with corresponding predictions for surface-level grid cells containing the monitoring sites. Several means of quantifying model performance have been developed (e.g., Bencala and Seinfeld, 1979; Hayes, 1979; Fox, 1981; Layland and Cole, 1963). Hayes (1979) reported a detailed examination of candidate evaluation measures for air quality dispersion models that identified five attributes of desirable model performance:

(1) Accuracy of the calculated peak concentration

(2) Absence of systematic bias

(3) Lack of gross error

(4) Temporal correlation

(5) Spatial alignment

The evaluation of UAM results for Philadelphia focused on quantitative assessments of each of these performance attributes. Some modifications to the performance measures suggested by Hayes (1979) were made to take into account the recommendations of the AMS workshop on air quality model performance (Fox, 1981).

BEST COPY AVAILABLE

Accuracy of the Calculated Peak Concentration

The accuracy of calculated 1-hour O_3 peak concentrations can be evaluated by several methods. The measured 1-hour O_3 peak concentrations can be compared with (1) the highest 1-hour O_3 concentrations calculated at the same monitoring station, (2) the highest 1-hour O_3 concentration calculated at any monitoring station (i.e., the calculated 1-hour O_3 peak station concentration), or (3) the highest 1-hour O_3 concentration calculated in any surface-level grid cell (i.e., the calculated 1-hour O_3 peak grid concentration).

Layland and Cole (1983) propose that of these three approaches, the comparison of the measured peak concentration with the calculated peak concentration at any monitoring station is the most useful method. They believe that the comparison of the measured peak concentration with the calculated peak concentration in any surface-level grid cell will bias the evaluation toward overestimation because the station monitoring network is less likely to report the highest O_3 concentrations occurring in the gridded area. They note also that a comparison of the peak predicted and observed concentrations for the same monitoring station would bias the evaluation toward underprediction because the model may not exactly reproduce the spatial pattern of the concentration field.

Consequently, in this study, the accuracy of the 1-hour O_3 peak concentration is evaluated by comparing the measured and calculated peak O_3 concentration at any of the monitoring stations. It should be noted that this model evaluation procedure is consistent with the regulatory aspect of the O_3 NAAQS since the concern in this case is with the peak 1-hour O_3 concentration occurring in the monitoring network regardless of time or location. The O_3 concentration at a monitoring station is calculated as the distance-weighted average of the surrounding four grid cells.

For completeness, the highest 1-hour O_3 concentrations calculated and measured at the same monitoring station are compared. These pairs of station peak O_3 concentrations are plotted on a scatter diagram of calculated versus measured values, and the correlation coefficient is calculated. The highest 1-hour O_3 concentration calculated in any surface-level grid cell is also reported.

Absence of Systematic Bias

Absence of systematic bias refers to the ability of a model to avoid either underestimating or overestimating pollutant concentrations. Estimates of the mean bias were calculated in the following manner:

BEST COPY AVAILABLE

$$\text{Mean Deviation} = \frac{1}{N} \sum_{i=1}^{N} (C_{m,i} - C_{c,i}) \quad ,$$

$$\text{Mean Normalized Deviation} = \frac{1}{N} \sum_{i=1}^{N} \frac{(C_{m,i} - C_{c,i})}{0.5 \times (C_{m,i} + C_{c,i})} \quad ,$$

where C_c and C_m are the calculated and measured concentrations, respectively, and N is the total number of comparisons. These measures are consistent with the recommendations made by the AMS workshop (Fox, 1981). A negative bias corresponds to model overprediction and a positive bias corresponds to model underprediction. The mean deviation is normalized with respect to the arithmetic mean of the measured and calculated concentrations according to Hayes (1979). The standard deviation for each of these measures of bias is also calculated to provide an indication of the variability of the quantities $(C_{m,i} - C_{c,i})$ and $(C_{m,i} - C_{c,i})/[0.5 \times (C_{m,i} + C_{c,i})]$. Mathematically, the expressions for the standard deviations (σ) are as follows:

$$\sigma\ (\text{Deviation}) = \left[\frac{1}{N} \sum_{i=1}^{N} \left[(C_{m,i} - C_{c,i}) - \frac{1}{N} \sum_{i=1}^{N} (C_{m,i} - C_{c,i}) \right]^2 \right]^{1/2} \quad ,$$

$$\sigma\ (\text{Normalized Deviation}) = \left[\frac{1}{N} \sum_{i=1}^{N} \left[\left(\frac{C_{m,i} - C_{c,i}}{0.5 \times (C_{m,i} + C_{c,i})} \right) - \frac{1}{N} \sum_{i=1}^{N} \left(\frac{C_{m,i} - C_{c,i}}{0.5 \times (C_{m,i} + C_{c,i})} \right) \right]^2 \right]^{1/2} \quad .$$

Because of the large uncertainties in measured values at low concentrations, overall bias estimates were performed only for those cases in which the measured concentration of O_3 exceeded 5 pphm. To illustrate further the nature of model bias, the mean normalized deviation was plotted as a function of measured concentration. Such graphs provide a convenient means of displaying concentration ranges for which the model tends to overpredict or underpredict the measured values. To examine the bias in peak O_3 concentrations, the mean deviation and mean normalized deviation were calculated using the pairs of calculated and measured peak 1-hour O_3 concentrations at monitoring stations.

BEST COPY AVAILABLE

Absence of Gross Error

The absence of gross error can be determined through the calculation of the mean absolute deviation and the mean normalized absolute deviation. These measures are given by the following expressions:

$$\text{Mean Absolute Deviation} = \frac{1}{N} \sum_{i=1}^{N} |C_{m,i} - C_{c,i}| \quad ,$$

$$\text{Mean Normalized Absolute Deviation} = \frac{1}{N} \sum_{i=1}^{N} \frac{|C_{m,i} - C_{c,i}|}{0.5 \times (C_{m,i} + C_{c,i})} \quad .$$

The standard deviation for each of these measures is calculated as follows:

$$\sigma \text{ (Absolute Deviation)} = \left[\frac{1}{N} \sum_{i=1}^{N} \left[\left| C_{m,i} - C_{c,i} \right| - \frac{1}{N} \sum_{i=1}^{N} \left| C_{M,i} - C_{c,i} \right| \right]^2 \right]^{1/2} \quad ,$$

$$\sigma \text{ (Normalized Absolute Deviation)} = \left[\frac{1}{N} \sum_{i=1}^{N} \left[\frac{|C_{m,i} - C_{c,i}|}{0.5 \times (C_{m,i} + C_{c,i})} - \frac{1}{N} \sum_{i=1}^{N} \frac{|C_{m,i} - C_{c,i}|}{0.5 \times (C_{m,i} + C_{c,i})} \right]^2 \right]^{1/2} \quad .$$

If the mean absolute deviation of the pairs of calculated and measured values is small, then the model is said to exhibit "skill" as a predictor. If the mean absolute deviation is large, the model suffers from the presence of large gross errors. As with the bias determination, these measures were calculated for O_3 for all cases in which the measured values exceeded a 5 pphm threshold. The mean normalized absolute deviation for O_3 was plotted as a function of measured concentration to complement the

BEST COPY AVAILABLE

corresponding bias displays discussed previously. The mean absolute deviation and mean normalized absolute deviation were also calculated for the pairs of measured and calculated peak 1-hour O_3 concentrations at monitoring stations. These pairs of peak station concentrations were also plotted on scatter diagrams.

Temporal Correlation

Temporal correlation refers to the "timing" or "phasing" of the measured and calculated ozone levels at a specified station. The temporal correlation for a given station can be determined by using the hourly pairs of measured and calculated concentrations to define the appropriate mean values. A correlation coefficient can then be calculated according to the following expression (Hoel, 1962):

$$\text{Correlation Coefficient} = \frac{\frac{1}{N}\left[\sum_{i=1}^{N}\left(C_{c,i} - \frac{1}{N}\sum_{i=1}^{N} C_{c,i}\right)\left(C_{m,i} - \frac{1}{N}\sum_{i=1}^{N} C_{m,i}\right)\right]}{\left[\frac{1}{N}\sum_{i=1}^{N}\left(C_{c,i} - \frac{1}{N}\sum_{i=1}^{N} C_{c,i}\right)^2\right]^{1/2}\left[\frac{1}{N}\sum_{i=1}^{N}\left(C_{m,i} - \frac{1}{N}\sum_{i=1}^{N} C_{m,i}\right)^2\right]^{1/2}} ,$$

where N is the number of comparisons for a particular station. Lack of temporal correlation can be ascribed to one or more causes, including inadequate characterization of emissions, wind, or mixing depth inputs.

To calculate an average temporal correlation coefficient on a particular day, the following change of variable is performed (Hoel, 1962):

$$\phi_j = \frac{1}{2} \ln\left(\frac{1 + r_j}{1 - r_j}\right) ,$$

where r_j is the computed correlation coefficient for station j. Next, the mean value of ϕ_j is estimated:

$$\bar{\phi} = \frac{\sum_{j=1}^{M} (n_j - 3)\,\phi_j}{\sum_{j=1}^{M} (n_j - 3)} ,$$

BEST COPY AVAILABLE

where M is the number of monitoring stations and n_j is the number of comparisons made for station j. This somewhat complicated transformation is used because the variance of an estimated correlation coefficient is a function of both sample size and the population correlation coefficient, ρ. The transformation to ϕ_j converts r_j to an approximately normally distributed random variable with a variance of $1/(n_j - 3)$ that is not dependent on the population value, ρ. The average of all ϕ_j is computed by weighting each value by its variance. Then ρ can be determined from the following equation:

$$\rho = \frac{\exp(2\bar{\phi}) - 1}{\exp(2\bar{\phi}) + 1} \quad .$$

Spatial Alignment

The spatial alignment of measured and calculated concentration fields is another useful measure of model performance. For a given hour, imagine two concentration isopleths, one constructed from measured pollutant concentrations, and the other from the corresponding model calculations. If one isopleth were placed over the other, the degree of spatial misalignment would be easy to discern. Spatial alignment can be quantified by considering a sequence of "time slices." The calculated and measured concentrations for a particular hour are employed to calculate a correlation coefficient using the formula given in the previous section. When applying the expression for the correlation coefficient for this example, N is equal to the number of comparisons available for a specific hour. Spatial correlation coefficients can thus be computed for each hour, and estimates of the average spatial correlation coefficient for each simulation day can also be made following the general procedure described in the previous section.

A high correlation coefficient means that the calculated spatial distribution of pollutants over the modeling region for a specific hour corresponds closely to that indicated by the measurements. Poor correlation is sometimes to be expected during hours when the measured values do not exhibit significant spatial variability. Although the absolute magnitudes of the calculated and measured values might be in reasonably close agreement, the small variations in pollutant levels from station to station might not be replicated in the variations of the calculated values, thus

BEST COPY AVAILABLE

yielding a relatively low spatial correlation coefficient. Common sources of spatial misalignment include discrepancies between modeled and observed wind velocities and directions, inaccuracies in the emission inventory, and improper treatment of photochemistry.

The results of the application of these performance measures to the UAM simulations of the 13 and 19 July 1979 ozone episodes in Philadelphia are presented next.

MODEL EVALUATION RESULTS FOR THE 13 JULY 1979 SIMULATION

Following the procedures outlined in the previous section, measures of overall model accuracy, bias, error, and temporal and spatial correlations were calculated. Bias and error were calculated for all pairs of ozone concentrations for which the measured value exceeded 5 pphm, as well as for pairs of station peak ozone concentrations. These results are summarized in Tables 6-1 and 6-2. Table 6-1 presents a detailed comparison of maximum measured and calculated ozone concentrations for each of the 22 monitoring stations. Table 6-2 presents the measures of model performance for this simulation.

Accuracy of Calculated Peak Concentrations

From a regulatory point of view, the ability of a model to reproduce measured peak concentrations is a major attribute of model performance. Table 6-1 presents the measured and calculated peak ozone concentrations at each monitoring station, the normalized residuals, the times of occurrence and the lag time. A scatter plot of these pairs of station peak ozone concentrations is presented in Figure 6-1; bias and gross error are given in Table 6-2.

The maximum measured 1-hour ozone concentration on 13 July was 20.5 pphm at the Conshohocken station at 1500-1700 EST. The peak calculated concentration at this same station was 18.5 pphm. The calculated ozone maximum concentration occurred two hours prior to the measured ozone peak value. The model-predicted maximum station value was 19.3 pphm, at the nearby Roxy Water Pump station, at 1300-1400 EST. This value is close to the measured peak concentration of 20 pphm at this same station and to the measured airshed-wide peak concentration of 20.5 pphm. The model underpredicts the station peak ozone concentration by 6 percent. The largest calculated 1-hour ozone concentration on the entire grid was 26.6 pphm at 1600-1700 EST.

BEST COPY AVAILABLE

TABLE 6-1. Maximum predictions/observations for 13 July 1979 for ozone (pphm).

STATIONS	OBSERVED MAXIMUM CONCENTRATION	PREDICTED MAXIMUM CONCENTRATION	RATIO OF PREDICTED TO OBSERVED CONCENTRATION	PERCENTAGE DIFFERENCE (PR - OB)/OB	HOUR OF OBSERVED MAXIMUM CONCENTRATION	HOUR OF PREDICTED MAXIMUM CONCENTRATION	LAG (HOURS)
ANS LAB	16.00	17.35	1.00	8	1300	1300	0
ANCORA	14.10	13.30	0.94	-5	1400	1300	-1
BRISTOL	13.00	17.95	1.38	38	1600	1500	-1
CAMDEN	16.10	15.47	0.96	-3	1300	1200	-1
CHESTER	10.30	14.56	0.60	-20	1200	1300	1
CLAYMONT	10.00	13.50	1.36	35	1400	1200	-2
CONSHOHOCKEN	20.50	18.46	0.90	-10	1600	1300	-3
DEFENSE SUPP	15.00	14.06	0.94	-6	1300	1200	-1
DOWNINGTON	12.30	12.93	1.05	5	1300	1500	2
FRANKLIN INS	15.00	14.12	0.94	-5	1300	1300	0
ISLAND RD AI	10.00	12.86	1.29	28	1100	1330	2
LUMBERTON	12.50	12.71	1.02	1	1500	1300	-2
NORRISTOWN A	10.30	19.26	1.05	5	1500	1400	-1
ROXY WATER P	20.00	19.32	0.97	-3	1400	1300	-1
SE SEWAGE PL	10.00	15.20	1.53	52	1300	1200	-1
SOUTH BROAD	14.00	14.34	1.02	2	1300	1300	0
SUMMIT BRIDG	8.70	9.79	1.13	12	1000	1200	2
TRENTON	11.30	16.41	1.45	45	1400	1600	2
VAN HISEVILL	9.00	11.32	1.26	25	1200	1600	4

BEST COPY AVAILABLE

TABLE 6-2. Performance measures for the UAM simulation of the 13 July 1979 episode in Philadelphia.

Performance Attribute	Performance Measure	Values
Accuracy of the airshed peak prediction	Ratio of predicted to measured station peaks	0.940
	Time difference between predicted and measured station peaks	-2 hours
	Station Peaks	
	Predicted	19.3 pphm (Roxy Water)
	Measured	20.5 pphm (Conshohocken)
Station peaks		
Systematic bias	Mean Deviation	
	Normalized	
	Average	-0.086
	Std. dev.	0.180
	Nonnormalized	
	Average	-0.998 pphm
	Std. dev.	2.491 pphm
	Bounds at the 90 percent confidence level	-2.790 and 0.793 pphm
Gross error	Mean absolute deviation	
	Normalized	
	Average	0.148
	Std. dev.	0.130
	Nonnormalized	
	Average	2.021 pphm
	Std. dev.	1.718 pphm

BEST COPY AVAILABLE

TABLE 6-2. (Concluded)

Performance Attribute	Performance Measure	Values
All O_3 Concentrations > 5 pphm		
Systematic bias	Mean deviation	
	Normalized	
	Average	-0.150
	Std. dev.	0.361
	Nonnormalized	
	Average	-1.660 pphm
	Std. dev.	2.885 pphm
Gross error	Mean absolute deviation	
	Normalized	
	Average	0.295
	Std. dev.	0.255
	Nonnormalized	
	Average	2.670 pphm
	Std. dev.	1.981 pphm
Temporal correlation	Temporal correlation coefficients	
	Each station	0.273 to 0.956
	All-station average	0.737
Spatial alignment	Spatial correlation coefficients	
	Each hour	0.041 to 0.735
	All-hour average	0.456

BEST COPY AVAILABLE

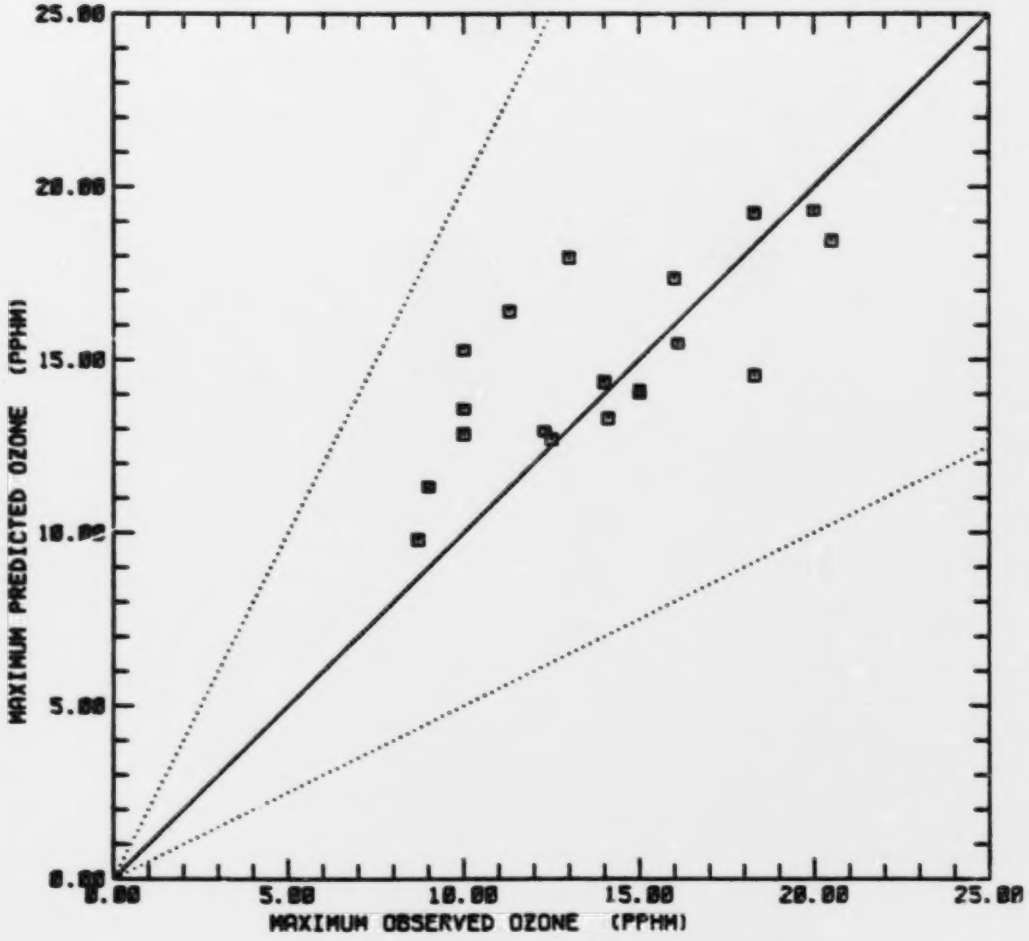

FIGURE 6-1. Scatter plot of predicted and observed station peak ozone concentrations for 13 July 1979. The correlation coefficient for the 19 pairs of station values is 0.731. The solid line represents perfect agreement between observed and predicted concentrations; the dotted lines represent the envelope of the predicted values that are within a factor of two of the corresponding observed values.

BEST COPY AVAILABLE

The scatter plot of station peak concentrations (Figure 6-1) shows a correlation of 0.731. The normalized bias and error are -0.086 and 0.148, respectively. The model appears to overestimate, on average, the station peak ozone concentrations by about 1 pphm. All the calculated peak station values are within a factor of 2 of the measured peak station values.

Estimates of Overall Systematic Bias

Measures of potential systematic bias were calculated as both nonnormalized and normalized quantities. Table 6-2 presents these biases for the 13 July 1979 simulation with the constraint that the measured ozone concentrations equaled or exceeded 5 pphm. Figure 6-2a shows a plot of the normalized bias as a function of the measured ozone concentrations. For measured ozone concentrations ranging from 5 to 16 pphm, the model tends to overestimate concentrations. The model tends to underestimate only at very low or very high ozone concentrations. The model also appears to overestimate ozone concentrations over the entire range of concentrations measured on 13 July 1979. For concentrations greater than 5 pphm, the model tends to overestimate measured values by 15 percent. The magnitude of the average overestimation is 1.66 pphm.

Estimates of Gross Error

The mean absolute deviation as an indication of gross error is estimated by averaging the absolute (unsigned) differences between the pairs of calculated and measured concentrations. This gross error is presented as both nonnormalized and normalized values in Table 6-2. Figure 6-2b presents the normalized gross error as a function of measured ozone concentrations. The average error for measured ozone concentrations greater than 5 pphm is 29.5 percent. The magnitude of the average error is 2.67 pphm. At elevated measured concentrations (i.e., above 12 pphm), the error is nearly independent of the measured ozone concentrations (see Figure 6-2b).

Temporal Correlation

The temporal evolution of observed and predicted ozone concentrations at 16 selected monitoring stations is presented in Figure 6-3.

The temporal correlation coefficients for ozone indicate a broad range of values for the individual monitoring stations (see Table 6-2). For ozone concentrations above 5 pphm, the average coefficient is 0.737. An examination of Figure 6-3 indicates that most of the observed temporal

BEST COPY AVAILABLE

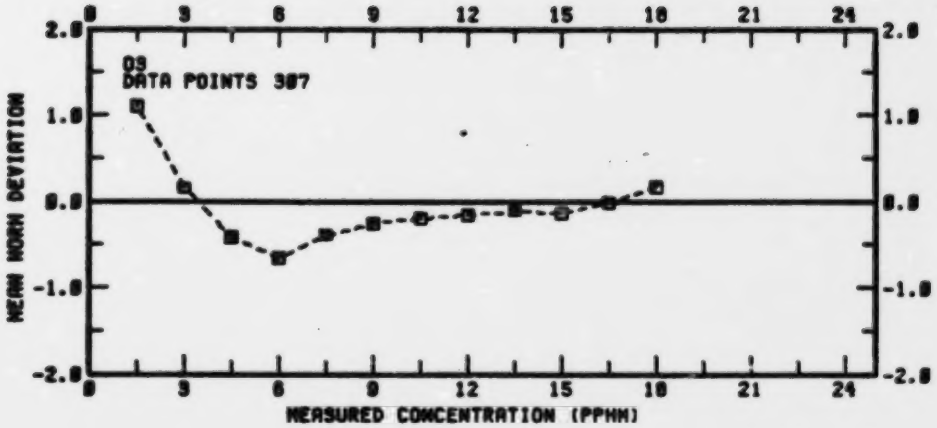

(a)

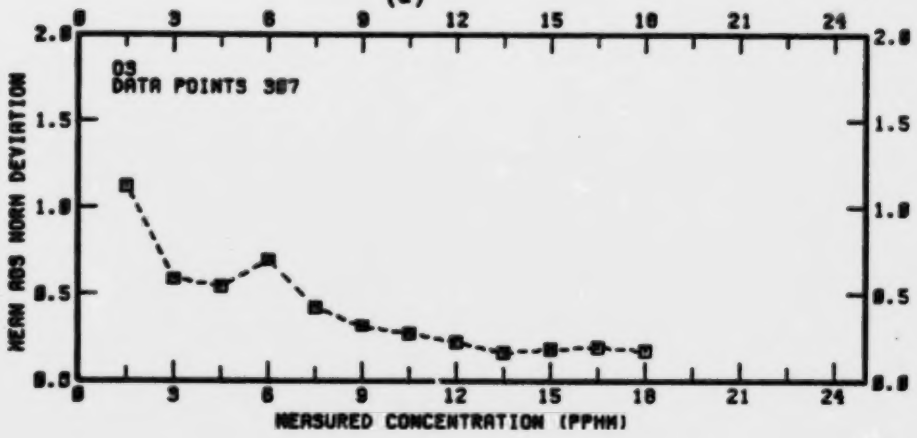

(b)

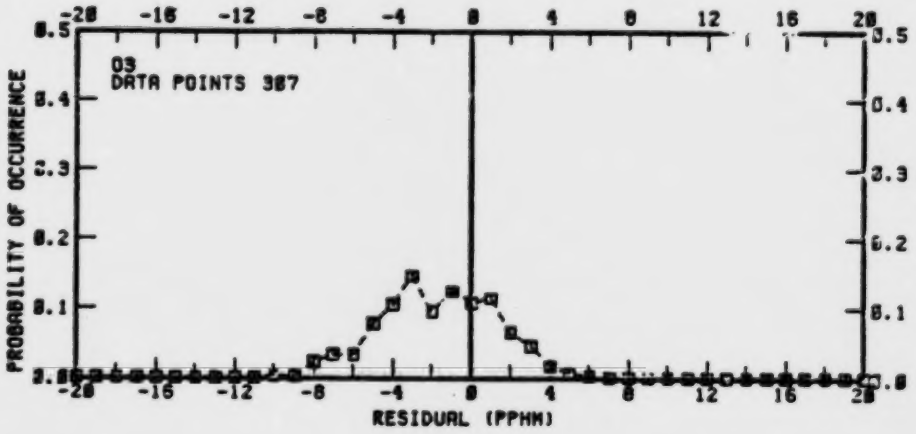

(c)

FIGURE 6-2. Mean normalized bias, mean normalized error as function of measured O_3 concentrations and distribution of residuals for 13 July 1979.

BEST COPY AVAILABLE

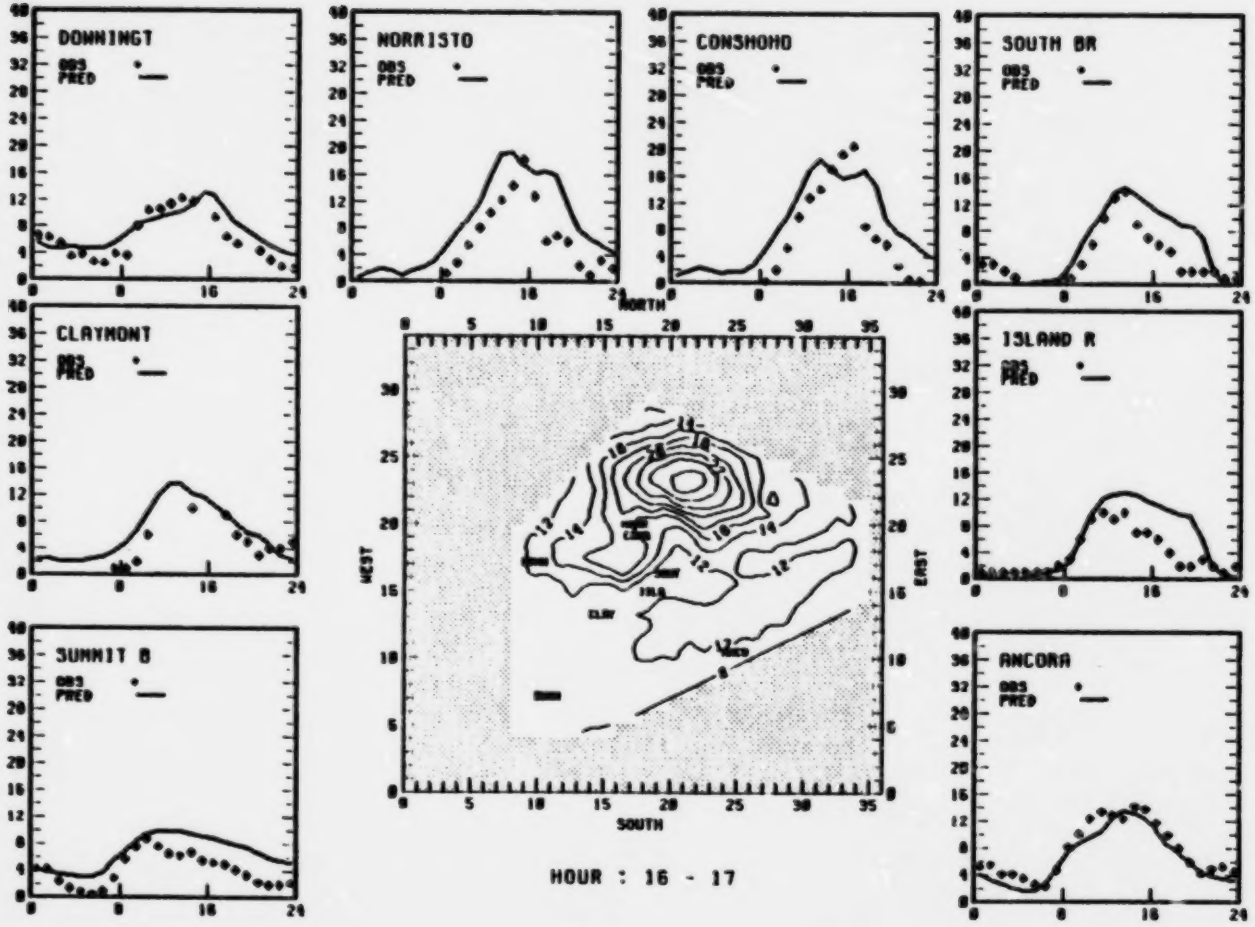

FIGURE 6-3. Time series (24 hours) of predicted versus observed ozone, and spatially predicted ozone (pphm), for the 13 July 1979 simulation, 1600-1700 EST.

BEST COPY AVAILABLE

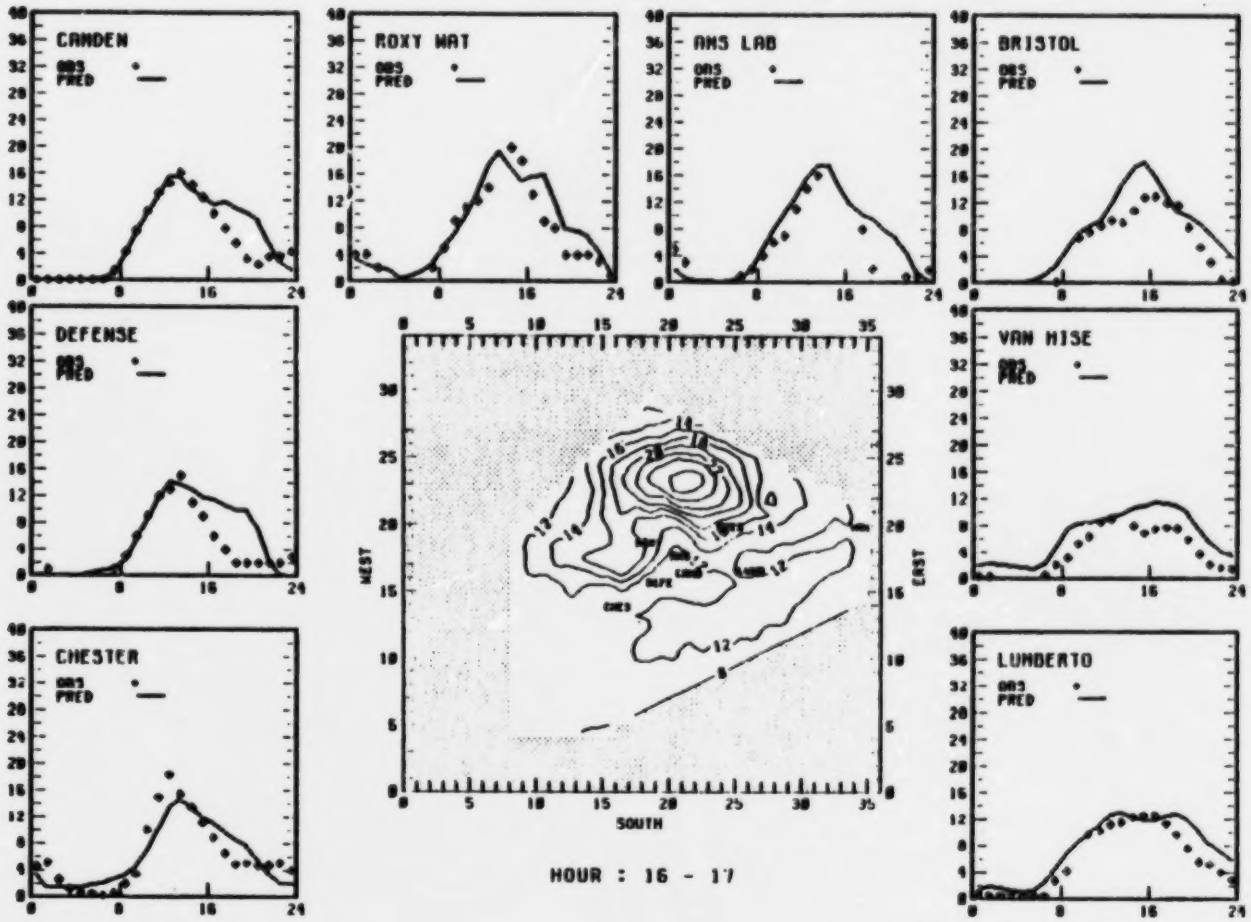

FIGURE 6-3 (concluded).

BEST COPY AVAILABLE

trends in the ozone measurements are represented in the model predictions; however, the model overestimates ozone levels after the time at which the peak observed value occurs.

Spatial Alignment

Spatial isopleths of calculated hourly averaged ozone concentrations at 1600-1700 EST are presented in Figure 6-3. Because of the consistent southerly wind flow established by late morning of 13 July 1979 in the Philadelphia region, the center of the ozone cloud depicted in Figure 6-3 is located north of the urban emission area. Spatial correlation coefficients are typically smaller than the corresponding temporal coefficients (see Table 6-2). For instance, for ozone levels greater than or equal to 5 pphm, the average spatial coefficient is 0.456. The spatial correlation is expected to be lower than the temporal correlation. The temporal correlation of calculated and measured concentrations will generally be satisfactory since the diurnal pattern of the ozone concentrations depends strongly on solar irradiation and will therefore be fairly well reproduced by a model such as the Urban Airshed Model that takes into account the effect of solar irradiation on ozone chemistry. On the other hand, uncertainties in meteorological inputs (e.g., wind speeds, wind directions, mixing heights, and mixing rates) can greatly affect the numerical value of the spatial correlation coefficient. For example, reduction of surface and upper-air meteorological data in Urban Airshed Model simulations of the Los Angeles basin had a large effect on the trajectories of air parcels and on the calculated ozone concentrations (Seigneur et al., 1981).

Overall Correlation

The distribution of the residuals (measured ozone concentrations minus calculated ozone concentration) is shown in Figure 6-2c. Most of the residuals are within ± 4 pphm, with a mean value of -1.7 pphm. A scatter plot of all ozone prediction-observation pairs is shown in Figure 6-4. Seventy-three percent of the predictions are within a factor of 2 of the observations. The correlation coefficient is 0.828.

MODEL EVALUATION RESULTS FOR THE 19 JULY 1979 SIMULATION

Following the procedures outlined in the first section, measures of overall model accuracy, bias, error, and temporal and spatial conditions were calculated. Bias and error were calculated for all pairs of ozone concentrations in which the measured value exceeded 5 pphm, as well as for

BEST COPY AVAILABLE

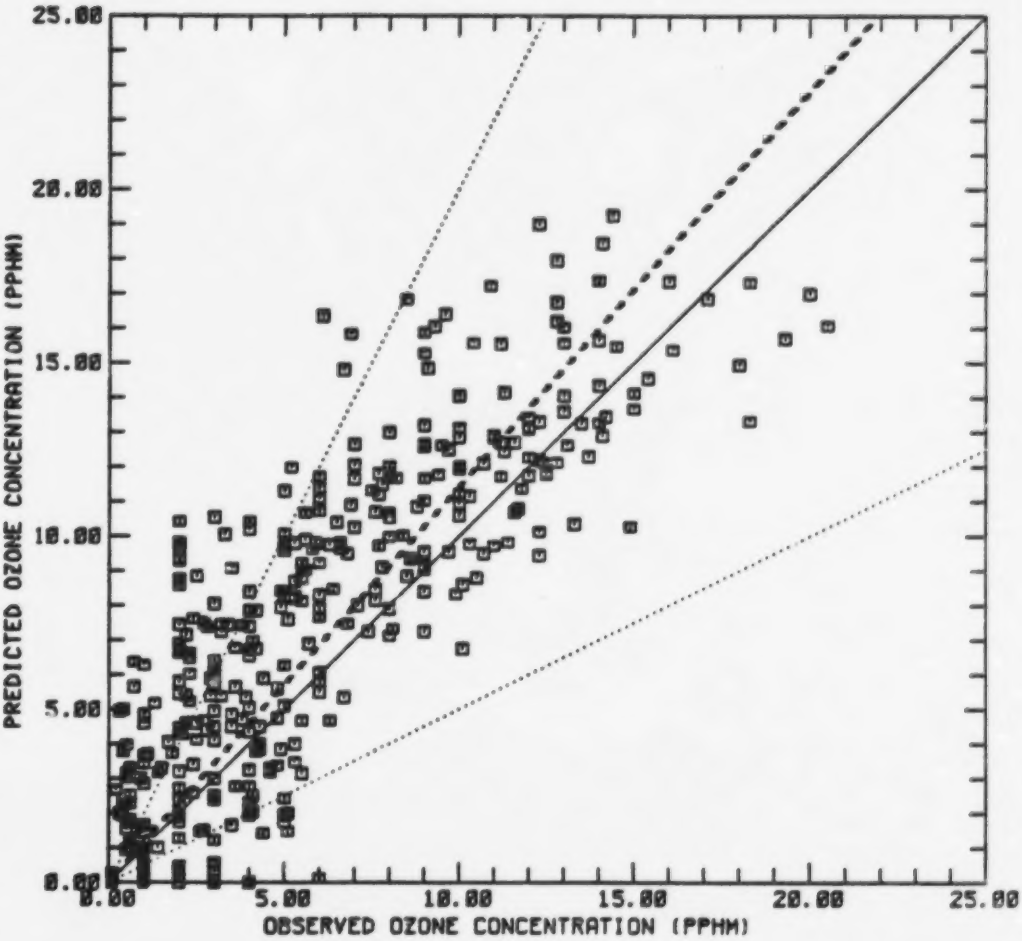

FIGURE 6-4. Scatter plot of predicted and observed ozone concentrations for 13 July 1979. The correlation coefficient for the 377 pairs of ozone concentrations is 0.828. The solid line represents perfect agreement between observed and predicted concentrations; the small dotted lines represent the envelope of the predicted values that are within a factor of two of the corresponding observed values, and the heavy dashed line represents the regression line forced through the origin.

BEST COPY AVAILABLE

pairs of station peak ozone concentrations. The results are summarized in Tables 6-3 and 6-4. Table 6-3 presents a detailed comparison of maximum measured and calculated ozone concentrations for each of the 22 monitoring stations. Table 6-4 presents the measures of model performance for this simulation.

Accuracy of Calculated Peak Concentrations

Table 6-3 compares the measured and calculated peak ozone concentrations at each monitoring station, the normalized residuals, the times of occurrence of the peak, and the lag times. A scatter plot of these pairs of peak O_3 concentrations is presented in Figure 6-5; bias and gross error are given in Table 6-4.

The maximum 1-hour concentration measured on 19 July was 17.0 pphm at the Roxy Water Pump station at 1400-1500 EST. The calculated peak concentration at this same station was 13.8 pphm. The largest station peak ozone concentration calculated by the model was 14.2 pphm at Downington at 1500-1600 EST. The model underpredicted the station peak ozone concentration by 16 percent. The largest 1-hour ozone concentration calculated by the model on the entire grid was 17.7 pphm.

The scatter plot of station peak concentrations (Figure 6-5) shows a correlation of 0.478. The normalized bias and error are -0.021 and 0.205, respectively. The model does not show any particular trend toward either over- or underestimation of the peak station ozone concentration. All calculated station peak ozone concentrations except one are within a factor of two of the measured station peak ozone concentrations.

Estimates of Systematic Bias

Normalized and nonnormalized measures of model bias are presented in Table 6-4 for ozone concentrations above 5 pphm. The normalized bias of 0.5 percent does not show a significant trend toward underestimation. The magnitude of the underestimation is only 0.024 pphm. The lack of under- or overestimation is exemplified in Figure 6-6a, which represents the normalized bias as a function of the measured ozone concentrations. It appears that the model overestimates ozone concentrations between 3 and 9 pphm and underestimates ozone concentrations below 3 pphm and above 9 pphm.

BEST COPY AVAILABLE

TABLE 6-3. Maximum predictions/observations for 19 July 1979 for ozone (pphm).

STATIONS	OBSERVED MAXIMUM CONCENTRATION	PREDICTED MAXIMUM CONCENTRATION	RATIO OF PREDICTED TO OBSERVED CONCENTRATION	PERCENTAGE DIFFERENCE (PR - OB)/OB	HOUR OF OBSERVED MAXIMUM CONCENTRATION	HOUR OF PREDICTED MAXIMUM CONCENTRATION	LAG (HOURS)
AMS LAB	13.00	13.39	1.03	3	1200	1500	3
ANCORA	9.70	10.88	1.12	12	1100	1300	2
BRISTOL	11.40	10.22	0.90	-10	1400	1300	-1
BRIGANTINE	5.10	6.80	1.33	33	1400	1200	-2
CAMDEN	13.80	13.31	0.96	-3	1300	1500	2
CHESTER	14.30	10.32	0.72	-27	1500	1400	-1
CLAYMONT	16.00	10.14	0.63	-36	1600	1400	-2
CONSHOHOCKEN	17.00	12.57	0.74	-26	1600	1800	2
DEFENSE SUPP	12.00	13.70	1.14	14	1300	1600	3
DOWNINGTON	15.70	14.21	0.91	-9	1500	1500	0
FRANKLIN INS	6.00	12.71	2.12	111	1100	1600	5
ISLAND RD AI	12.00	13.74	1.14	14	1200	1700	5
LUMBERTON	10.40	9.58	0.92	-7	1100	1200	1
NORRISTOWN A	13.80	13.22	0.96	-4	1600	1500	-1
NORTHEAST AI	10.00	12.61	1.26	26	1400	1400	0
ROXY WATER P	17.00	13.84	0.81	-18	1400	1700	3
SE SEWAGE PL	8.00	13.47	1.68	68	1300	1600	3
SOUTH BROAD	11.00	12.86	1.17	16	1300	1600	3
SUMMIT BRIDG	12.00	8.56	0.71	-28	1400	1200	-2
TRENTON	7.10	8.71	1.23	22	1200	1300	1
VAN HISEVILL	8.30	7.99	0.96	-3	1000	1100	1
VINELAND	10.30	10.53	1.02	2	1300	1400	1

BEST COPY AVAILABLE

TABLE 6-4. Performance measures for the UAM simulation of the 19 July 1979 episode in Philadelphia.

Performance Attribute	Performance Measure	Values
Accuracy of the airshed peak prediction	Ratio of predicted to measured station peaks	0.836
	Time difference between predicted and measured station peaks	1 hour
	Station Peaks	
	Predicted	14.2 pphm (Downington)
	Measured	17.0 pphm (Roxy Water)
Station peaks		
Systematic bias	Mean deviation	
	Normalized	
	Average	-0.021
	Std. dev.	0.275
	Nonnormalized	
	Average	0.047 pphm
	Std. dev.	3.038 pphm
	Bounds at the 90 percent confidence level	-1.437 and 1.531 pphm
Gross error	Mean absolute deviation	
	Normalized	
	Average	0.205
	Std. dev.	0.179
	Nonnormalized	
	Average	2.293 pphm
	Std. dev.	1.930 pphm

BEST COPY AVAILABLE

TABLE 6-4 (Concluded)

Performance Attribute	Performance Measure	Values
All O_3 concentrations > 5 pphm		
Systematic bias	Mean Deviation	
	Normalized	
	Average	0.005
	Std. dev.	0.398
	Nonnormalized	
	Average	0.024 pphm
	Std. dev.	3.163 pphm
Gross error	Mean absolute deviation	
	Normalized	
	Average	0.288
	Std. dev.	0.273
	Nonnormalized	
	Average	2.400 pphm
	Std. dev.	2.051 pphm
Temporal correlation	Temporal correlation coefficients	
	Each station	-0.914 to 0.970
	All-station average	0.525
Spatial alignment	Spatial correlation coefficients	
	Each hour	-0.421 to 0.643
	All-hour average	0.202

BEST COPY AVAILABLE

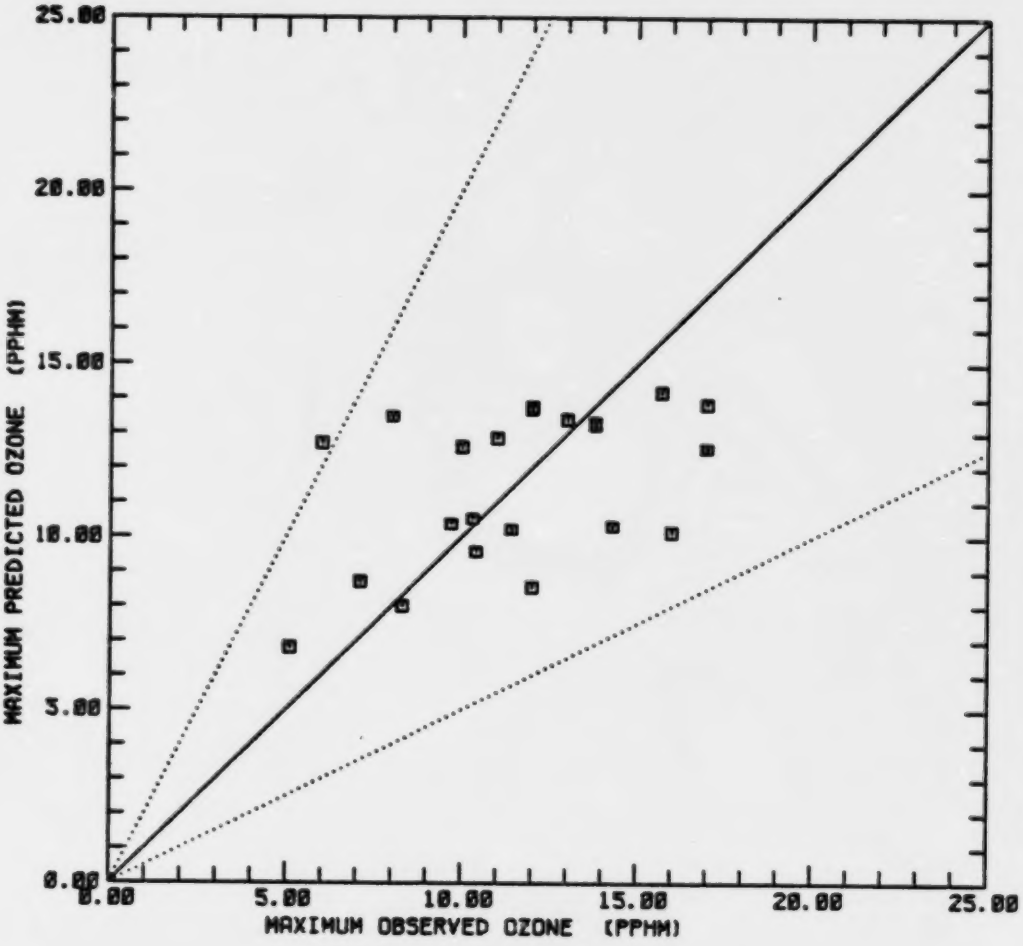

FIGURE 6-5. Scatter plot of predicted and observed station peak ozone concentrations for 19 July 1979. The correlation coefficient for the 22 pairs of station values is 0.478. The solid line represents perfect agreement between observed and predicted concentrations; the dotted lines represent the envelope of the predicted values that are within a factor of two of the corresponding observed values.

BEST COPY AVAILABLE

Estimates of Gross Error

The normalized and nonnormalized gross errors are presented in Table 6-4. The average error for measured ozone concentrations greater than 5 pphm is 28.8 percent. The magnitude of the error is 2.4 pphm. The normalized gross error is presented as function of the measured ozone concentrations in Figure 6-6b. The normalized gross error appears to decrease as the measured ozone concentration increases.

Temporal Correlation

The temporal evolution of observed and predicted ozone concentrations at 16 selected monitoring stations is presented in Figure 6-7. The temporal correlation coefficients are presented in Table 6-4. They indicate a large variation among stations. The overall temporal correlation is 0.525, which is lower than that obtained for the 13 July 1979 simulation. This lower temporal correlation may result from uncertainties in the boundary concentrations for the 19 July 1979 simulation since the ozone inflow through the Northeast and East boundaries strongly affects the airshed ozone field. This pattern is characteristic of the 19 July 1979 simulation and is discussed in the next paragraph.

Spatial Correlation

Spatial isopleths of calculated hourly averaged ozone concentrations at 1400-1500 EST are presented in Figure 6-7. The ozone isopleths show three centers of predicted high ozone buildup for that hour: one southwest of Downington, Pennsylvania, another just southwest of Norristown, Pennsylvania; and the third just west of Ancora, New Jersey. Because of the wind flow through the airshed on this particular day, high ozone concentrations were generally anticipated west of the Philadelphia urban center. The ozone isopleths for 1400-1500 EST clearly show this pattern. The large mass of ozone aligned in a north-south direction north of Vineland, New Jersey results from oxidant precursor material advected from the New York City area into the Philadelphia region on 19 July. This inflow is specified in the model by the boundary concentrations for the Northeast and East boundaries (see Section 5).

The average spatial correlation for ozone levels greater than or equal to 5 pphm is 0.202. This value is lower than the temporal correlation coefficient. This feature has been discussed with the results of the 13 July 1979 simulation. The spatial correlation is lower than that obtained for the 13 July 1979 simulation. This lower spatial correlation may result from uncertainties in the Northeast and East boundary concentrations for

BEST COPY AVAILABLE

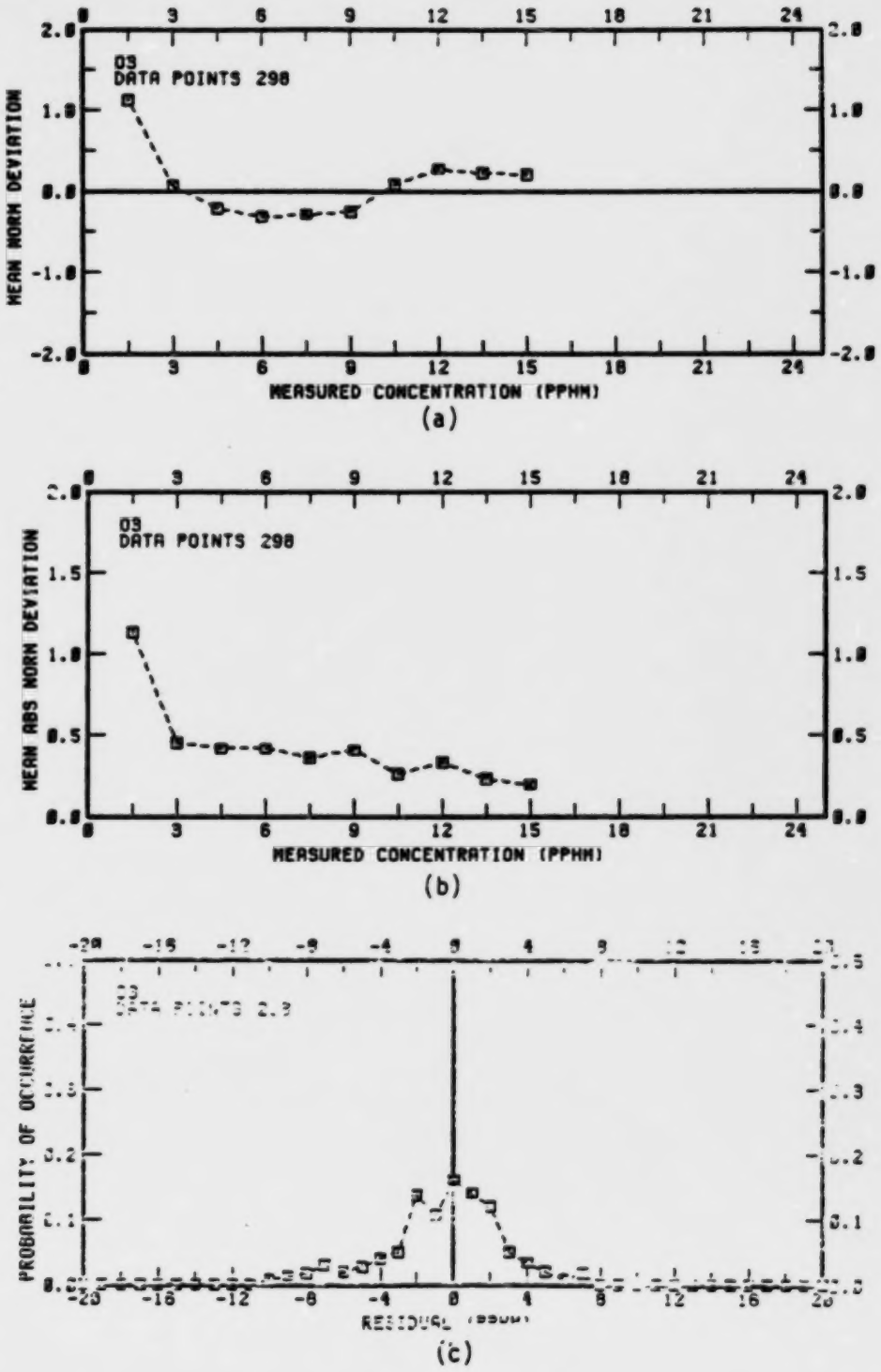

FIGURE 6-6. Mean normalized bias, mean normalized error as function of measured O_3 concentrations and distribution of residuals for 19 July 1979.

BEST COPY AVAILABLE

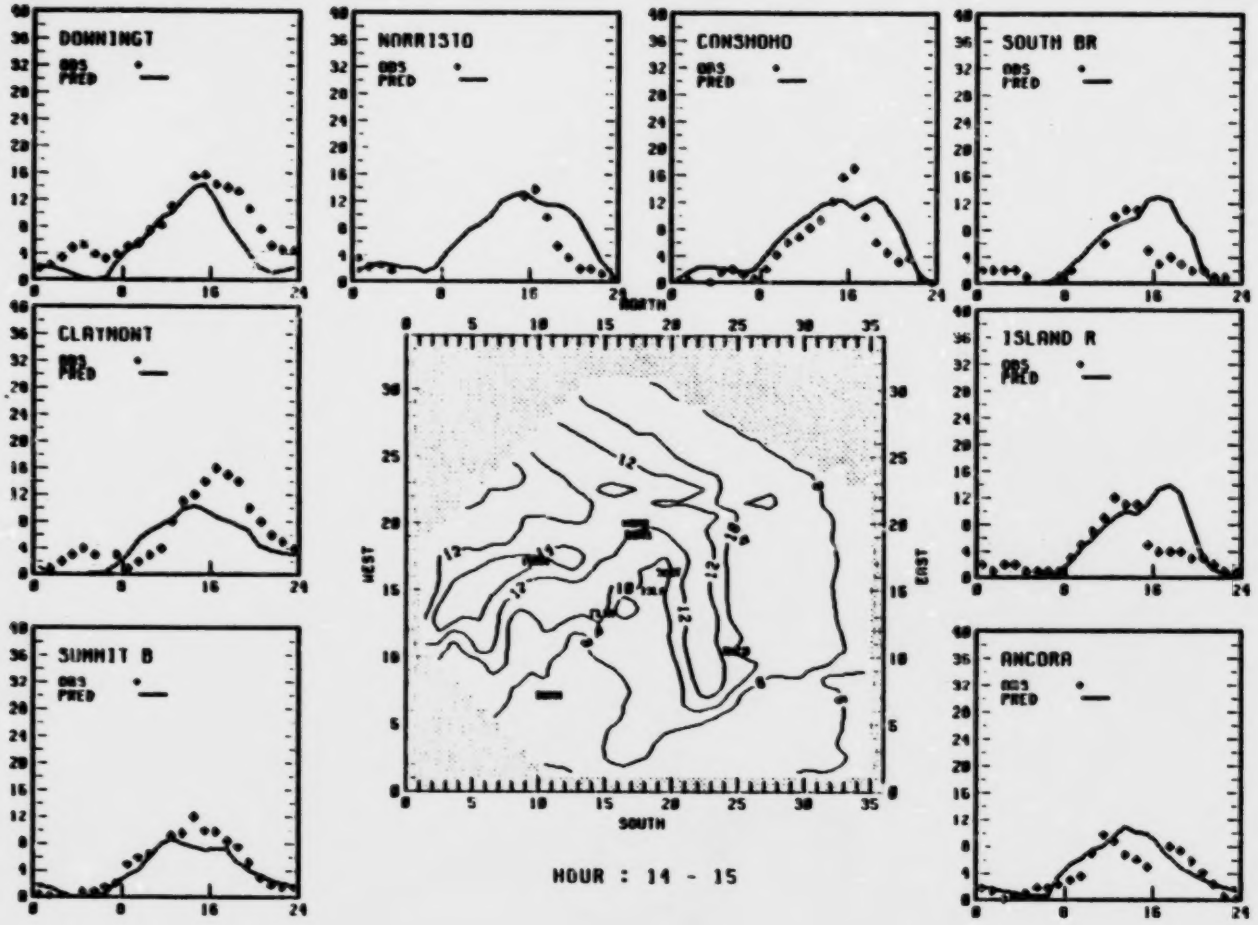

FIGURE 6-7. Time series (24 hours) of predicted versus observed ozone and spatially predicted ozone for the simulation of 19 July 1979, 1400 - 1500 EST.

BEST COPY AVAILABLE

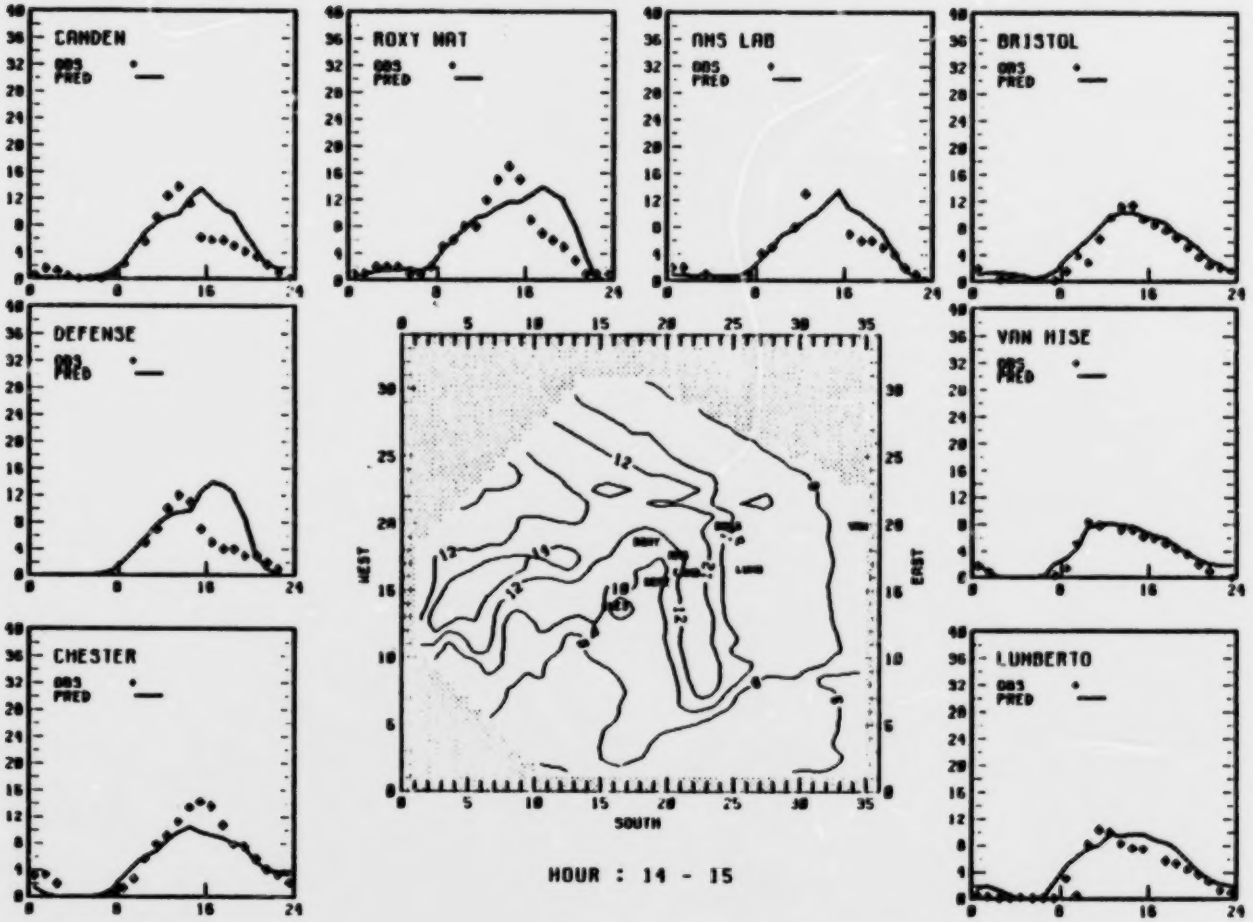

FIGURE 6-7 (concluded).

BEST COPY AVAILABLE

the 19 July 1979 simulation since the ozone field appears to be sensitive to these boundary concentrations and air quality data were insufficient to determine these concentrations with accuracy.

Overall Correlation

The distribution of the residuals (measured ozone concentration minus calculated ozone concentrations) is shown in Figure 6-6c. Most of the residuals are within ± 3 pphm, with a mean value of -0.6 pphm. A scatter plot of the pairs of calculated and measured ozone concentrations is presented in Figure 6-8. Seventy-five percent of the predictions are within a factor of 2 of the observations. The correlation coefficient is 0.769.

COMPARISON OF PHILADELPHIA RESULTS WITH UAM PERFORMANCE IN OTHER CITIES

To provide perspective on how the Philadelphia simulation compares with other recent model applications, Table 6-5 summarizes the results of simulations for Los Angeles, Tulsa, Sacramento, and Denver. These data indicate that the model generally tends to underpredict by from 1 to 15 percent. The cases of overprediction are the Tulsa simulation of 2 September, the Los Angeles simulation of 26 June, and the Philadelphia simulations of both 13 and 19 July 1979.

The Philadelphia simulations show gross errors of 34 and 31 percent for the 13 and 19 July 1979 simulations, respectively. Other Airshed Model simulations show gross errors ranging from 21 to 57 percent. Thus, model performance for the Philadelphia simulations appears to be commensurate with performance obtained in previous model applications.

In a study of the expected accuracy of photochemical air quality simulation models (AQSM) arising from likely uncertainties in model inputs, Seinfeld (1977) stated that "one is inclined to place an overall uncertainty on oxidant level predictions from current AQSM of ± 50 percent." The results of the application of the UAM to Philadelphia appear to be consistent with this expected level of performance, which is the only available stated "standard" of photochemical grid model performance.

BEST COPY AVAILABLE

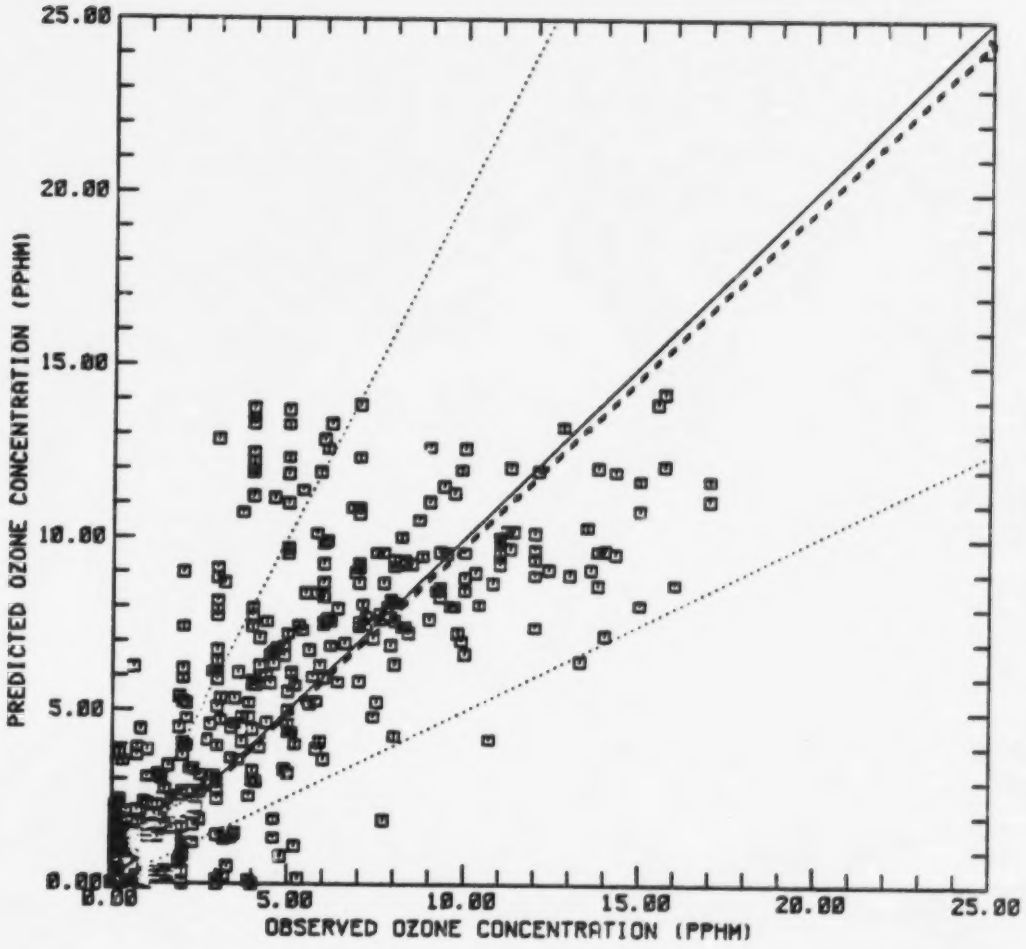

FIGURE 6-8. Scatter plot of predicted and observed ozone concentrations for 19 July 1979. The correlation coefficient for the 445 pairs of O_3 concentrations is 0.769. The solid line represents perfect agreement between observed and predicted concentrations; the dotted lines represent the envelope of the predicted values that are within a factor of two of the corresponding observed values, and the heavy dashed line represents the regression line forced through the origin.

BEST COPY AVAILABLE

BLANK PAGE

BLANK PAGE

BLANK PAGE

TABLE 6-5. Comparison of UAM performance evaluation for ozone in Los Angeles, Tulsa, Sacramento, Denver, and Philadelphia.

City	Simulation	Mean Normalized Deviation[a]	Mean Normalized Absolute Deviation[a]	Number of Comparisons
Los Angeles[b]	26 June 1974	-0.05	0.37	246
	27 June 1974	0.10	0.33	320
Tulsa[c]	21 July 1977	0.04	0.37	129
	29 July 1977	0.07	0.21	136
	3 August 1977	0.04	0.31	115
	2 September 1977	-0.22	0.34	110
Sacramento[d]	28 June 1976	0.01	0.22	42
	24 August 1976	0.22	0.29	52
Denver[e]	29 July 1975	0.09	0.50	62
	28 July 1976	0.15	0.57	91
Philadelphia	13 July 1979	-0.28	0.34	307
Philadelphia	19 July 1979	-0.08	0.31	335

[a] All statistics for all cases were computed using the same method, and mean deviations were normalized with respect to the measured O_3 concentrations. This differs from Tables 6-2 and 6-3, where the mean deviations were normalized with respect to the arithmetic average of the measured and calculated O_3 concentrations. All values reported in this column are for comparisons with measured values > 2 pphm, with the exception of Philadelphia, where the cutoff is > 5 pphm.

[b] The Los Angeles results are discussed by Tesche et al. (1982a, b).

[c] The Tulsa results are discussed by Reynolds et al. (1982).

[d] The Sacramento results are described by Reynolds et al. (1979).

[e] The Denver results are described by Reynolds et al. (1979).

109

BEST COPY AVAILABLE

BLANK PAGE

7 OZONE SENSITIVITY ANALYSIS

METHODOLOGY

After the base case simulations for 13 and 19 July were completed, a number of ozone sensitivity simulations were performed. These simulations were carried out to examine the UAM's sensitivity to the principal factors that might affect National Ambient Air Quality Standard (NAAQS) ozone attainment control strategy development. In these sensitivity simulations only hydrocarbon emissions and initial conditions were reduced; emissions and initial conditions of NO_x were left unchanged. Along with the emission and initial condition reductions, simulations were performed to test the sensitivity of predicted ozone levels to key inputs for the simulation (e.g., boundary conditions and assumed background concentrations). A total of 34 sensitivity simulations were performed combining hydrocarbon emission reductions with various assumptions of boundary conditions and background concentrations specified for hydrocarbons and ozone. The list of simulations is presented in Table 7-1. All simulations cover the time period 0000-2000 EST.

Hydrocarbons were reduced in the low-level area source and elevated point source files by multiplying all source emission rates by appropriate factors, resulting in a total reduction of hydrocarbon emissions by 25, 50, or 75 percent. Initial condition concentrations were reduced in a different manner. Reduced initial concentrations at stations with available data were obtained by first subtracting a background total RHC value of 0.06 ppmC (Killus, 1982) from the base case initial concentrations, then reducing the resulting value by the appropriate factor (25, 50, or 75 percent), and finally, by adding the background value of 0.06 ppmC to this value to obtain a new initial value. Table 7-2 presents the initial conditions for RHC used in the base case and the hydrocarbon reduction simulations for 13 July. The observed value for Summit Bridge (0.05 ppmC) was close to background initially and was left unchanged in the hydrocarbon reduction simulations. Initial conditions in surface grid cells without monitors were obtained by employing a Poisson interpolation. After this surface field was computed, a vertical interpolation method was chosen such that the background concentration at the top of the modeling region (TOPCONC) was used in levels 3 and 4, and the level 2 value was obtained by a linear interpolation between the surface (level 1) value and the

BEST COPY AVAILABLE

Table 7-1. Simulation Designations for Philadelphia Airshed Sensitivity Analysis for 13 and 19 July 1979 .

Simulation Name	Date	Description
D.BASE	13 July	Base Case
D.25BC	"	Reduce BC's 25% in Emiss and Initial conditions
D.50BC	"	Reduce BC's 50% " " " " "
D.75BC	"	Reduce BC's 75% " " " " "
D.B50BC	"	Reduce BC's 50% in Emiss, Initial, SE Boundary
D.BKBC	"	Reduce Background BC's in Run D.BASE
D.25BC.BKBC	"	Reduce Background BC's in Run D.25BC
D.50BC.BKBC	"	" " " in Run D.50BC
D.75BC.BKBC	"	" " " in Run D.75BC
D.BKO3	"	Reduce Background O3 in Run D.BASE
D.25BC.BKO3	"	Reduce Background O3 in Run D.25BC
D.50BC.BKO3	"	" " " in Run D.50BC
D.75BC.BKO3	"	" " " in Run D.75BC
D.BKBC.O3	"	Reduce Background BC's, O3 in Run D.BASE
D.25BC.BKBC.O3	"	Reduce Background BC's, O3 in Run D.25BC
D.50BC.BKBC.O3	"	" " " " in Run D.50BC
D.75BC.BKBC.O3	"	" " " " in Run D.75BC
6.BASE	19 July	Base case
6.25BC	"	Reduce BC's 25% in Emiss and Initial conditions
6.50BC	"	Reduce BC's 50% " " "
6.75BC	"	Reduce BC's 75% " " "
6.B25BC	"	Reduce BC's 25% in Emiss, Initial, NE Boundary
6.B50BC	"	Reduce BC's 50% " " " "
6.B75BC	"	Reduce BC's 75% " " " "
6.BKBC	"	Reduce Background BC's in Run 6.BASE
6.B25BC.BKBC	"	Reduce Background BC's in Run 6.B25BC
6.B50BC.BKBC	"	" " " in Run 6.B50BC
6.B75BC.BKBC	"	" " " in Run 6.B75BC
6.BKO3	"	Reduce Background O3 in Run 6.BASE
6.B25BC.BKO3	"	Reduce Background O3 in Run 6.B25BC
6.B50BC.BKO3	"	" " " in Run 6.B50BC
6.B75BC.BKO3	"	" " " in Run 6.B75BC
6.BKBC.O3	"	Reduce Background BC's and O3 in Run 6.BASE
6.B25BC.BKBC.O3	"	Reduce Background BC's, O3 in Run 6.B25BC
6.B50BC.BKBC.O3	"	" " " " in Run 6.B50BC
6.B75BC.BKBC.O3	"	" " " " in Run 6.B75BC

BEST COPY AVAILABLE

TABLE 7-2. Total RHC concentrations used as initial conditions for base case and hydrocarbon reduction simulations for 13 July.

Station	Base Case RHC (ppmC)	25 Percent Reduction RHC (ppmC)	50 Percent Reduction RHC (ppmC)	75 Percent Reduction RHC (ppmC)
AMS Lab	1.05	0.803	0.555	0.308
Chester	2.10	1.59	1.08	0.570
Lumberton	0.2	0.165	0.13	0.095
Norristown	0.39	0.308	0.225	0.1425
South Broad	0.30	0.24	0.180	0.120
Summit Bridge	0.05	0.05	0.050	0.050

BEST COPY AVAILABLE

level-3 value. This method was used to initialize all grid cells in all levels with appropriate concentrations for all species before commencement of the ozone sensitivity simulation. Initial concentrations for 19 July were obtained using the same procedure as that for 13 July. These values are presented in Table 7-3.

For 13 July, the base-case emissions and initial conditions were reduced by 25, 50, and 75 percent, respectively, for three simulations (D.25HC, D.50HC, and D.75HC). The analysis was extended by examining the sensitivity of predicted ozone to reductions in background hydrocarbons and background ozone in separate simulations and by reducing both background hydrocarbon and ozone in the same simulations along with the reduced hydrocarbon emissions and initial conditions. Only one simulation involving a reduction of the Southeast boundary hydrocarbon concentrations was performed for 13 July. Differences of less than 1 ppb for predicted ozone were found for this simulation (D.B50HC). Because of this result and the fact that the designated boundary hydrocarbon concentrations along the Southeast boundary were already close to background when inflow from this boundary occurred, all subsequent sensitivity simulations for 13 July used combinations of reduced emissions, initial conditions, and background, but did not reduce concentrations along the Southeast boundary.

For 19 July, ozone precursors from the New Jersey/New York urban area that were transported through the Northeast and East boundaries mixed with the local emissions to produce high levels of ozone. Hydrocarbon emissions and initial conditions were reduced in three simulations (6.25HC, 6.50HC, and 6.75HC). In all subsequent hydrocarbon reduction simulations for 19 July, boundary conditions on the Northeast and East boundaries were also reduced by 25, 50, or 75 percent. These simulations were performed to test the sensitivity of ozone by control of hydrocarbons in the local airshed (Philadelphia) and a neighboring airshed (New Jersey/New York urban area). Values of reduced hydrocarbons for the Northeast and East boundaries were obtained in a manner similar to that used to obtain the reduced initial conditions. Background concentrations of the speciated hydrocarbons (see Table 5-3) were subtracted from the base-case hourly hydrocarbon boundary value (Table 5-5). This intermediate value was then reduced by 25, 50, or 75 percent, and the background was added, resulting in a new hourly value for the boundary concentration. Boundary conditions for hydrocarbons already below background were left unchanged.

Background values for hydrocarbons and ozone were reduced in a number of the sensitivity simulations. These background values were designated for the top of the modeling region, as initial conditions above the mixing height, and for all boundaries, except the Southeast boundary for 13 July and the Northeast and East boundaries for 19 July below the mixing

BEST COPY AVAILABLE

TABLE 7-3. Total RHC concentrations used as initial conditions for base case and hydrocarbon reduction simulations for 19 July.

Station	Base Case RHC (ppmC)	25 Percent Reduction RHC (ppmC)	50 Percent Reduction RHC (ppmC)	75 Percent Reduction RHC (ppmC)
AMS Lab	0.35	0.2775	0.205	0.1325
Chester	0.95	0.7275	0.505	0.2825
Downington	0.05	0.05	0.05	0.05
Lumberton	0.4	0.315	0.23	0.145
Norristown	0.29	0.2325	0.175	0.1175
South Broad	0.25	0.2025	0.155	0.1075
Summit Bridge	0.1	0.09	0.08	0.07

BEST COPY AVAILABLE

height. These values are presented in Table 7-4. The reduced RHC background values for both days represent a reduction of nearly 50 percent from the base-case values. For 13 July, the background ozone value was reduced 50 percent, and for 19 July, the background ozone was reduced 33 percent.

RESULTS OF OZONE SENSITIVITY SIMULATIONS FOR 13 JULY

A total of 16 ozone sensitivity simulations were performed for 13 July (Table 7-1). Ozone response in all simulations, compared to base-case predictions, was obtained by examining both the predicted maximum over the entire grid for the simulation day and the predicted distance-weighted* average maximum value at the two highest monitors. Both peak grid and peak station maxima were examined because previous evaluations of the UAM (EPA, 1983b) have shown that when hydrocarbon emissions are reduced, the daily maximum ozone predictions may migrate and "... emission control requirements should not be based on ozone predictions constrained to a particular monitoring site" (Layland and Cole, 1983). The peak predicted grid value is the actual peak value obtained in a particular grid cell, whereas the maximum at a station monitor is a distance-weighted average value of the four closest grid cell values. Table 7-5 presents the hourly predicted maximum ozone for the base case and all sensitivity simulations for the Philadelphia urban plume peak (located north of urban center), the Roxy Water monitor, and the Norristown monitor. Also included in the table are the relative and total ozone reductions for each sensitivity case. The relative reductions were obtained by comparing the emission reduction simulation with the corresponding simulation without reduced emissions (e.g., compare D.BKHC with D.50HC.BKHC). The total ozone reduction value was obtained by comparing sensitivity simulations to the base case (D.BASE).

The values in Table 7-5 are presented graphically in two ways. The first type of graph compares the percent hydrocarbon emission reduction with the peak predicted hourly average ozone value, while the second type compares the percent of hydrocarbon emission reduction with either the total or relative percent of ozone reduction. Also depicted on the former graph is the level of the NAAQS (12 pphm) for ozone.

Figure 7-1 presents a comparison of the peak predicted hourly average ozone of the Philadelphia urban plume for all sensitivity simulations

---

* The distance weighted average concentration is obtained by computing the distance weighted average of the concentrations at the centroids of the four grid cells closest to the station monitor in question.

BEST COPY AVAILABLE

TABLE 7-4. Reduced background concentrations used in the ozone sensitivity simulations of 13 and 19 July.

Species	Concentration (ppm)
ETH	0.0
OLE	0.0
PAR	0.03
CARB	0.003
ARO	0.0
CO	0.1
O_3	0.04

BEST COPY AVAILABLE

TABLE 7-5. Hourly predicted maximum ozone and ozone reductions for the ozone sensitivity simulations of 13 July.

Simulation	Philadelphia Urban Plume Peak			Roxy Water, PA			Norristown, PA		
	Ozone Prediction (pphm)	Ozone Reduction (percent)		Ozone Prediction (pphm)	Ozone Reduction (percent)		Ozone Prediction (pphm)	Ozone Reduction (percent)	
		Relative	Total		Relative	Total		Relative	Total
D.BASE	26.6	-	-	19.3	-	-	19.3	-	-
D.25HC	20.6	22.5	22.5	14.3	25.8	25.8	15.6	19.2	19.2
D.50HC	14.7	44.7	44.7	11.5	40.4	40.4	12.0	37.8	37.8
D.75HC	12.4	53.4	53.4	9.5	50.7	50.7	9.7	49.8	49.8
D.BKHC	23.3	-	12.4	15.9	-	17.6	16.0	-	17.1
D.25HC.BKHC	16.5	29.2	38.0	11.3	29.1	41.4	12.1	24.4	37.3
D.50HC.BKHC	10.4	55.4	60.9	8.0	49.7	58.5	8.8	45.2	54.4
D.75HC.BKHC	8.6	63.1	67.7	6.0	62.5	68.9	6.7	58.3	65.3
D.BK03	25.6	-	3.7	17.9	-	7.3	17.9	-	7.3
D.25HC.BK03	19.3	24.6	27.4	12.9	28.1	33.2	14.0	21.8	27.5
D.50HC.BK03	13.0	49.2	51.1	9.7	46.1	49.7	10.2	43.1	47.1
D.75HC.BK03	10.4	59.4	60.9	7.4	59.0	61.7	7.5	58.1	61.1
D.BKHC.03	22.2	-	16.5	14.5	-	24.9	14.4	-	25.4
D.25HC.BKHC.03	14.9	32.9	44.0	9.6	34.0	50.3	10.2	28.9	47.1
D.50HC.BKHC.03	8.4	62.2	68.4	5.8	60.1	69.9	6.6	54.2	65.8
D.75HC.BKHC.03	5.9	73.4	77.8	4.8	67.1	75.1	4.1	71.5	78.8

BEST COPY AVAILABLE

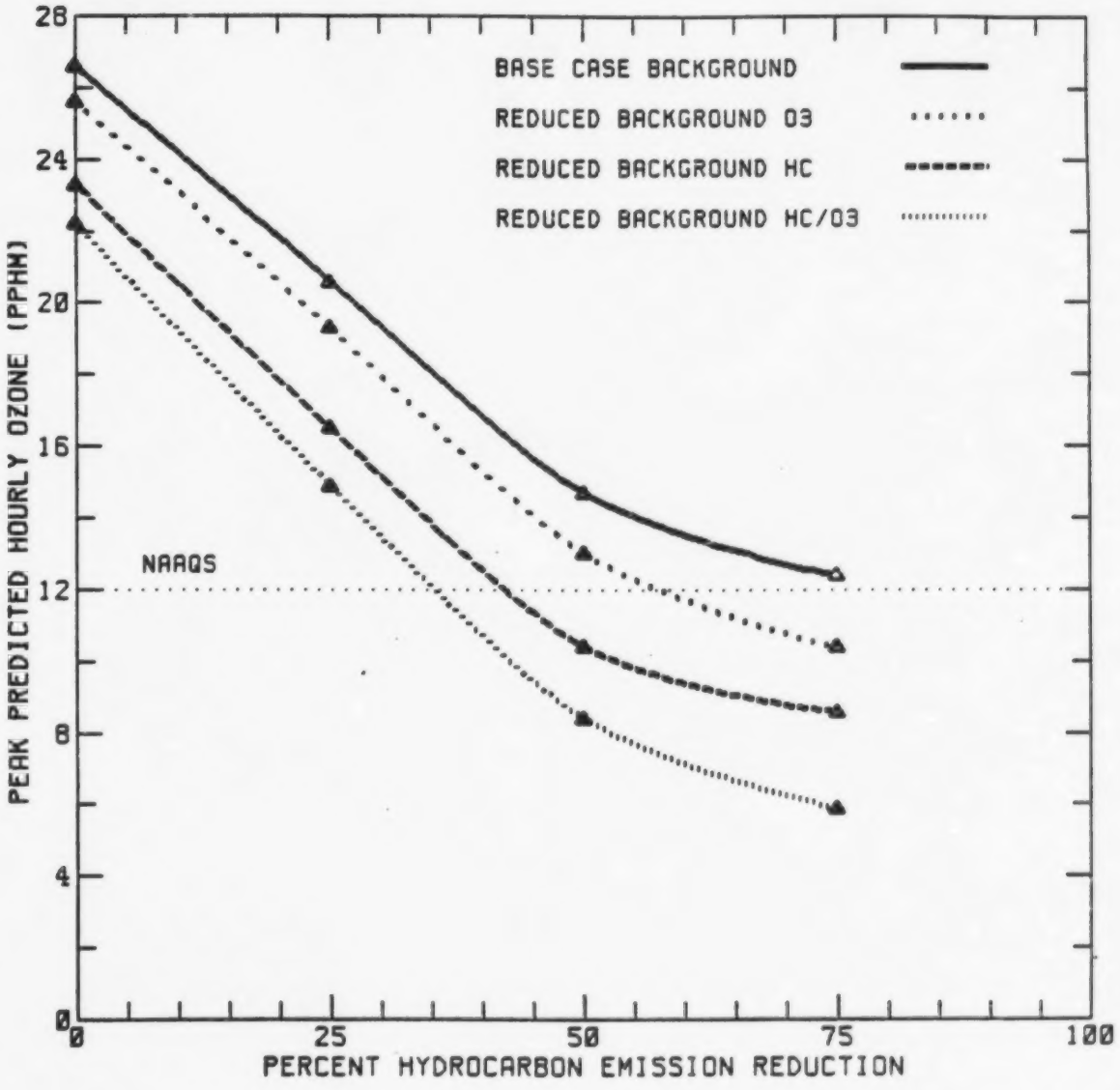

FIGURE 7-1. Predicted ozone response to hydrocarbon emission reductions for peak regional ozone in the Philadelphia urban plume for 13 July.

BEST COPY AVAILABLE

with the percent of hydrocarbon emission reduction. Similar graphs are presented in Figures 7-2 and 7-3 for the station monitors of Roxy Water and Norristown (both located in Pennsylvania, northwest of the urban center of Philadelphia), respectively. Figures 7-4, 7-5, and 7-6 present response curves of relative ozone reductions for the peak of the urban plume, the Roxy Water, and Norristown monitors, respectively. Figures 7-7, 7-8, and 7-9 present response curves of total ozone reduction for the urban plume, Roxy Water, and Norristown monitors, respectively.

All of the figures contain information that might guide the possible formulation of broad control requirements for attaining the ozone NAAQS; however, since specific source categories were not addressed (e.g., mobile and stationary sources), the results cannot be used directly to formulate an ozone NAAQS attainment strategy. Figure 7-1, for example, shows that the peak predicted value in the base case (26.6 pphm) would not meet ambient standards for ozone even with a 75 percent reduction in hydrocarbon emissions, assuming no change in background levels for hydrocarbons and ozone. If, however, background ozone levels are reduced by 50 percent, the standard can be met with only a 58 percent reduction of hydrocarbon emissions. If hydrocarbon background levels are reduced by 50 percent, with ozone background unchanged, then modeling analysis shows that the ozone standard will be met with only a 43 percent hydrocarbon emission reduction. If background hydrocarbon and ozone levels are reduced by 50 percent, Figure 7-1 reveals that ambient ozone levels will meet the national standard with only a 35 percent reduction in hydrocarbon emissions. The percent of hydrocarbon emission reductions needed to reach the standard at the Roxy Water and Norristown monitors is lower for the four cases as shown in Figures 7-2 and 7-3, respectively. All emission reduction values required to meet the ozone standard for all sensitivity simulations of 13 July are summarized in Table 7-6. This table shows a wide spectrum of control requirements both in comparison of the regional peak with the highest station predictions, and in comparisons of the various assumptions for background hydrocarbons or ozone. Using the values of the regional peak is a conservative approach for estimating control requirements because the peak predicted ozone (26.6 pphm) is more than 30 percent greater than that observed during the entire summer field program. Control requirements at the two highest monitors are very similar for the four sets of sensitivity simulations, with nearly 50 percent hydrocarbon control needed, assuming no change in background concentrations, and only 14 percent control needed if background for both ozone and hydrocarbon is decreased by 50 percent.

Spatial patterns of predicted ozone can be illustrated with the use of Deficit/Enhancement (D/E) plots which show the areal extent of the decrease or increase for ozone in the Philadelphia airshed for each sensitivity simulation compared to the base case simulation. Ozone decreases

BEST COPY AVAILABLE

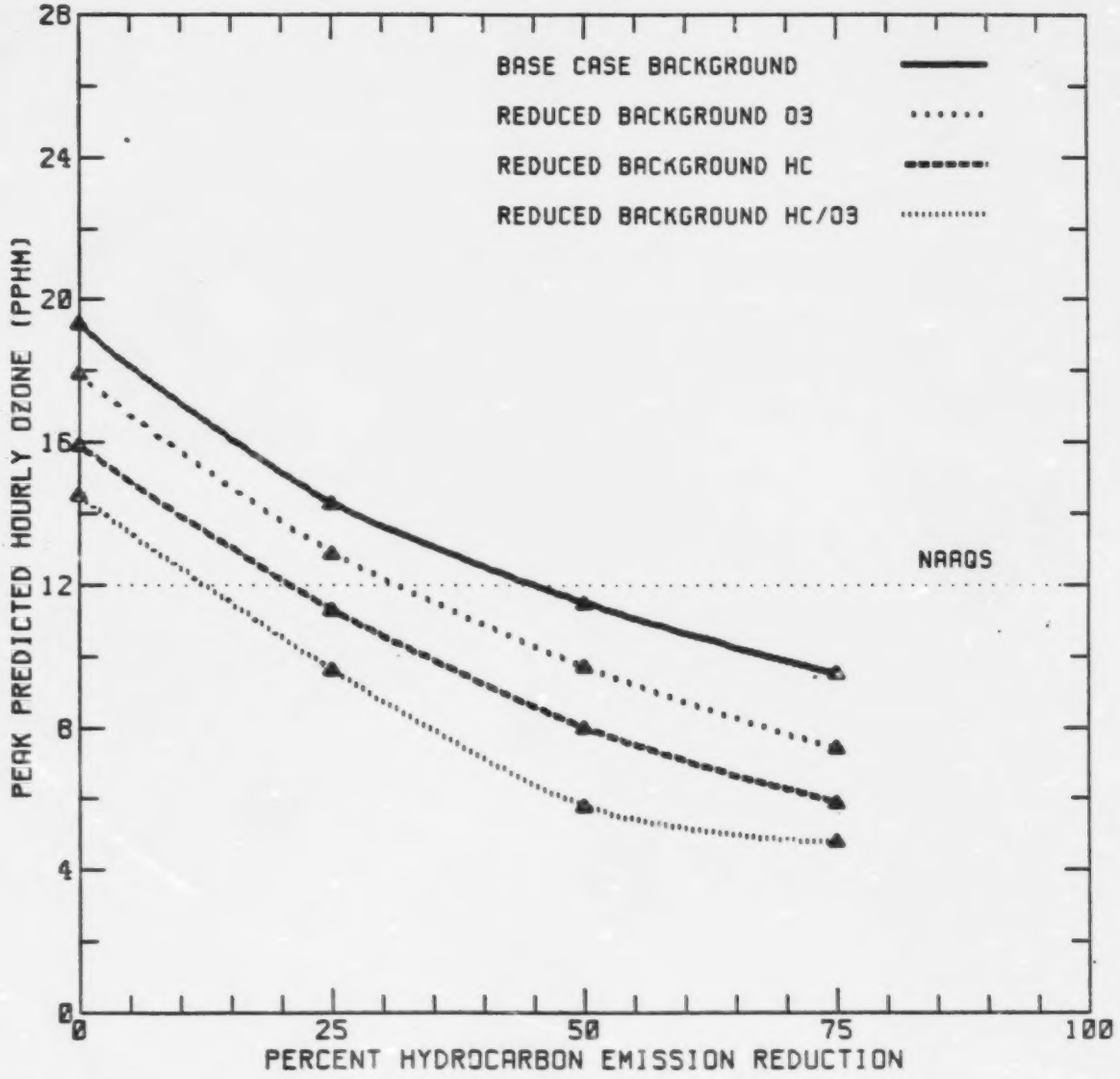

FIGURE 7-2. Predicted ozone response to hydrocarbon emission reductions for 13 July at the Roxy Water, PA monitor.

BEST COPY AVAILABLE

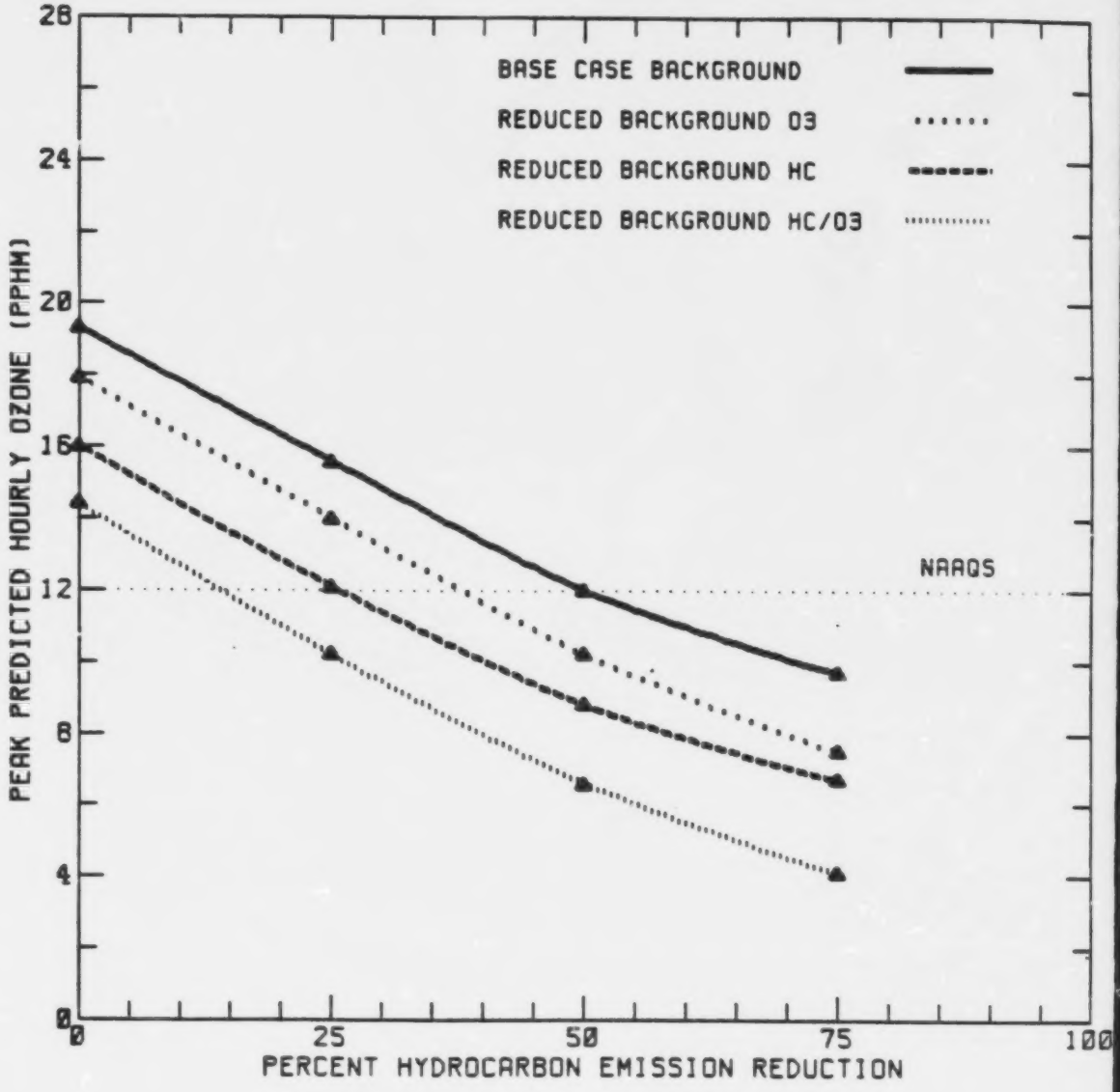

FIGURE 7-3. Predicted ozone response to hydrocarbon emission reductions for 13 July at the Norristown, PA monitor.

BEST COPY AVAILABLE

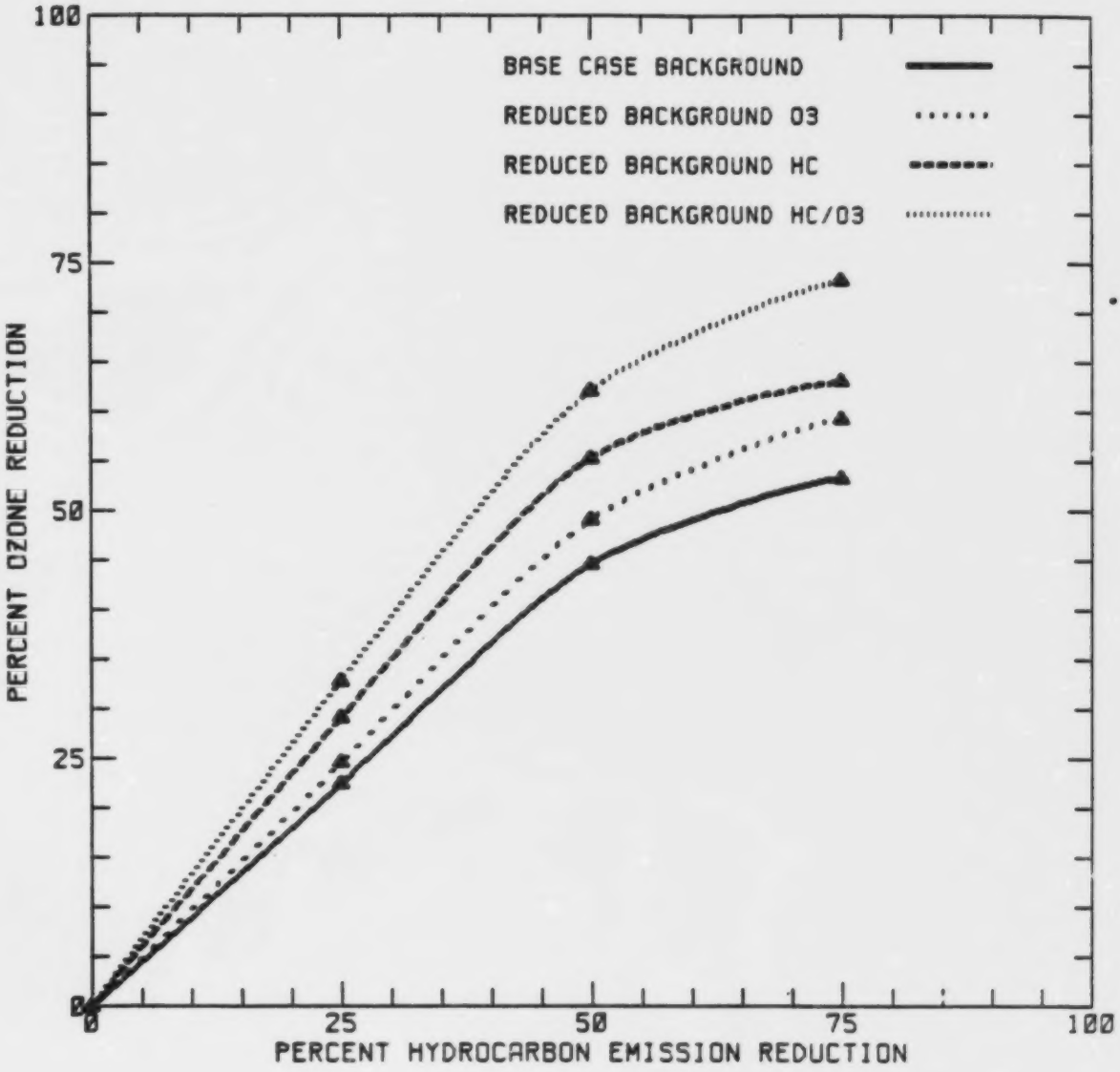

FIGURE 7-4. Relative ozone reduction (%) versus percent hydrocarbon emission reduction for peak regional ozone in the Philadelphia urban plume for 13 July.

BEST COPY AVAILABLE

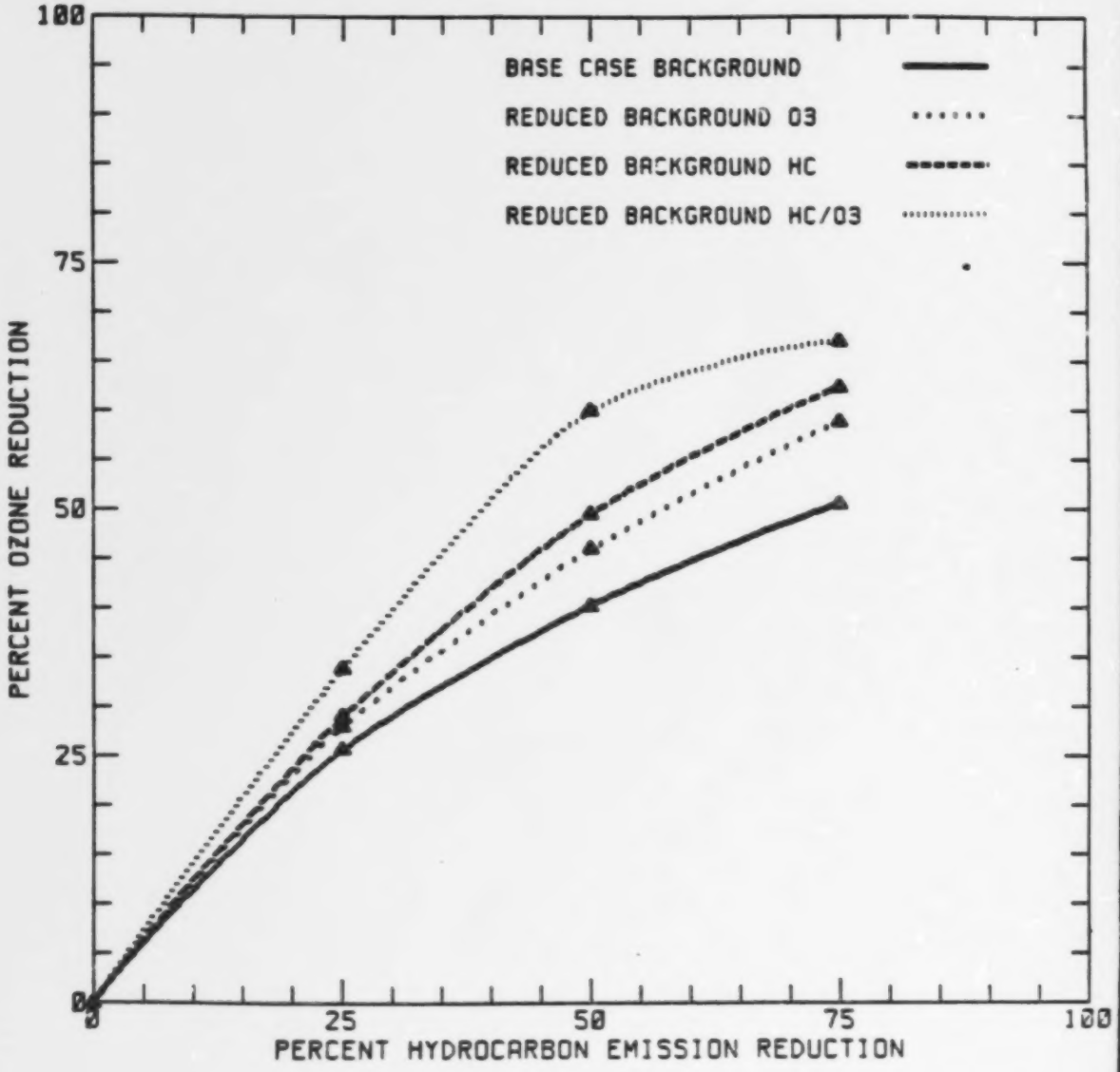

FIGURE 7-5. Relative ozone reduction (%) versus percent hydrocarbon emission reduction fr · 13 July at the Roxy Water, PA monitor.

BEST COPY AVAILABLE

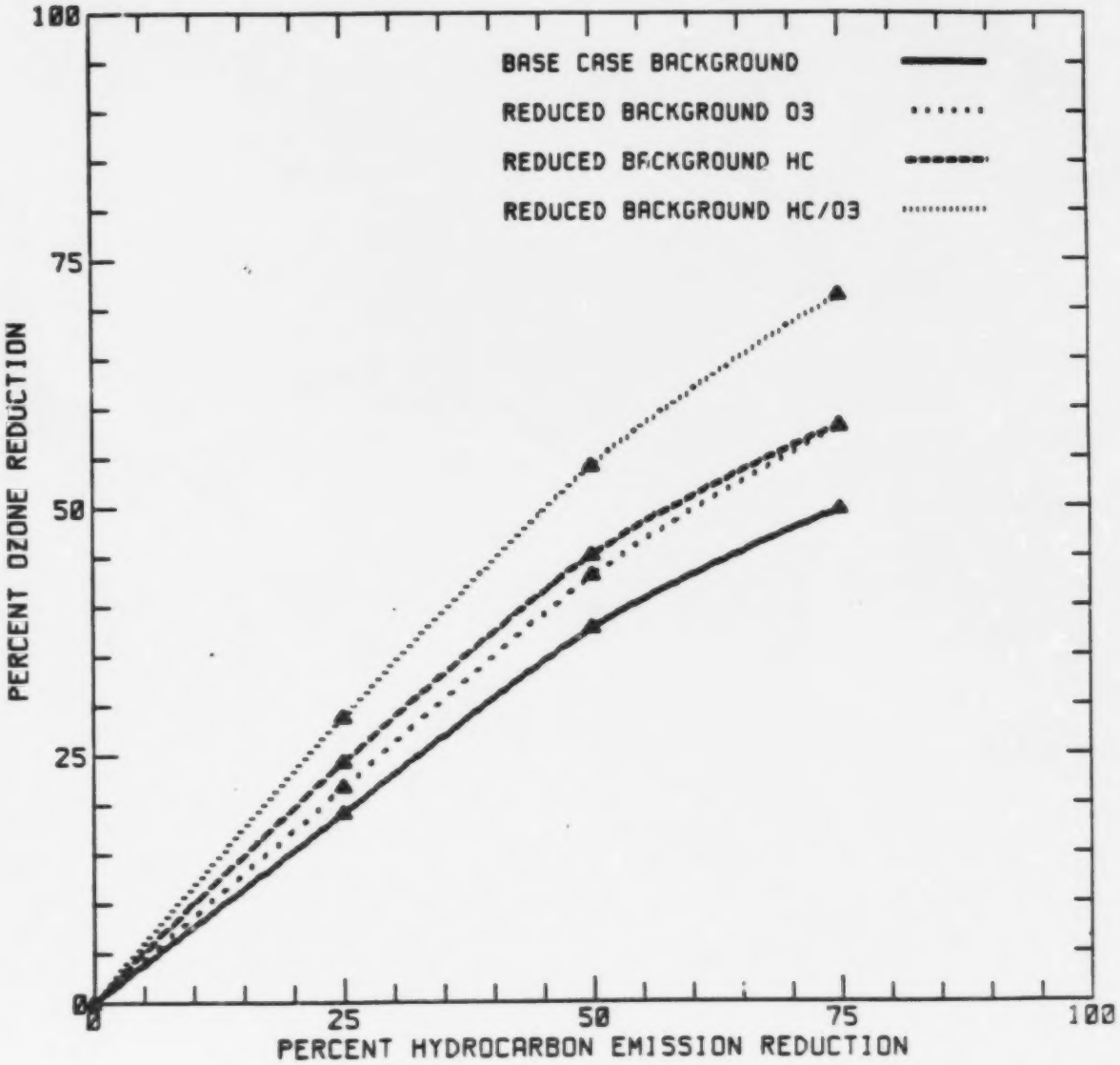

FIGURE 7-6. Relative ozone reduction (%) versus percent hydrocarbon emission reduction for 13 July at the Norristown, PA monitor.

BEST COPY AVAILABLE

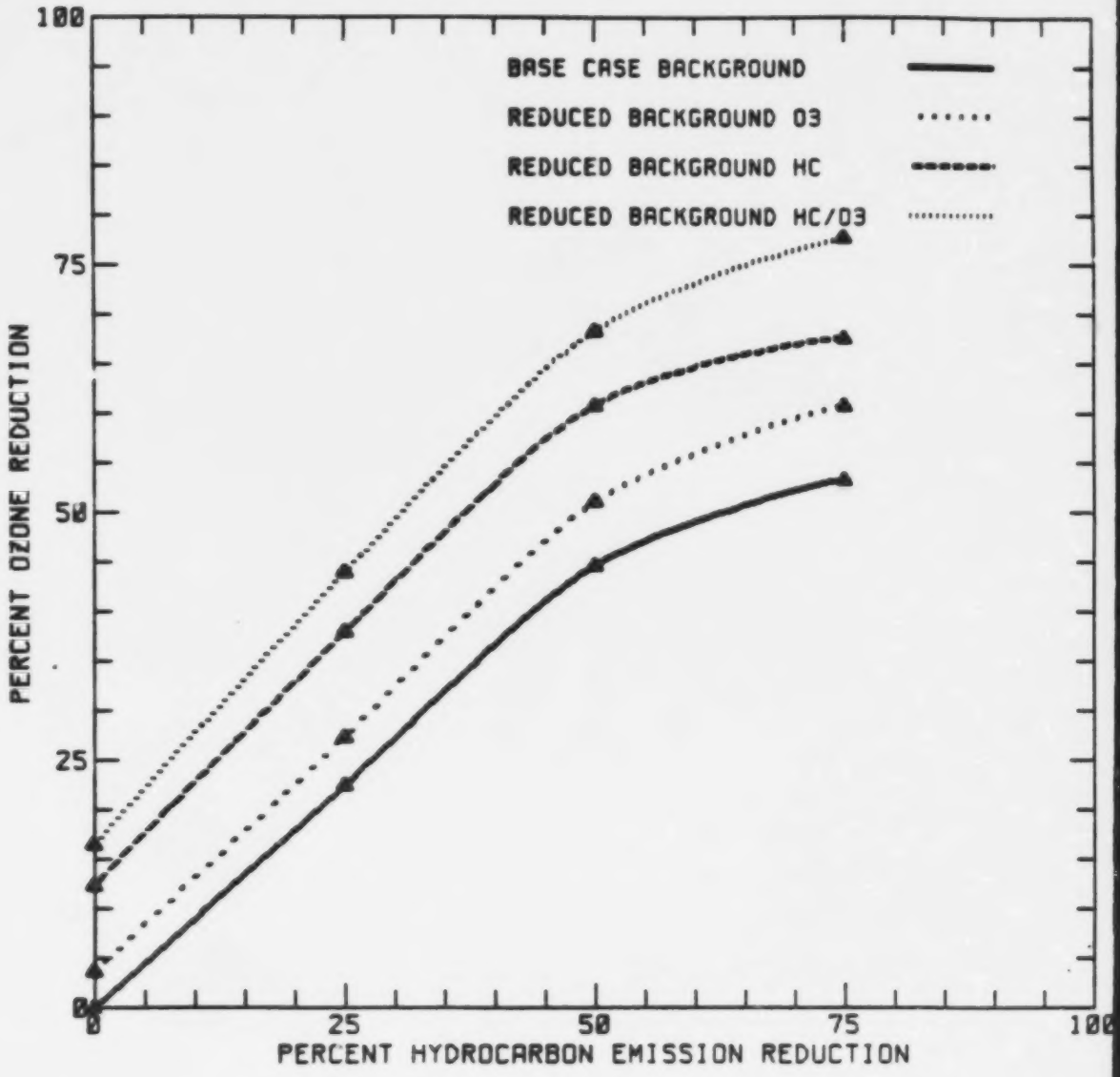

FIGURE 7-7. Total ozone reduction (%) versus percent hydrocarbon emission reduction for peak regional ozone in the Philadelphia urban plume for 13 July.

BEST COPY AVAILABLE

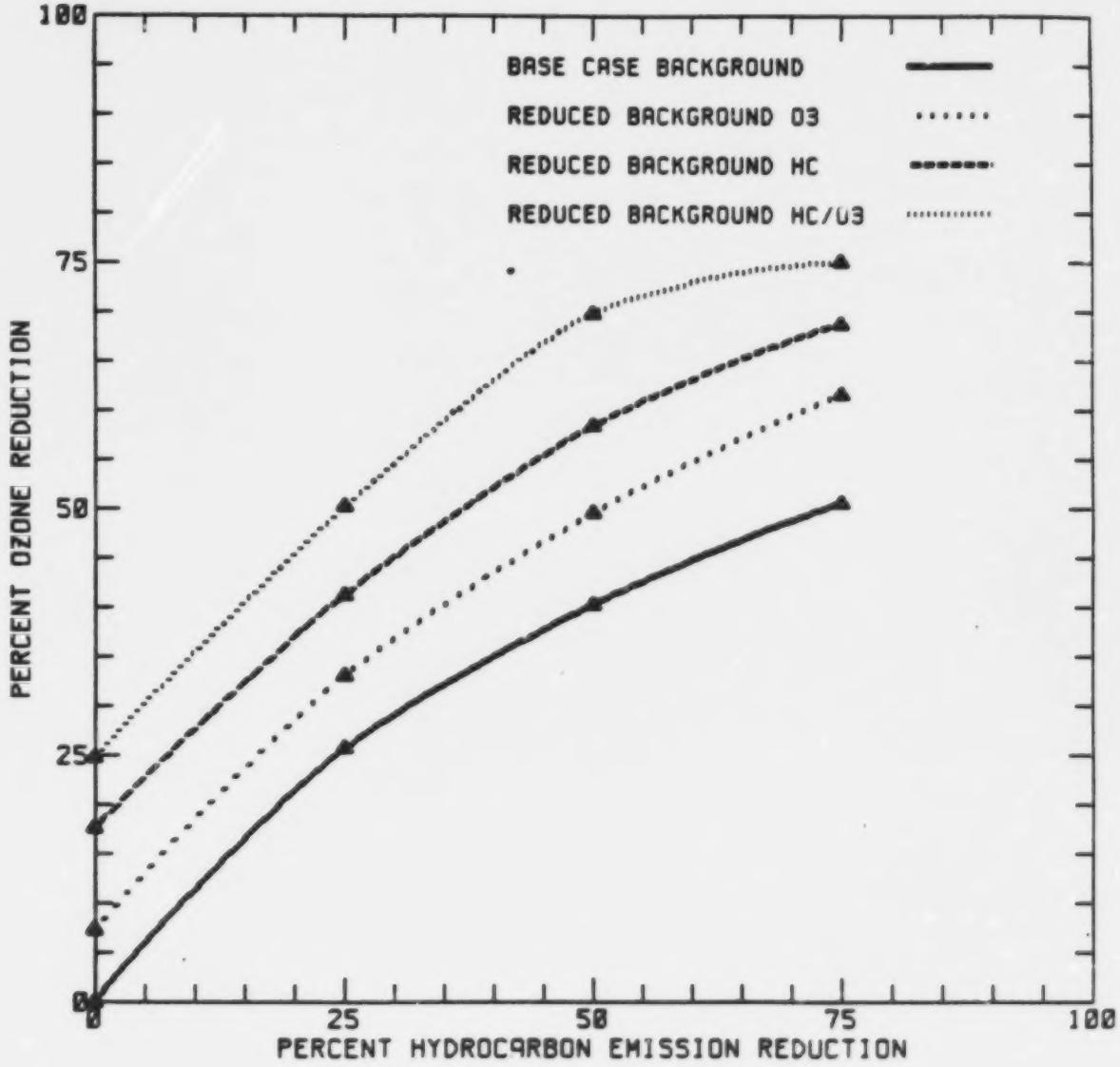

FIGURE 7-8. Total ozone reduction (%) versus percent hydrocarbon emission reduction for 13 July at the Roxy Water, PA monitor.

BEST COPY AVAILABLE

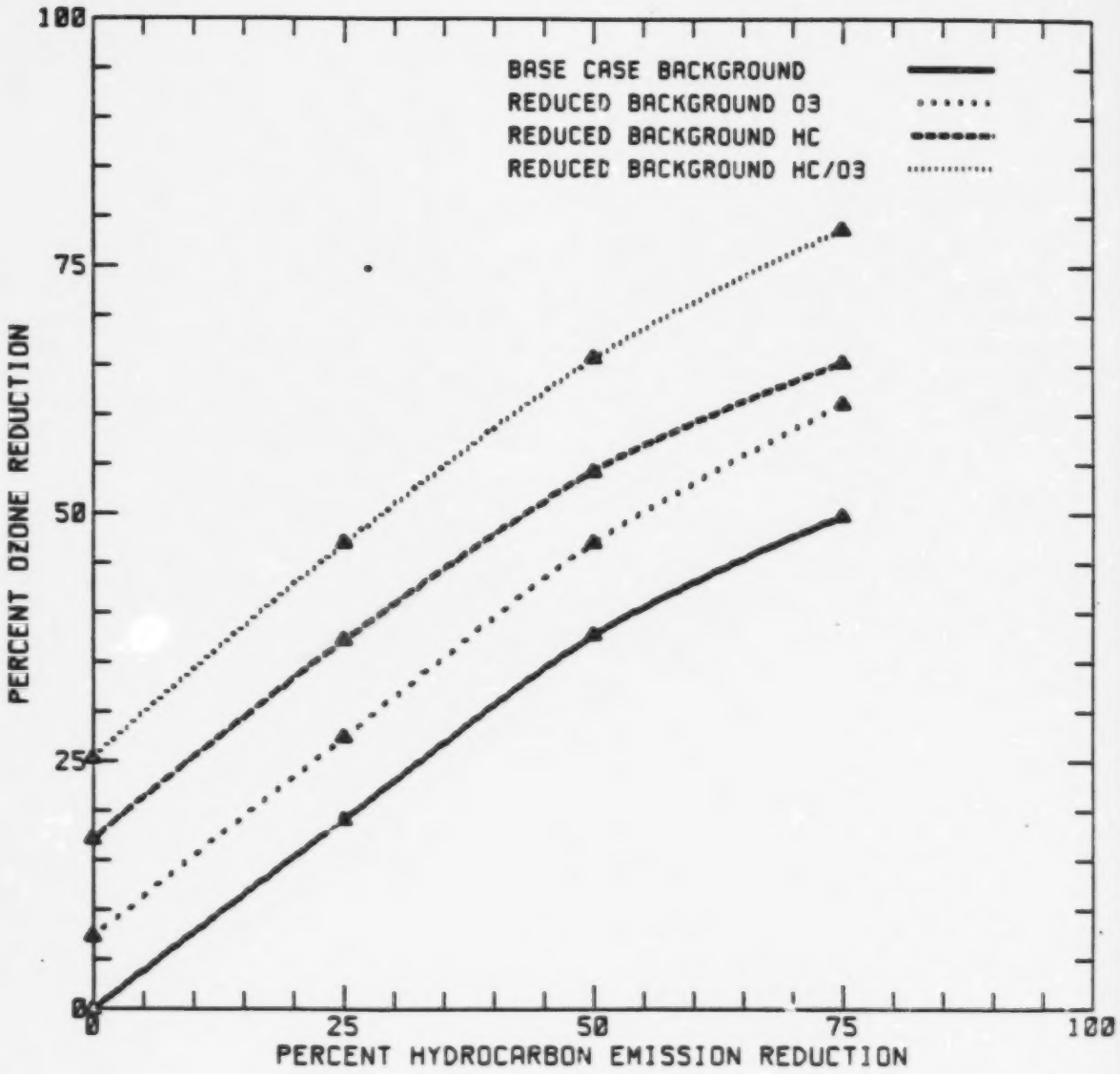

FIGURE 7-9. Total ozone reduction (%) versus percent hydrocarbon emission reduction for 13 July at the Norristown, PA monitor.

BEST COPY AVAILABLE

TABLE 7-6. Hydrocarbon emission reductions required to meet the NAAQS for ozone from the sensitivity simulations of 13 July.

Sensitivity Simulation	Percent Hydrocarbon Emission Reduction		
	Regional Peak	Roxy Water	Norristown
Base case background	> 75	45	50
Reduced background ozone	58	32	38
Reduced background hydrocarbons	43	21	27
Reduced background ozone and hydrocarbons	35	13	14

BEST COPY AVAILABLE

or increases can be depicted hourly, or the maximum D/E can be shown with one plot summarizing the maximum hourly increase or decrease for each grid cell over the entire simulation day. In this analysis, the maximum D/E patterns are presented for a number of the sensitivity simulations in Figures 7-10 through 7-21, as summarized in Table 7-7. Some of the Deficit/Enhancement plots show comparisons with the overall base case simulation (D.BASE), whereas others show comparisons with the corresponding simulation without hydrocarbon emission reduction (e.g., compare D.50HC.BKHC with D.BKHC). All the Deficit/Enhancement plots presented show decreases in predicted ozone. This is due to the fact that in the sensitivity simulations, combinations of urban emissions, background concentrations, and boundary conditions were reduced.

Figures 7-10 through 7-12 depict areal changes in ozone that resulted from reducing hydrocarbon emissions without changing background hydrocarbon or ozone levels. The largest decrease in ozone was 16 pphm (located in the center of the peak in the base case) with a 75 percent decrease in hydrocarbon emissions.

If no controls were specified for urban hydrocarbon emissions, the largest reduction in ozone would be 3 pphm if background ozone levels were halved (Figure 7-13). Similarly, a reduction of 4 pphm ozone over limited areas was obtained in the simulation by decreasing only background hydrocarbons (Figure 7-14). By decreasing both background ozone and hydrocarbons, the simulation revealed large areas to the north and west of the urban center where decreases of 5 pphm were calculated to occur (Figure 7-15). Figures 7-16 through 7-18 show comparisons with the base case of combinations of 50 percent hydrocarbon emission reduction and various assumptions for background hydrocarbon and ozone. Figure 7-18 compares the sensitivity simulation of 50 percent emission reduction and 50 percent decrease in both background ozone and hydrocarbon with the base case. This figure shows a decrease in predicted ozone of 18 pphm in an area north of the urban center. Figures 7-19 through 7-21 show relative differences between simulations with 50 percent reduction in hydrocarbon emissions and those with no emission reductions. The magnitude and areal extent of these patterns are, as expected, similar to the pattern depicted in Figure 7-11 where emissions were also reduced 50 percent.

RESULTS OF OZONE SENSITIVITY SIMULATIONS FOR 19 JULY

For the meteorological conditions of 19 July, a total of 18 ozone sensitivity simulations were performed (Table 7-1). As was done for 13 July, both the peak regional predicted ozone and the peak station ozone are examined. Because 19 July was a transport day with inflow of fresh precursors from the New Jersey/New York urban area, the peak predicted ozone

BEST COPY AVAILABLE

TABLE 7-7. Deficit/enhancement Figures for ozone for the 13 July sensitivity simulations.

Figure	Sensitivity Simulation	minus	Base Case Simulation
7-10	D.25BC	minus	D.BASE
7-11	D.50BC	minus	D.BASE
7-12	D.75BC	minus	D.BASE
7-13	D.BRO3	minus	D.BASE
7-14	D.BKBC	minus	D.BASE
7-15	D.BKBC.O3	minus	D.BASE
7-16	D.50BC.BRO3	minus	D.BASE
7-17	D.50BC.BKBC	minus	D.BASE
7-18	D.50BC.BKBC.O3	minus	D.BASE
7-19	D.50BC.BRO3	minus	D.BRO3
7-20	D.50BC.BKBC	minus	D.BKBC
7-21	D.50BC.BKBC.O3	minus	D.BKBC.O3

BEST COPY AVAILABLE

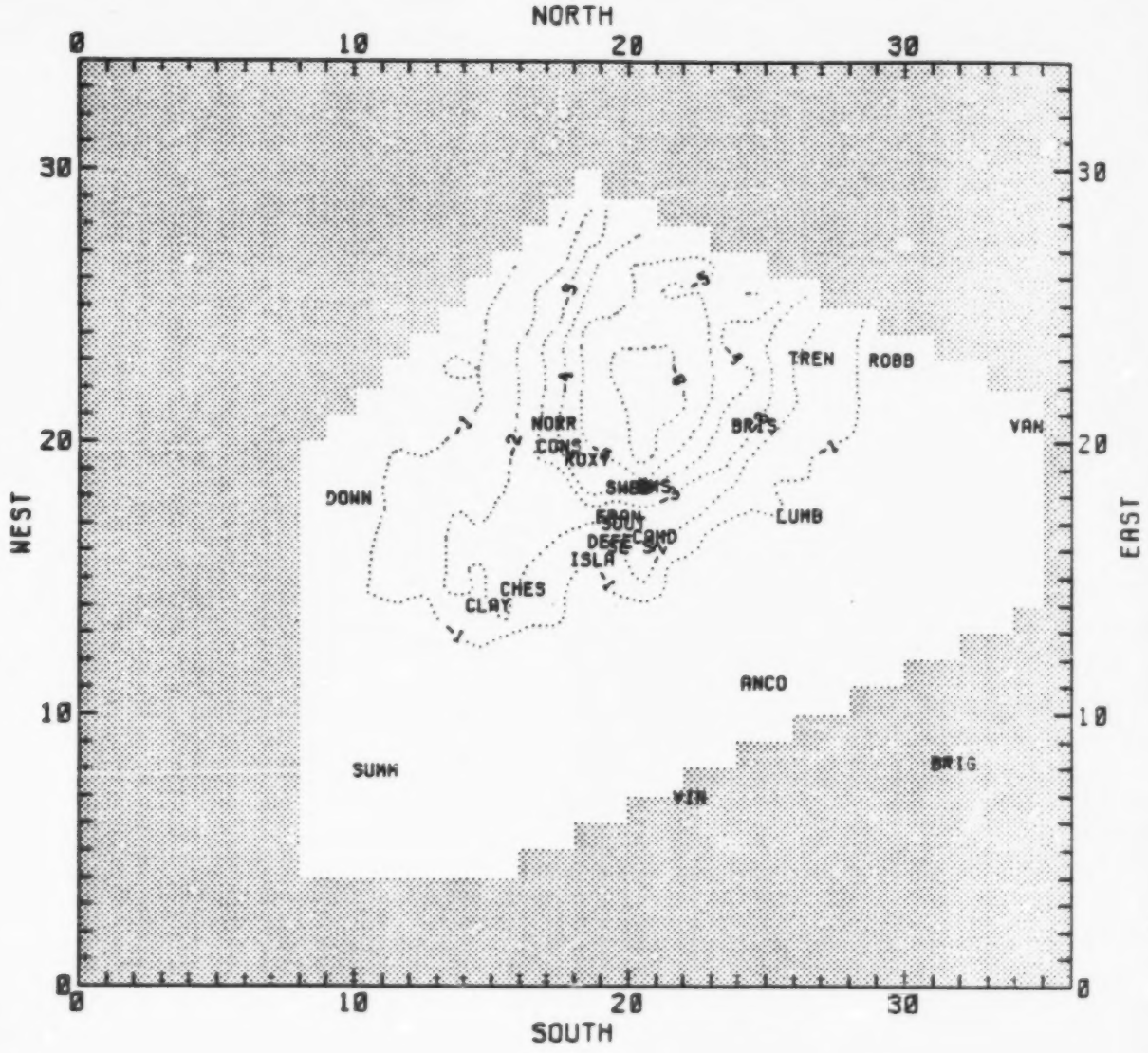

FIGURE 7-10. Maximum deficit/enhancement for ozone (pphm) for all hours for 13 July [D.25HC minus D.BASE].

BEST COPY AVAILABLE

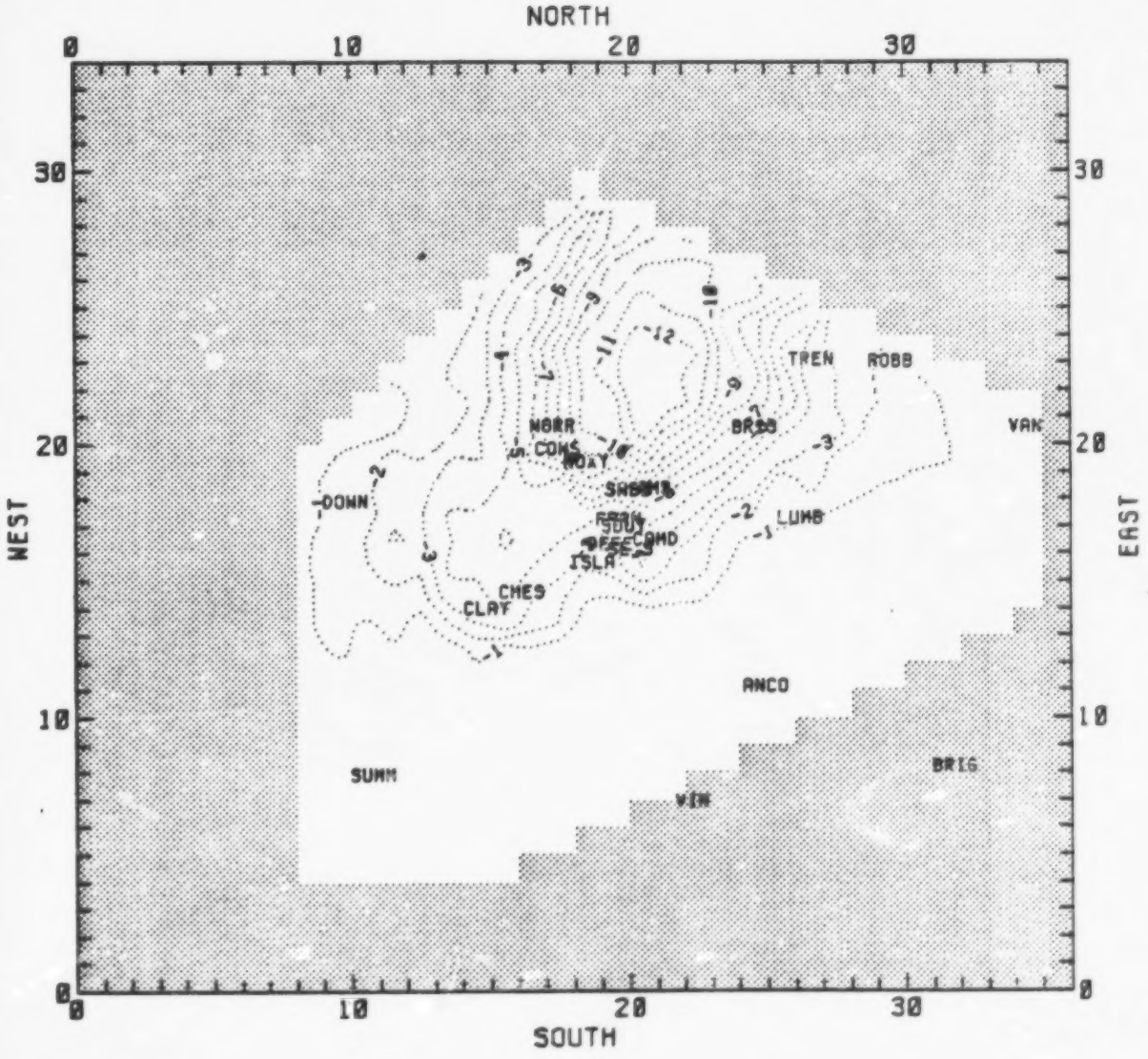

FIGURE 7-11. Maximum deficit/enhancement for ozone (pphm) for all hours for 13 July [D.50HC minus D.BASE].

BEST COPY AVAILABLE

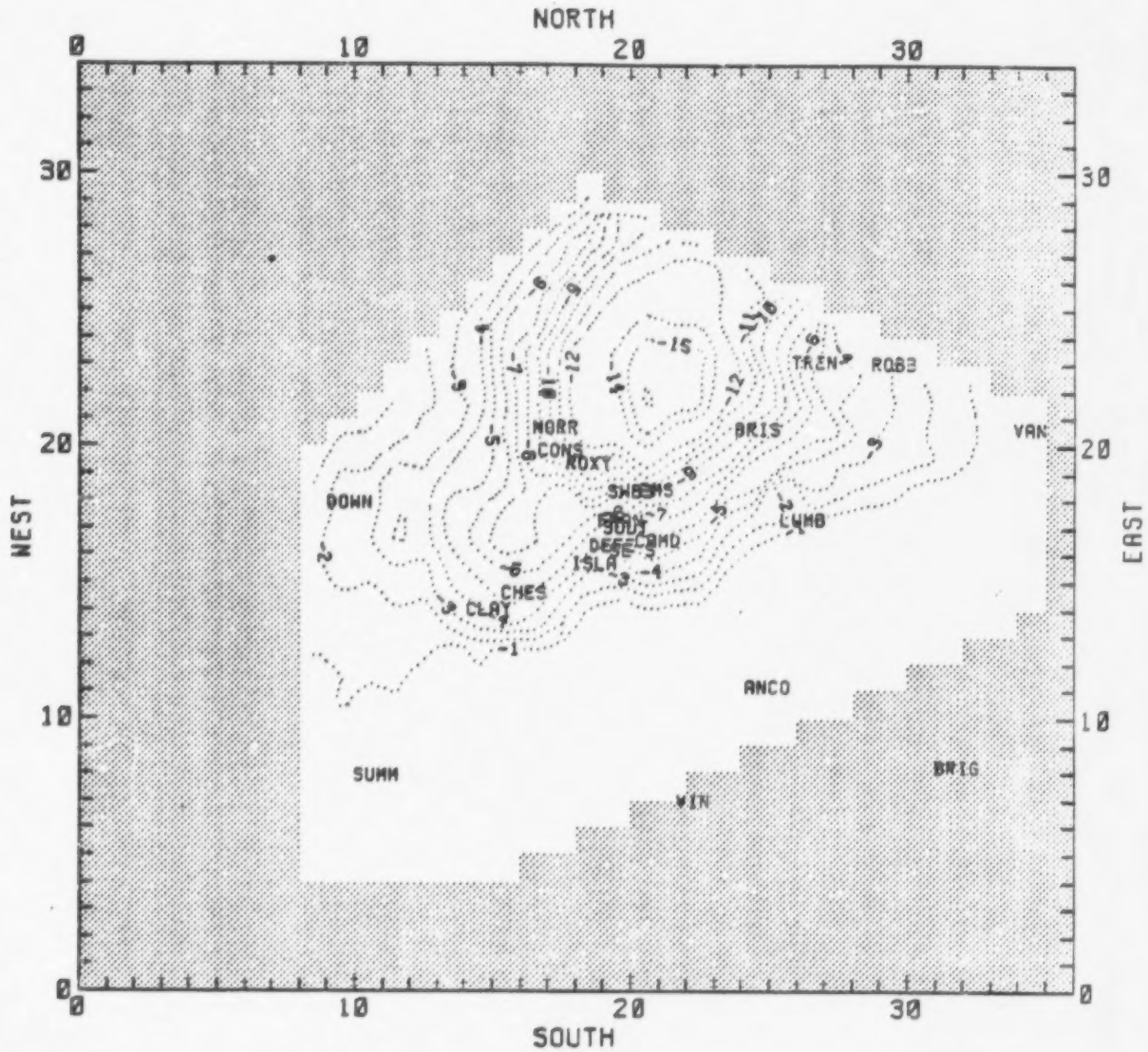

FIGURE 7-12. Maximum deficit/enhancement for ozone (pphm) for all hours for 13 July [D.75HC minus D.BASE].

BEST COPY AVAILABLE

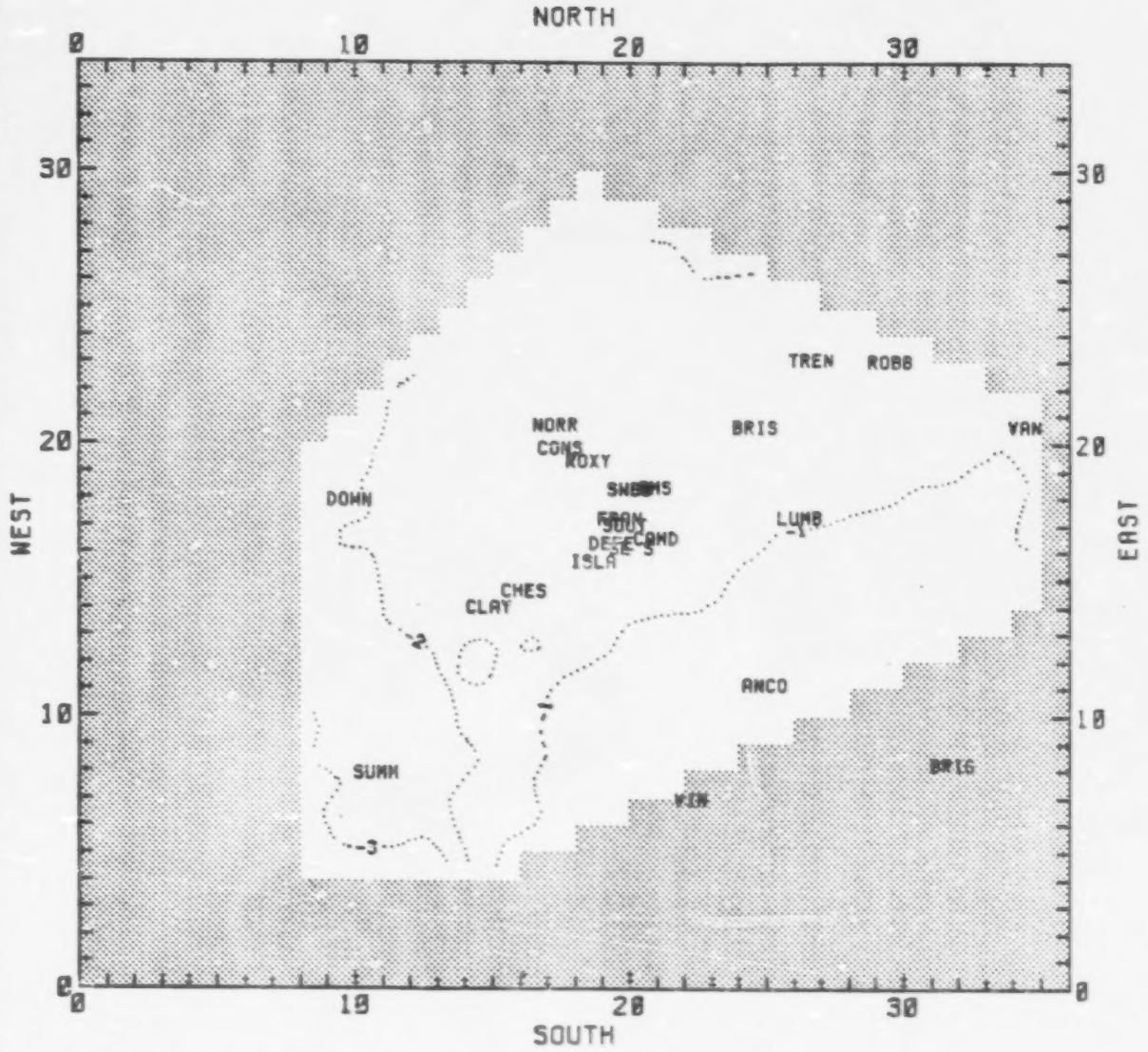

FIGURE 7-13. Maximum deficit/enhancement for ozone (pphm) for all hours for 13 July [D.BKO3 minus D.BASE].

BEST COPY AVAILABLE

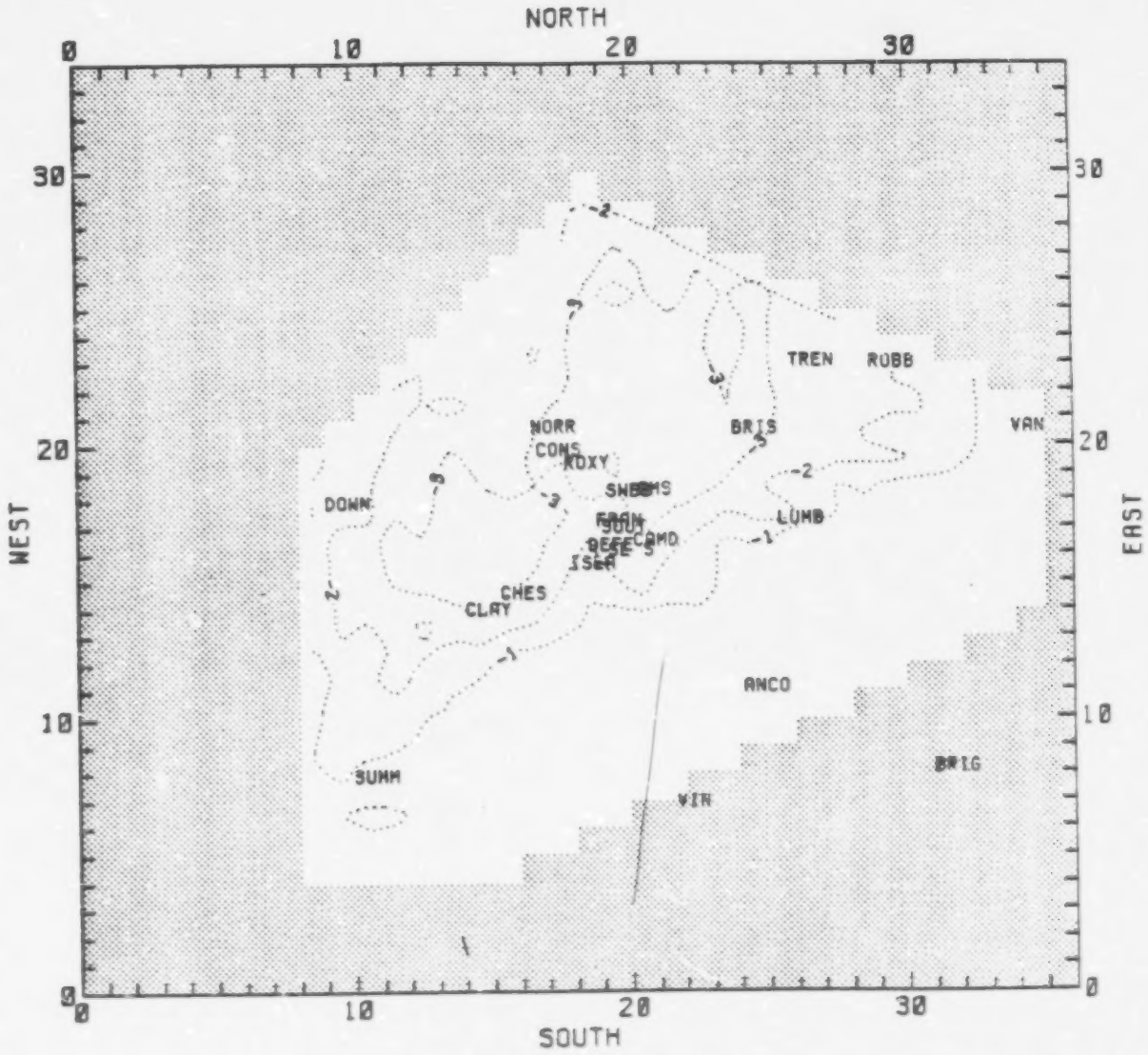

FIGURE 7-14. Maximum deficit/enhancement for ozone (pphm) for all hours for 13 July [D.BKHC minus D.BASE].

BEST COPY AVAILABLE

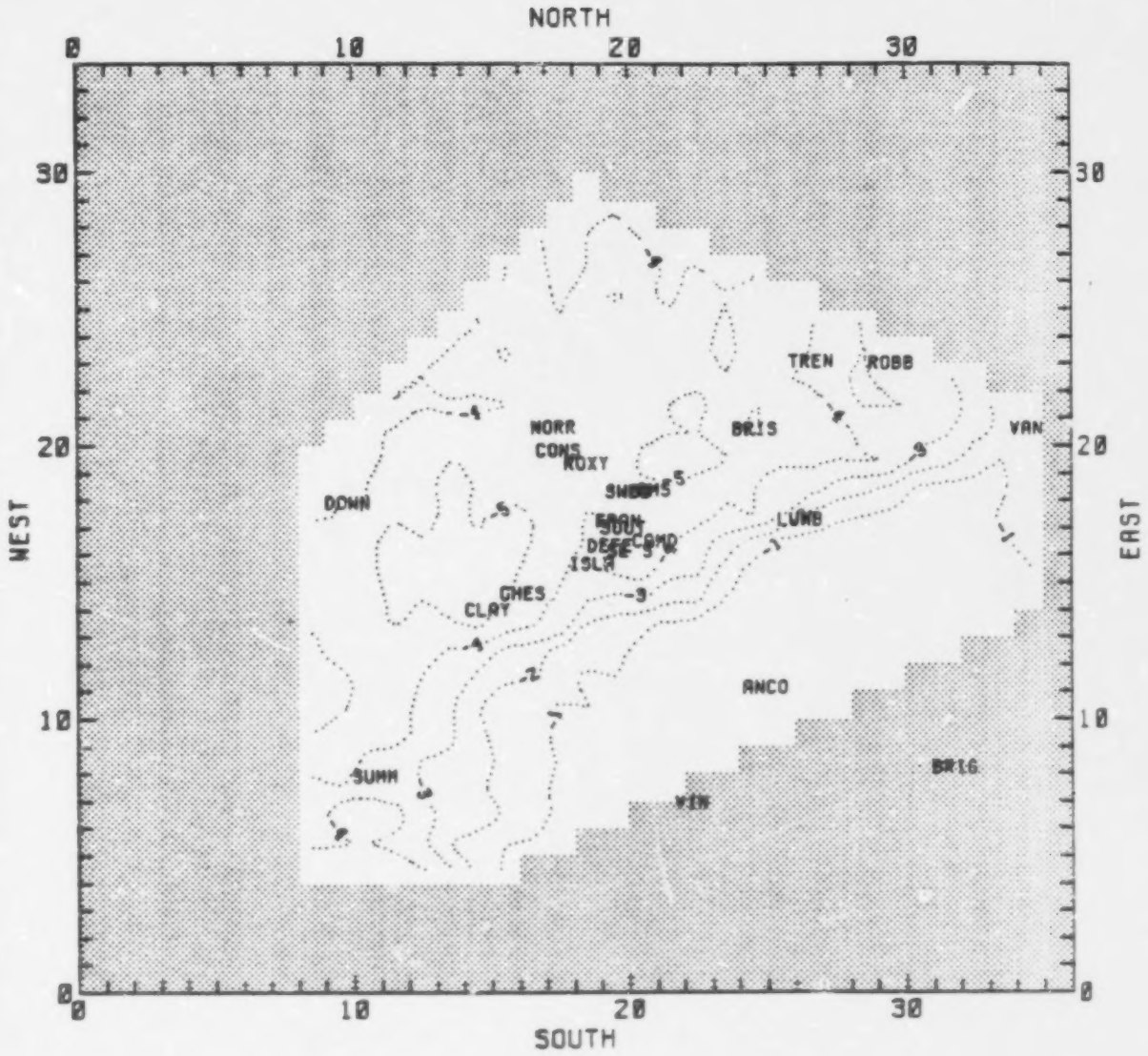

FIGURE 7-15. Maximum deficit/enhancement for ozone (pphm) for all hours for 13 July [D.BKHC.03 minus D.BASE].

BEST COPY AVAILABLE

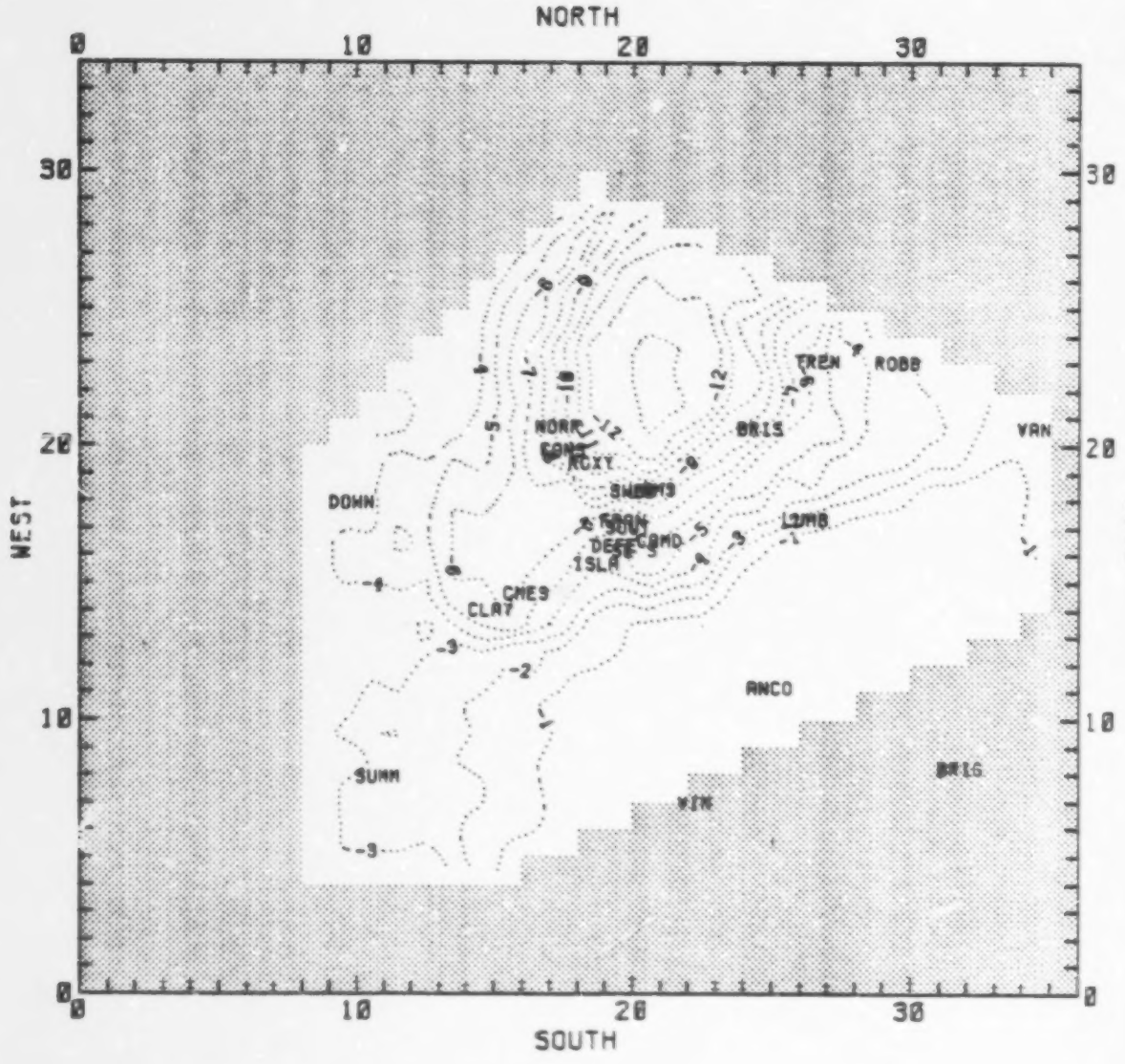

FIGURE 7-16. Maximum deficit/enhancement for ozone (pphm) for all hours for 13 July [D.50HC.BK03 minus D.BASE].

BEST COPY AVAILABLE

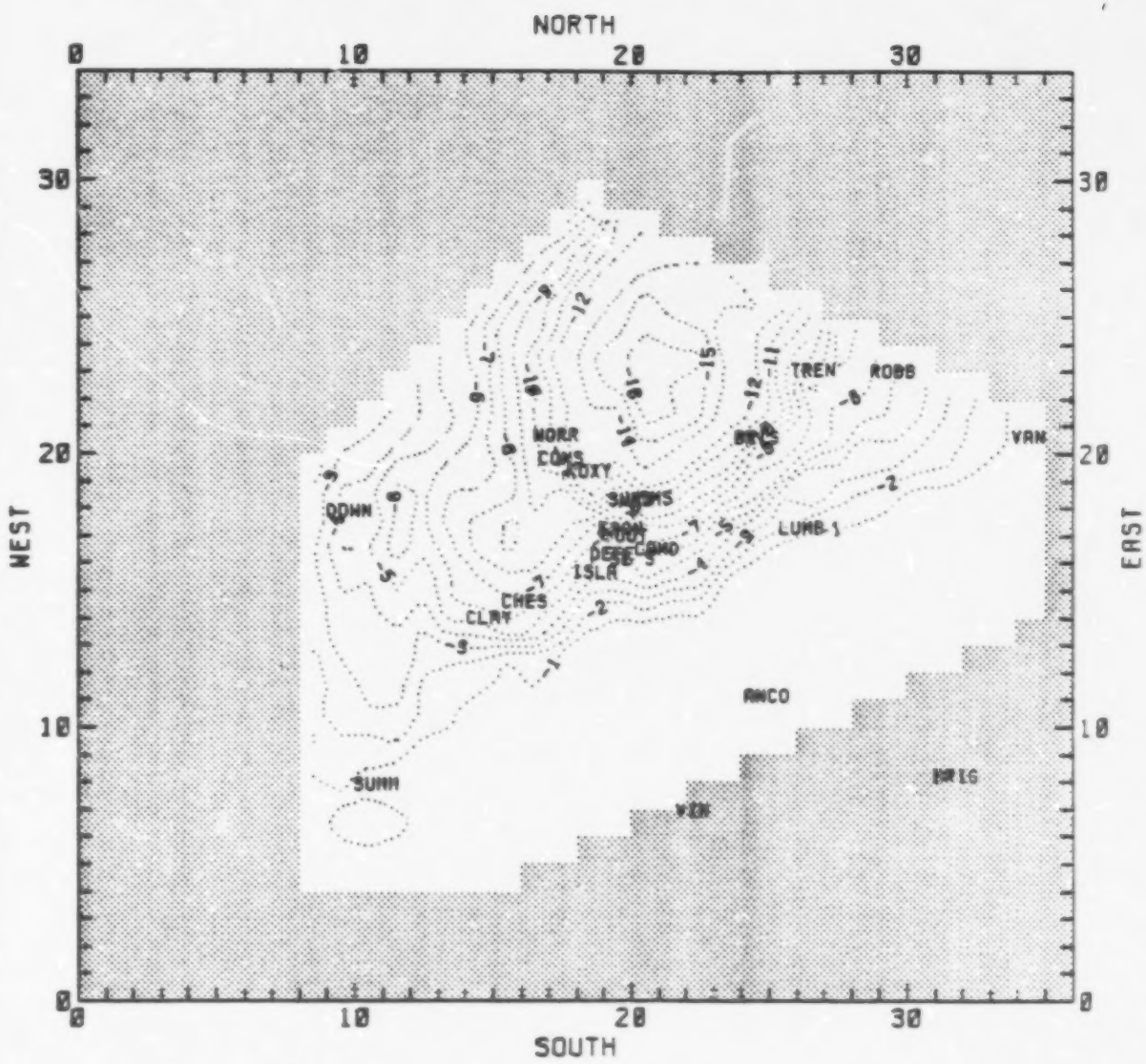

FIGURE 7-17. Maximum deficit/enhancement for ozone (pphm) for all hours for 13 July [D.5OHC.BKHC minus D.BASE].

BEST COPY AVAILABLE

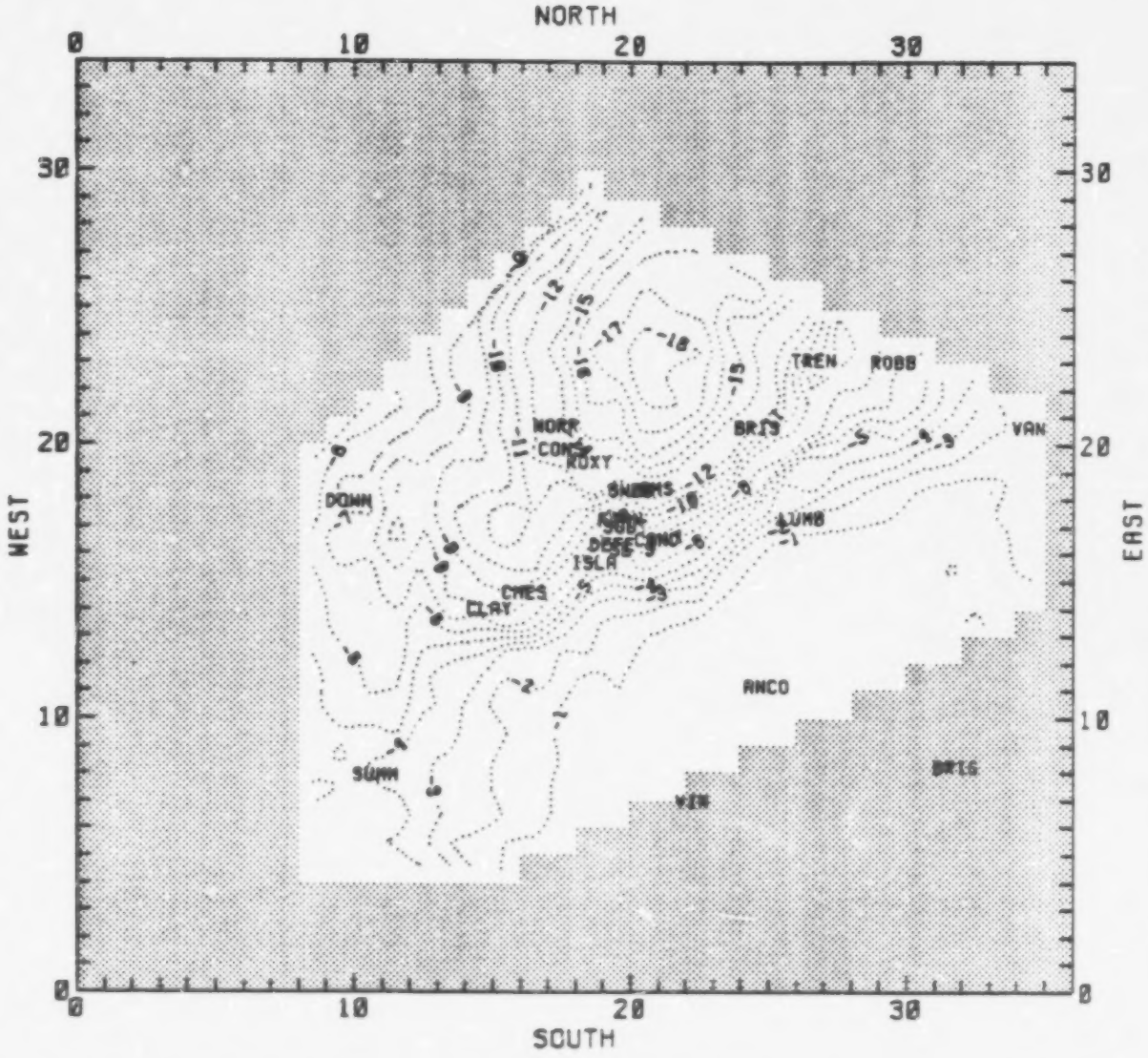

FIGURE 7-18. Maximum deficit/enhancement for ozone (pphm) for all hours for 13 July [D.50HC.BKHC.03 minus D.BASE].

BEST COPY AVAILABLE

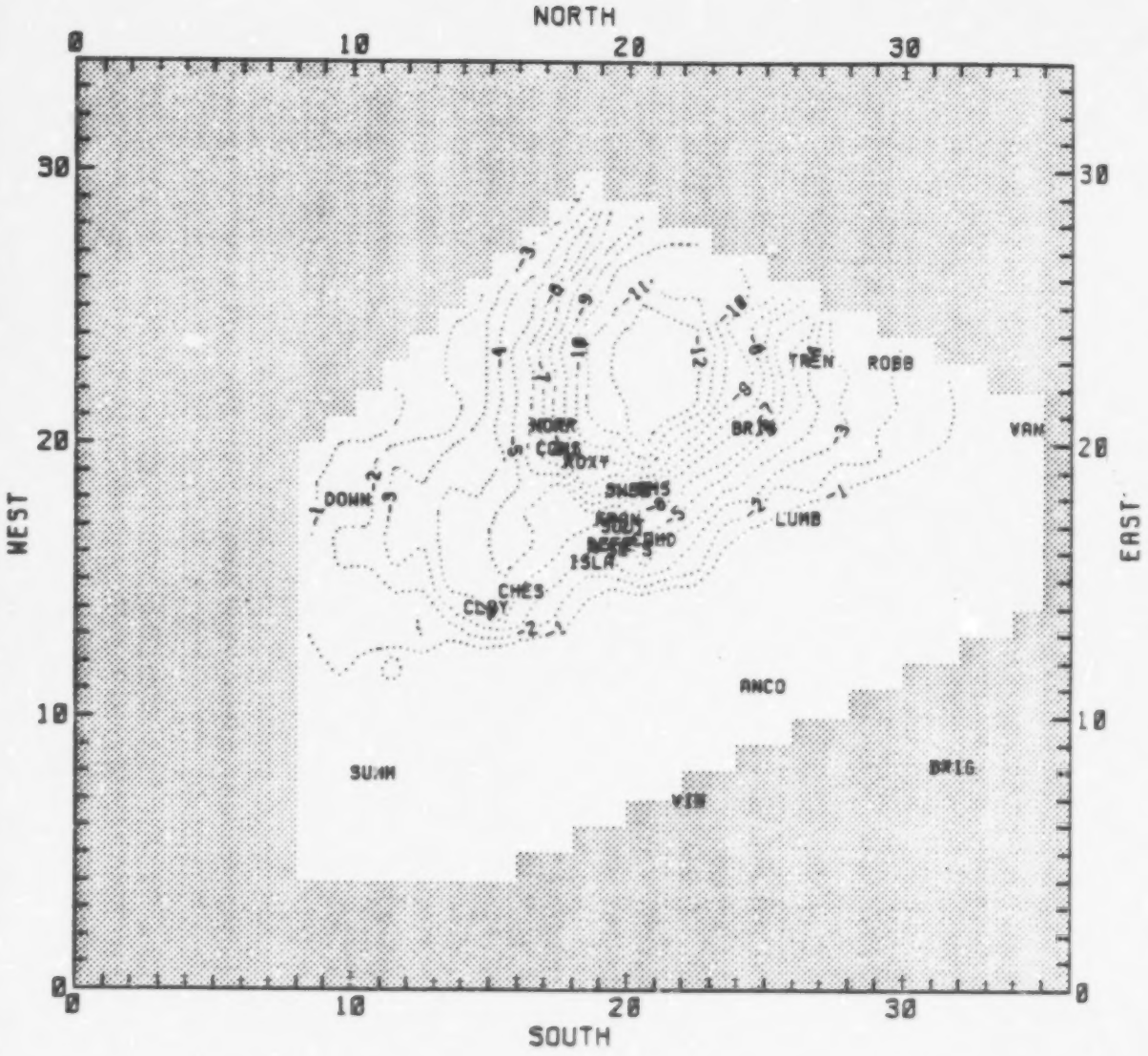

FIGURE 7-19. Maximum deficit/enhancement for ozone (pphm) for all hours for 13 July [D.50HC.BK03 minus D.BK03].

BEST COPY AVAILABLE

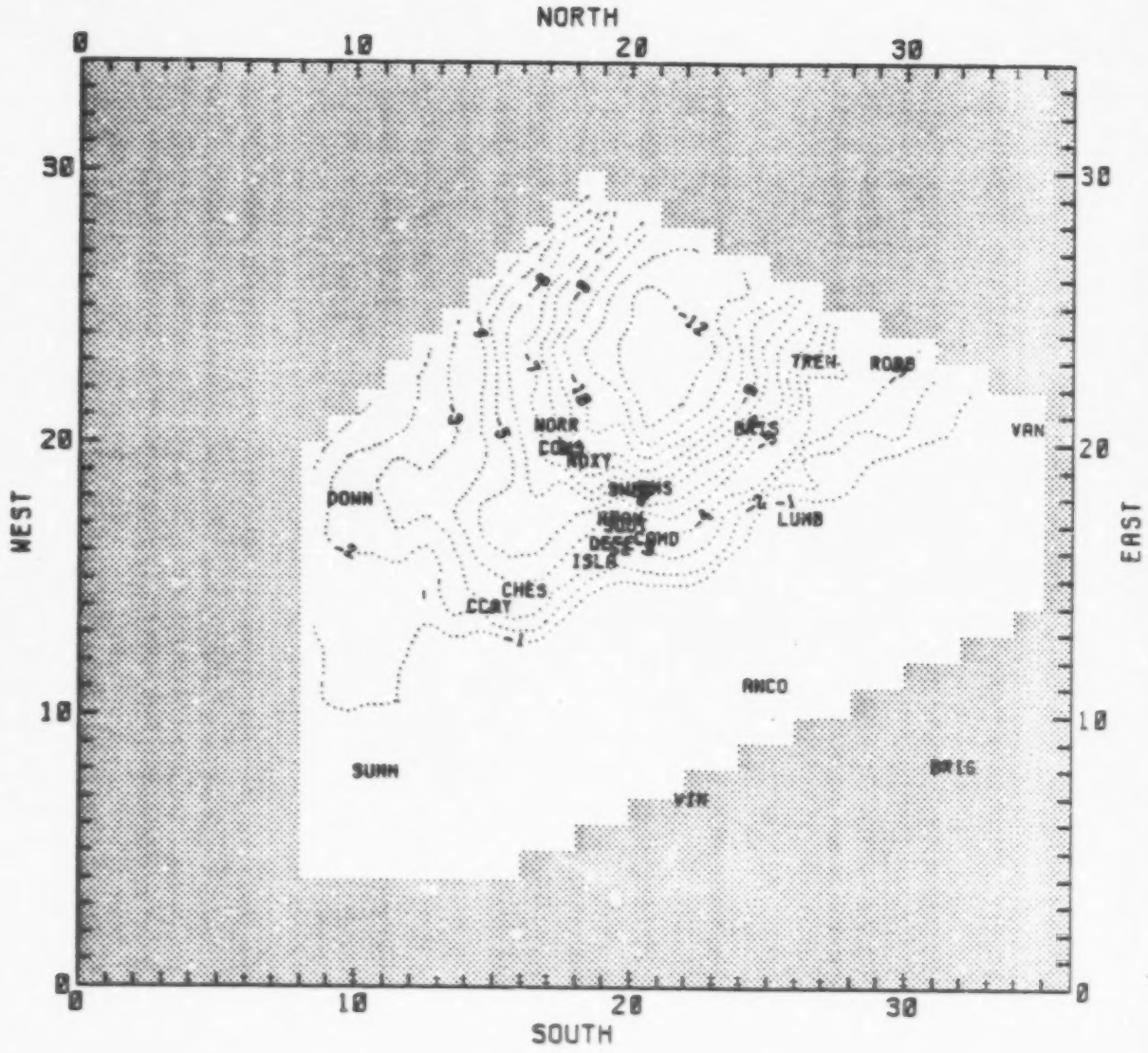

FIGURE 7-20. Maximum deficit/enhancement for ozone (pphm) for all hours for 13 July [D.50HC.BKHC minus D.BKHC].

BEST COPY AVAILABLE

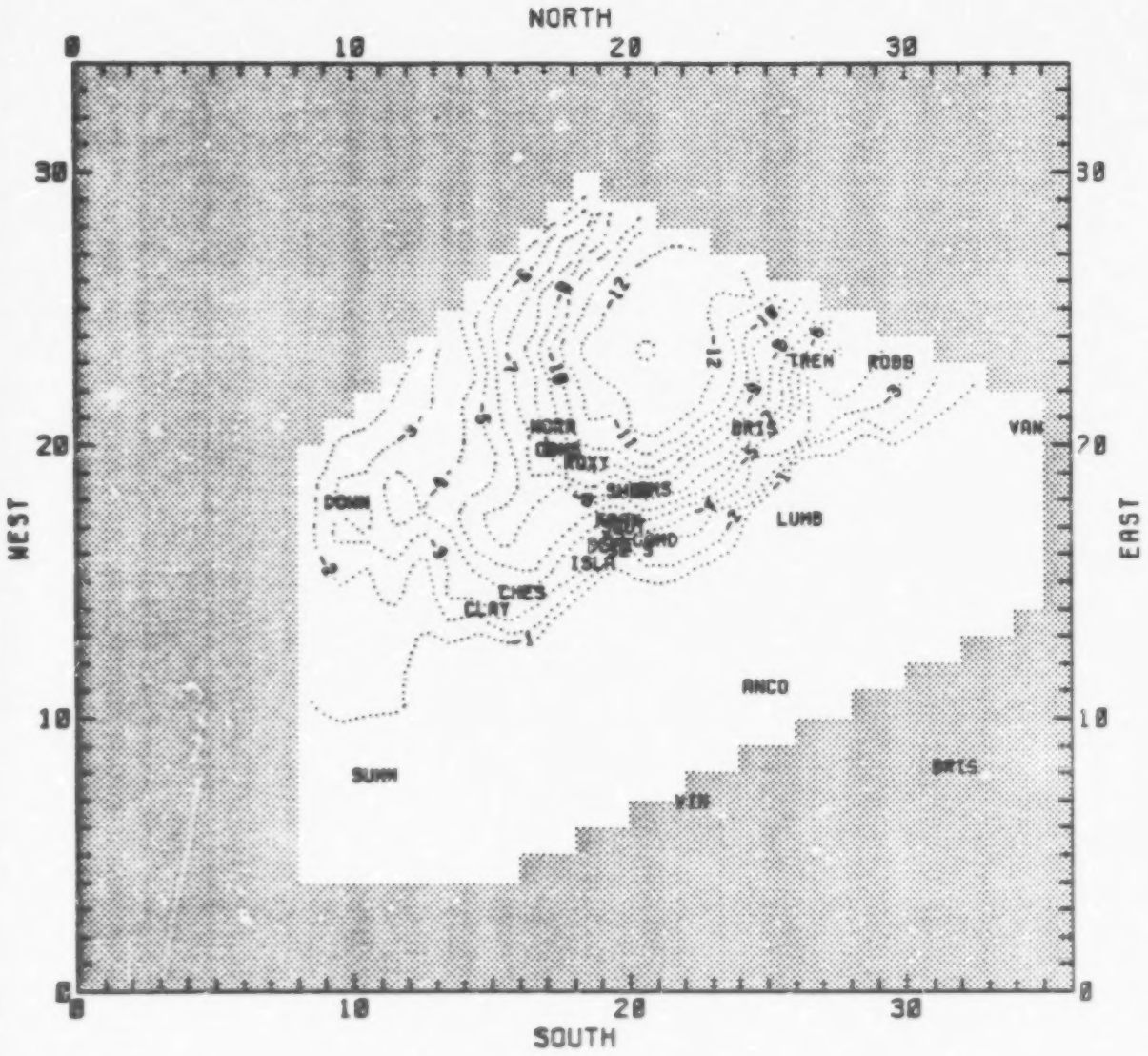

FIGURE 7-21. Maximum deficit/enhancement for ozone (pphm) for all hours for 13 July [D.50HC.BKHC.03 minus D.BKHC.03].

BEST COPY AVAILABLE

at a station affected by this interurban transport is also examined. As is shown in the base case for this day (Figure 6-7), the simulated urban ozone plume from Philadelphia was transported nearly 90 km west of the urban center. As a result, the station of Downington, Pennsylvania received the highest predicted ozone. In the simulation, this station was affected almost exclusively by urban Philadelphia emissions, whereas all other stations were affected to a large degree by the New Jersey/New York plume. Of those stations affected by this plume, the one for which maximum ozone was predicted was the Roxy Water, Pennsylvania monitor. Table 7-8 presents the hourly predicted maximum for the base case and all sensitivity simulations for the Philadelphia urban plume (located west of Downington, Pennsylvania), the Downington monitor, and the Roxy Water monitor. Also included in the table are the relative and total ozone reductions for each sensitivity simulation. Because 19 July experienced interurban transport of ozone precursors, all but three of the sensitivity simulations (6.25HC, 6.50HC, and 6.75HC) resulted in reductions in boundary condition hydrocarbons on the Northeast and East boundaries by 25, 50, and 75 percent, along with the corresponding reduction in hydrocarbon emissions and initial conditions.

For 13 July, the information contained in Table 7-8 is presented graphically for ease of interpretation.

Figure 7-22 compares, for all sensitivity simulations, peak predicted hourly averaged ozone from the Philadelphia urban plume with the percent of hydrocarbon emissions reduction. Similar figures are presented for the Downington and Roxy Water monitors in Figures 7-23 and 7-24, respectively. Figures 7-25 through 7-27 present relative ozone response, and Figures 7-28 through 7-30 present total ozone response for the Philadelphia urban plume, the Downington monitor, and the Roxy Water monitor, respectively.

Figure 7-22 shows the effects on ozone of possible hydrocarbon and ozone reduction scenarios, both from the Philadelphia emission region and from the neighboring emission area of New Jersey and New York. This figure shows that the peak regional value located west of Philadelphia is also influenced by transport through the boundaries to the northeast. This is evident in a comparison of the curve representing the no-change boundary conditions with the curve for the simulation in which the Northeast and East boundary hydrocarbons are decreased by 25, 50, or 75 percent concurrently with emissions and initial conditions. In these simulations, background hydrocarbon and ozone were left unchanged. In the no-change boundary condition emission reduction simulations, a value of 57 percent hydrocarbon reduction is needed to meet the standard for ozone, but with Northeast and East boundary conditions reduced, only 44 percent hydrocarbon reduction is required. This difference is an important consideration

BEST COPY AVAILABLE

TABLE 7-8. Hourly predicted maximum ozone and ozone reductions for the ozone sensitivity simulations of 19 July.

Simulation	Philadelphia Urban Plume Peak			Downington, PA			Roxy Water, PA		
	Ozone Prediction (pphm)	Ozone Reduction (percent)		Ozone Prediction (pphm)	Ozone Reduction (percent)		Ozone Prediction (pphm)	Ozone Reduction (percent)	
		Relative	Total		Relative	Total		Relative	Total
6.BASE	17.7	-	-	14.2	-	-	13.8	-	-
6.25HC	15.1	14.7	14.7	12.1	15.2	15.2	13.7	0.7	0.7
6.50HC	12.4	29.9	29.9	10.0	29.6	29.6	13.6	1.6	1.6
6.75HC	11.1	37.3	37.3	9.0	36.9	36.9	13.5	2.6	2.6
6.B25HC	14.6	17.5	17.5	11.7	17.9	17.9	11.0	20.6	20.6
6.B50HC	11.3	36.2	36.2	9.4	33.7	33.7	9.8	29.4	29.4
6.B75HC	9.6	45.7	45.7	8.2	42.3	42.3	8.8	36.5	36.5
6.BKHC	14.7	-	16.9	11.1	-	21.8	11.8	-	14.5
6.B25HC.BKHC	11.3	23.1	36.2	8.6	22.8	39.4	8.2	30.5	40.6
6.B50HC.BKHC	7.8	46.9	55.9	7.0	37.0	50.7	6.5	45.0	52.9
6.B75HC.BKHC	6.5	55.8	63.3	6.3	43.4	55.6	5.7	52.1	62.3
6.BK03	17.2	-	2.8	13.4	-	5.6	13.3	-	3.6
6.B25HC.BK03	14.0	18.6	20.9	10.8	19.4	23.9	10.4	22.0	24.6
6.B50HC.BK03	10.6	38.4	40.1	8.5	36.6	40.1	8.8	34.1	36.2
6.B75HC.BK03	8.7	49.4	50.8	7.3	45.3	48.6	7.7	42.3	44.2
6.BKHC.03	14.4	-	18.6	10.3	-	27.5	11.2	-	18.8
6.B25HC.BKHC.03	10.6	26.4	40.1	7.7	25.3	45.8	7.4	33.9	46.4
6.B50HC.BKHC.03	7.0	51.4	60.4	6.0	41.6	57.7	5.6	50.2	59.4
6.B75HC.BKHC.03	5.1	64.6	71.2	5.2	49.3	63.4	4.3	61.5	68.8

BEST COPY AVAILABLE

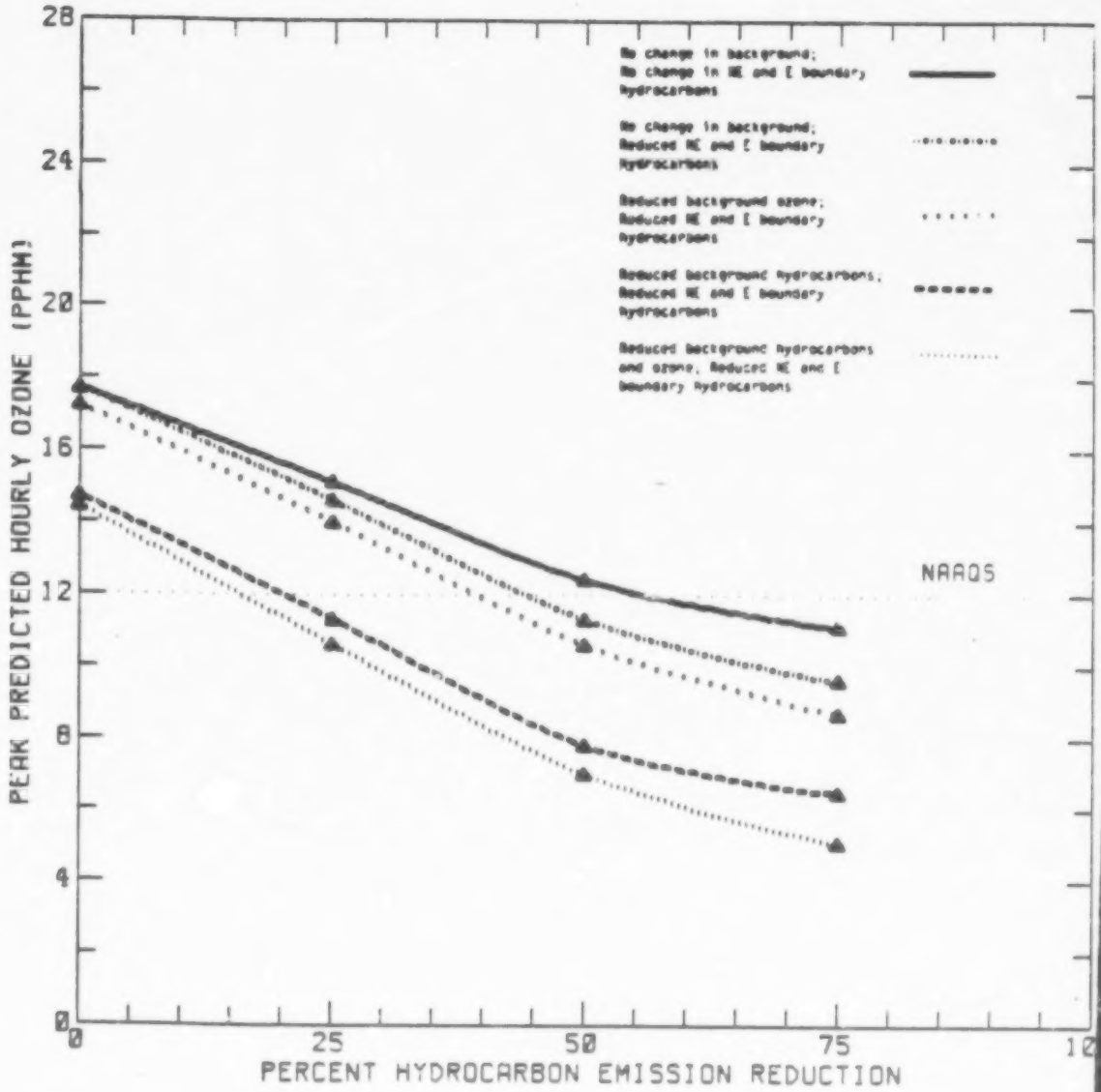

FIGURE 7-22. Predicted ozone response to hydrocarbon emission reductions for peak regional ozone in the Philadelphia urban plume for 19 July.

BEST COPY AVAILABLE

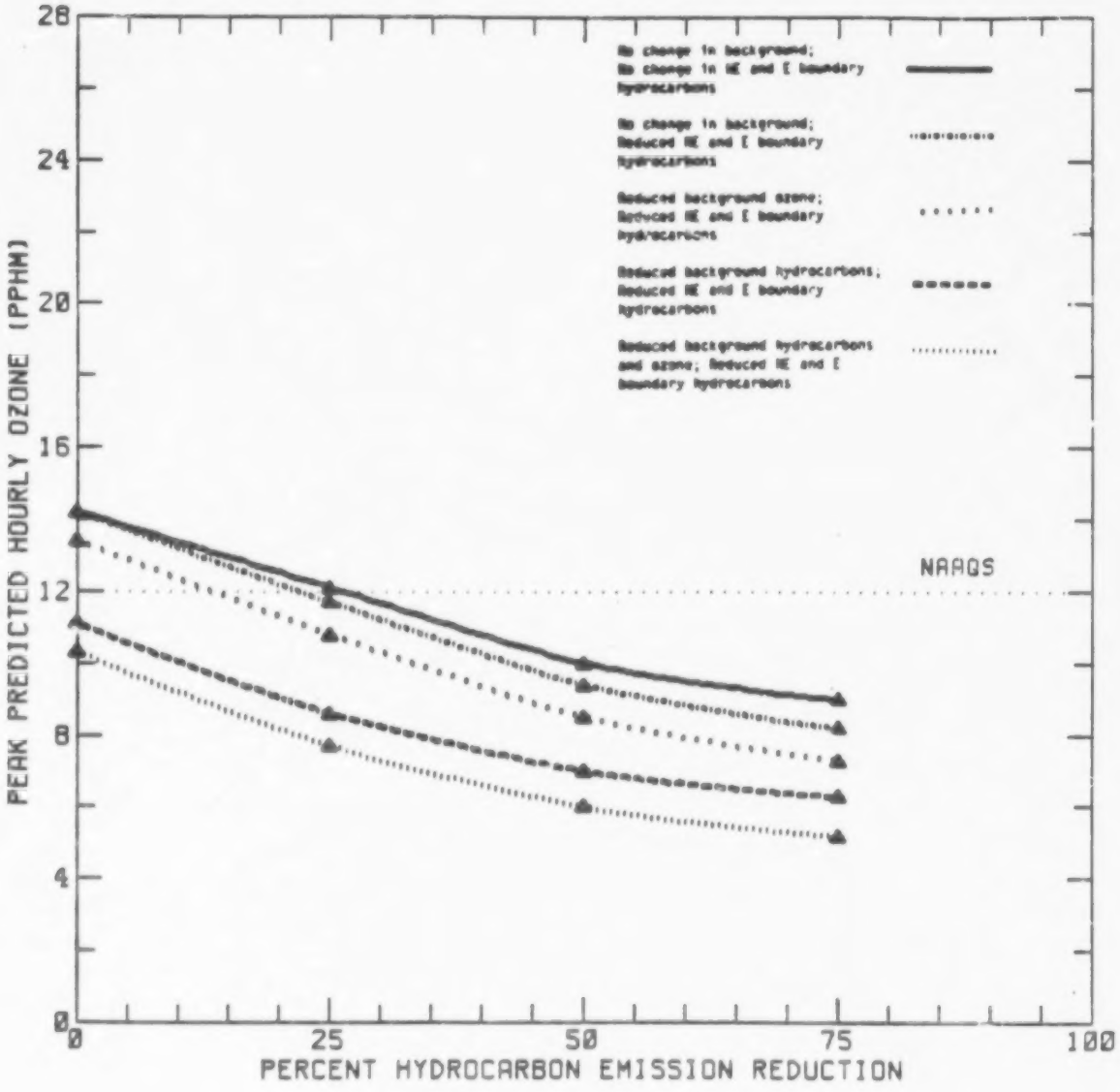

FIGURE 7-23. Predicted ozone response to hydrocarbon emission reductions for 19 July at the Downington, PA monitor.

BEST COPY AVAILABLE

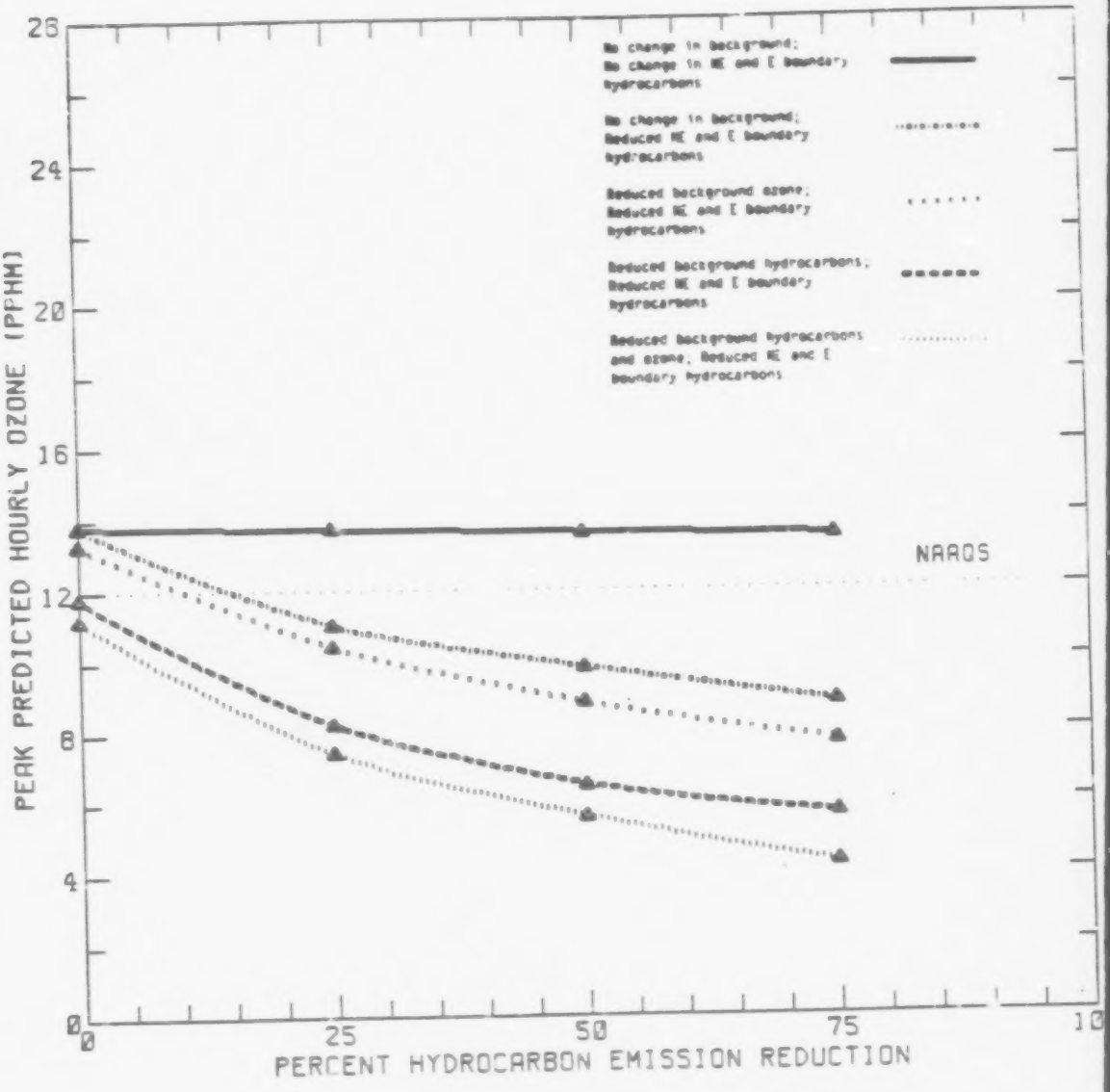

FIGURE 7-24. Predicted ozone response to hydrocarbon emission reductions for 19 July at the Roxy Water, PA monitor.

BEST COPY AVAILABLE

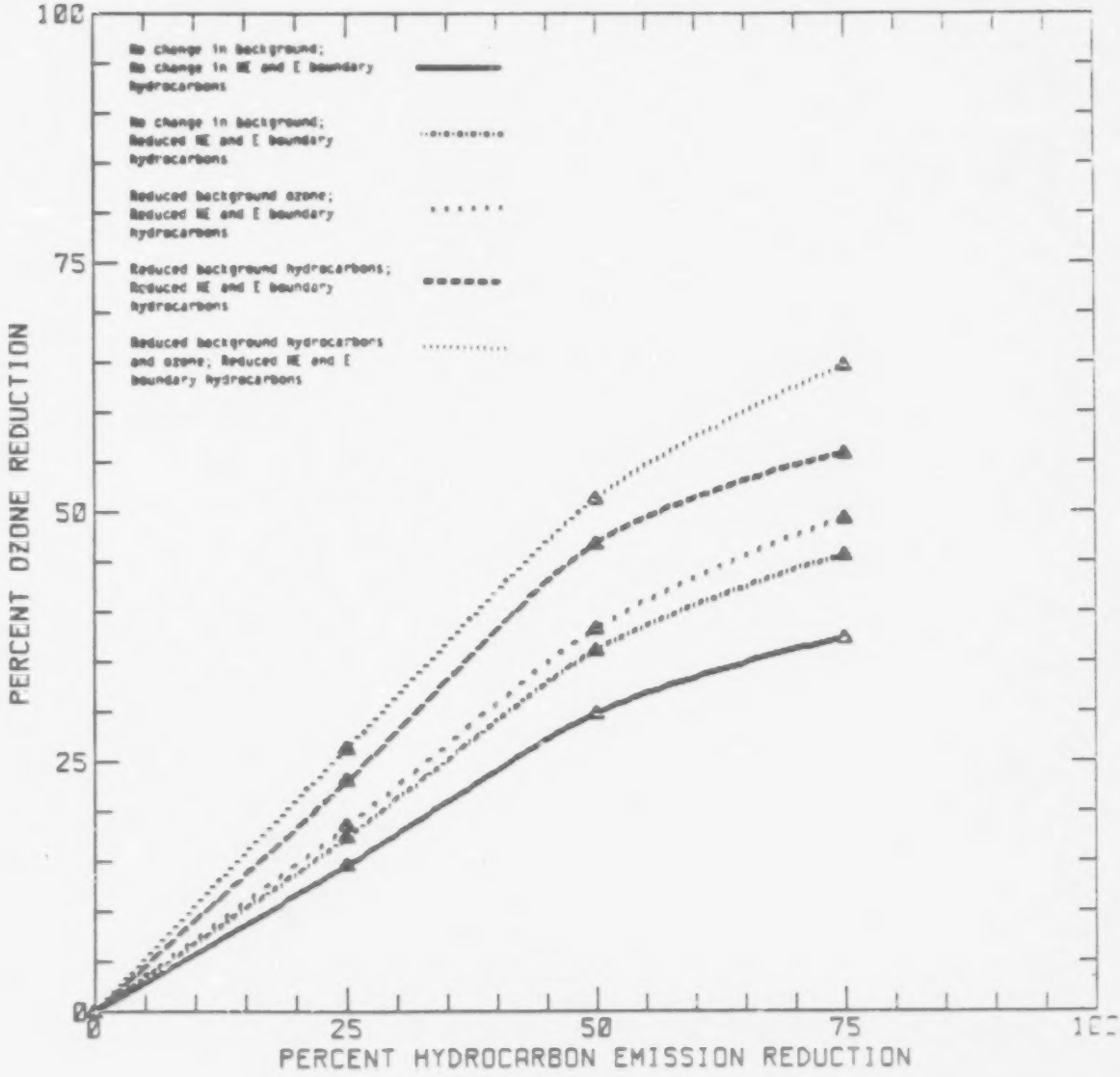
100
75
50
25
0
PERCENT OZONE REDUCTION
No change in background; No change in NE and E boundary hydrocarbons
No change in background; Reduced NE and E boundary hydrocarbons
Reduced background ozone; Reduced NE and E boundary hydrocarbons
Reduced background hydrocarbons; Reduced NE and E boundary hydrocarbons
Reduced background hydrocarbons and ozone; Reduced NE and E boundary hydrocarbons
0
25
50
75
PERCENT HYDROCARBON EMISSION REDUCTION

FIGURE 7-25. Relative ozone reduction (%) versus percent hydrocarbon emission reduction for peak regional ozone in the Philadelphia urban plume for 19 July.

BEST COPY AVAILABLE

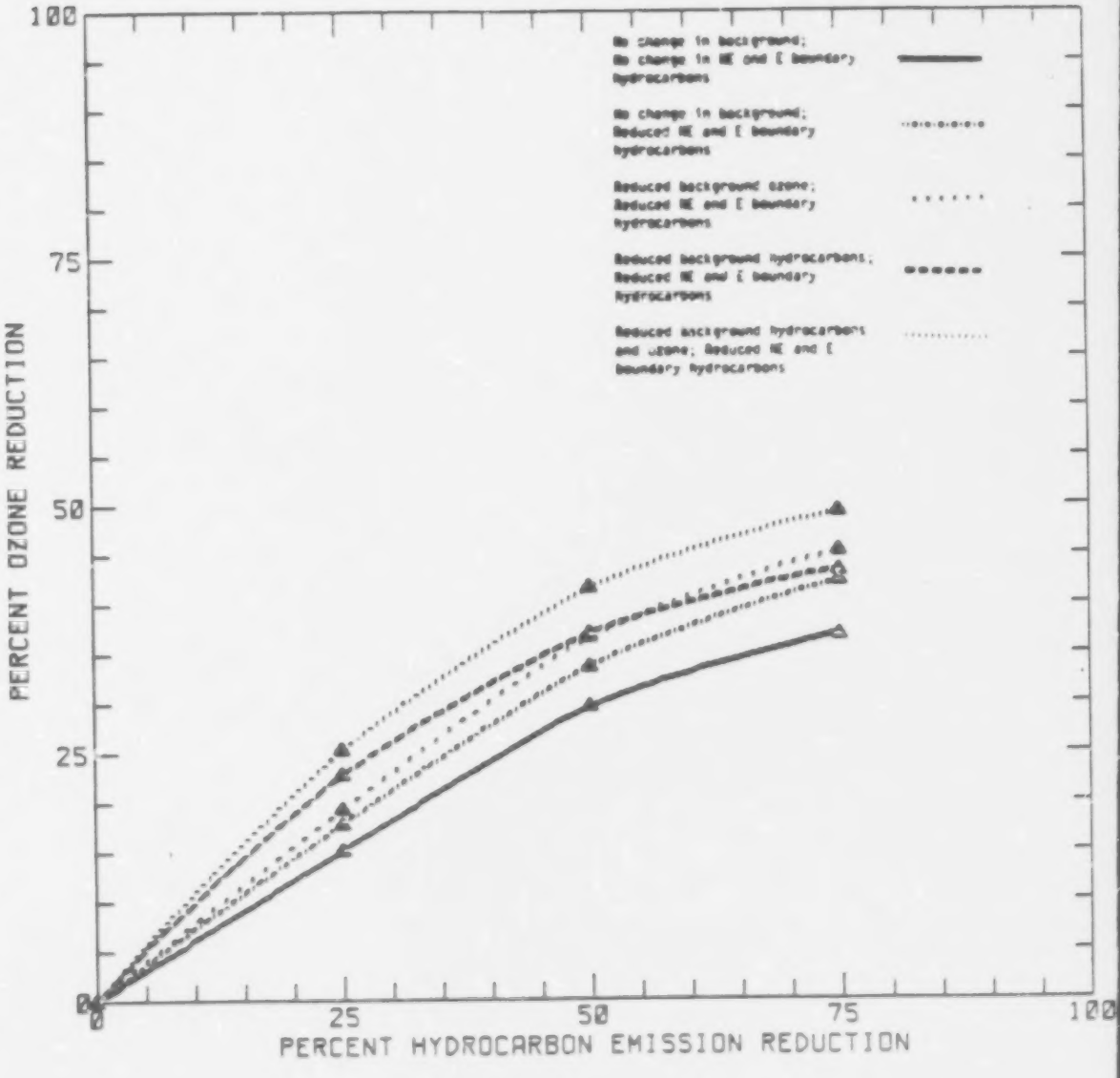
100
75
50
25
0
0
25
50
75
100
PERCENT OZONE REDUCTION
PERCENT HYDROCARBON EMISSION REDUCTION
No change in background; No change in NE and E boundary hydrocarbons
No change in background; Reduced NE and E boundary hydrocarbons
Reduced background ozone; Reduced NE and E boundary hydrocarbons
Reduced background hydrocarbons; Reduced NE and E boundary hydrocarbons
Reduced background hydrocarbons and ozone; Reduced NE and E boundary hydrocarbons

FIGURE 7-26. Relative ozone reduction (%) versus percent hydrocarbon emission reduction for 19 July at the Downington, PA monitor.

BEST COPY AVAILABLE

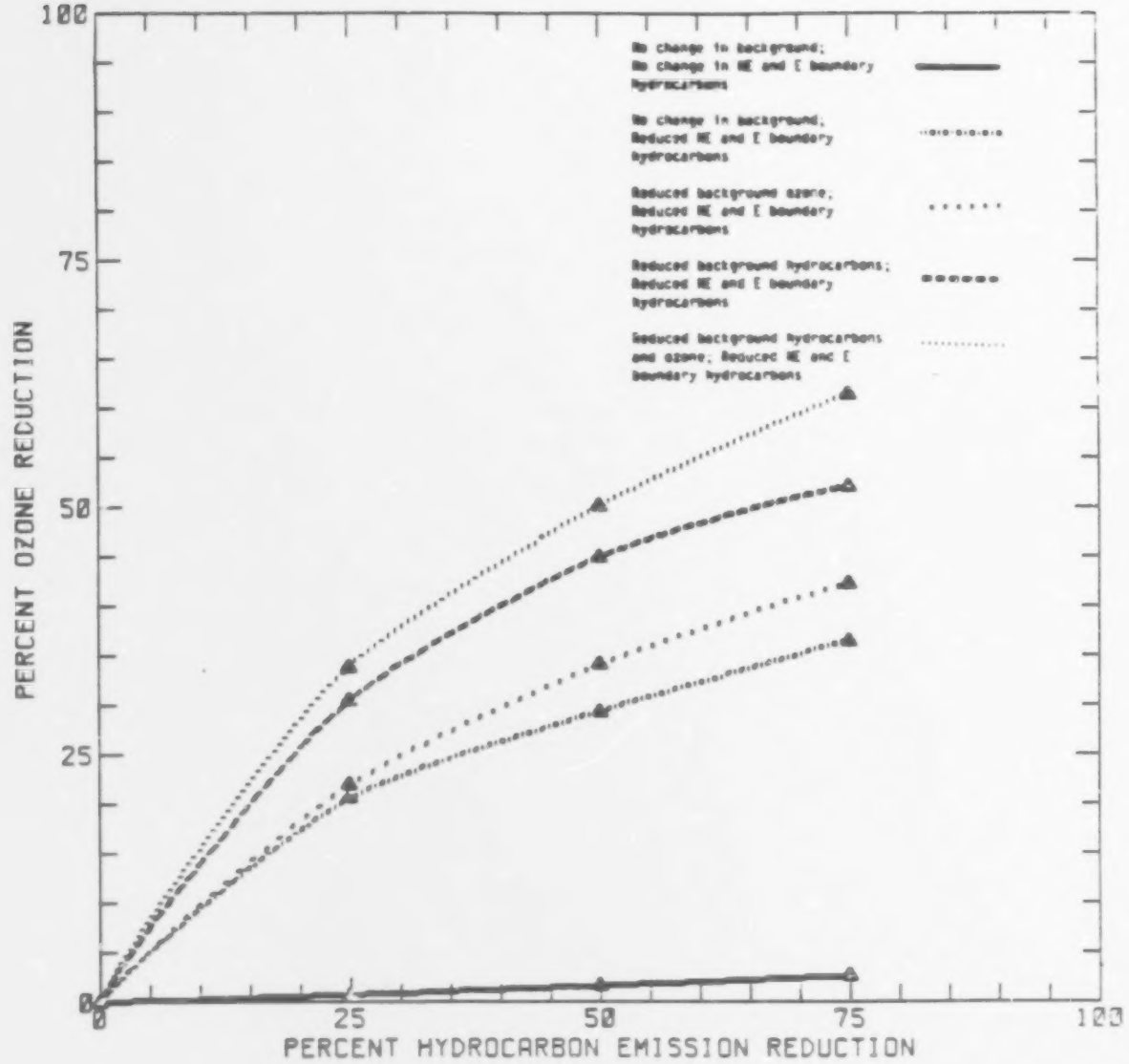
100
75
50
25
0
0
25
50
75
100
PERCENT OZONE REDUCTION
PERCENT HYDROCARBON EMISSION REDUCTION
No change in background; No change in NE and E boundary hydrocarbons
No change in background; Reduced NE and E boundary hydrocarbons
Reduced background ozone; Reduced NE and E boundary hydrocarbons
Reduced background hydrocarbons; Reduced NE and E boundary hydrocarbons
Reduced background hydrocarbons and ozone; Reduced NE and E boundary hydrocarbons

FIGURE 7-27. Relative ozone reduction (%) versus percent hydrocarbon emission reduction for 19 July at the Roxy Water, PA monitor.

BEST COPY AVAILABLE

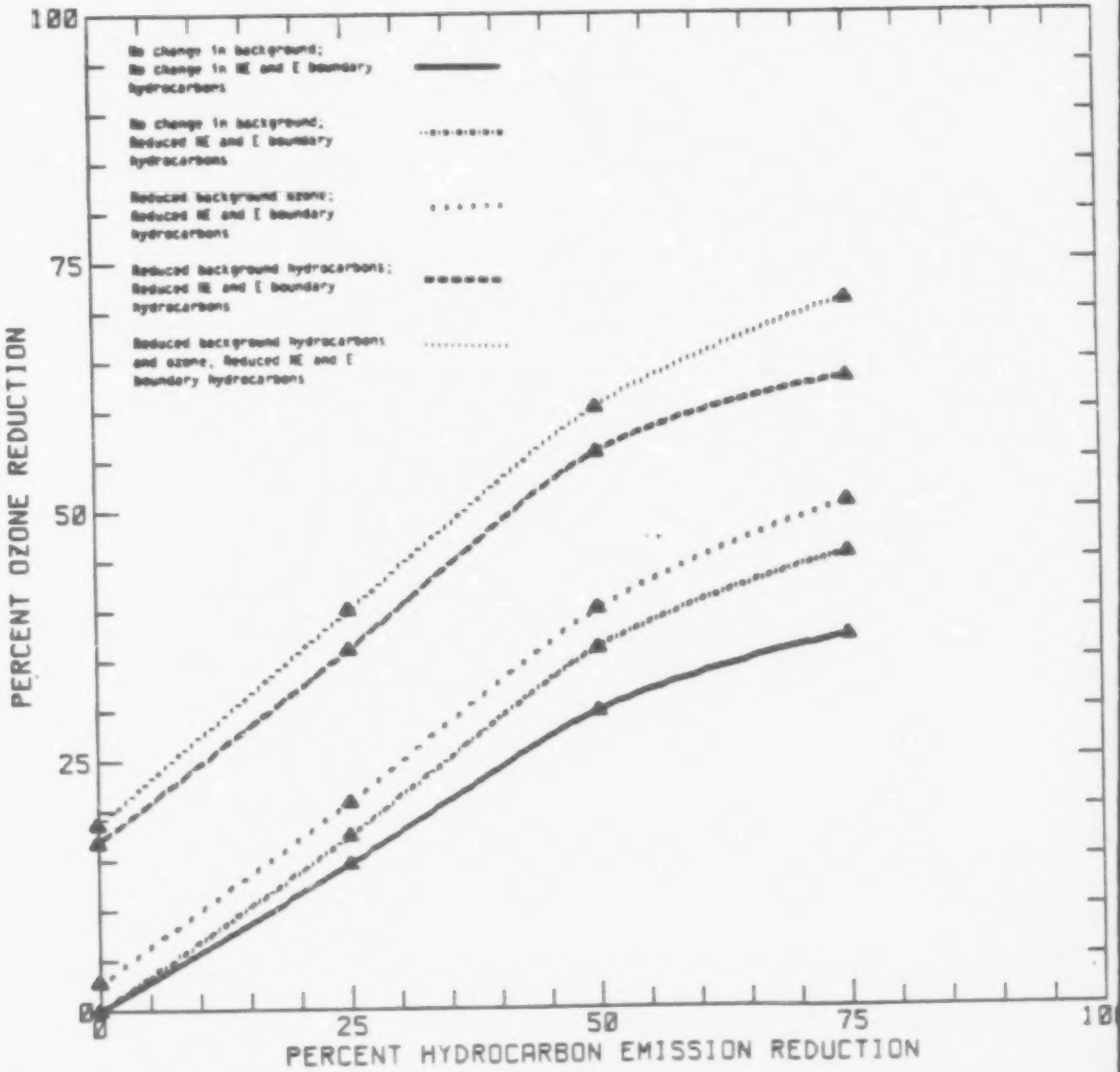
100
75
50
25
0
0
25
50
75
10
PERCENT OZONE REDUCTION
PERCENT HYDROCARBON EMISSION REDUCTION
No change in background; No change in NE and E boundary hydrocarbons
No change in background; Reduced NE and E boundary hydrocarbons
Reduced background ozone; Reduced NE and E boundary hydrocarbons
Reduced background hydrocarbons; Reduced NE and E boundary hydrocarbons
Reduced background hydrocarbons and ozone, Reduced NE and E boundary hydrocarbons

FIGURE 7-28. Total ozone reduction (%) versus percent hydrocarbon emission reduction of peak regional ozone in the Philadelphia urban plume for 19 July.

BEST COPY AVAILABLE

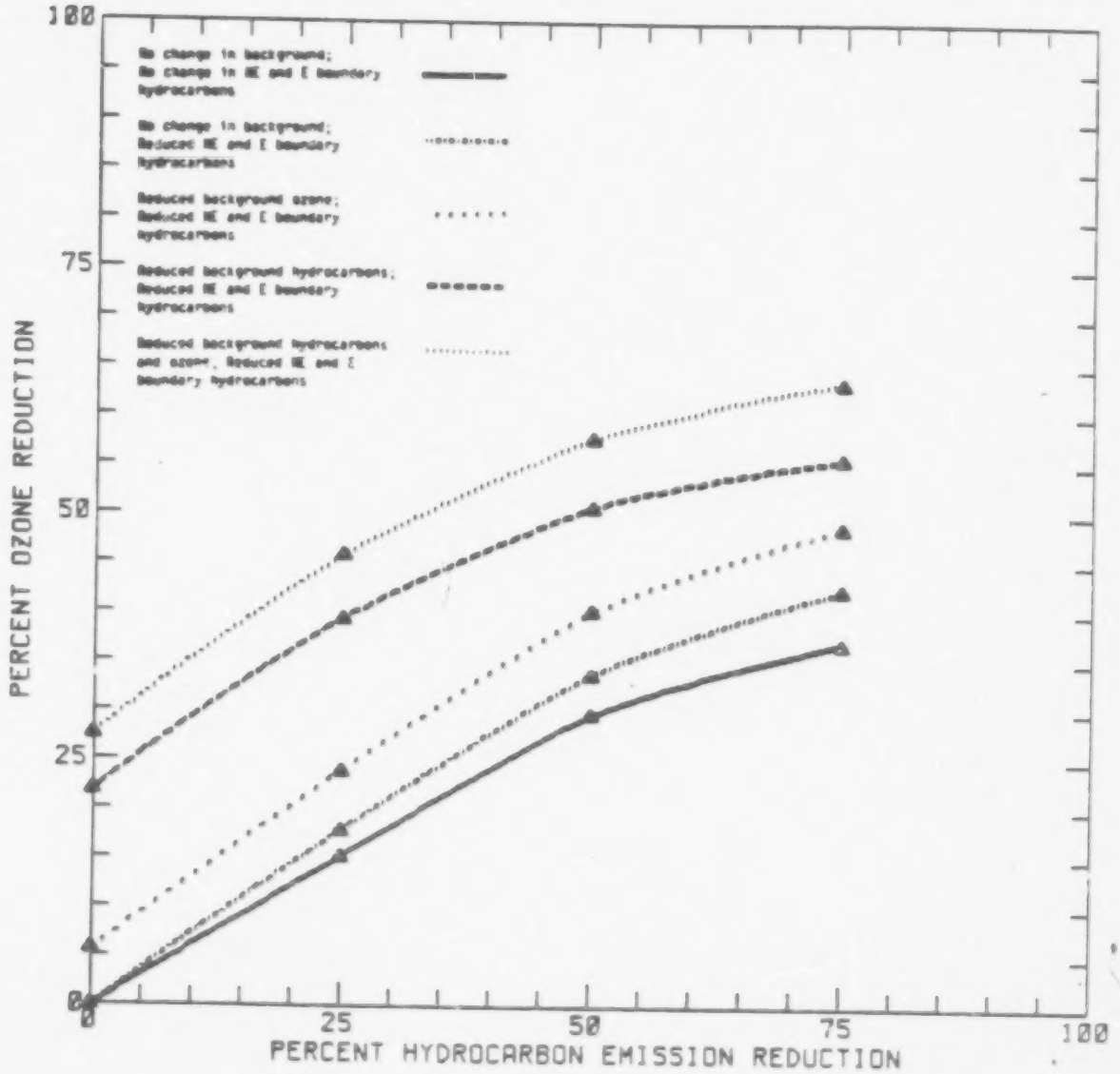

FIGURE 7-29. Total ozone reduction (%) versus percent hydrocarbon emission reduction for 19 July at the Downington, PA monitor.

BEST COPY AVAILABLE

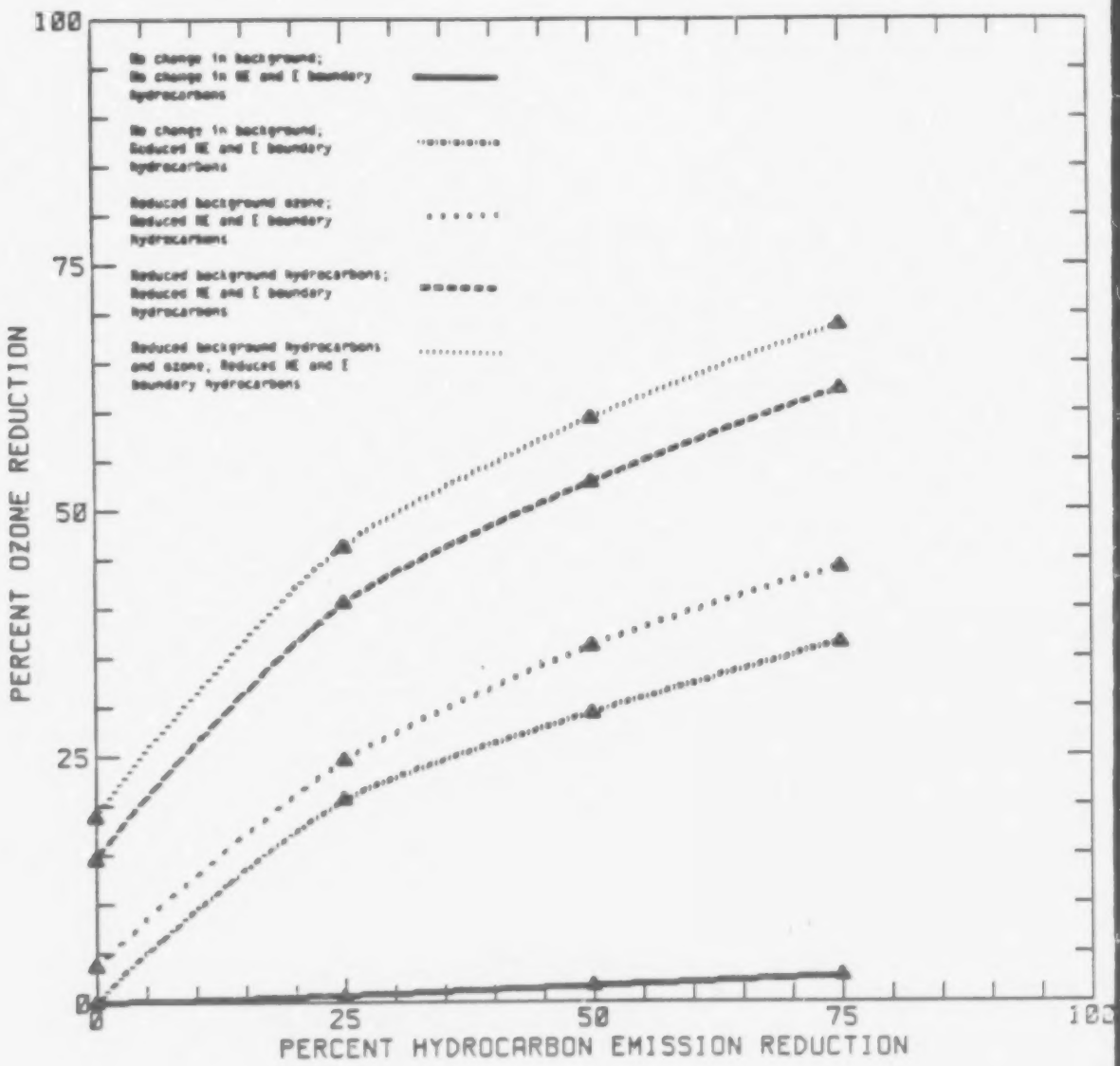
100
75
50
25
0
0
25
50
75
100
PERCENT OZONE REDUCTION
PERCENT HYDROCARBON EMISSION REDUCTION
No change in background; No change in NE and E boundary hydrocarbons
No change in background; Reduced NE and E boundary hydrocarbons
Reduced background ozone; Reduced NE and E boundary hydrocarbons
Reduced background hydrocarbons; Reduced NE and E boundary hydrocarbons
Reduced background hydrocarbons and ozone, Reduced NE and E boundary hydrocarbons

FIGURE 7-30. Total ozone reduction (%) versus percent hydrocarbon emission reduction for 19 July at the Roxy Water, PA monitor.

BEST COPY AVAILABLE

for air quality planners in Northeast Corridor cities. This finding suggests that reduced ozone levels in one airshed may not be maintained if neighboring cities do not also make comparable emission reductions.

A summary of hydrocarbon reductions required to meet the ambient standard for ozone for all sensitivity simulations of 19 July is presented in Table 7-9. In the no-change background simulations with no decreases of boundary hydrocarbons, the peak predicted ozone value at the Roxy Water monitor decreases very slightly with increased hydrocarbon control. This shows that the peak predicted ozone value at the Roxy Water monitor is the result of inflow of ozone precursors from the Northeast and East boundaries. Peak predicted ozone, however, is decreased as boundary concentrations for hydrocarbons are decreased, as illustrated in Figure 7-24.

At the Downington and Roxy Water monitors, no hydrocarbon controls are needed to meet the ozone standard if either background hydrocarbons alone or both background hydrocarbons and ozone are decreased, because the peak predicted values in the simulation without emission control are already below 12 pphm for ozone (Table 7-9). Hydrocarbon controls needed to meet the standard for the regional peak predicted ozone drop from 57 percent to 16 percent if background hydrocarbon is reduced by 50 percent, background ozone is reduced by 33 percent, and the inflow of hydrocarbons from the New Jersey/New York urban area is reduced by the same amount as the reduction in the Philadelphia emissions.

Relative and total ozone response curves for the regional peak in the Philadelphia urban plume, Downington, and Roxy Water monitors are presented in Figures 7-25 through 7-27 and Figures 7-28 through 7-30, respectively. The decrease in predicted maximum ozone for the regional peak (71 percent) as shown in Figure 7-28 is nearly equal to the reduction in hydrocarbon emissions and boundary conditions (75 percent) if the background ozone is decreased by 33 percent and the background hydrocarbons are decreased by 50 percent. As is evident in Figure 7-30, the calculated percentage reduction in ozone concentration at the Roxy Water monitor is only slightly affected by hydrocarbon emission reductions from the Philadelphia area alone. Substantial ozone reductions can be calculated only if UAM input changes that correspond to emission reductions from the New York City/New Jersey airshed are achieved.

For 13 July, spatial patterns of changes in predicted ozone for the sensitivity simulations are displayed with the use of Deficit/Enhancement (D/E) plots. The list of D/E plots for the sensitivity simulations of 19 July is presented in Table 7-10. Figures 7-31 through 7-33 present D/Es for the sensitivity simulation in which only hydrocarbon emissions from Philadelphia were reduced 25, 50, and 75 percent, respectively. No noticeable decrease in ozone is found in central Philadelphia for any of these three

BEST COPY AVAILABLE

TABLE 7-9. Hydrocarbon emission reductions required to meet the NAAQS for ozone from the sensitivity simulations of 19 July.

Sensitivity Simulation	Percent Hydrocarbon Emission Reduction		
	Philadelphia Urban Plume	Downington	Roxy Water
No change in background; No change in NE and E boundary hydrocarbons	57	27	> 75
No change in background; Reduced NE and E boundary hydrocarbons	44	23	15
Reduced background ozone; Reduced NE and E boundary hydrocarbons	40	15	12
Reduced background hydrocarbons; Reduced NE and E boundary hydrocarbons	20	0	0
Reduced background hydrocarbons and ozone; Reduced NE and E boundary hydrocarbons	16	0	0

BEST COPY AVAILABLE

TABLE 7-10. Deficit/enhancement figures for ozone for 19 July sensitivity simulations.

Figure	Sensitivity Simulation	minus	Base Case Simulation
7-31	6.25BC	minus	6.BASE
7-32	6.50BC	minus	6.BASE
7-33	6.75BC	minus	6.BASE
7-34	6.B25BC	minus	6.BASE
7-35	6.B50BC	minus	6.BASE
7-36	6.B75BC	minus	6.BASE
7-37	6.BKO3	minus	6.BASE
7-38	6.BKBC	minus	6.BASE
7-39	6.BKBC.O3	minus	6.BASE
7-40	6.B50BC.BKO3	minus	6.BASE
7-41	6.B50BC.BKBC	minus	6.BASE
7-42	6.B50BC.BKBC.O3	minus	6.BASE
7-43	6.B50BC.BKO3	minus	6.BKO3
7-44	6.B50BC.BKBC	minus	6.BKBC
7-45	6.B50BC.BKBC.O3	minus	6.BKBC.O3

BEST COPY AVAILABLE

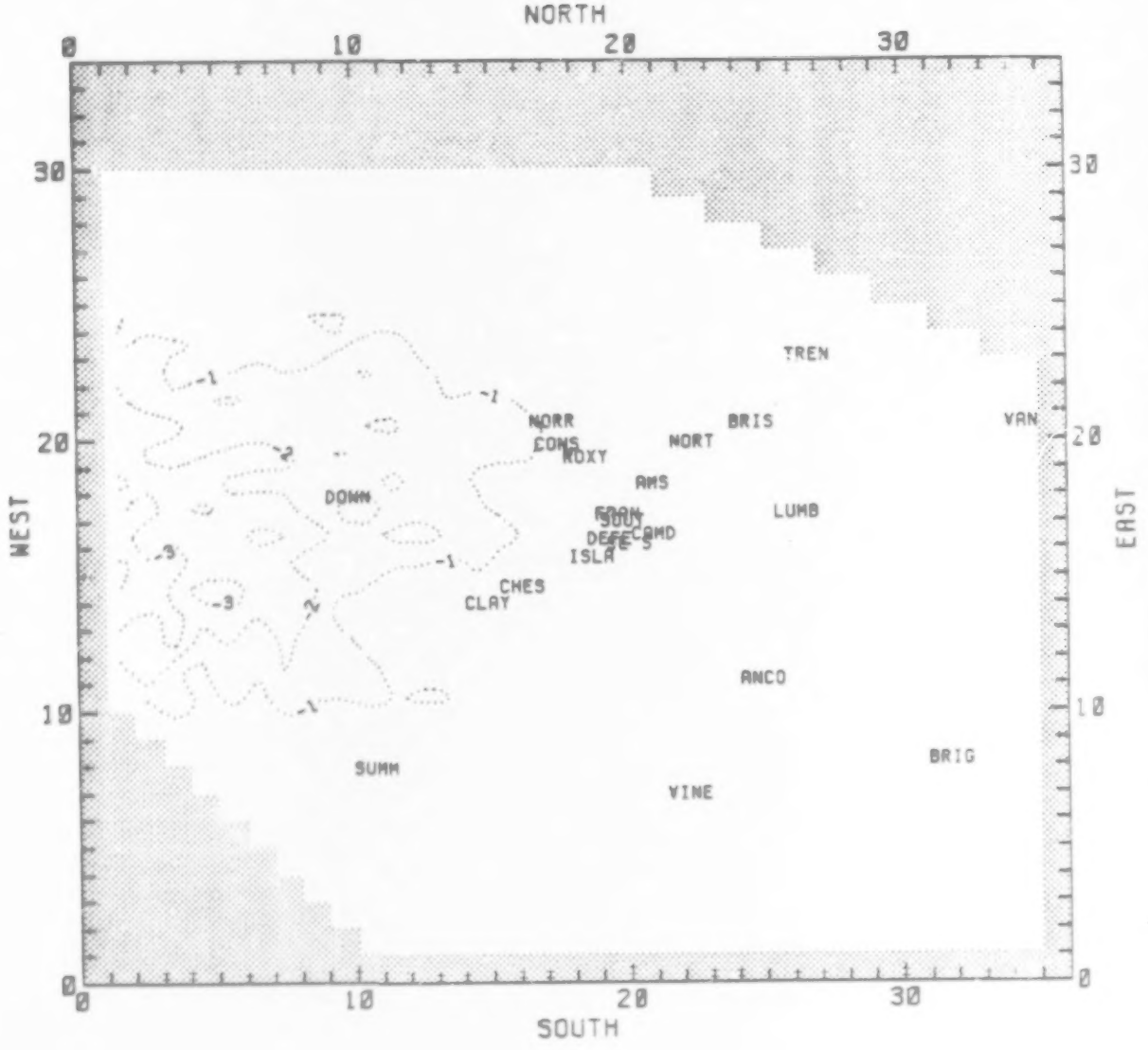

FIGURE 7-31. Maximum deficit/enhancement for ozone (pphm) for all hours on 19 July [6.25HC minus 6.BASE].

BEST COPY AVAILABLE

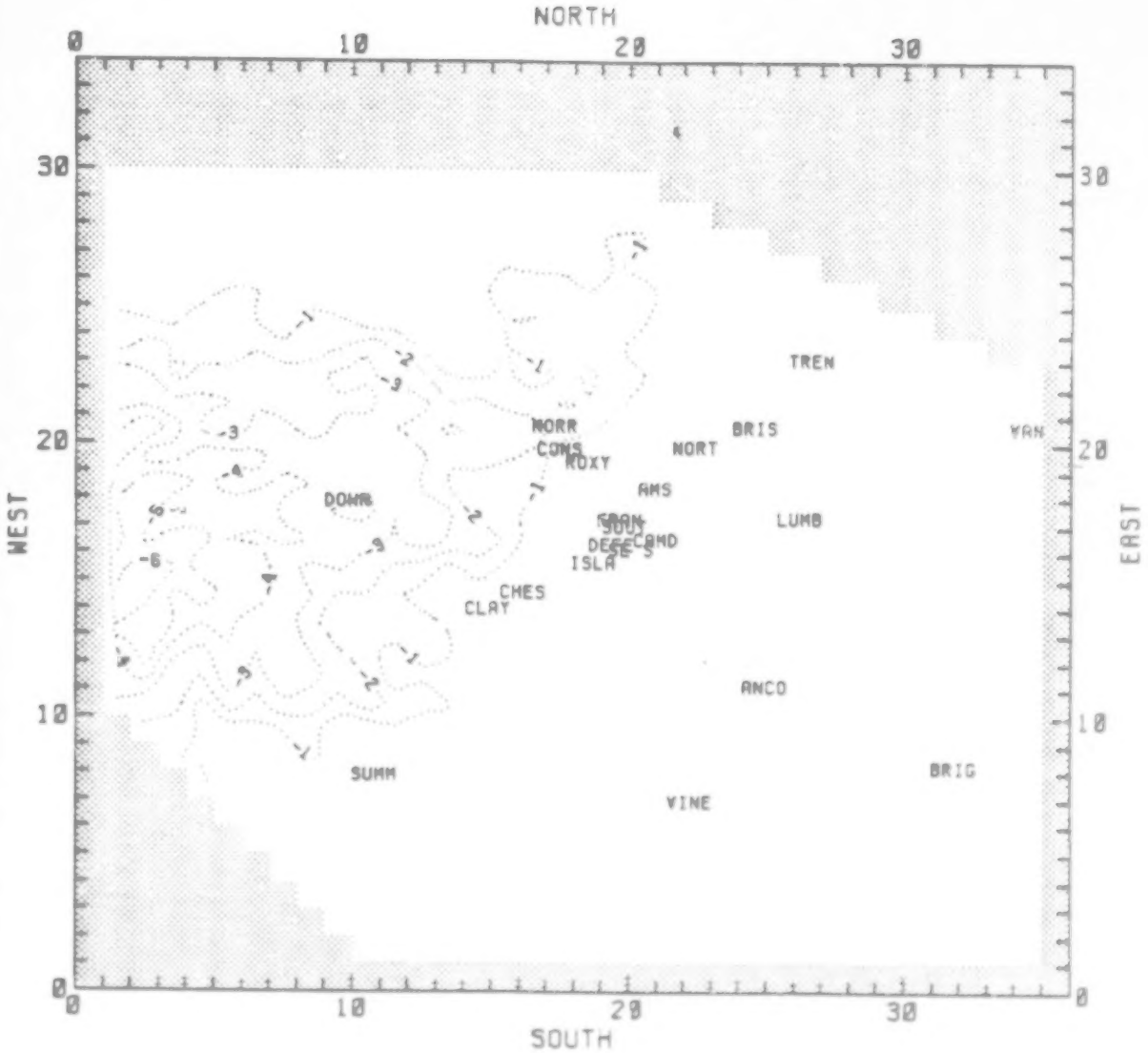

FIGURE 7-32. Maximum deficit/enhancement for ozone (pphm) for all hours on 19 July [6.5OHC minus 6.BASE].

BEST COPY AVAILABLE

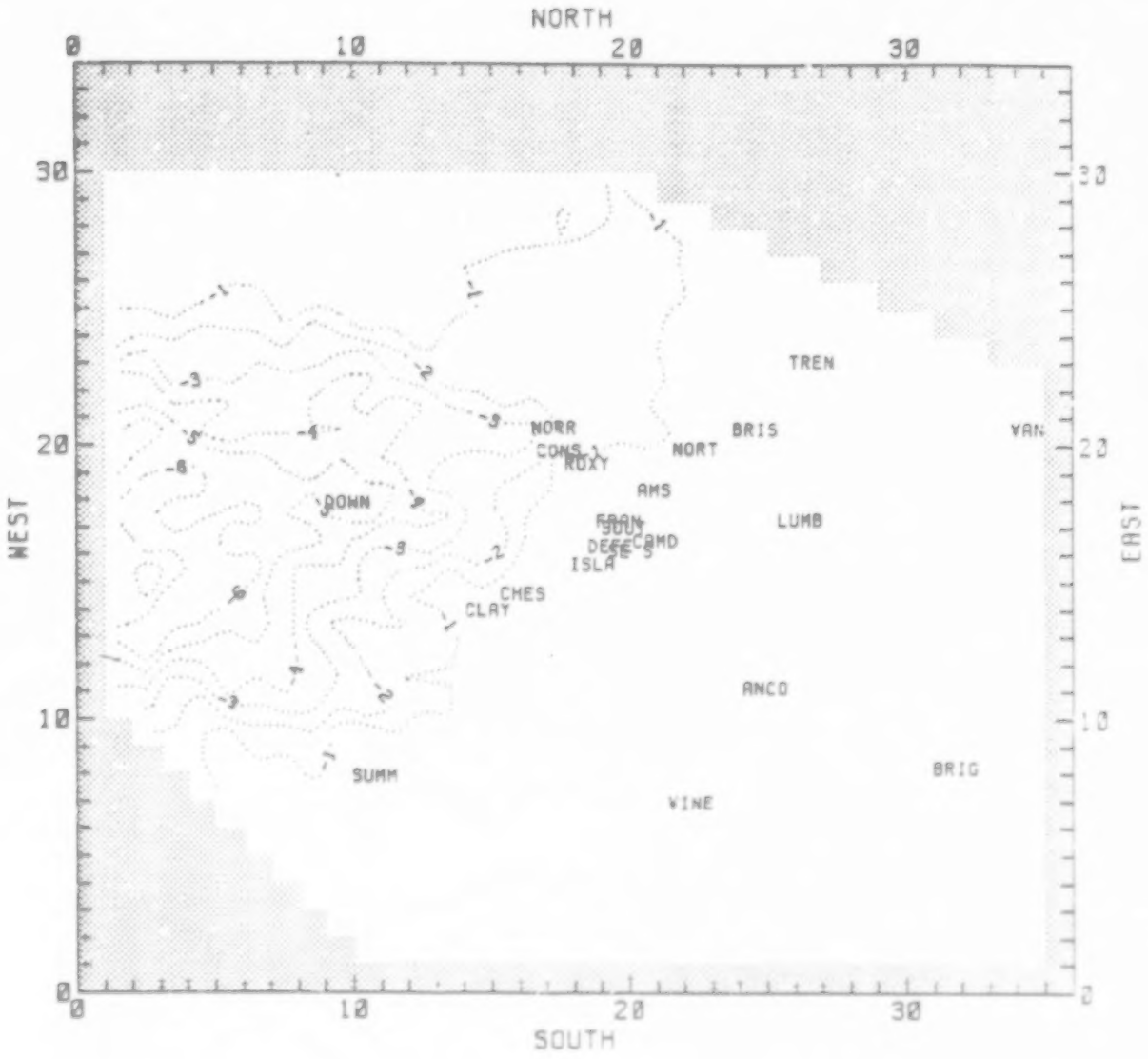

FIGURE 7-33. Maximum deficit/enhancement for ozone (pphm) for all hours on 19 July [6.75HC minus 6.BASE].

BEST COPY AVAILABLE

simulations, consistent with the hypothesis that ozone levels in the New York plume must be decreased before substantial reductions in Philadelphia ozone levels can be achieved on 19 July-type days. The decreases in ozone occur, as expected, west of the urban center, in the area of the Philadelphia urban plume in the base case. If, however, hydrocarbon emissions being transported through the Northeast and East boundaries are decreased along with the urban emissions, then decreases for ozone occur throughout the region as illustrated in Figures 7-34 through 7-36. Maximum changes in predicted ozone for the regional peak were approximately 8 pphm when hydrocarbon emissions were decreased 75 percent, as shown in Figures 7-33 and 7-36. Figures 7-37 through 7-39 were created to assess the changes in ozone predictions with no change in hydrocarbon emissions and decreased background estimates for ozone and hydrocarbons. For 19 July, background estimates for ozone and hydrocarbons represent a decrease of 33 and 50 percent, respectively. When ozone background was decreased, changes of less than 1 pphm occurred, as presented in Figure 7-37. By decreasing hydrocarbon background, ozone decreases of nearly 4 pphm were calculated, as shown in Figure 7-38. After decreasing both background hydrocarbons and ozone, decreases of as much as 5 pphm were predicted, as shown in Figure 7-39.

Maximum calculated changes in ozone from the base case simulation (6.BASE) were evaluated for the simulations with a 50 percent decrease in hydrocarbon emissions and boundary conditions, and various background assumptions for hydrocarbons and ozone. Figures 7-40 through 7-42 present the spatial patterns of these changes. By decreasing urban hydrocarbon emissions and boundary hydrocarbons 50 percent, and assuming a 33 percent decrease in background ozone and a 50 percent decrease in background hydrocarbons, predicted ozone was decreased by 11 pphm in a small area west of Downington (Figure 7-42).

Patterns showing relative changes in predicted ozone for those simulations with decreases of 50 percent in urban hydrocarbon emissions and boundary concentrations are given in Figures 7-43 through 7-45. The patterns are fairly similar to those in Figure 7-35, with minor differences due to the nonlinearity of the atmospheric chemistry in the model.

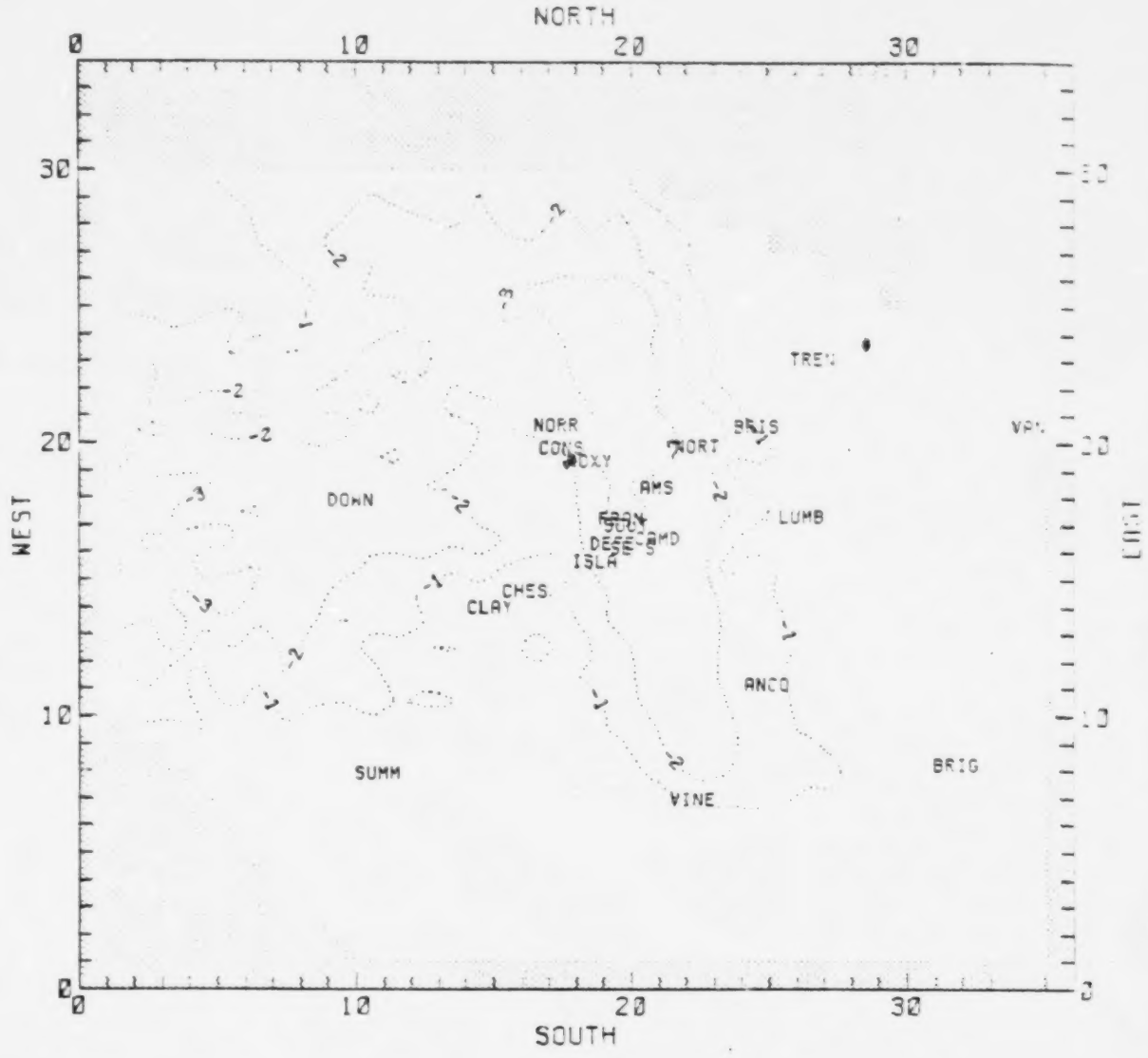

FIGURE 7-34. Maximum deficit/enhancement for ozone (pphm) for all hours on 19 July [6.B25HC minus 6.BASE].

BEST COPY AV

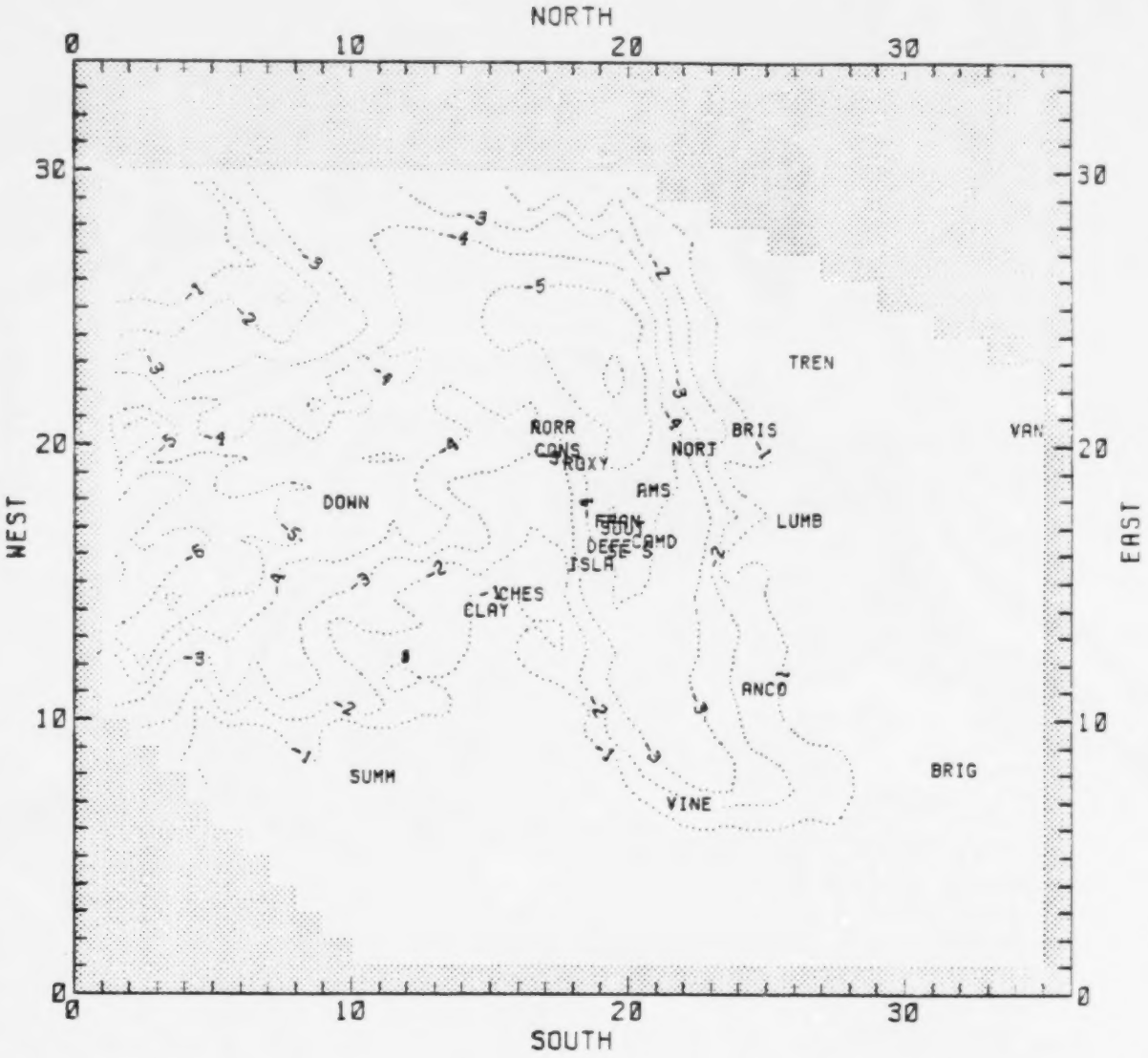

FIGURE 7-35. Maximum deficit/enhancement for ozone (pphm) for all hours on 19 July [6.B50HC minus 6.BASE].

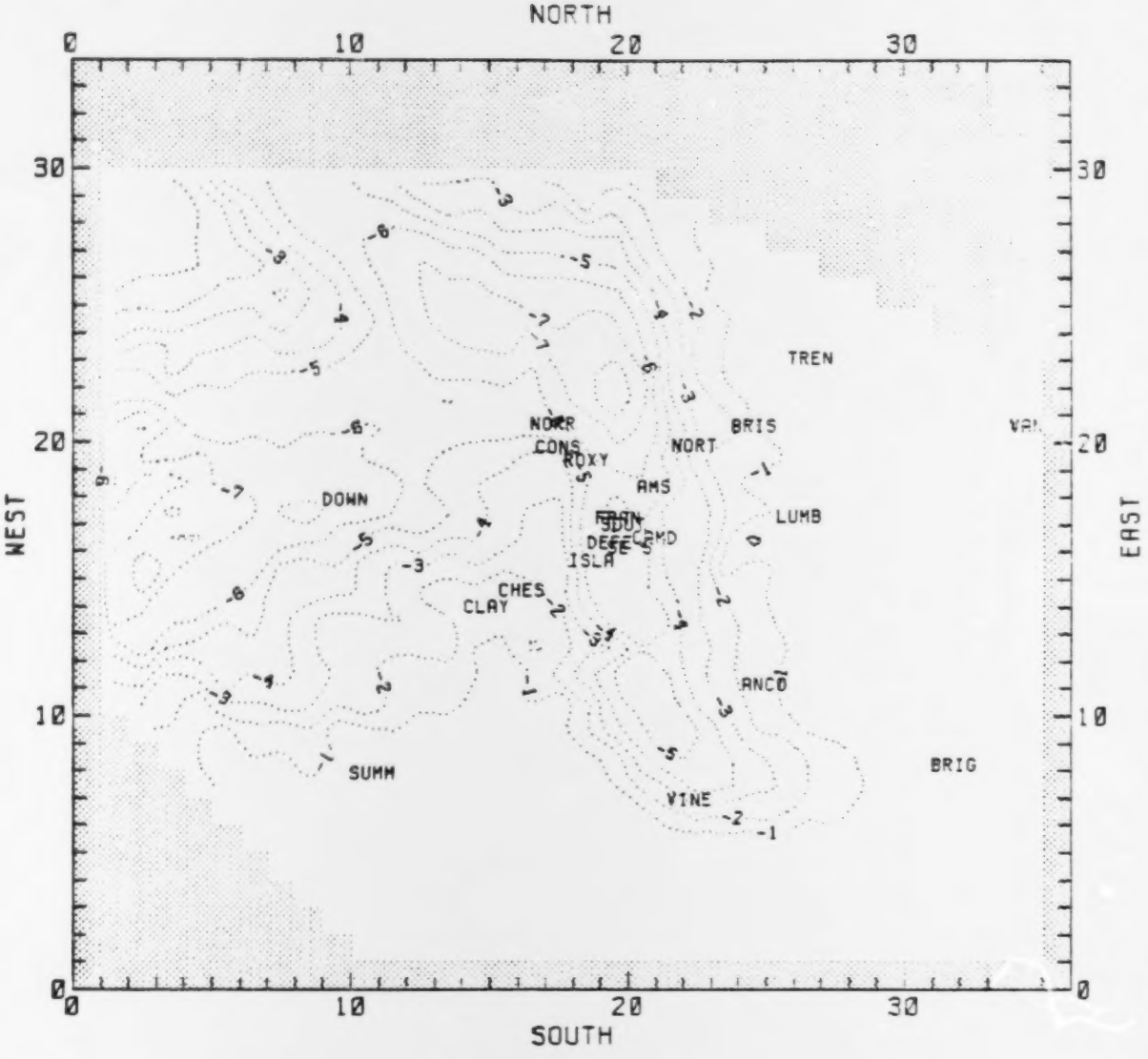

FIGURE 7-36. Maximum deficit/enhancement for ozone (pphm) for all hours on 19 July [6.B75HC minus 6.BASE]

BEST COPY AVAILABLE

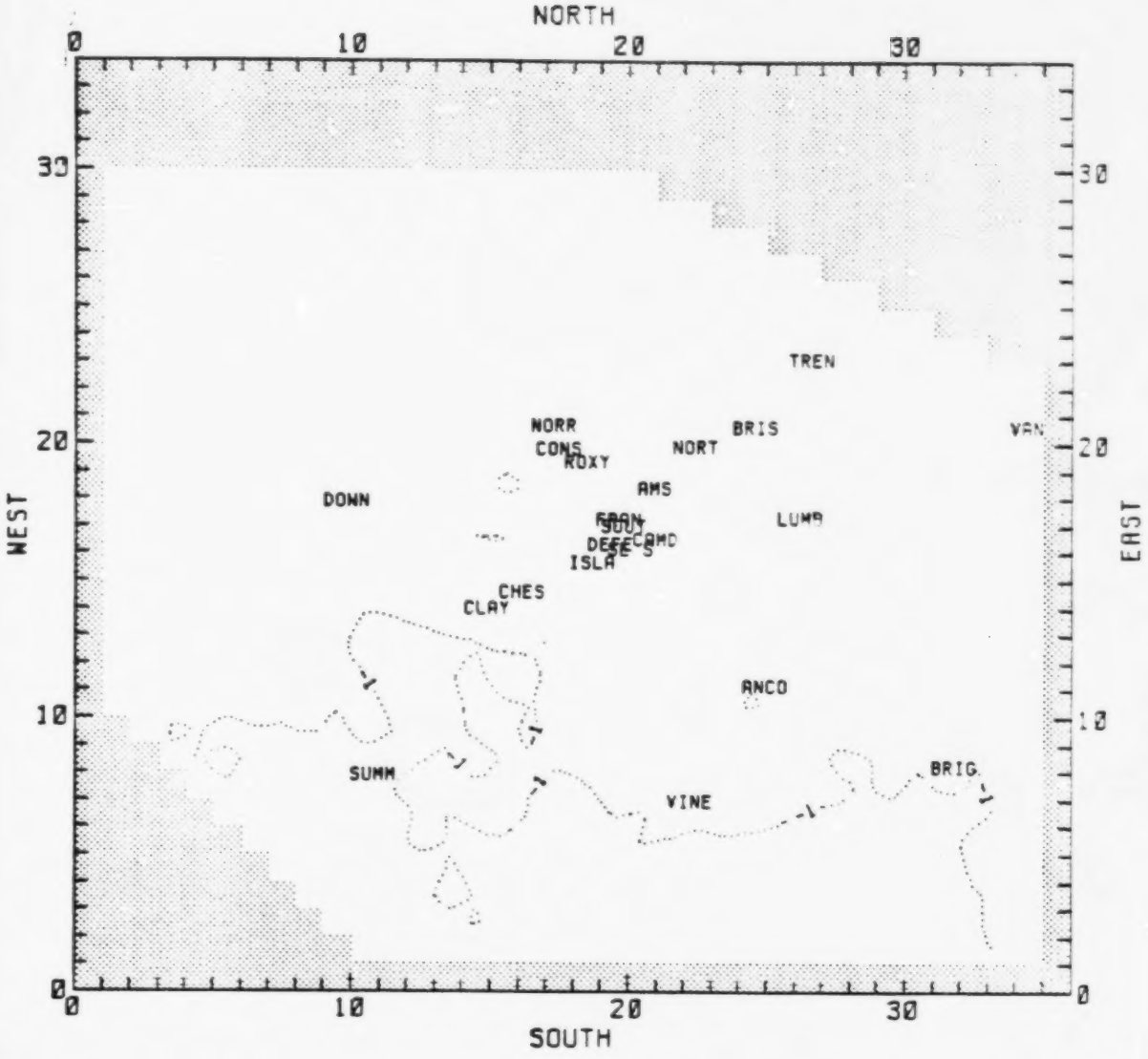

FIGURE 7-37. Maximum deficit/enhancement for ozone (pphm) for all hours on 19 July [6.BK03 minus 6.BASE]

BEST COPY AVAILABLE

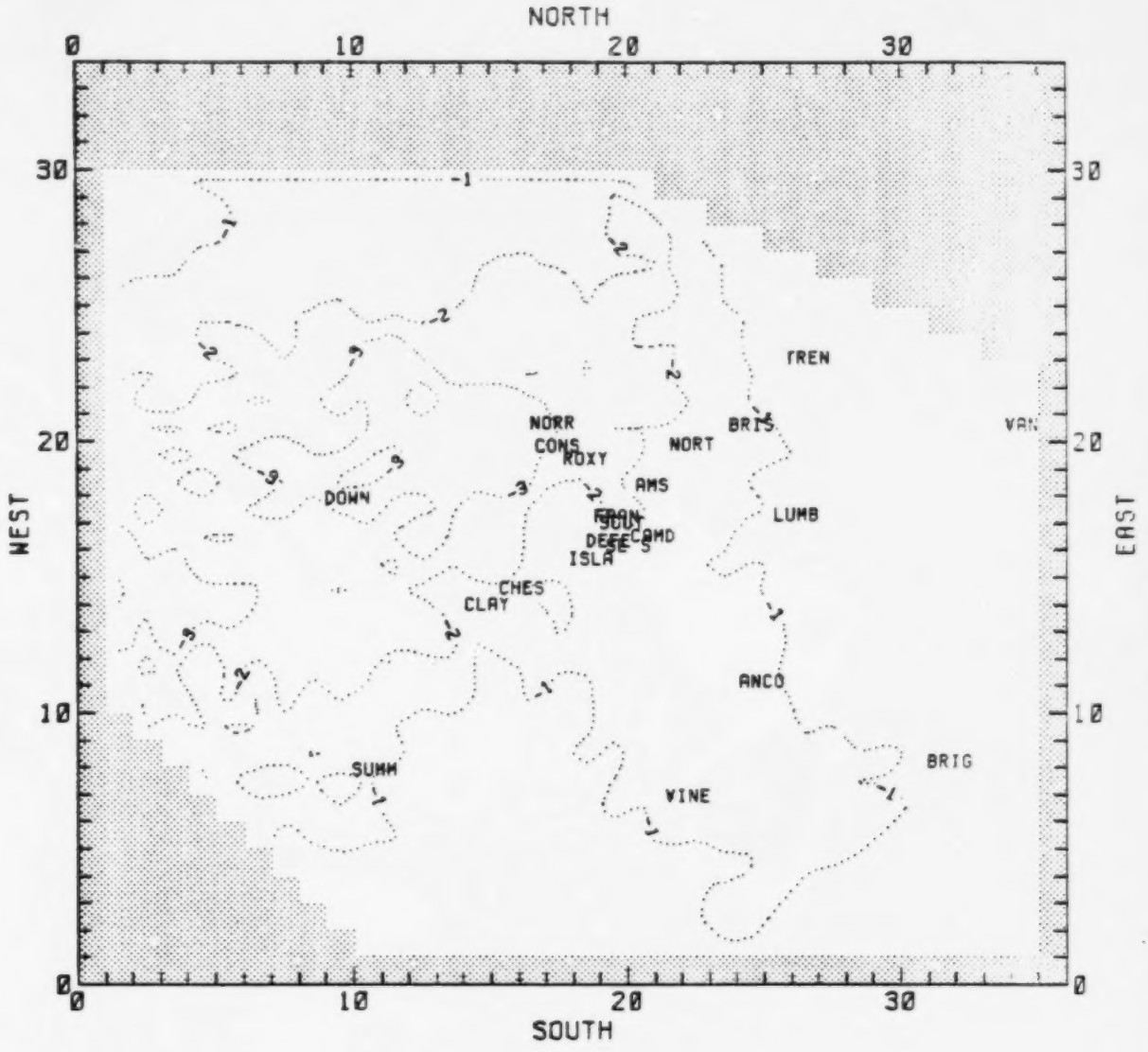

FIGURE 7-38. Maximum deficit/enhancement for ozone (pphm) for all hours on 19 July [6.BKHC minus 6.BASE]

BEST COPY AVAILABLE

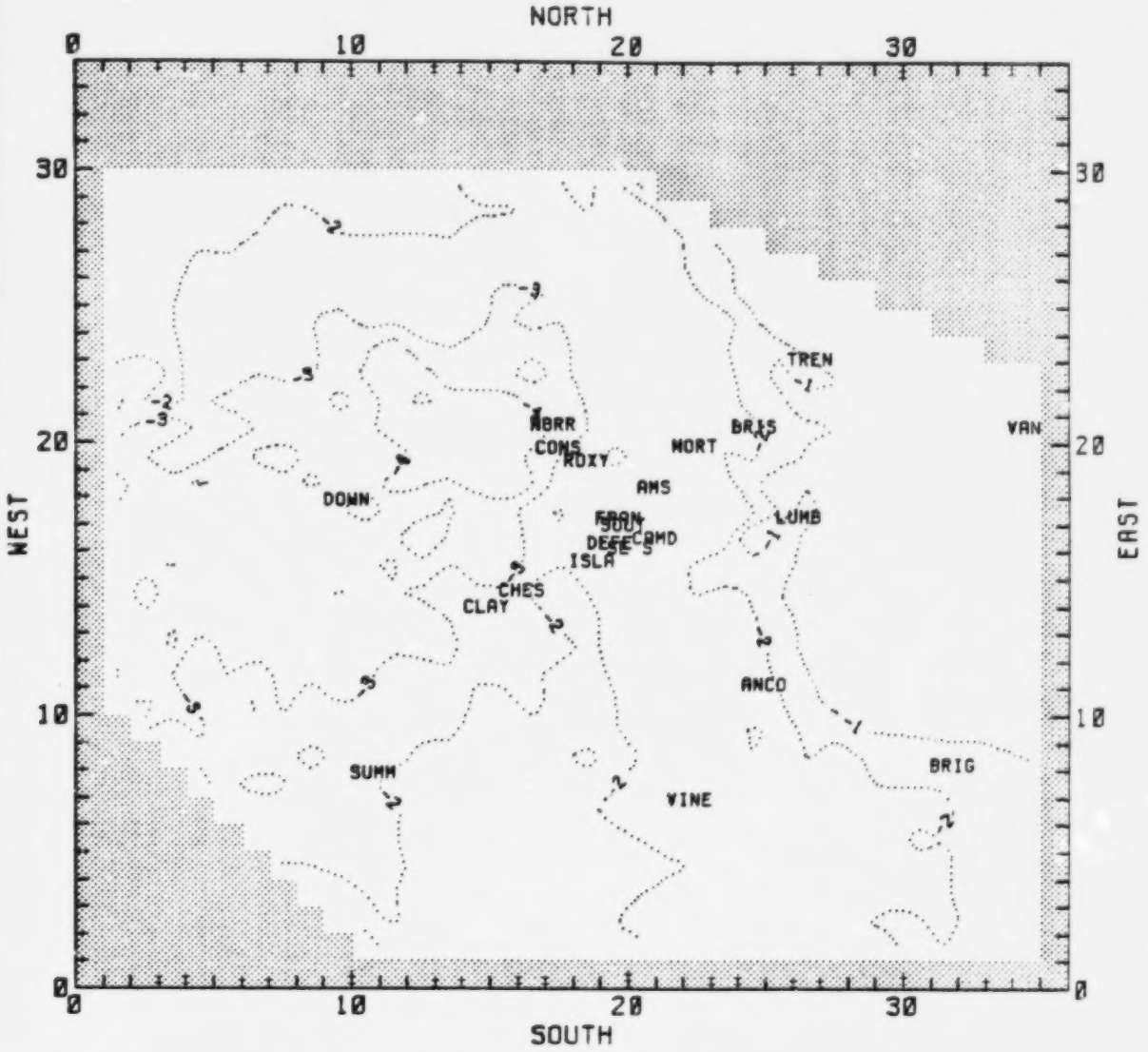

FIGURE 7-39. Maximum deficit/enhancement for ozone (pphm) for all hours on 19 July [6.BKHC.03 minus 6.BASE]

BEST COPY AVAILABLE

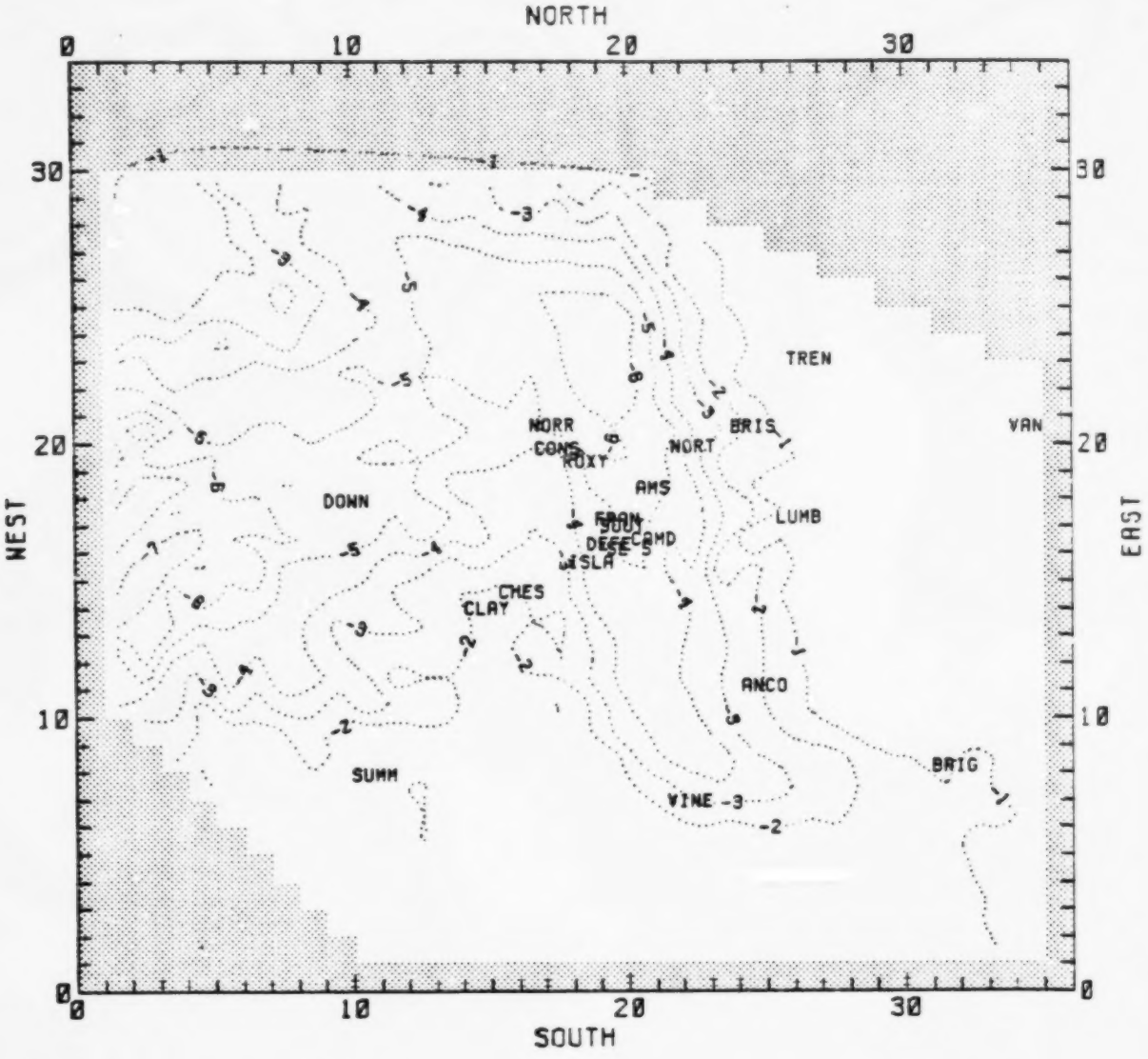

FIGURE 7-40. Maximum deficit/enhancement for ozone (pphm) for all hours on 19 July [6B50HC.BK03 minus 6.BASE]

BEST COPY AVAILABLE

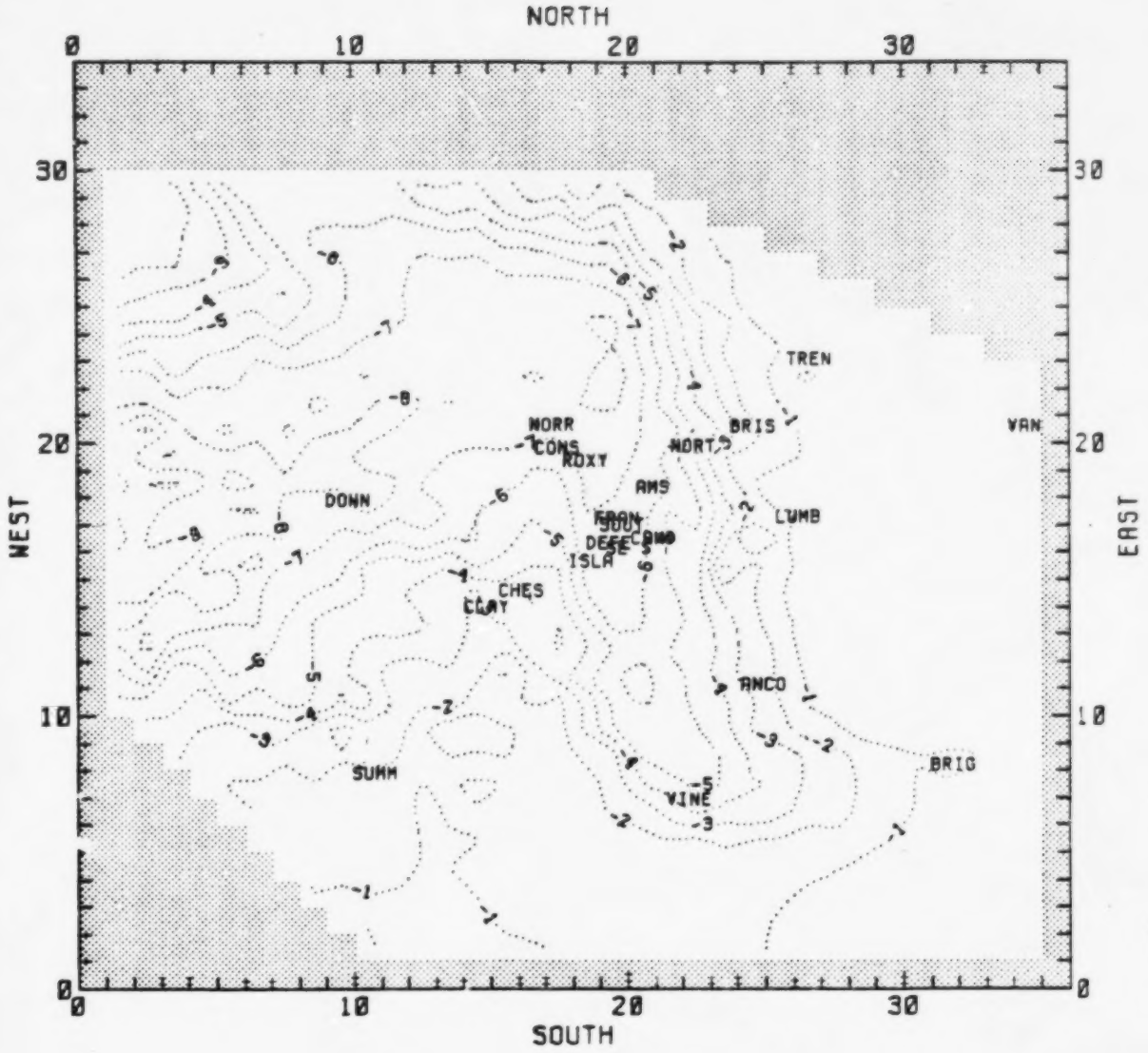

FIGURE 7-41. Maximum deficit/enhancement for ozone (pphm) for all hours on 19 July [6.B50HC.BKHC minus 6.BASE]

BEST COPY AVAILABLE

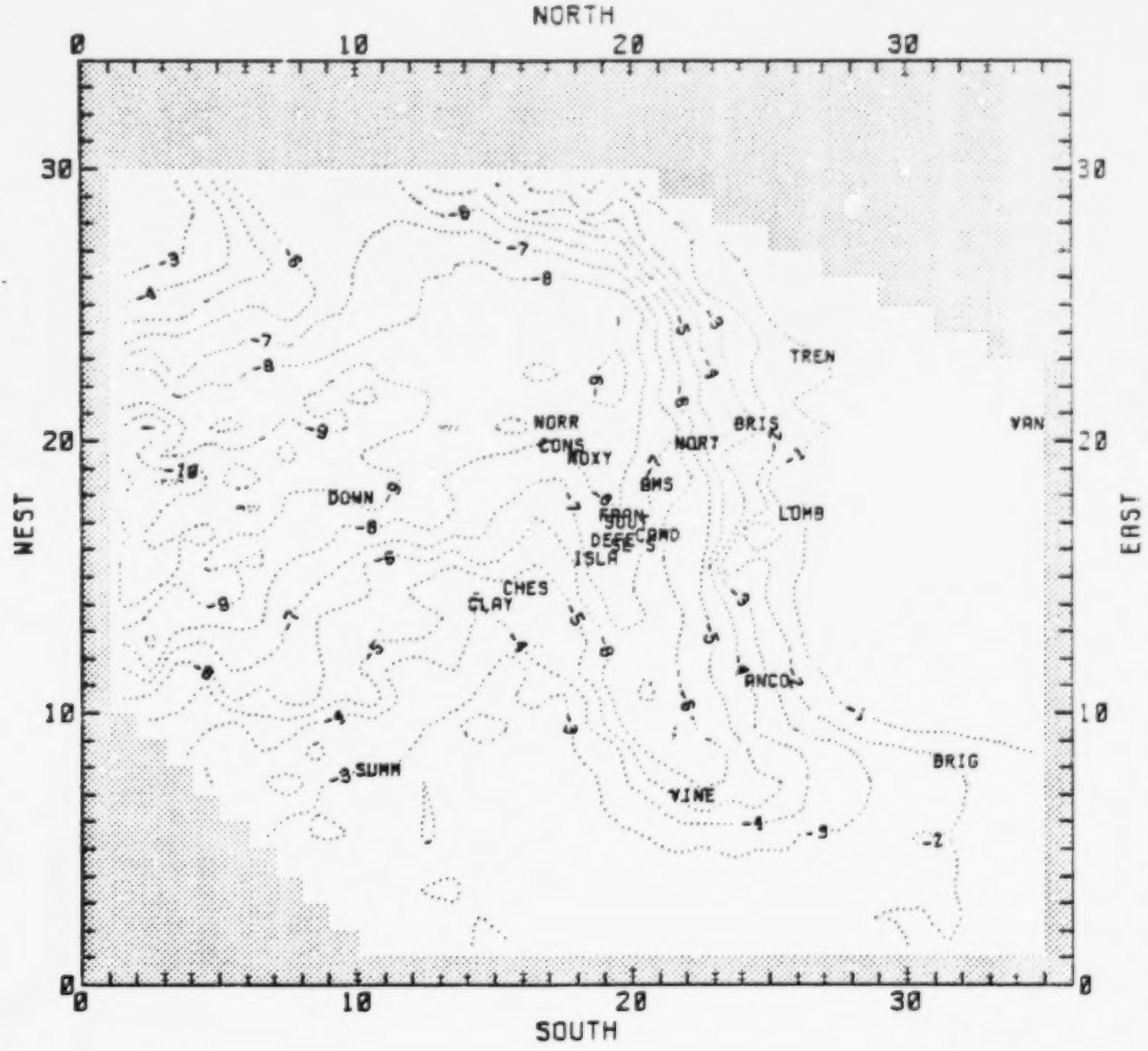

FIGURE 7-42. Maximum deficit/enhancement for ozone (pphm) for all hours on 19 July [6B50HC.BKHC.03 minus 6.BASE]

BEST COPY AVAILABLE

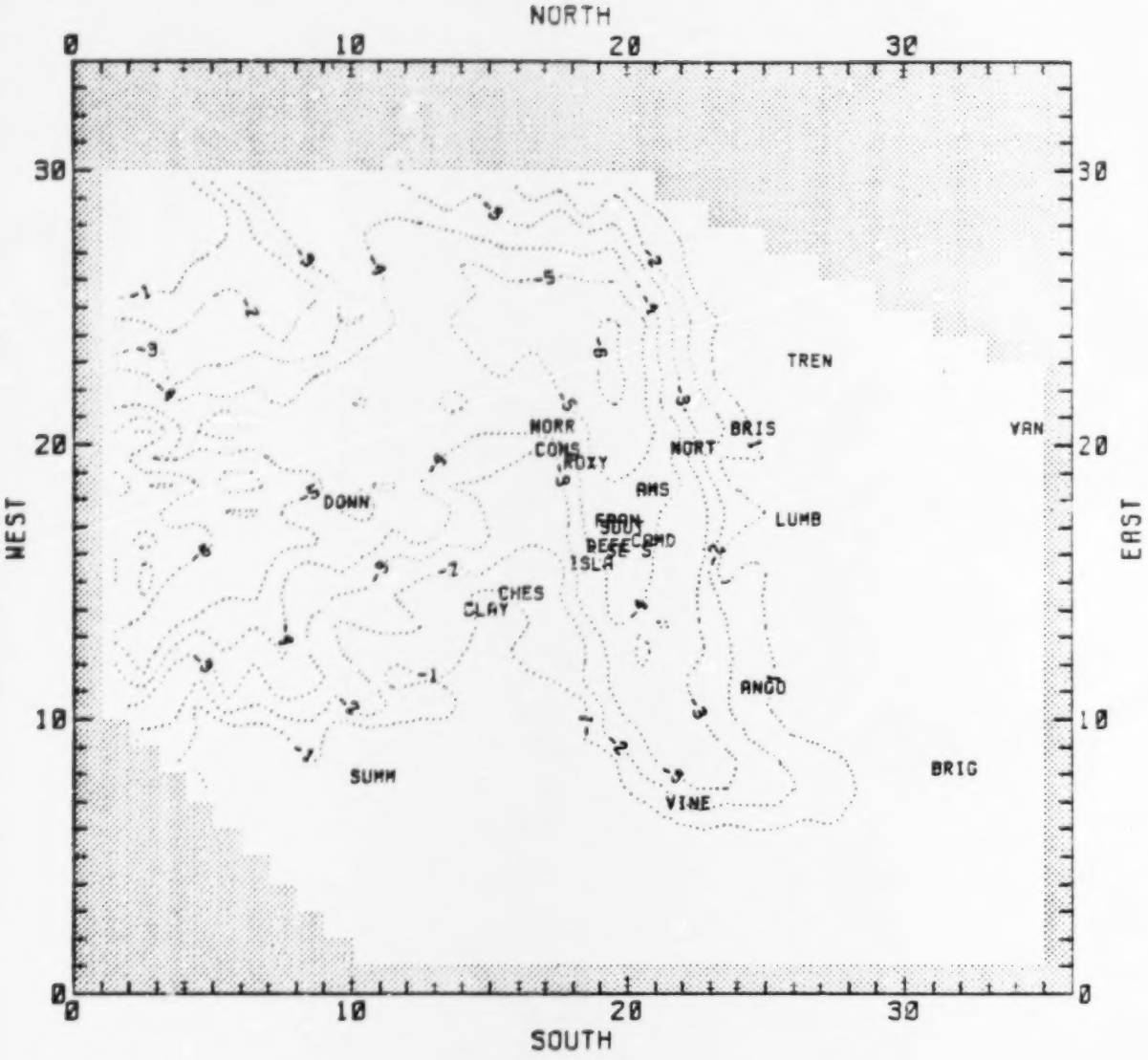

FIGURE 7-43. Maximum deficit/enhancement for ozone (pphm) for all hours on 19 July [6.B50HC.BK03 - 6.BK03]

BEST COPY AVAILABLE

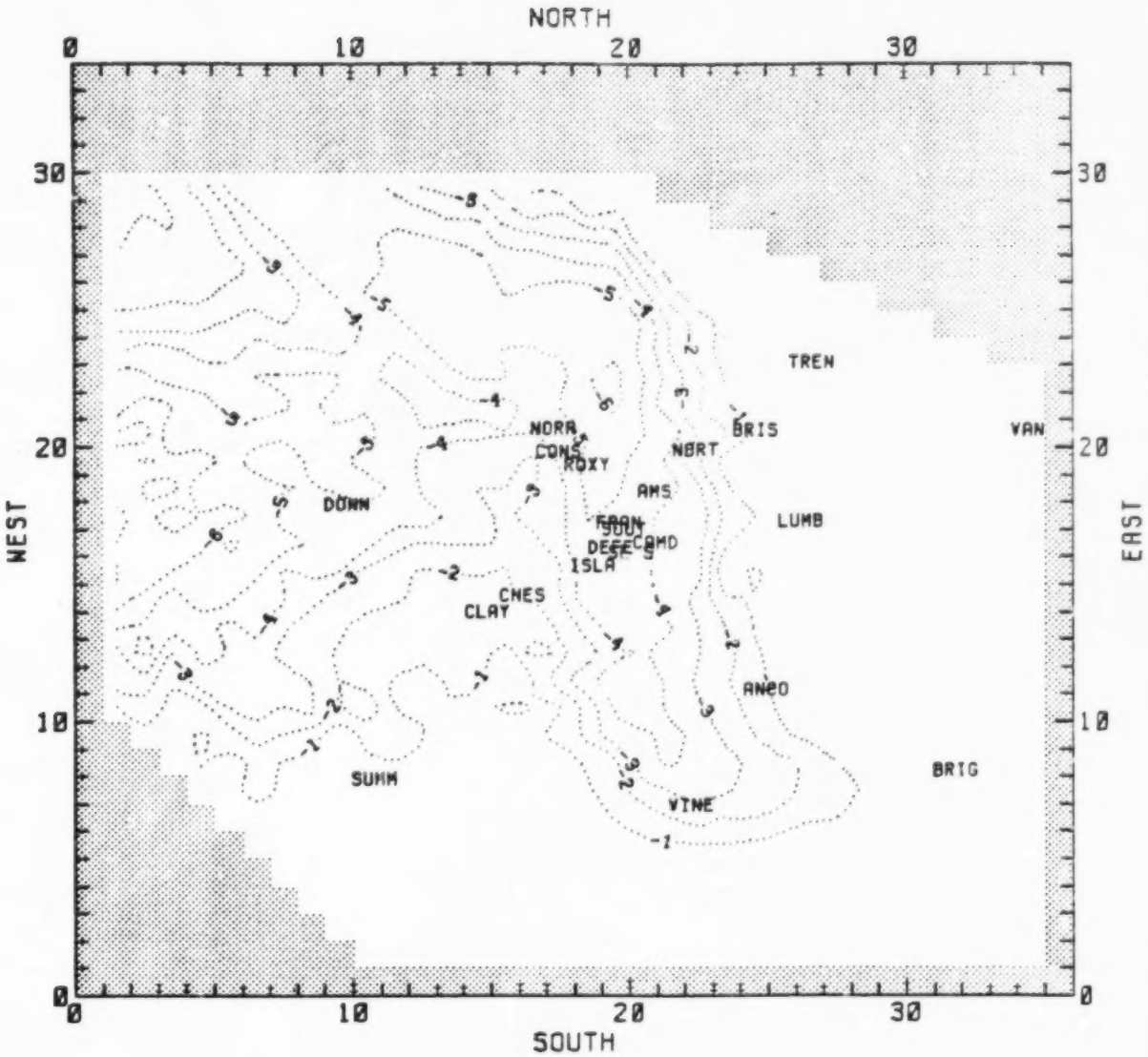

FIGURE 7-44. Maximum deficit/enhancement for ozone (pphm) for all hours on 19 July [6.B50HC.BKHC minus 6.BKHC]

BEST COPY AVAILABLE

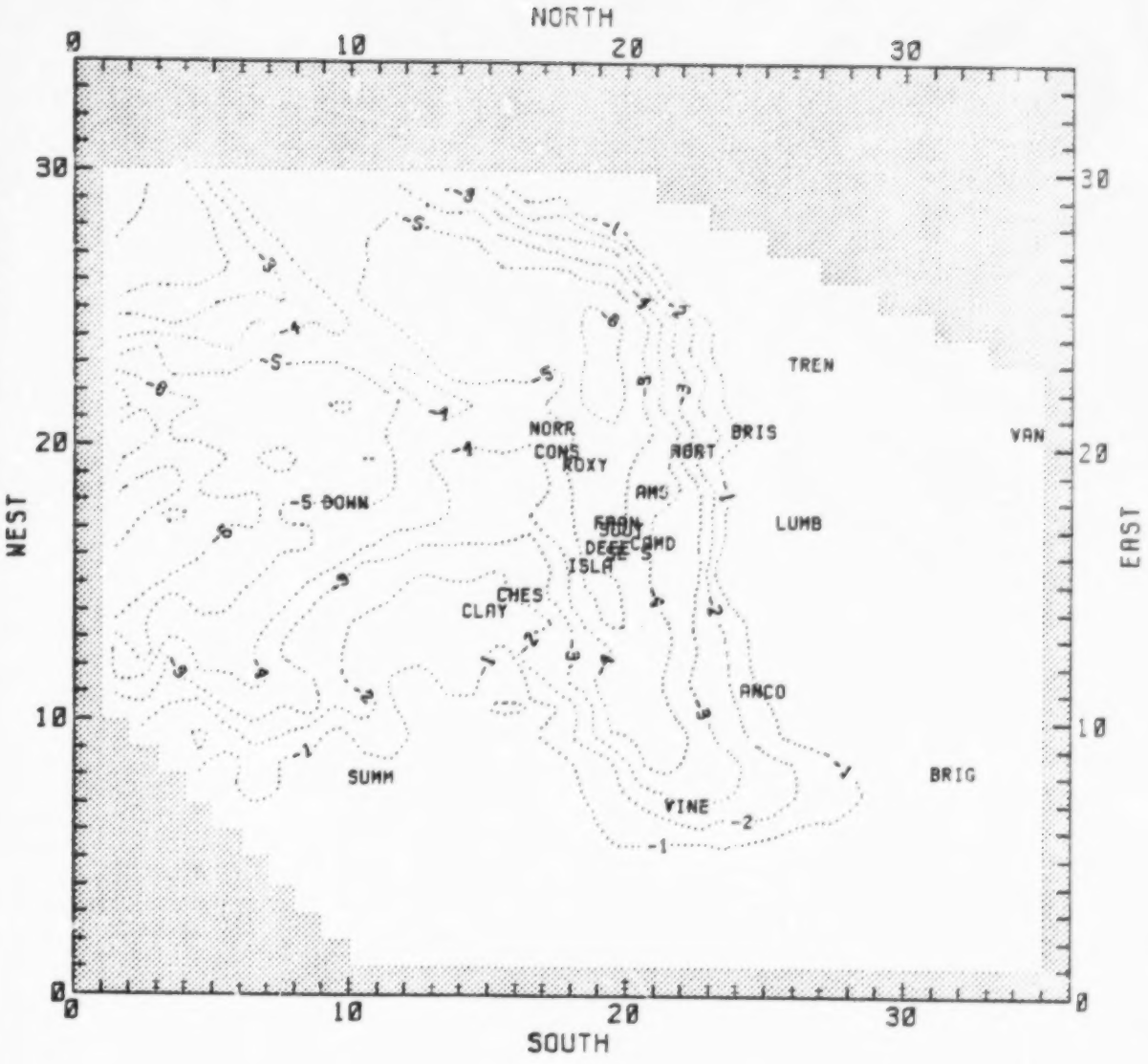

FIGURE 7-45. Maximum deficit/enhancement for ozone (pphm) for all hours on 19 July [6.B50HC.BKHC.03 minus 6.BKHC.03]

BEST COPY AVAILABLE

BLANK PAGE

8 SUMMARY AND CONCLUSIONS

Two summer days experiencing the highest and second-highest observed region-wide ozone concentrations during the 1979 Philadelphia Oxidant Data Enhancement Study were simulated with the Urban Airshed Model (UAM). This study is one of a number of recent applications of the UAM to large metropolitan areas sponsored by the EPA. Other applications have involved the cities of Tulsa, Denver, and St. Louis; work is currently under way to evaluate and apply the UAM to the New York metropolitan area.

The Philadelphia application is unique because the Philadelphia airshed is nested in the expansive and emission-rich Northeast Urban Corridor. Under certain meteorological conditions, interurban transport of fresh oxidant precursors plays a key role in determining ozone levels in Philadelphia due to the proximity of the Baltimore/Washington D.C. urban area to the southwest, and the New Jersey/New York urban area to the northeast. In this study, two distinct meteorological regimes were successfully simulated. On 13 July 1979, high pressure, light winds, and carryover of urban emissions from the previous day created conditions that led to the highest and most widespread high ozone readings recorded during the summer of 1979. The second day simulated, 19 July, was characterized by an influx of fresh migratory precursor emissions from the New Jersey/New York urban area to the northeast into the Philadelphia region. The bulk of the Philadelphia urban plume was advected to the west of the urban center on this day, while the New Jersey/New York plume moved toward the Philadelphia urban center, affecting most station readings. The occurrence of this transport was substantiated by the fact that a parcel trajectory reaching the station recording a high concentration at the time of the peak (Claymont, Delaware) did not travel over high-density emission areas, but originated well to the northeast of the region in the New Jersey/New York urban complex.

The first phase of the model evaluation study involved the preparation of UAM inputs using day-specific air quality and meteorological data. These inputs included estimates of initial conditions, boundary conditions, modeling region specifications, surface land-use features, background concentrations, meteorological scalars, mixing heights, and wind fields. An emission inventory for a typical 1979 summer weekday was prepared and evaluated by the EPA prior to the commencement of this study and was used

BEST COPY AVAILABLE

in all model simulations for both days. Boundary conditions, initial conditions, and background concentrations were specified after examining day-specific air quality and meteorological data. Meteorological scalars (e.g., humidity, surface pressure, etc.), mixing heights, and wind fields were prepared using meteorological data routinely collected in the region and additional data such as radiosonde, pibal, solar radiation, and other surface data from sites which operated specifically for the 1979 summer oxidant data enhancement program in Philadelphia.

Base-case simulations were obtained for both days after a number of preliminary partial-day simulations were performed. For the 13 July base case, the regional peak predicted hourly average ozone concentration was 26.6 pphm, and the peak ozone concentration calculated at a station monitor (Conshohocken, Pennsylvania) was 19.3 pphm; the peak concentration observed at a station monitor was 20.5 pphm. The peak predicted value in the region was 30 percent greater than the peak observed value. This fact may indicate that the model is overestimating the region-wide peak ozone; however, it is unlikely that a limited number of monitors will capture the actual peak ozone that occurred in the region, especially when the urban plume is advected downwind of the urban emission center to the fringe of the metropolitan area where few monitors are located. Model evaluation statistics for peak ozone prediction/observation values paired in space but not paired in time show that the model slightly overestimates peak concentrations by 8.6 percent, with an average overestimate of 1 pphm. For all predictions/observations paired in space and time for observations above 5 pphm, the model overestimates by 15 percent, with an average overestimate of 1.7 pphm. The gross error or mean absolute deviation was 14.8 percent for station peak pairs and 29.5 percent for all pairs. These statistics reveal that for this simulation day, the model shows a tendency toward overestimation of hourly ozone; however, overall model performance is still fairly good.

The development of an appropriate base case simulation for 19 July was more difficult because of the uncertainty in specifying the quantity of precursor inflow from the New Jersey/New York urban area with boundary concentrations on the Northeast and East boundaries. If data from an extended network of monitors at the surface and aloft along a particular boundary provided information on the quantity of inflow material, some degree of uncertainty would still remain in the transport, mixing, and photochemical transformation of this material because of the uncertainty involved in specifying a suitably representative flow field on the surface and aloft from a limited number of wind measurements. Not only is the quantity of precursor material important for boundary specifications, but the timing of the boundary inflow is also critical to the ozone-formation-dependent factors of mixing, turbulent diffusion, and solar radiation as the material is advected through the airshed. Trajectory analysis using

BEST COPY AVAILABLE

the surface wind field prepared for the 19 July simulations was used to verify parcel trajectory paths to the peak observed station ozone value. Parcels originated in the early morning hours northeast of Philadelphia, and data from an upwind monitor (Van Hiseville, New Jersey) were used to estimate hourly precursor inflow along the boundary.

For this simulation, the predicted peak hourly ozone concentration was 17.7 pphm in the urban plume located west of the Downington, Pennsylvania monitor compared to an observed peak value of 17.0 pphm recorded at the Roxy Water, Pennsylvania monitor. The predicted maximum ozone value was 14.2 pphm for the Downington monitor, whereas a value of 15.7 pphm was observed for the same hour. The peak regional value predicted for this same hour was located 30 km west of Downington. This suggests that perhaps spatial alignment errors were introduced because of the possible overestimation of wind speeds due to the technique used in preparing the wind field. In spite of possible minor spatial alignment errors, evaluation statistics show good model performance for the 19 July base case. Statistics on peak station predictions/observations paired in space but not paired in time reveal that the model slightly overestimates peak ozone by 2.1 percent, with an average overestimate of 0.05 pphm. Statistics for predictions/observations paired in space and time show nearly zero bias. The mean absolute deviation or gross error for all pairs, however, is 28.8 percent, with a nonnormalized average absolute deviation of 2.4 pphm. The model underestimated ozone in the lower and upper ranges of ozone observations and overestimated ozone in the mid-range of observations. These model performance evaluation statistics are important considerations for both 13 and 19 July in the light of the next phase of the study, which tested the sensitivity of ozone to changes in critical inputs (such as boundary and background conditions) and used the model to simulate hypothetical urban hydrocarbon emission-reduction scenarios.

A total of 16 20-hour ozone sensitivity simulations were carried out for the 13 July episodes, and a total of 18 simulations were performed for the 19 July episodes. These simulations addressed various assumptions for background ozone and hydrocarbons, inflow boundary hydrocarbons, and across-the-board reductions in urban hydrocarbon emissions (reductions of 25, 50, or 75 percent). Background hydrocarbons were decreased for both simulation days by approximately 50 percent, while background ozone was decreased 50 percent for 13 July and 33 percent for 19 July. Only one simulation was performed in which hydrocarbon boundary conditions on the Southeast inflow boundary were decreased by 50 percent for 13 July. Boundary value hydrocarbons on Northeast and East inflow boundaries for 19 July were decreased by factors corresponding to reductions in the hydrocarbon inventory of 25, 50, and 75 percent. Ozone response in all 13 July sensitivity simulations was obtained by examining the peak predicted hourly ozone in the Philadelphia urban plume and at the two monitors with

BEST COPY AVAILABLE

the highest hourly predicted ozone. For 19 July, the peak predicted regional ozone from Philadelphia urban emissions, as well as the highest station affected by these emissions, was examined. The ozone response at the station with the calculated highest ozone affected by the simulated New Jersey/New York urban emission plume was also examined. Ozone response in the sensitivity simulations revealed the model's sensitivity to various model input assumptions such as background conditions. However, simulated emission reduction scenarios were performed to broadly demonstrate the real purpose of the Urban Airshed Model, which is the prediction of (1) future air quality and (2) controls on present-day emission sources needed to attain and maintain the ozone NAAQS. It is not the intent of this study to dictate the actual control measures needed to improve future air quality in the Philadelphia AQCR; however, the results demonstrate the model's ability to identify critically important planning variables (e.g., HC reductions planned in neighboring influential cities), and thus its use in regulatory settings by air quality planners.

Results for the 13 July sensitivity simulations show that, for the peak predicted ozone concentration in the entire grid, the hydrocarbon emission controls needed to show attainment of the NAAQS for ozone range from 75 percent reduction, assuming no change in background, to 35 percent reduction if background ozone and hydrocarbons are decreased by 50 percent. Background values for hydrocarbons and ozone in the Philadelphia AQCR are the result of atmospheric loading in the entire eastern United States, encompassing the northeast urban emission corridor. Background values in the future can decrease only if other AQCRs also control precursor emissions throughout the region. It is beyond the scope of this study to quantify the reduction in background levels under various urban emission control scenarios throughout the East; however, the model results show the response of ozone to a hypothetical decrease of 50 percent for backgrounds of ozone and hydrocarbons using the meteorological conditions of 13 July. The effect of emission controls in upwind urban areas could be quantitatively assessed if a regional oxidant model were used to define the boundary conditions of the Airshed Model. Regional oxidant models have been developed and applied to the northeastern United States (Liu et al., 1984; Lamb, 1983; Schere and Possiel, 1984). By simulating the effect of emission controls at the regional scale with a regional model, it would be possible to determine the resulting reduction in background hydrocarbons and ozone. These reduced background concentrations could then be used as input to UAM simulations. Examination of the peak predicted regional ozone for the sensitivity simulation of 13 July shows that the difference in urban hydrocarbon emission control needed to meet the standard for two background assumption cases (no-change background case vs. 50 percent decrease in background hydrocarbons and ozone) is large--75 percent compared to 35 percent. This difference is significant for air

BEST COPY AVAILABLE

quality planners and operators of urban emission sources because any change in present-day emission levels has a large effect on the economic factors involved in operating such sources. Similar large differences were obtained from ozone response on 13 July at the peak station examined--45 percent urban hydrocarbon reduction with no change in background compared to 13 percent reduction needed if background for hydrocarbons and ozone is decreased 50 percent.

The 19 July sensitivity simulations were complicated by the transport regime and influx of urban emissions from the New York city area. For the regional peak predicted ozone concentration from the Philadelphia urban plume, there were large differences in control requirements to attain the ozone NAAQS (similar to those of 13 July)--57 percent control of urban hydrocarbon emissions with no change in boundary conditions or background hydrocarbon and ozone assumptions, compared to only 16 percent control required if ozone background is decreased 33 percent, hydrocarbon background is decreased 50 percent, and Northeast and East boundary hydrocarbons are reduced by the same amount as are Philadelphia emissions. Because overall peak ozone predictions in the simulation of 19 July were substantially less than those for 13 July, lower control requirements for urban hydrocarbon emissions were needed to show attainment. For 19 July, all but three of the sensitivity simulations decreased boundary inflow hydrocarbons by 25, 50, and 75 percent. The three simulations in which boundary hydrocarbons were not reduced reveal that attainment may not be maintained for ozone in the Philadelphia AQCR under certain meteorological conditions if neighboring emission-rich areas do not also control emissions. This is due to the close proximity of these emission areas and the meteorological regimes under which interurban transport occurs.

Specific conclusions of this urban photochemical modeling study can be summarized as follows:

(1) The UAM has been demonstrated to successfully simulate two distinct meteorological regimes in the Philadelphia AQCR--stagnation and interurban transport--that led to widespread high ozone concentrations. Model performance, using output statistical measures recommended by EPA/AMS, was judged to be good for both simulation days. For the 13 July base case, the model tended to overpredict peak ozone by an average of 8.6 percent at all station monitors. For 19 July, the model overpredicted peak ozone by 2.1 percent. Because of the slight tendency to overpredict peak ozone and because this tendency is conservative, the model can be considered a satisfactory predictor of ozone in the Philadelphia AQCR.

BEST COPY AVAILABLE

(2) Using the simplified urban hydrocarbon emission/initial condition reduction scenarios in this study, the UAM-calculated urban hydrocarbon emission control requirements for Philadelphia needed to attain the NAAQS for ozone for 13 July were as follows: greater than 75 percent reduction using the calculated peak regional ozone, or 45 percent reduction if the calculated peak ozone at a station monitor is used. For 19 July the hydrocarbon control requirements were as follows: 57 percent hydrocarbon reduction using the calculated peak ozone of the Philadelphia plume, 27 percent reduction using the peak value calculated at a station monitor influenced by the Philadelphia urban plume, and greater than 75 percent using the peak value calculated at a station monitor influenced by the New York plume. The latter control requirement indicates that this monitor was almost entirely influenced by the simulated New Jersey/New York urban plume, because no change in peak ozone was found for those simulations that used reduced Philadelphia urban hydrocarbons coupled with no change in the Northeast and East inflow boundary hydrocarbons.

(3) Urban hydrocarbon control requirements vary widely depending on the background levels assumed for ozone and hydrocarbons. For 13 July, if ozone background is reduced by 50 percent, the hydrocarbon control requirement (using the peak regional value) to meet the ozone NAAQS is decreased from greater than 75 percent to 58 percent. If background hydrocarbons are reduced by 50 percent, with ozone background unchanged, the hydrocarbon control requirement is decreased to 43 percent. Reducing both ozone and hydrocarbon by 50 percent decreases the hydrocarbon control requirement to 35 percent. For 19 July, the hydrocarbon control requirement for the Philadelphia urban plume is reduced from 57 to 44 percent when Northeast and East inflow boundary hydrocarbons are reduced by the same amount as are the Philadelphia emissions. In addition, when background ozone and hydrocarbons are reduced, the following results are obtained: if background ozone is reduced 33 percent, the hydrocarbon control requirement is decreased from 44 to 40 percent; if background hydrocarbon is reduced 50 percent, with ozone background unchanged, the hydrocarbon control requirement is decreased to 20 percent; and if background ozone is reduced 33 percent and background hydrocarbons are reduced 50 percent, the hydrocarbon control requirement to meet the NAAQS for ozone drops to 16 percent. For both days modeled, reductions in background hydrocarbons yield a much greater decrease in hydrocarbon control requirements than do comparable reductions in background ozone.

BEST COPY AVAILABLE

(4) Regional cooperation in reducing area emissions in the eastern United States appears to be required if background levels for hydrocarbons and ozone are to be lowered. Reducing background levels of ozone and hydrocarbons will reduce control requirements for individual sources to achieve attainment. Under certain meteorological conditions, interurban transport of fresh hydrocarbon emissions may lead to violations of the ozone standard in the Philadelphia AQCR regardless of the Philadelphia AQCR emissions levels. It is, therefore, important for neighboring emission source regions to also lower emissions.

BEST COPY AVAILABLE

BLANK PAGE

REFERENCES

Alkezweeny, A. T., K. M. Basness, R. C. Eastie, and T. S. Wetzel (1981), "Northeast Corridor Regional Modeling Project: Aircraft Measurements - New York and Vicinity," EPA-450/4-81-012, March 1981, pp. 235.

Allard, D., M. Chan, C. Marlia, and E. Stephens (1981), "Philadelphia Oxidant Data Enhancement Study--Analysis and Interpretation of Measured Data," EPA-450/4-81-011, U.S. Environmental Protection Agency, Research Triangle Park, North Carolina.

Ames, J., T. C. Meyers, L. E. Reid, D. C. Whitney, S. H. Golding, S. R. Hayes, and S. D. Reynolds (1985), "SAI Airshed Model Operations Manuals Volume I--User's Manual and Volume II--Systems Manual," EPA-600/8-85/007a,b, U.S. Environmental Protection Agency, Research Triangle Park, North Carolina.

[AMS] American Meteorological Society (1981), "Air Quality Modeling and the Clean Air Act: Recommendations to EPA on Dispersion Modeling for Regulatory Applications," American Meteorology Society, Boston, Massachusetts.

Anderson, G. E., S. R. Hayes, M. J. Hillyer, J. P. Killus, and P. V. Mundkur (1977), "Air Quality in the Denver Metropolitan Region--1974-2000," 77-222, Systems Applications, Inc., San Rafael, California.

Bencala, K. E., and J. H. Seinfeld (1979), "An Air Quality Model Performance Assessment Package," Atmos. Environ., Vol. 13, pp. 1181-1185.

Boris, J. P., and D. L. Book (1973), "Flux Corrected Transport, I: SHASTA, an Algorithm That Works," J. Comp. Phys., Vol. 11, pp. 38-69.

Bornstein, R. D. (1968), "Observations of the Urban Heat Island Effect in New York City," J. Appl. Meteorol., Vol. 7, pp. 575-582.

Chock, D. P., and A. M. Dunker (1982), "A Comparison of Numerical Methods for Solving the Advection Equation," Environmental Science Department, General Motors Research Laboratories, Warren, Michigan.

BEST COPY AVAILABLE

Clark, T. L., and R. E. Eskridge (1977), "Non-Divergent Wind Analysis Algorithm for the St. Louis RAPS Network," Environmental Sciences Research Laboratory Report EPA-600/4-77-049, U.S. Environmental Protection Agency, Research Triangle Park, North Carolina.

Clarke, J. F. (1969), "Nocturnal Urban Boundary Layer over Cincinnati, Ohio," Mon. Wea. Rev., Vol. 97, No. 8, pp. 582-589.

Demerjian, K. L., K. L. Schere, and J. T. Peterson (1980), "Theoretical Estimates of Actinic (Spherically Integrated) Flux and Photolytic Rate Constants of Atmospheric Species in the Lower Troposphere," in Advances in Environmental Science and Technology, Vol. 10, pp. 369-459, J. Pitts and R. Metcalf, eds., John Wiley & Sons, New York, New York.

[EPA] U.S. Environmental Protection Agency (1981), "Interim Procedures for Evaluating Air Quality Models," Office of Air Quality Planning and Standards, Research Triangle Park, North Carolina.

[EPA] U.S. Environmental Protection Agency (1982), "Emissions Inventories for Urban Airshed Model Application in the Philadelphia AQCR," 450/4-82-005, Research Triangle Park, North Carolina.

[EPA] U.S. Environmental Protection Agency (1983a), "The St. Louis Ozone Modeling Project," 450/4-83-019, Office of Air Quality Planning and Standards, Research Triangle Park, North Carolina.

[EPA] U.S. Environmental Protection Agency (1983b), "Evaluation of Performance Measures for an Urban Photochemical Model," 450/4-83-021, Office of Air Quality Planning and Standards, Research Triangle Park, North Carolina.

Fox, D. G. (1981), "Judging Air Quality Model Performance," Bull. Am. Meteorol. Soc., Vol. 62, pp. 599-609.

Godowitch, J. M. (1984), personal communication.

Godowitch, J. M., J.K.S. Ching, and J. F. Clarke (1984a), "Spatial Variation of the Evolution and Structure of the Urban Boundary Layer," submitted for publication to Bound. Layer Meteorol.

Godowitch, J. M., J.K.S. Ching, and J. F. Clarke (1984b), "Evolution of the Nocturnal Inversion Layer at an Urban and a Nonurban Location," submitted for publication to J. Climate and Appl. Meteorol.

BEST COPY AVAILABLE

Hayes, S. R. (1979), "Performance Measures and Standards for Air Quality Simulation Models," 78-93R, Systems Applications, Inc., San Rafael, California.

Hillyer, M. J., S. D. Reynolds, and P. M. Roth (1979), "Procedures for Evaluating the Performance of Air Quality Simulation Models," 79-25R, Systems Applications, Inc., San Rafael, California.

Hoel, T. G. (1962), Introduction to Mathematical Statistics, John Wiley & Sons, New York, New York.

Holzworth, G. C. (1972), "Mixing Heights, Wind Speeds, and Potential for Urban Air Pollution Throughout the Contiguous United States," Office of Air Programs Publication No. AP-101, U.S. Environmental Protection Agency, Research Triangle Park, North Carolina.

Jeffries, H. E., R. M. Kamens, K. G. Sexton, and A. A. Gerhardt (1982), "Outdoor Smog Chamber Experiments to Test Photochemical Models," EPA Cooperative Agreement No. 805843, University of North Carolina, Chapel Hill, North Carolina.

Kaimal, J. C., N. L. Abshire, R. B. Chadwick, M. T. Decker, W. H. Hooke, R. A. Kropfli, W. D. Neff, F. Pasqualucci, and P. H. Hildebrand (1982), "Estimating the Depth of the Daytime Convective Boundary Layer," J. Appl. Meteorol., Vol. 21, pp. 1123-1129.

Killus, J. P. (1982), "Background Reactivity Estimates for Atmospheric Modeling Studies," presented at the XV Informal Conference on Photochemistry, June 27-July 1, 1982, Stanford, California.

Killus, J. P., and M. K. Liu (1981), "Development and Evaluation of a Regional-Scale Photochemical Air Quality Simulation Model," paper presented at the 62nd annual meeting, Pacific Division AAAS, University of Oregon, Eugene, Oregon, 14-19 June 1981.

Killus, J. P., and G. Z. Whitten (1981), "A New Carbon-Bond Mechanism for Air Quality Simulation Modeling," SAI No. 81245, prepared for the U.S. Environmental Protection Agency under contract #68-02-3281, Systems Applications, Inc., San Rafael, California.

Killus, J. P., J. P. Meyer, D. R. Durran, G. E. Anderson, T. N. Jerskey, S. D. Reynolds, and J. Ames (1977), "Continued Research in Mesoscale Air Pollution Simulation Modeling: Volume V--Refinements in Numerical Analysis, Transport, Chemistry, and Pollutant Removal," 77-142R, Systems Applications, Inc., San Rafael, California.

BEST COPY AVAILABLE

Lamb, R. G. 1983. "A Regional Scale (1000 km) Model of Photochemical Air Pollution, Part 1, Theoretical Formulation," EPA-600/3-83-035, U.S. Environmental Protection Agency, Research Triangle Park, North Carolina.

Layland, D. E., and H. S. Cole (1983), "A Review of Recent Applications of the SAI Urban Airshed Model," EPA-450/4-84-004, U.S. Environmental Protection Agency, Research Triangle Park, North Carolina.

Liu, M. K., R. E. Morris, and J. P. Killus (1984), Development of a Regional Oxidant Model and Application to the Northeastern United States, Atmos. Environ., Vol. 18, No. 16, pp. 1145-1161.

McRae, G. J., W. R. Goodin, and J. H. Seinfeld (1982), "Mathematical Modeling of Photochemical Air Pollution," Environmental Quality Laboratory, California Institute of Technology, Pasadena, California.

Noonkester, V. R. (1976), The Evolution of the Clear Air Convective Layer Revealed by Surface Based Remote Sensors," J. Appl. Meteorol., Vol. 15, pp. 594-606.

Possiel, N. C., C. W. Spicer, P. R. Sticksel, G. M. Sverdrup, A. T. Alkezweeny, and W. E. Davis (1984), "Northeast Corridor Regional Modeling Project: Ozone and Precursor Transport in New York City and Boston During the 1980 Field Program, EPA-450/4-84-011, U.S. Environmental Protection Agency, Research Triangle Park, North Carolina.

Reynolds, S. D., H. Hogo, W. R. Oliver, and L. E. Reid (1982), "Application of the SAI Airshed Model to the Tulsa Metropolitan Area," SAI No. 82004, report to U.S. Environmental Protection Agency, Contract No. 68-02-3370, Systems Applications, Inc., San Rafael, California.

Reynolds, S. D., L. Reid, M. Hillyer, J. P. Killus, T. W. Tesche, R. I. Pollack, G. E. Anderson, and J. Ames (1979), "Photochemical Modeling of Transportation Control Strategies. I. Model Development, Performance Evaluation, and Strategy Assessment," Federal Highway Administration, Office of Research, U.S. Department of Transportation, Washington, D.C.

Roth, P. M., C. Seigneur, S. D. Reynolds, and T. W. Tesche (1983), "Assessment of NO_x Emission Control Requirements in the California South Coast Air Basin, Vol. III," SYSAPP-83/019, report to Western Oil and Gas Association, Systems Applications, Inc., San Rafael, California.

BEST COPY AVAILABLE

Schere, K. L., and K. L. Demerjian (1977), "Calculation of Selected Photolytic Rate Constants over a Diurnal Range: A Computer Algorithm," EPA-600/4-77-015, U.S. Environmental Protection Agency, Research Triangle Park, North Carolina.

Schere, K. L., and N. C. Possiel. 1984. "U.S. EPA Regional Oxidant Model--Background and Overview." 77th Air Pollution Control Association Annual Meeting, San Francisco, California, 25-29 June 1984.

Seigneur, C., T. W. Tesche, P. M. Roth, and M. K. Liu (1983), "On the Treatment of Point Source Emissions in Urban Air Quality Modeling," Atmospheric Environment, Vol. 17, No. 9, pp. 1655-1676.

Seigneur, C., T. W. Tesche, P. M. Roth, and L. E. Reid (1981), "Sensitivity of a Complex Urban Air Quality Model to Input Data," J. Appl. Meteorol., Vol. 20, pp. 1020-1040.

Seinfeld, J. H. (1977), "Review and Analysis," in International Conference on Oxidants, 1976--Analysis of Evidence and Viewpoints--Part VI. The Issue of Air Quality Simulation Model Utility, EPA-600/3-77-118, U.S. Environmental Protection Agency, Research Triangle Park, North Carolina.

Singh, H. B., and P. L. Hanst (1981), "Peroxyacetyl Nitrate (PAN) in the Unpolluted Atmosphere: An Important Reservoir for Nitrogen Oxides," Geophys. Res. Lett., Vol. 8, No. 8, pp. 941-944.

Spangler, T. C., and R. A. Dirks (1974), "Meso-Scale Variations of the Urban Mixing Height," Bound. Layer Meteorol., Vol. 6, pp. 423-441.

Tesche, T. W., W. R. Oliver, H. Hogo, P. Saxena, and J. L. Haney (1982a), "Assessment of NO_x Emission Control Measurements in the California South Coast Air Basin--Appendix A: Performance Evaluation of the Systems Applications Airshed Model for the 26-27 June 1974 O_3 Episode in the South Coast Air Basin," SAI No. 82064, Systems Applications, Inc., San Rafael, California.

Tesche, T. W., W. R. Oliver, H. Hogo, P. Saxena, and J. L. Haney (1982b), "Assessment of NO_x Emission Control Requirements in the California South Coast Air Basin--Appendix B: Performance Evaluation of the Systems Applications' Airshed Model for the 7-8 November 1978 NO_2 Episode in the South Coast Air Basin," SAI No. 82230, Systems Applications, Inc., San Rafael, California.

BEST COPY AVAILABLE

Wesely, M. L. (1983), "Turbulent Transport of Ozone to Surfaces Common in the Eastern Half of the United States," in Trace Atmospheric Constituents: Properties, Transformations, and Rates, pp. 345-370, Advances in Environmental Science and Technology, Vol. 12, S. E. Schwartz, ed. (H. Wiley-Interscience Publication).

Westburg, H., and P. Sweany (1980), "Philadelphia Oxidant Enhancement Study: Hydrocarbon Analysis," EPA-450/4-80-022, U.S. Environmental Protection Agency, Research Triangle Park, North Carolina.

Whitten, G. Z., and H. Hogo (1978), "User's Manual for Kinetics Model and Ozone Isopleth Plotting Package," EPA-600/8-78-014a, U.S. Environmental Protection Agency, Research Triangle Park, North Carolina.

Yanenko, N. N. (1971), The Method of Fractional Steps, Springer Verlag, New York.

Zalesak, S. T. (1979), "Fully Multidimensional Flux-Corrected Transport Algorithms for Fluids," J. Computational Physics, Vol. 31, pp. 335-362.

BEST COPY AVAILABLE

APPENDIX A

COMPILATION OF AIRSHED RESULTS FOR 13 JULY 1979

BEST COPY AVAILABLE

BLANK PAGE

APPENDIX A

COMPILATION OF AIRSHED RESULTS FOR 13 JULY 1979

This appendix compiles various sets of Airshed Model ozone results. Figure A-1 is a complete set of hourly average ozone isopleths in the Philadelphia area throughout the day. Time-series plots comparing distance-weighted average and maximum/minimum ozone predictions within one cell's distance with observations at 19 monitoring stations are presented in Figure A-2. Model results presented in this manner are helpful in developing a better qualitative understanding of the simulation results. These grid model concentration estimates used in comparison with the observed data are defined as follows:

Distance-Weighted Average. The solid lines presented in Figure A-2 represent an average model prediction (for comparison with observed values), which is obtained by computing the distance-weighted average concentration of the four grid cells nearest to the monitor where the observed value was recorded.

Maximum/Minimum One Cell Away. The dashed lines presented in Figure A-2 represent the maximum and minimum concentrations predicted in the block of nine cells centered on the grid cell containing the monitoring station. This envelope provides an indication of the spatial variability of the predicted concentration values in the immediate vicinity of the station.

These plots reveal the presence of steep spatial gradients in the concentration field and the qualitative effect that wind field errors might have on the performance results. In calculating the model evaluation statistics, the distance-weighted average estimates produced by the simulation are used.

BEST COPY AVAILABLE

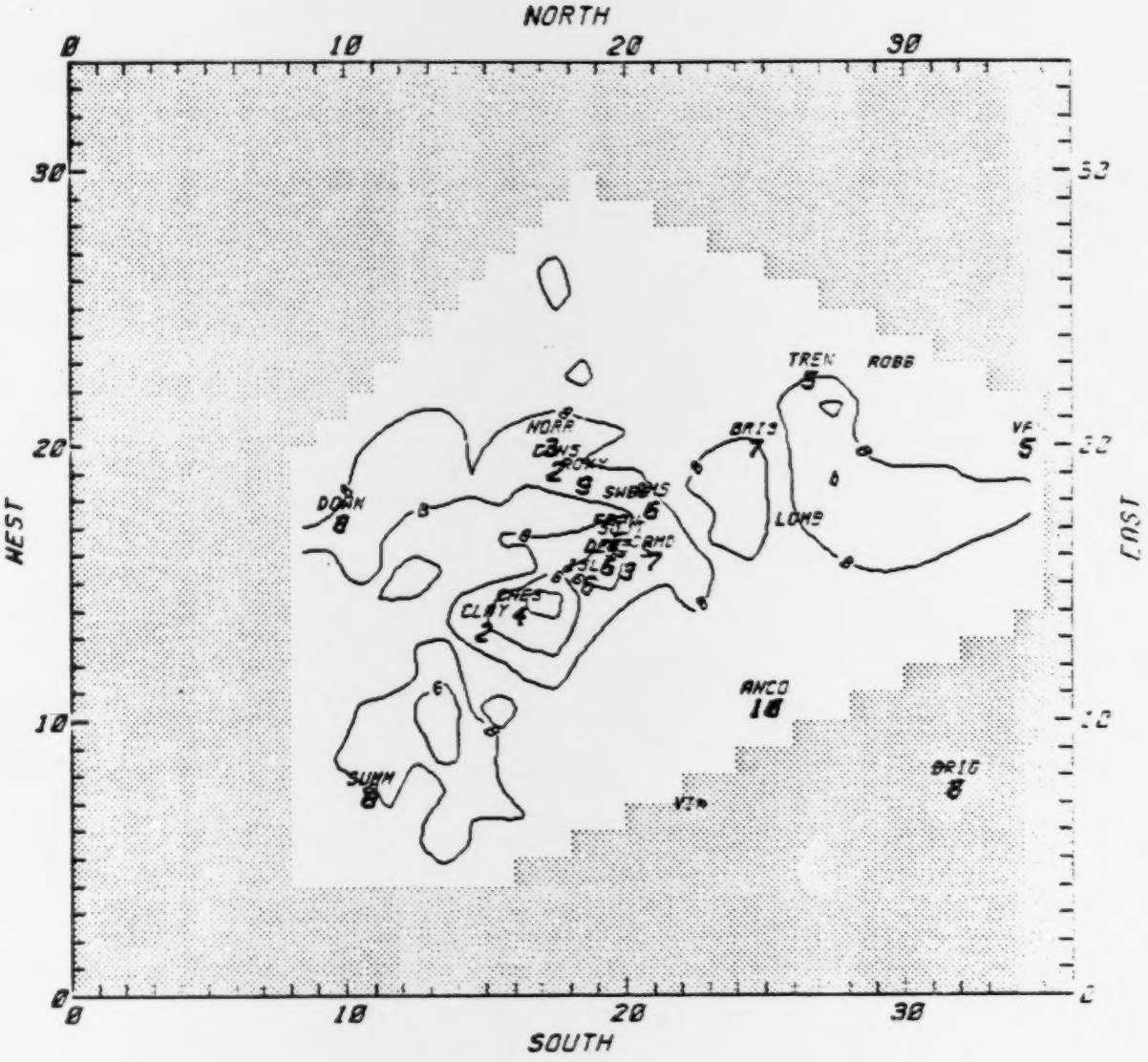

(a) BETWEEN THE HOURS OF 9 AND 10

FIGURE A-1. Hourly variation in predicted ground-level ozone concentration fields (pphm) for Philadelphia, 13 July 1979 (bold numbers correspond to station observations).

BEST COPY AVAILABLE

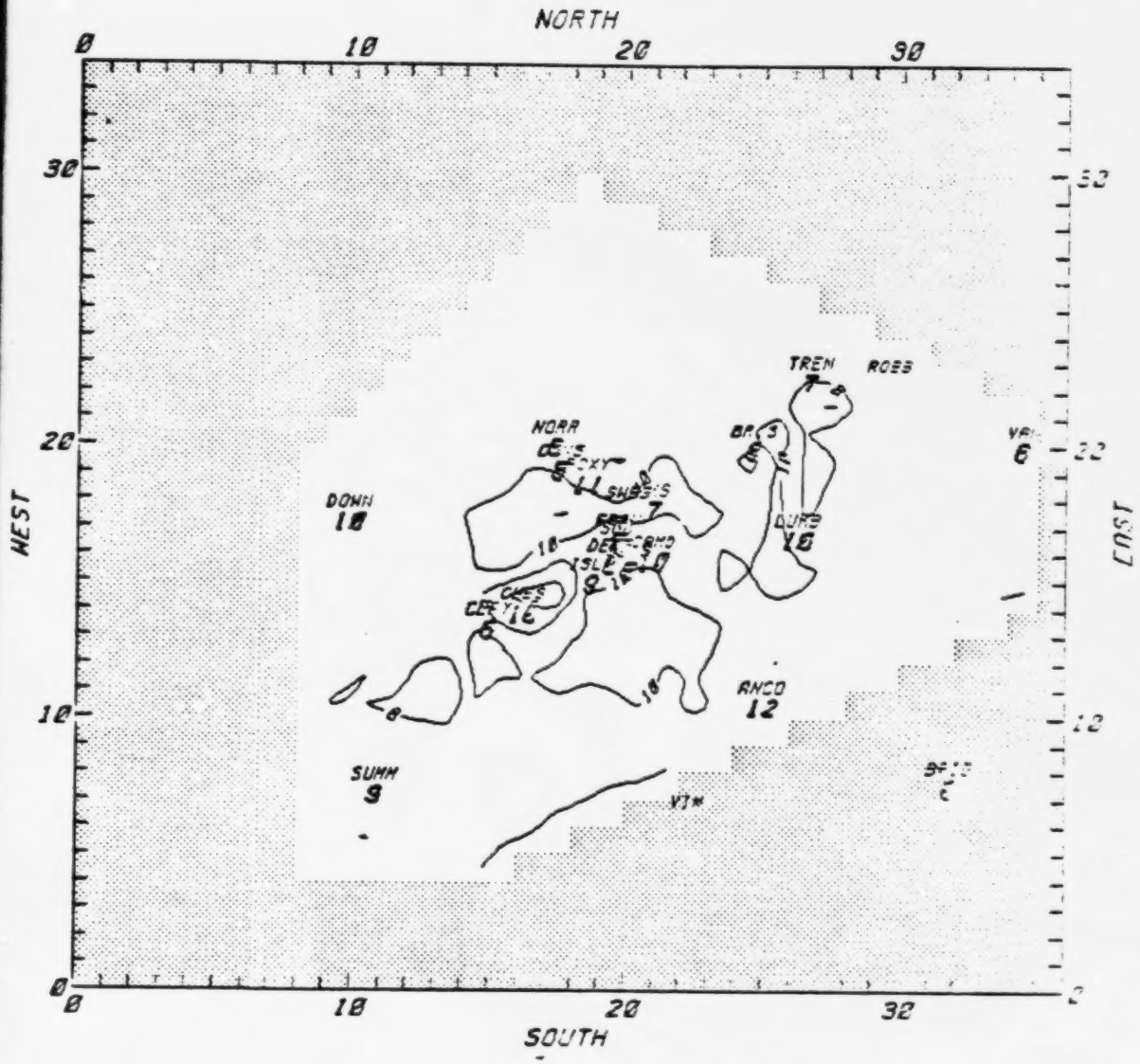

(b) BETWEEN THE HOURS OF 10 AND 11

FIGURE A-1 continued.

BEST COPY AVAILABLE

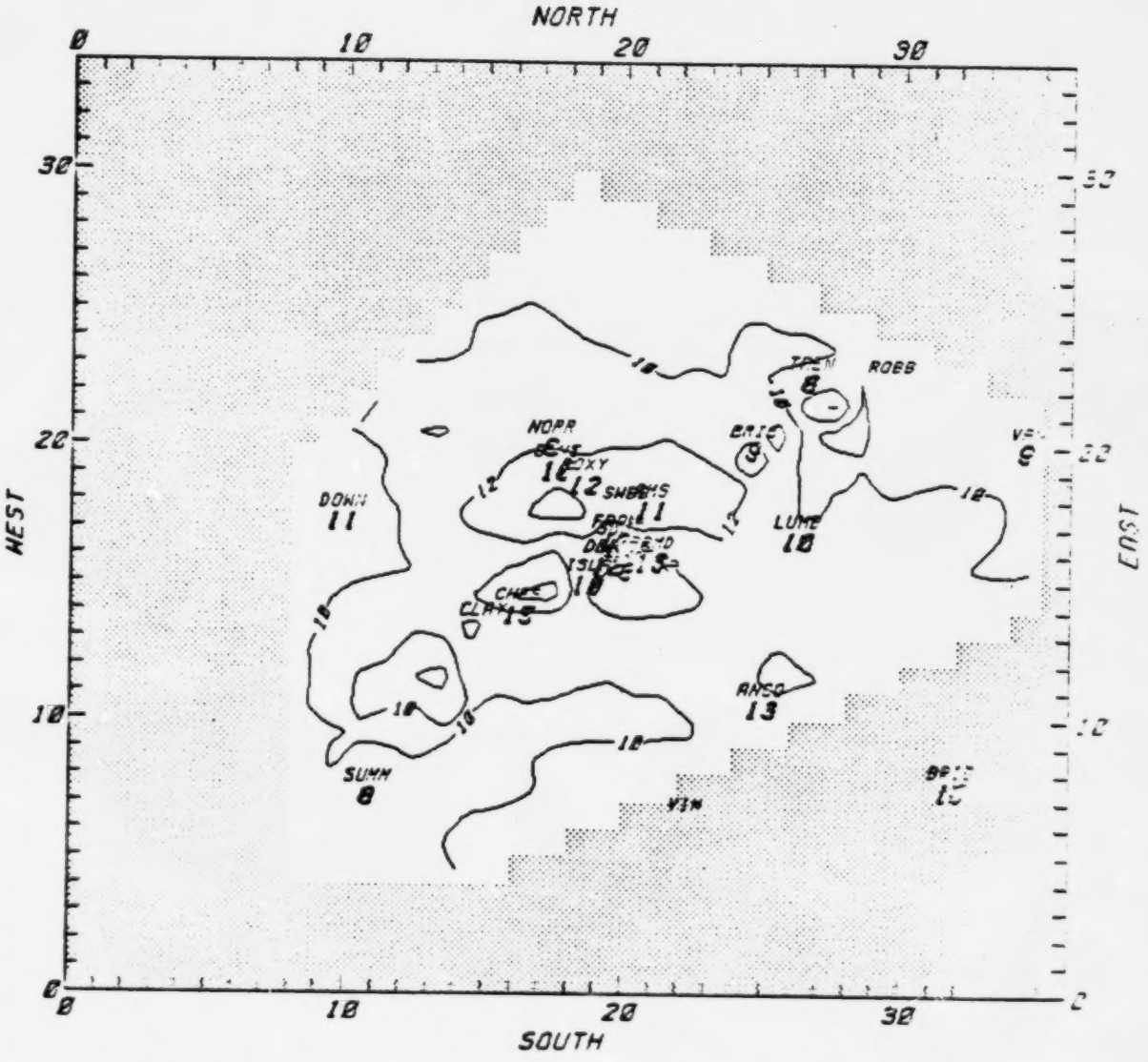

(c) BETWEEN THE HOURS OF 11 AND 12

FIGURE A-1 continued.

BEST COPY AVAILABLE

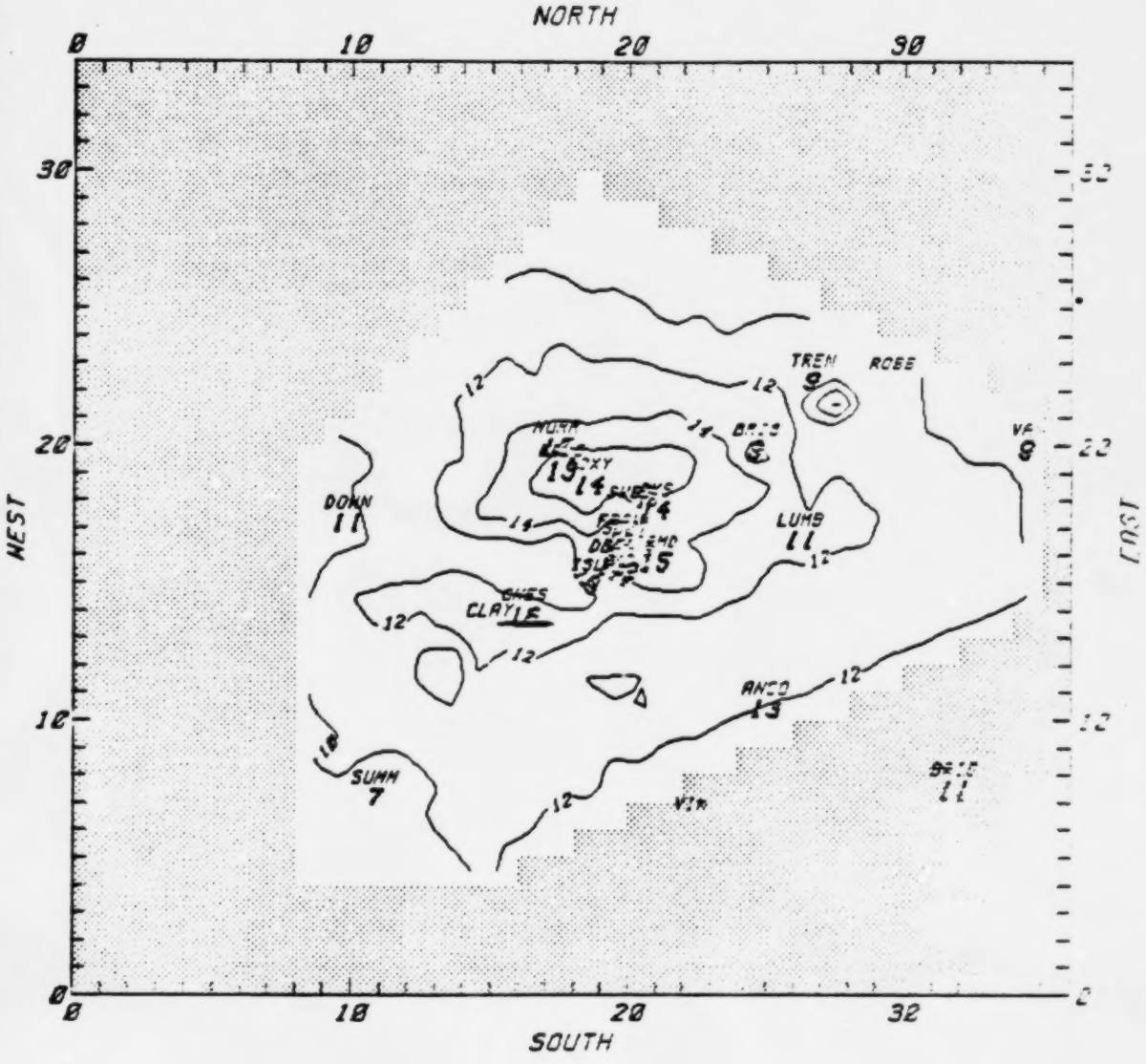

(d) BETWEEN THE HOURS OF 12 AND 13

FIGURE A-1 continued.

BEST COPY AVAILABLE

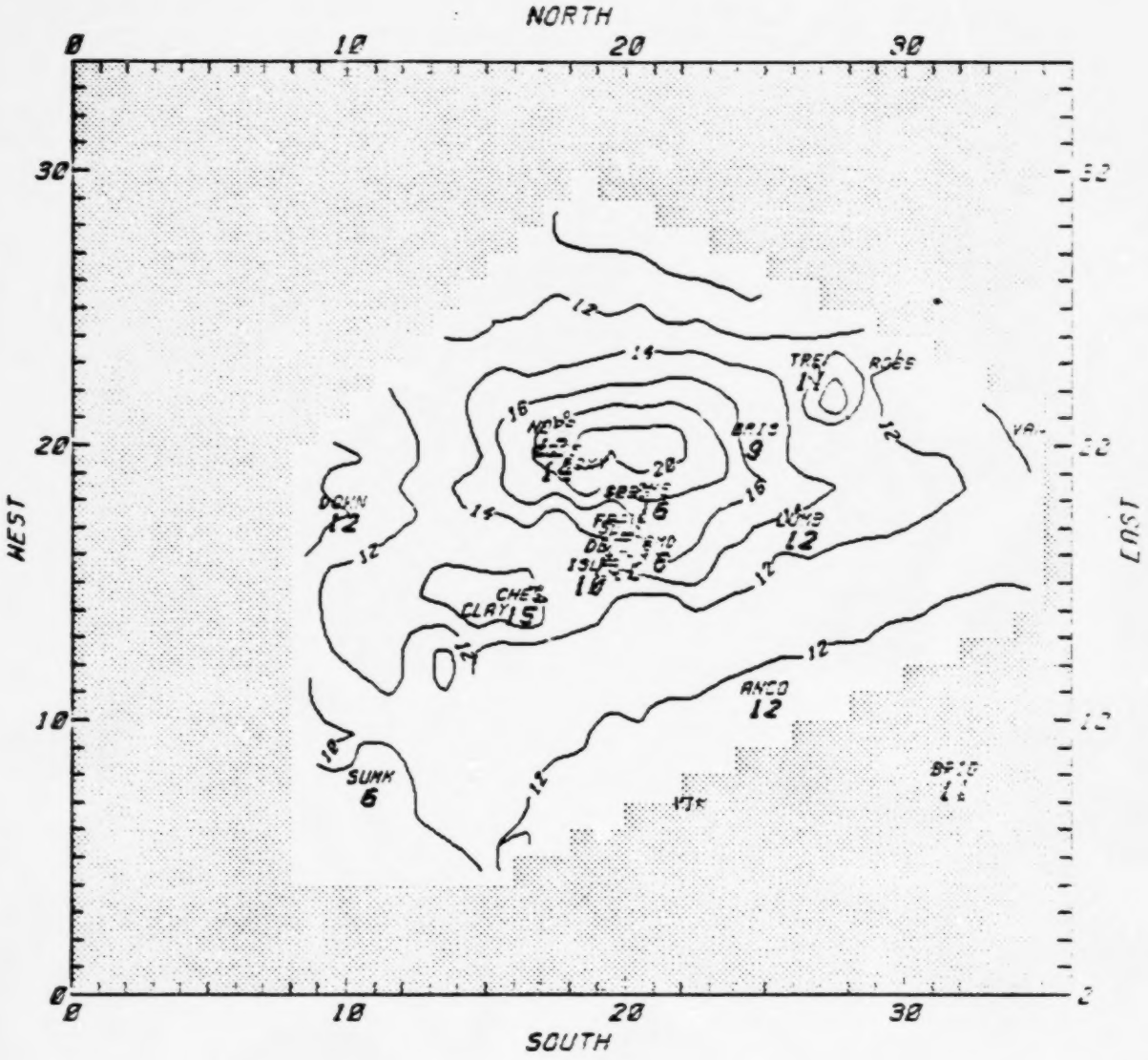

(e) *BETWEEN THE HOURS OF 13 AND 14*

FIGURE A-1 continued.

BEST COPY AVAILABLE

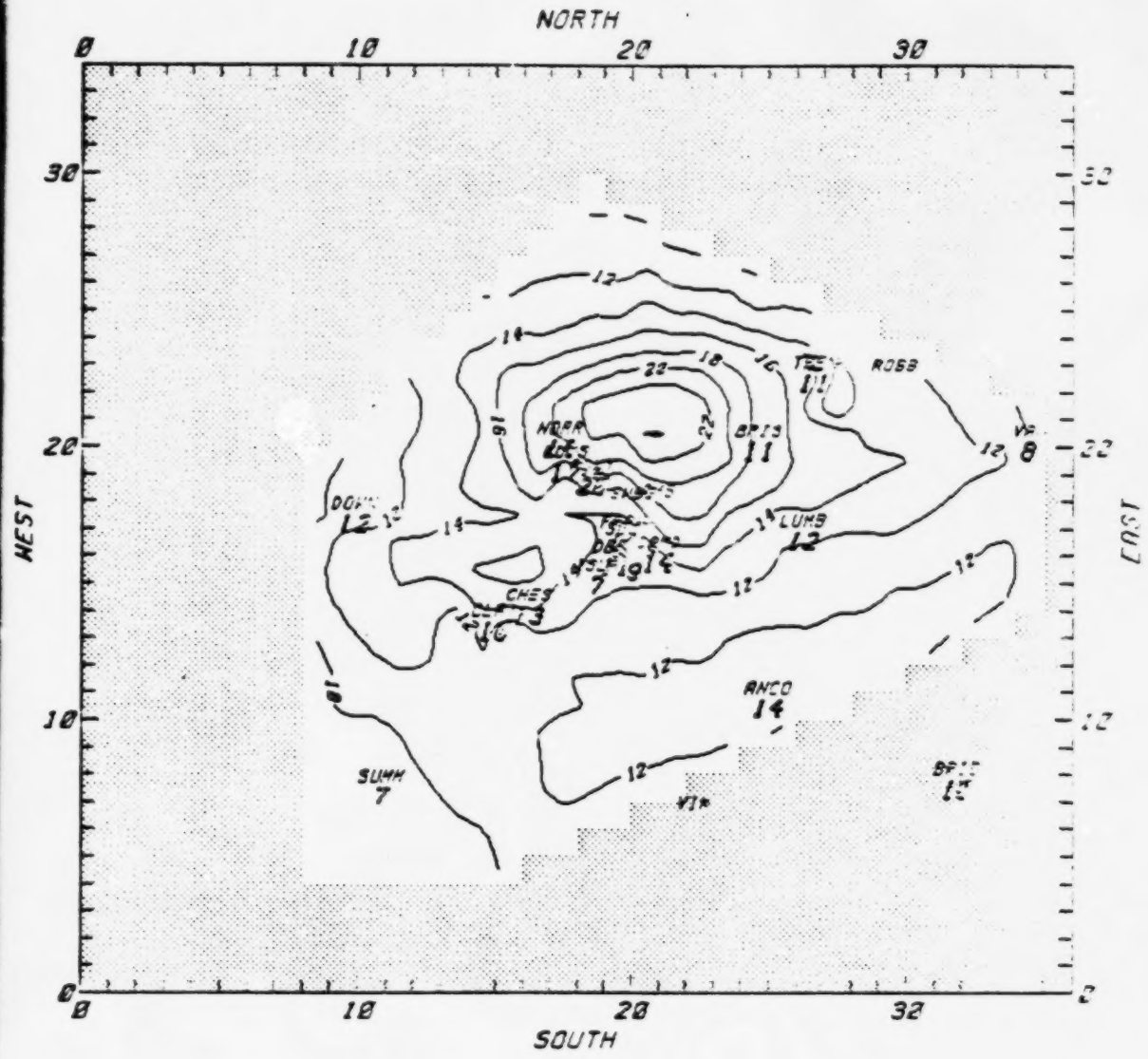

(f) BETWEEN THE HOURS OF 14 AND 15

FIGURE A -1 continued.

BEST COPY AVAILABLE

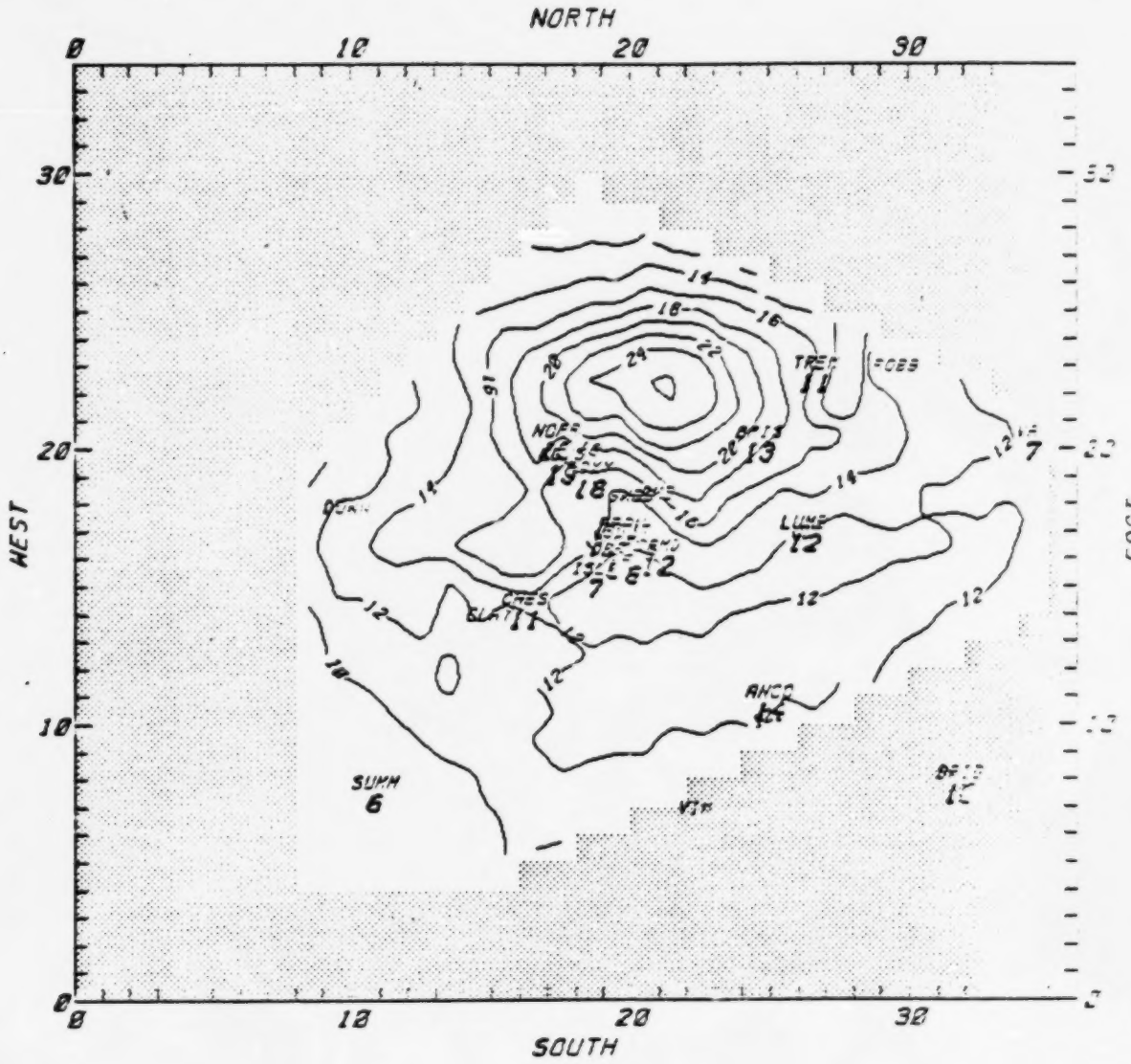

(g) BETWEEN THE HOURS OF 15 AND 16

FIGURE A-1 continued.

BEST COPY AVAILABLE

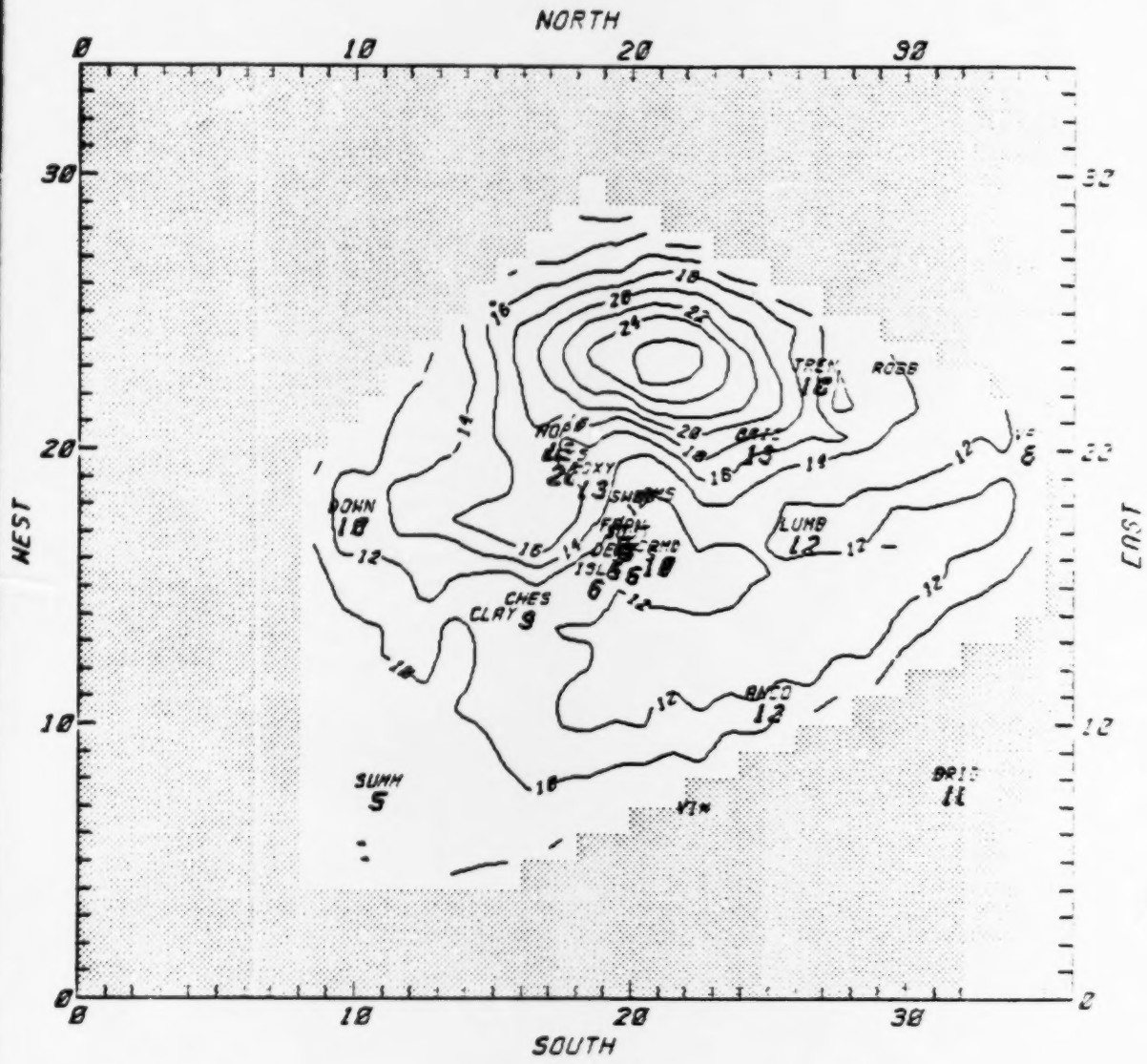

(h) BETWEEN THE HOURS OF 16 AND 17

FIGURE A-1 continued.

BEST COPY AVAILABLE

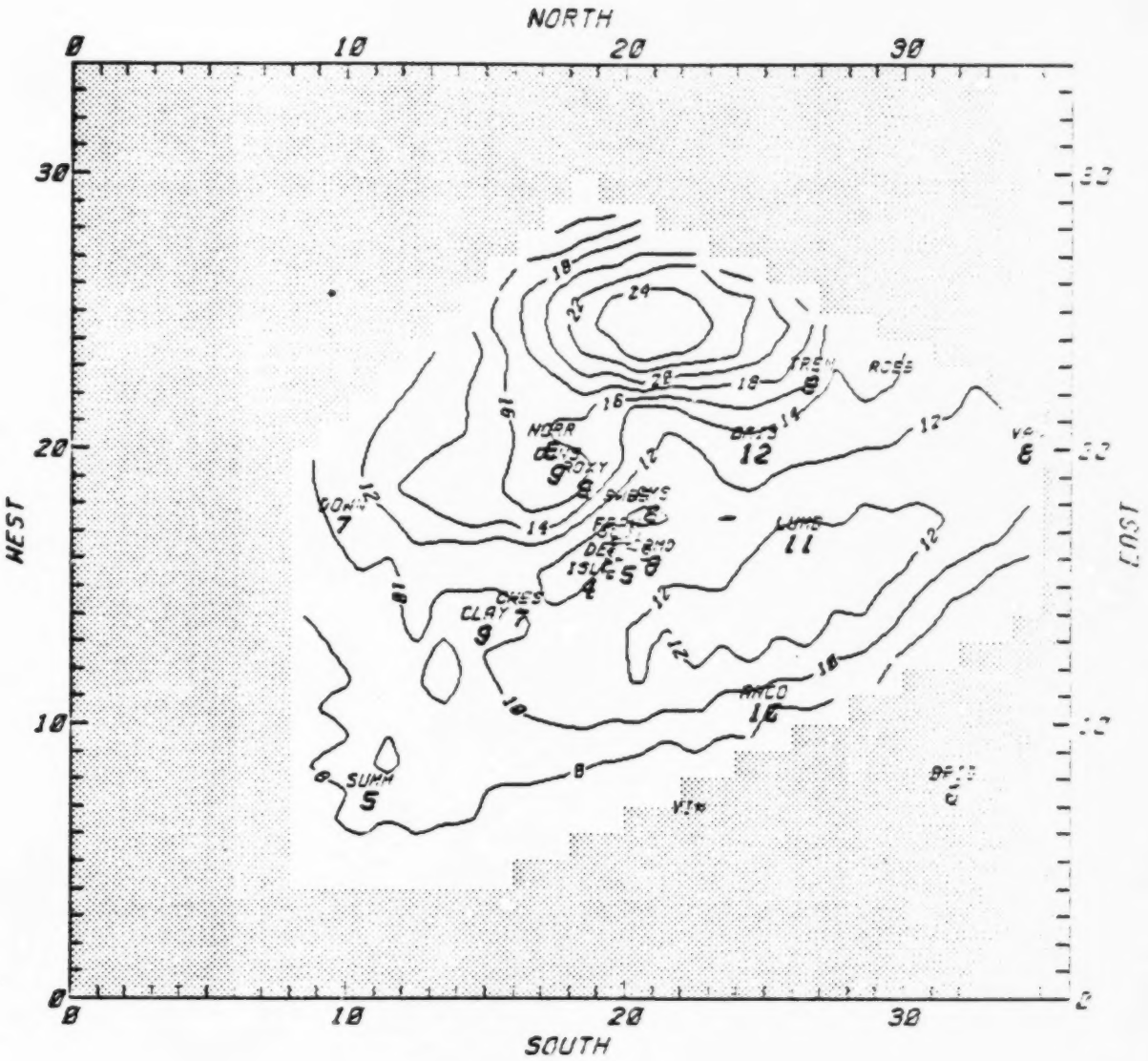

(i) BETWEEN THE HOURS OF 17 AND 18

FIGURE A-1 continued.

BEST COPY AVAILABLE

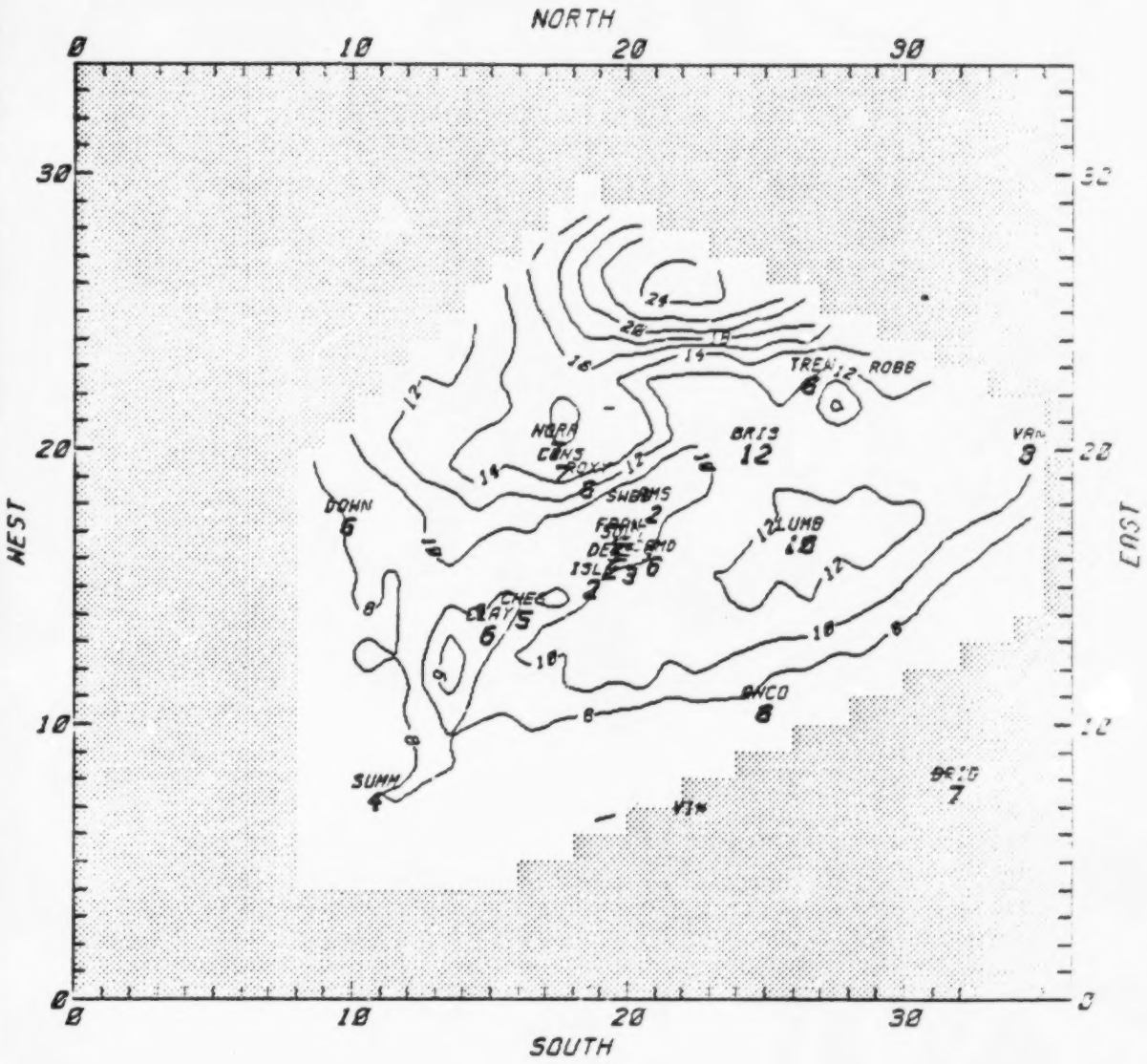

(j) BETWEEN THE HOURS OF 18 AND 19

FIGURE A-1 concluded.

BEST COPY AVAILABLE

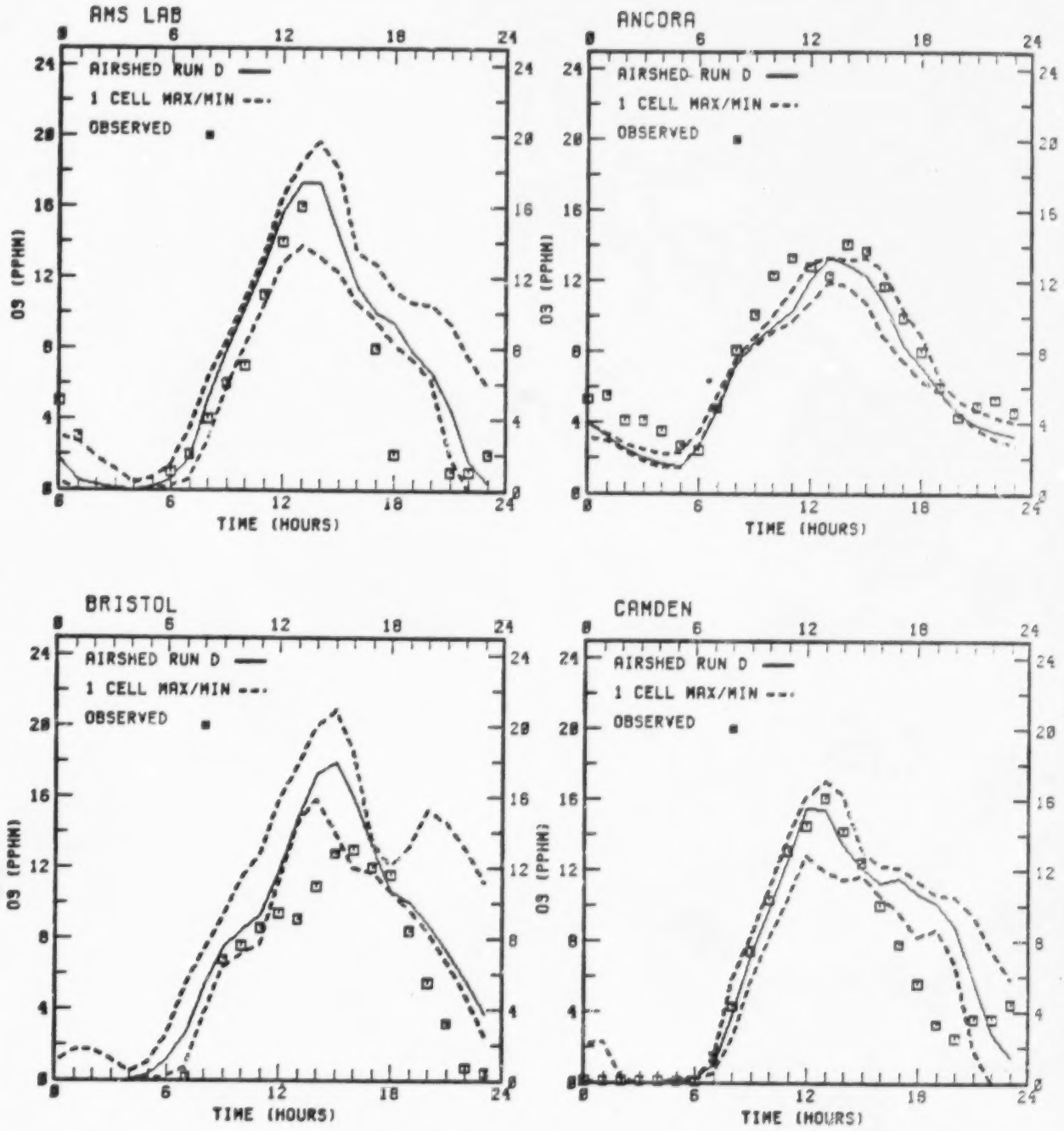

FIGURE A-2. Comparison of Airshed Model predictions and ozone observations for the 13 July 1979 episode, Philadelphia, Pennsylvania.

BEST COPY AVAILABLE

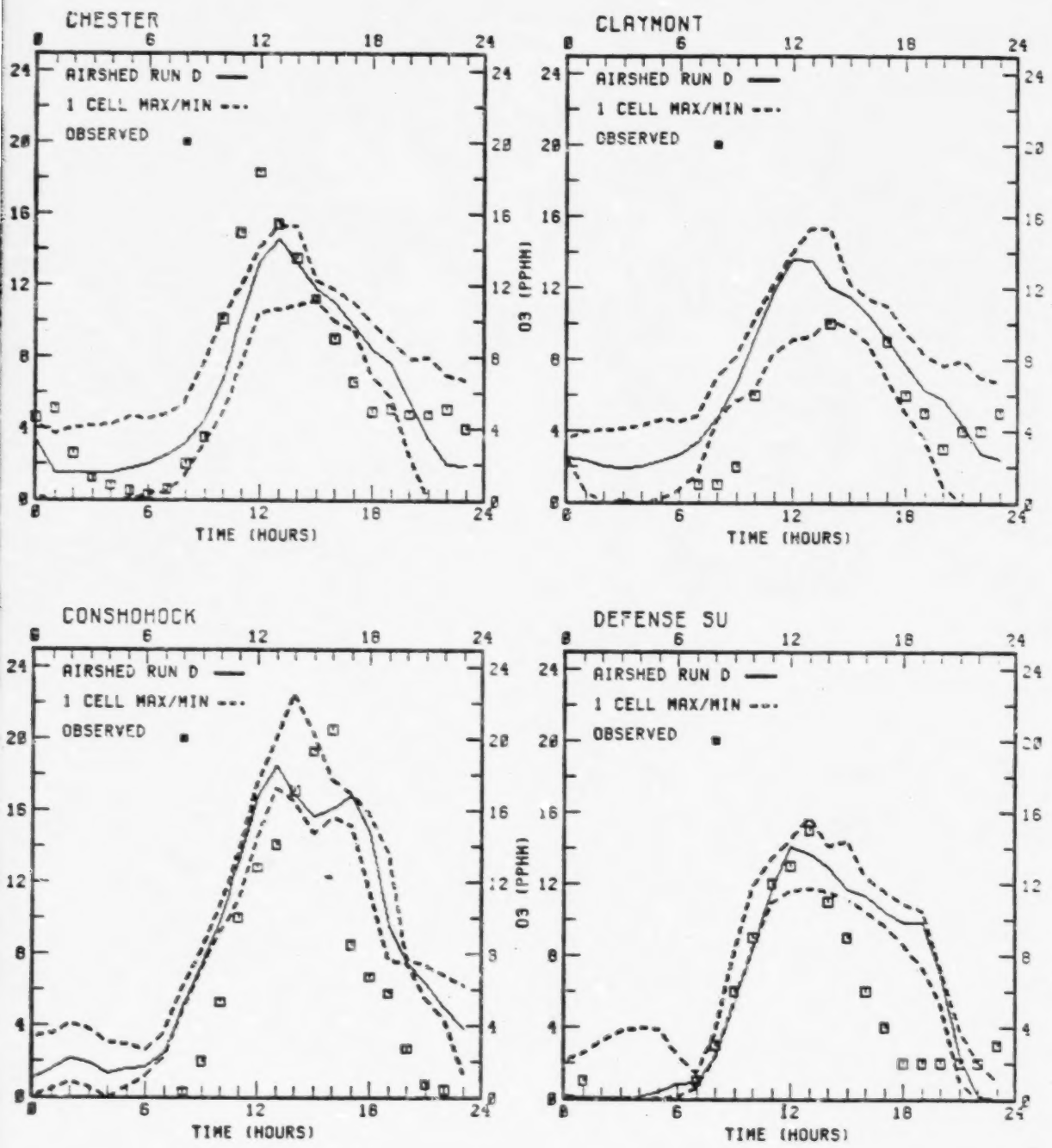

FIGURE A-2 continued.

BEST COPY AVAILABLE

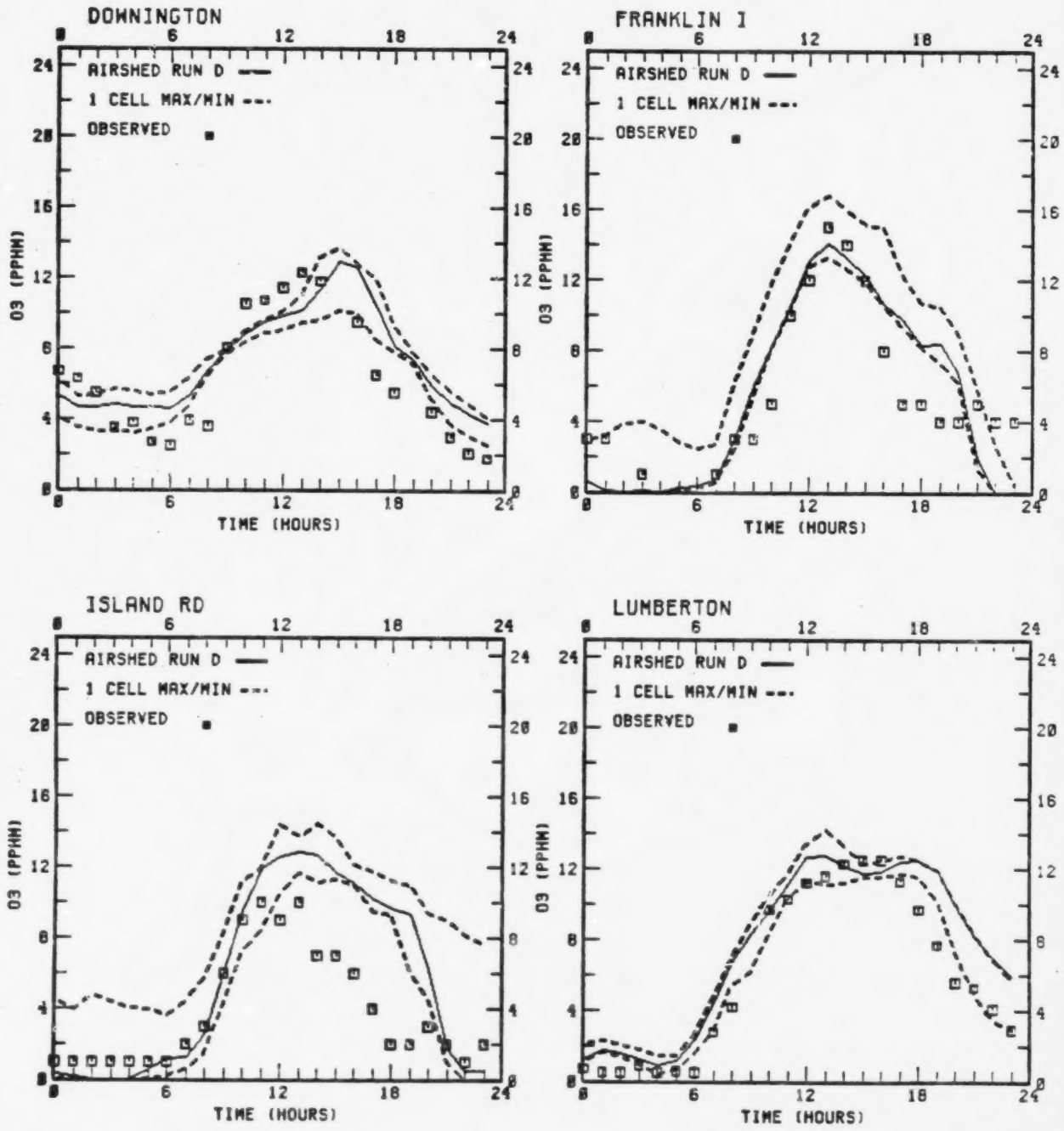

FIGURE A-2 continued.

BEST COPY AVAILABLE

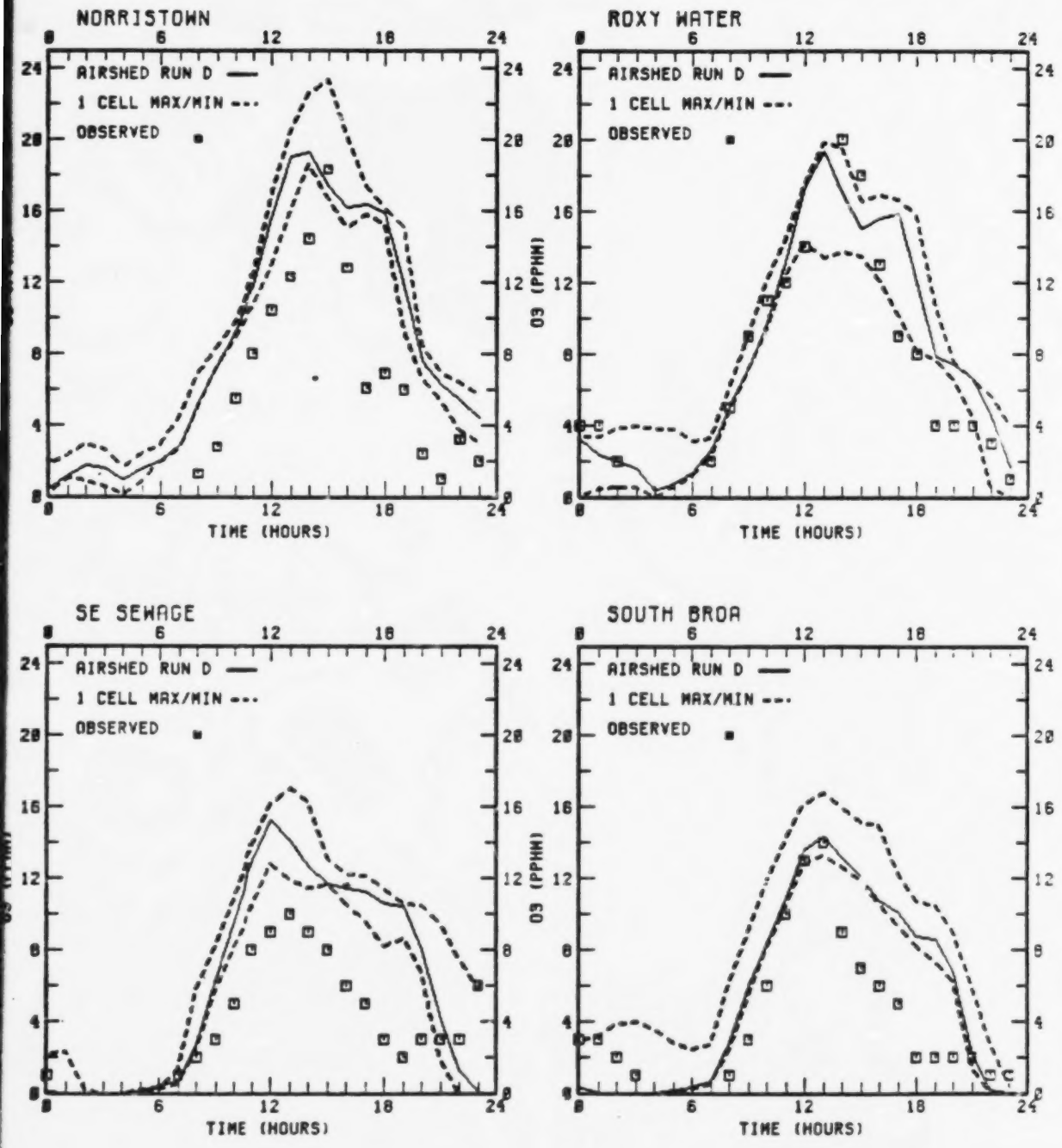

FIGURE A-2 continued.

BEST COPY AVAILABLE

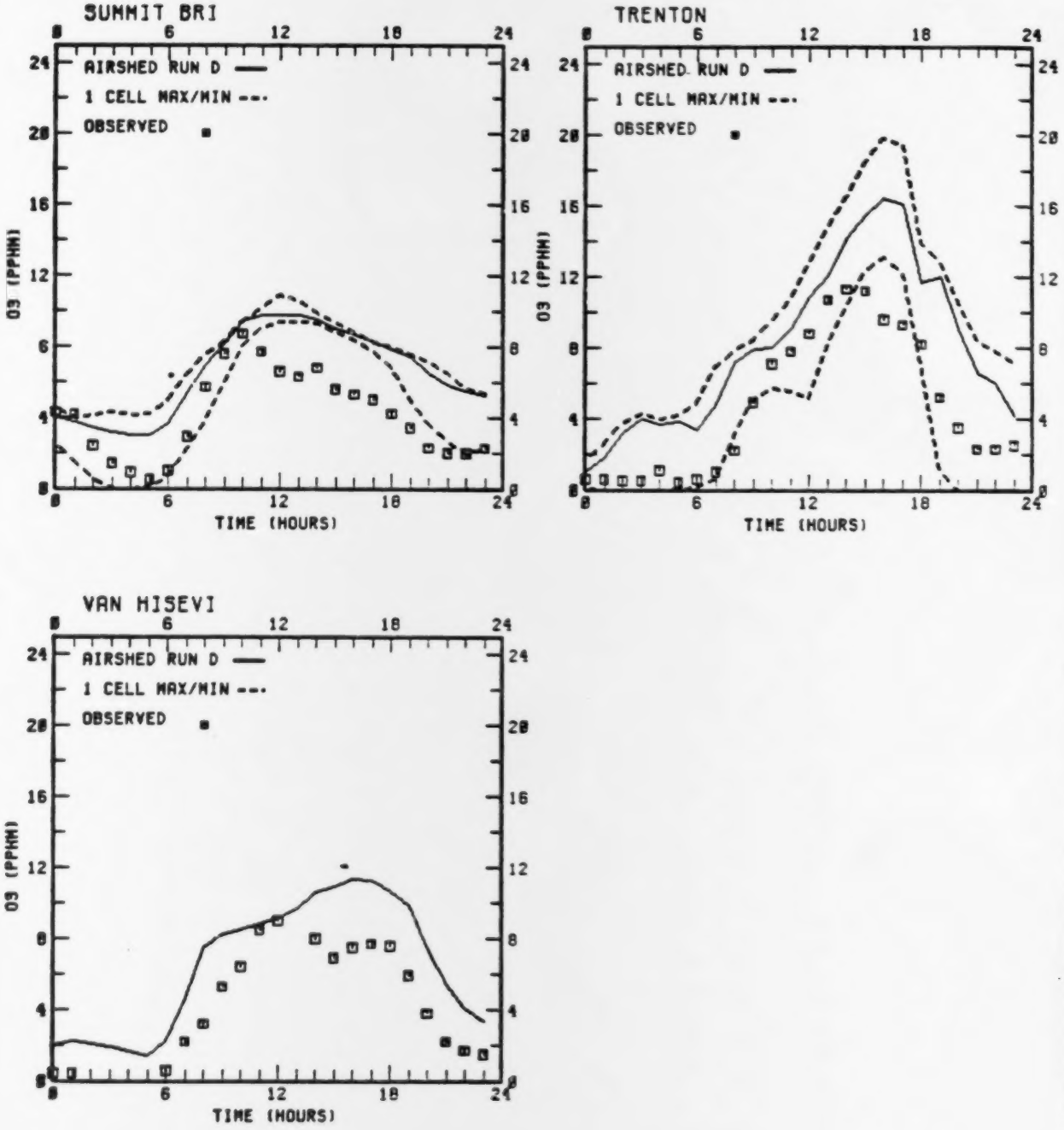

FIGURE A-2 concluded.

BEST COPY AVAILABLE

APPENDIX B

COMPILATION OF AIRSHED RESULTS FOR 19 JULY 1979

BEST COPY AVAILABLE

BLANK PAGE

APPENDIX B

COMPILATION OF AIRSHED RESULTS FOR 19 JULY 1979

This appendix compiles various sets of Airshed Model ozone results. Figure B-1 is a complete set of hourly average ozone isopleths in the Philadelphia area throughout the day. Time-series plots comparing distance-weighted average and maximum/minimum ozone predictions within one cell's distance with observations at 20 monitoring stations are presented in Figure B-2. Model results presented in this manner are helpful in developing a better qualitative understanding of the simulation results. These grid model concentration estimates used in comparison with the observed data are defined as follows:

Distance-Weighted Average. The solid lines presented in Figure B-2 represent an average model prediction (for comparison with observed values), which is obtained by computing the distance-weighted average concentration of the four grid cells nearest to the monitor where the observed value was recorded.

Maximum/Minimum One Cell Away. The dashed lines presented in Figure B-2 represent the maximum and minimum concentrations predicted in the block of nine cells centered on the grid cell containing the monitoring station. This envelope provides an indication of the spatial variability of the predicted concentration values in the immediate vicinity of the station.

These plots reveal the presence of steep spatial gradients in the concentration field and the qualitative effect that wind field errors might have on the performance results. In calculating the model evaluation statistics, the distance-weighted average estimates produced by the simulation are used.

BEST COPY AVAILABLE

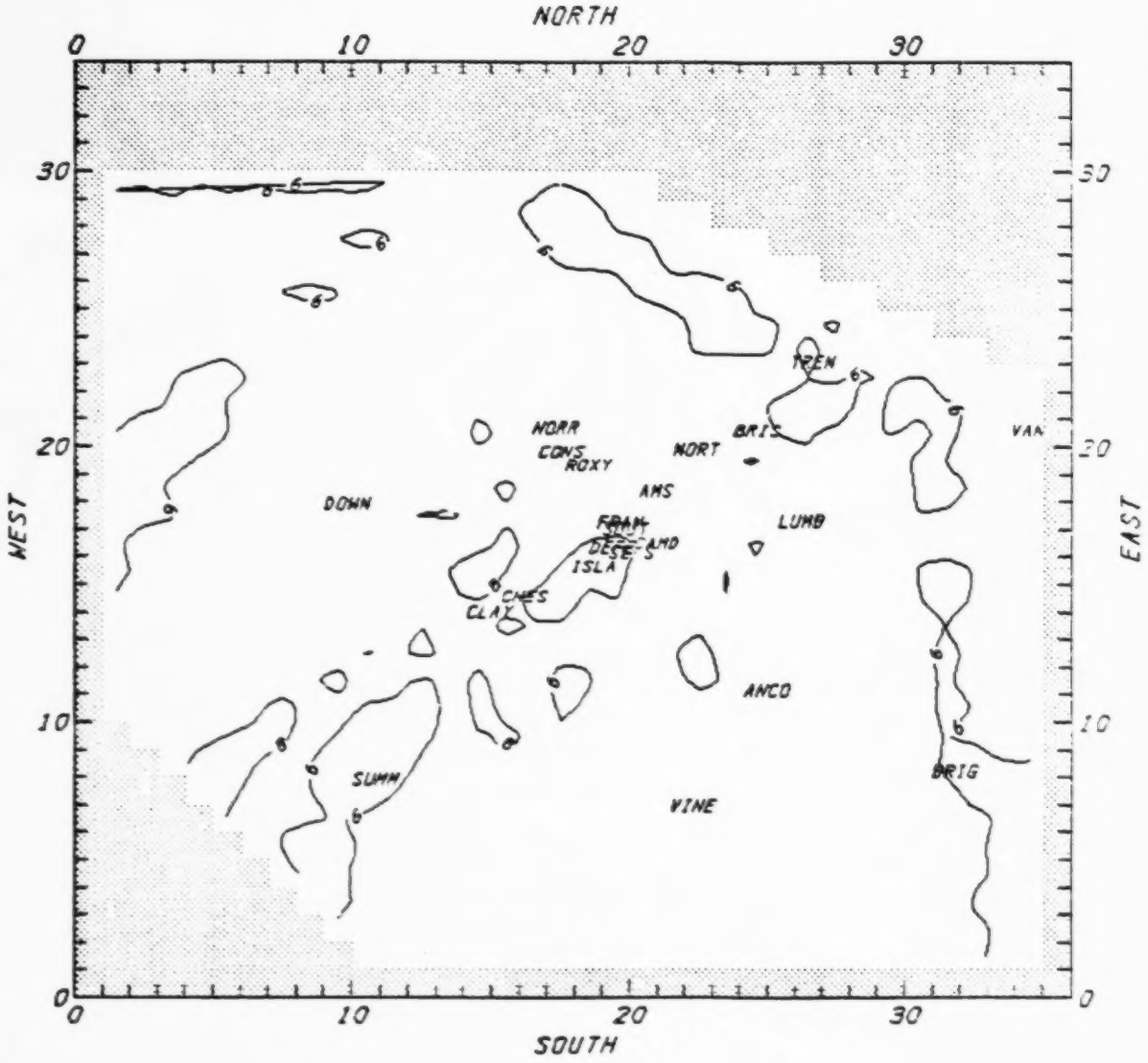

(a) *BETWEEN THE HOURS OF 10 AND 11*

FIGURE B-1. Hourly variation in predicted ground-level ozone concentration fields (pphm) for Philadelphia, 19 July 1979. (Bold numbers correspond to station observations.)

BEST COPY AVAILABLE

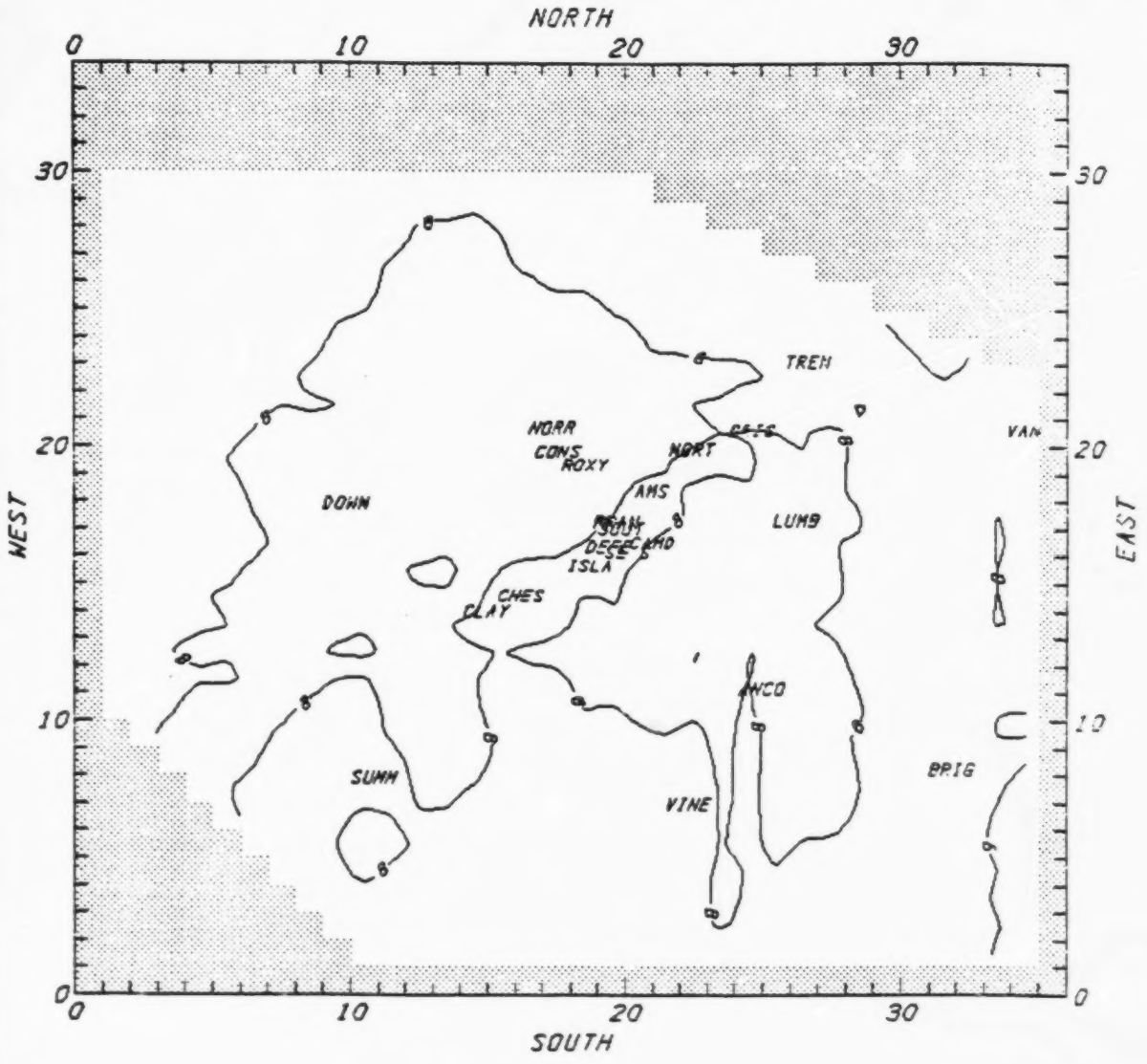

(b) BETWEEN THE HOURS OF 11 AND 12

FIGURE B-1 continued .

BEST COPY AVAILABLE

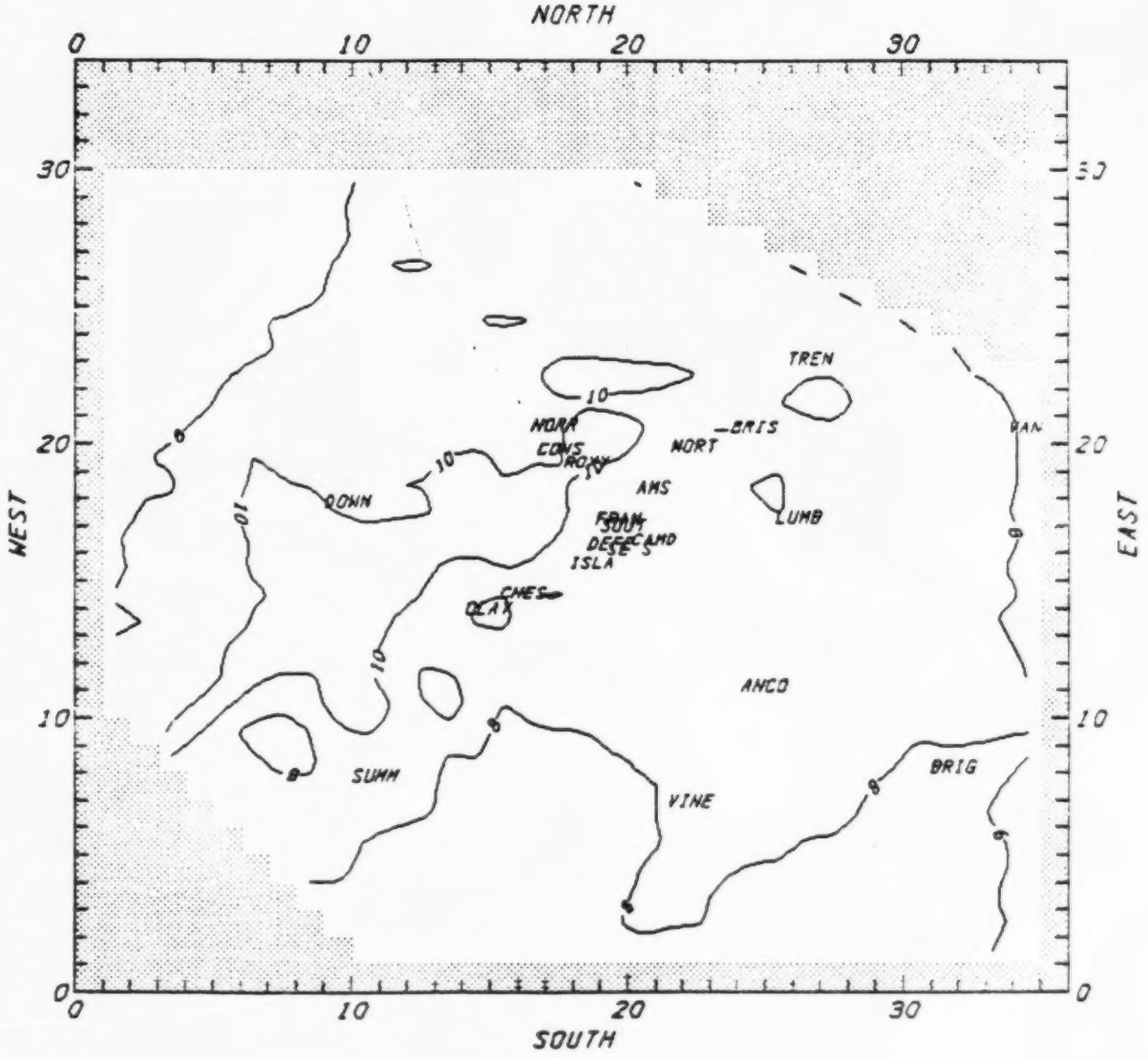

(c) BETWEEN THE HOURS OF 12 AND 13

FIGURE B-1 continued .

BEST COPY AVAILABLE

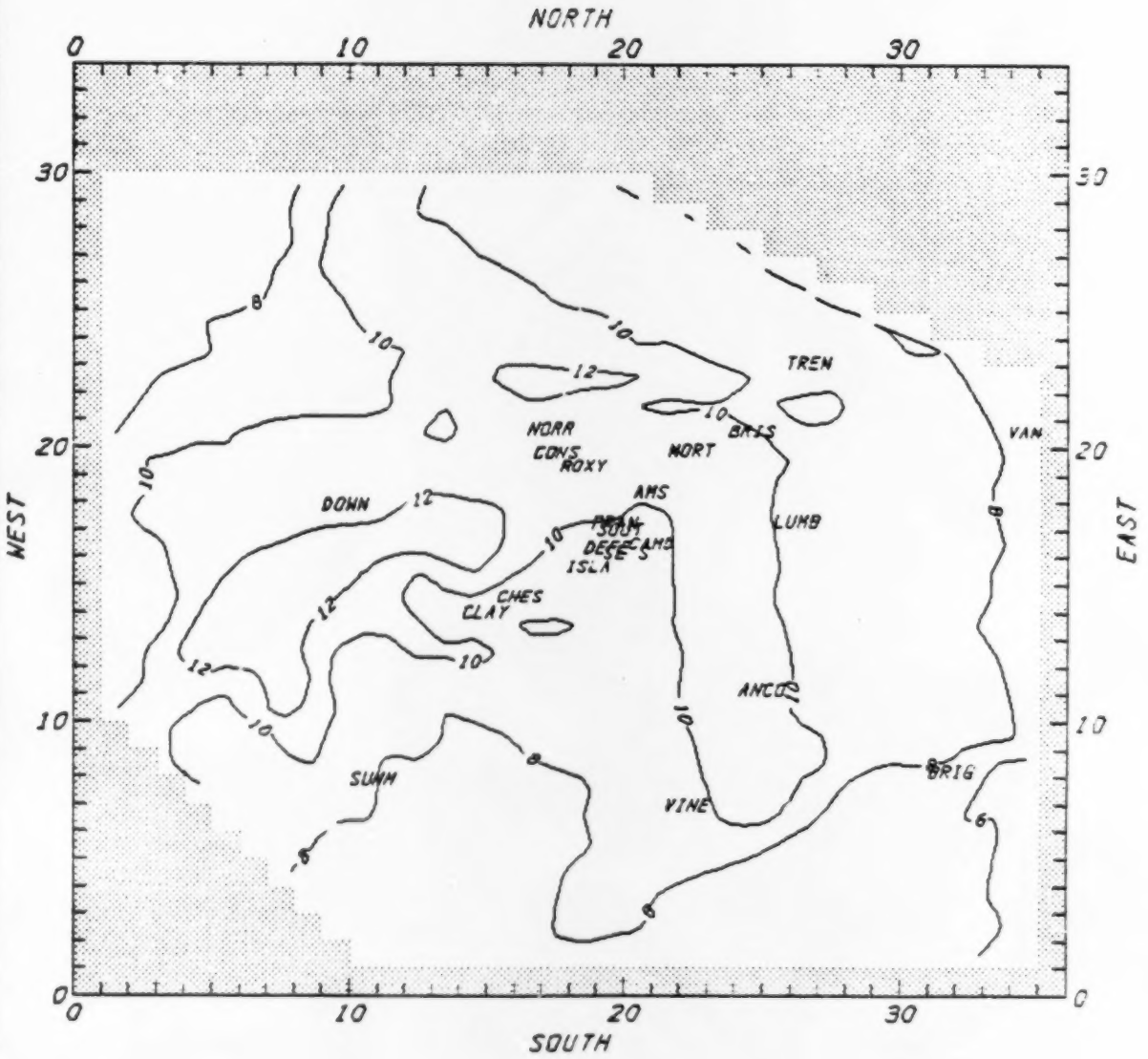

(d) BETWEEN THE HOURS OF 13 AND 14

FIGURE B-1 continued .

BEST COPY AVAILABLE

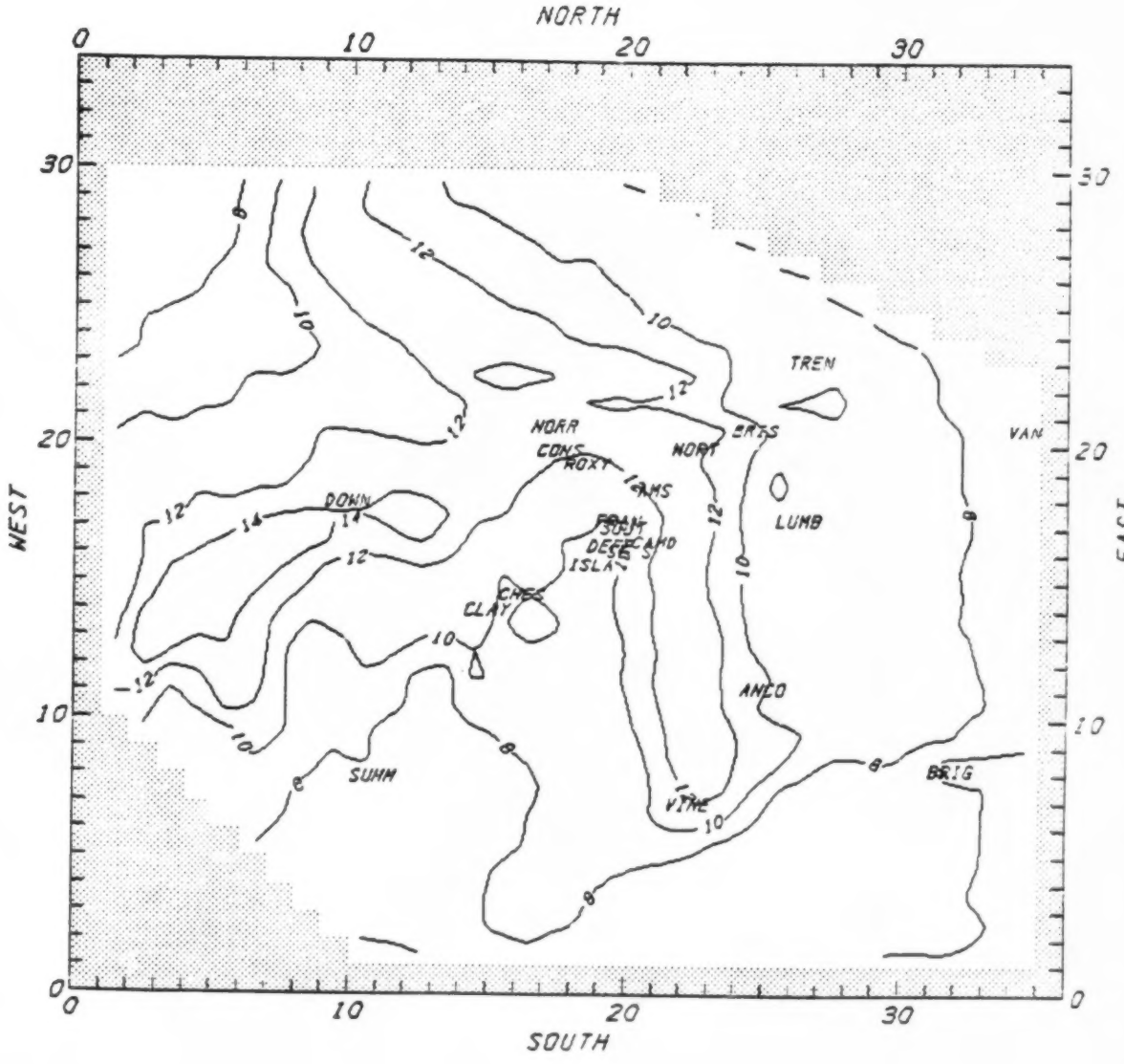

(e)BETWEEN THE HOURS OF 14 AND 15

FIGURE B-1 continued .

BEST COPY AVAILABLE

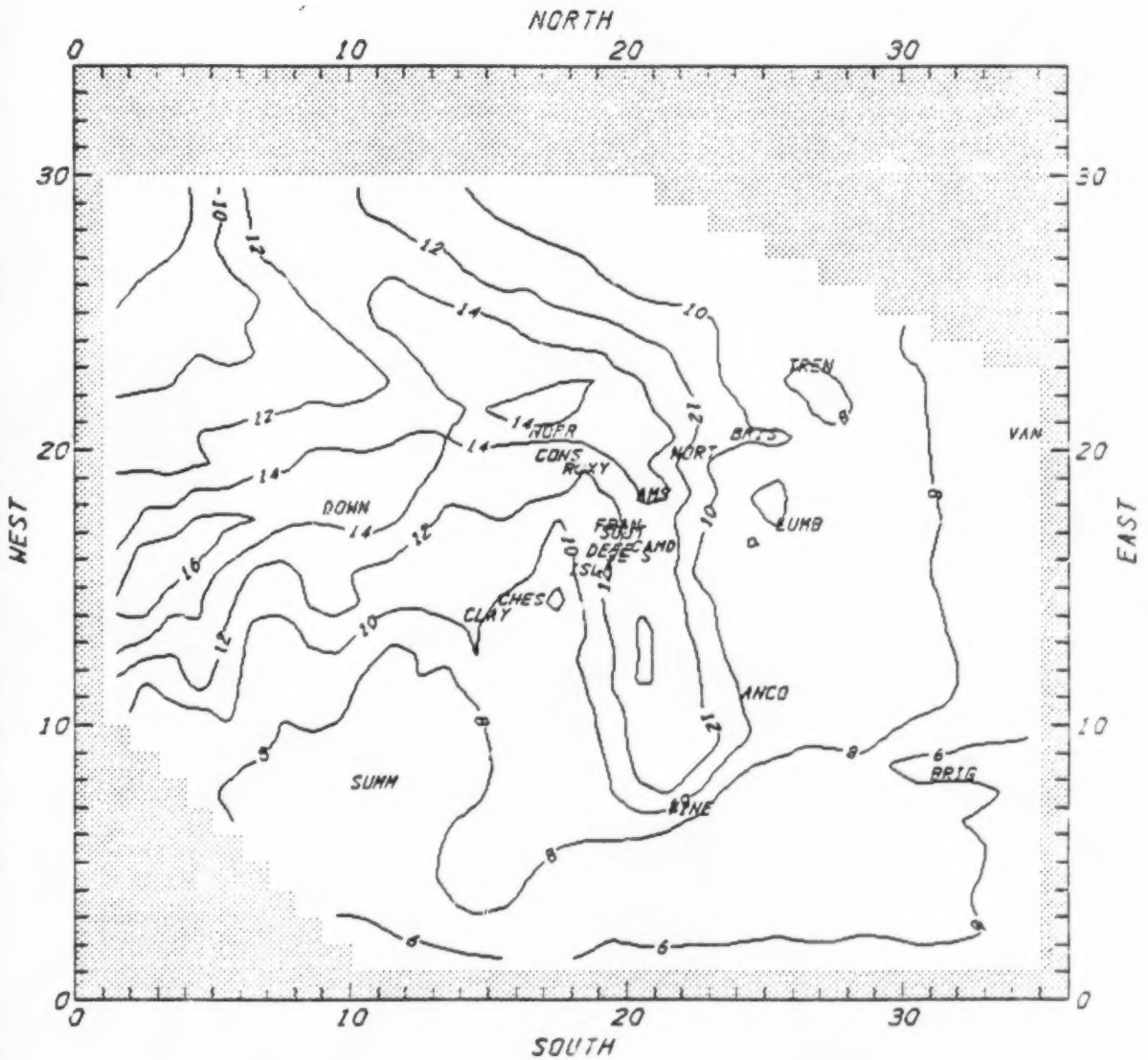

(f) BETWEEN THE HOURS OF 15 AND 16

FIGURE B-1 continued .

BEST COPY AVAILABLE

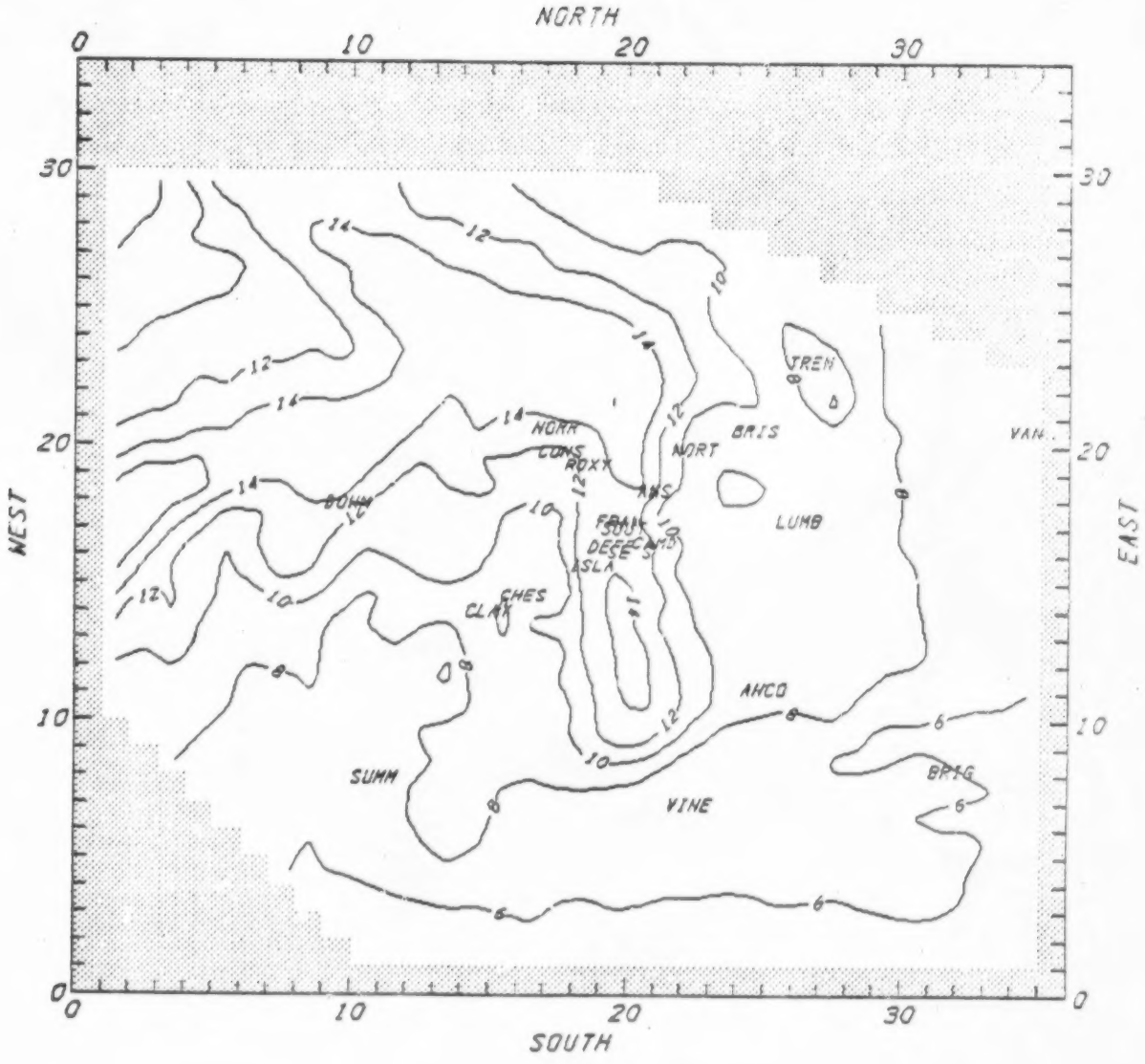

(g)BETWEEN THE HOURS OF 16 AND 17

FIGURE B-1 continued .

BEST COPY AVAILABLE

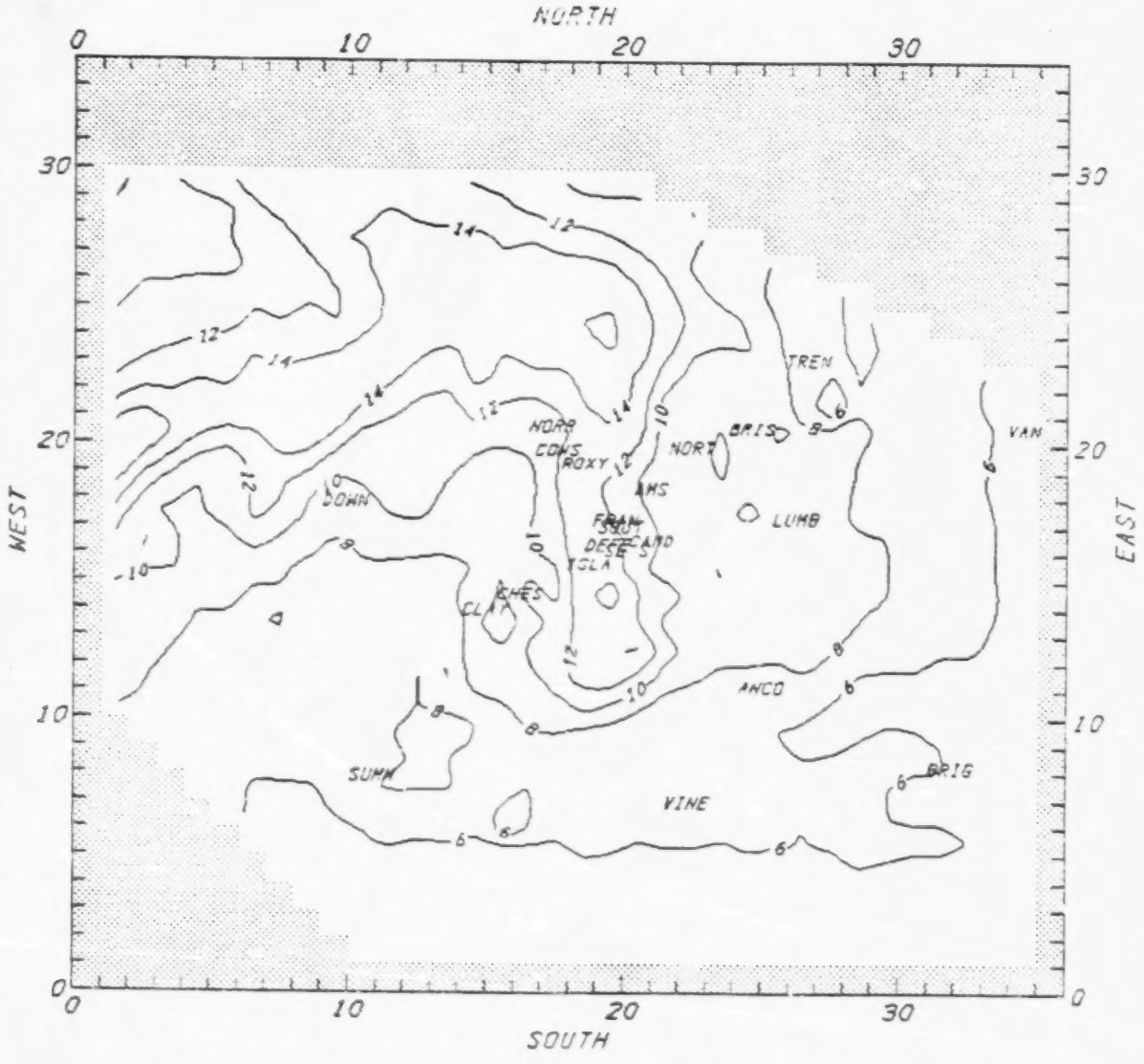

(h) BETWEEN THE HOURS OF 17 AND 18

FIGURE B-1 continued .

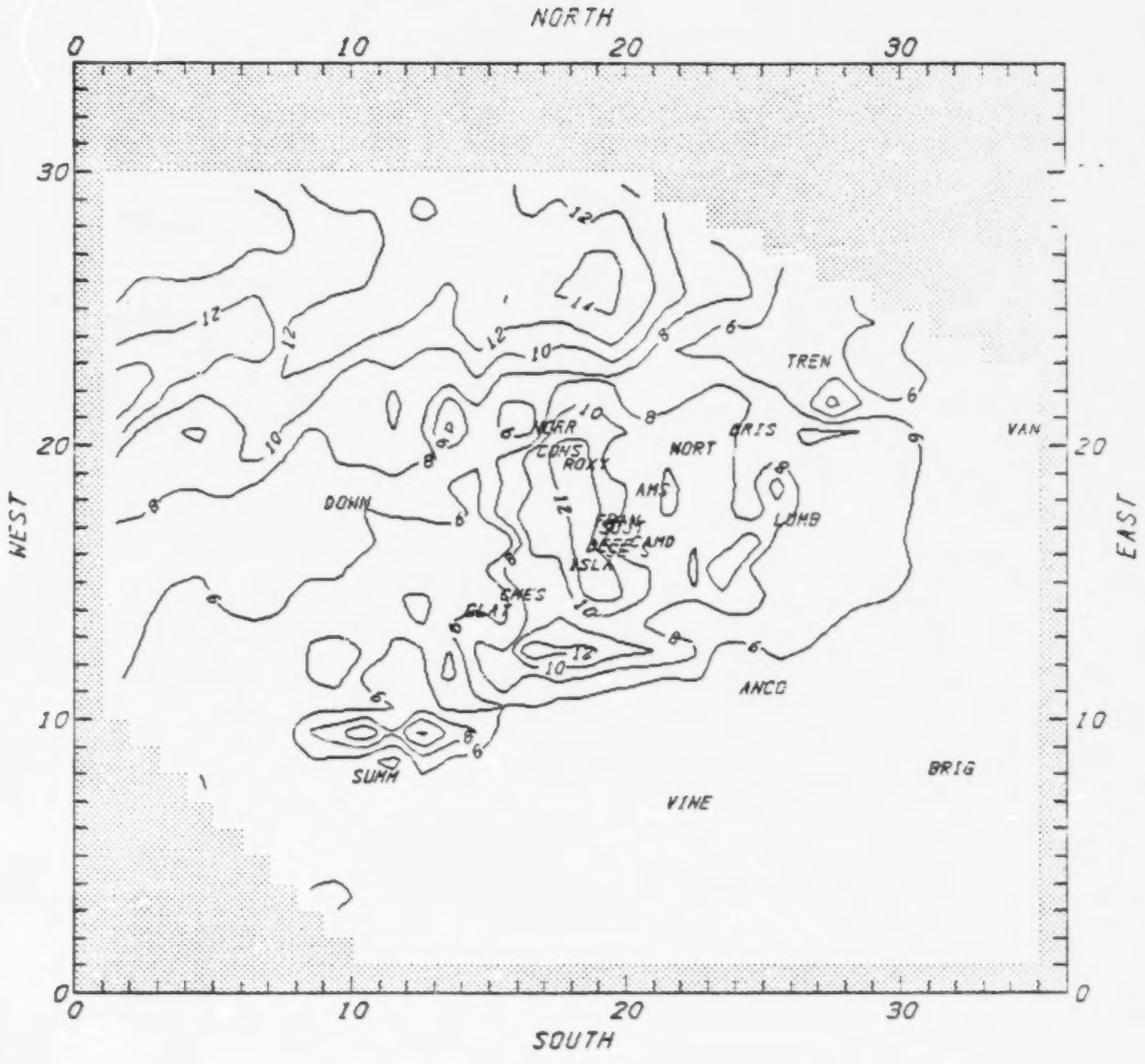

(i) BETWEEN THE HOURS OF 18 AND 19

FIGURE B-1 continued .

BEST COPY AVAILABLE

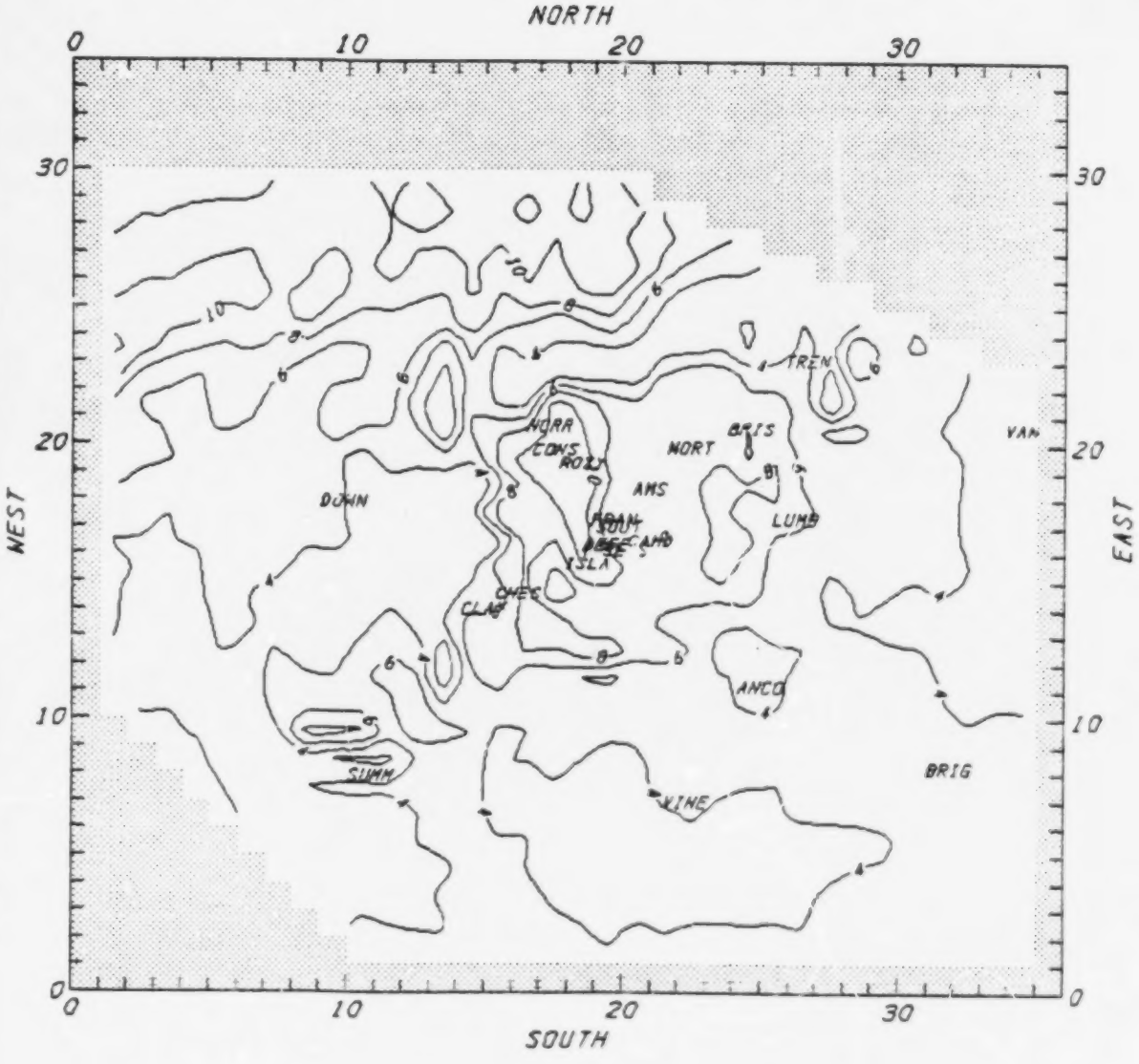

(j) BETWEEN THE HOURS OF 19 AND 20

FIGURE B-1 concluded .

BEST COPY AVAILABLE

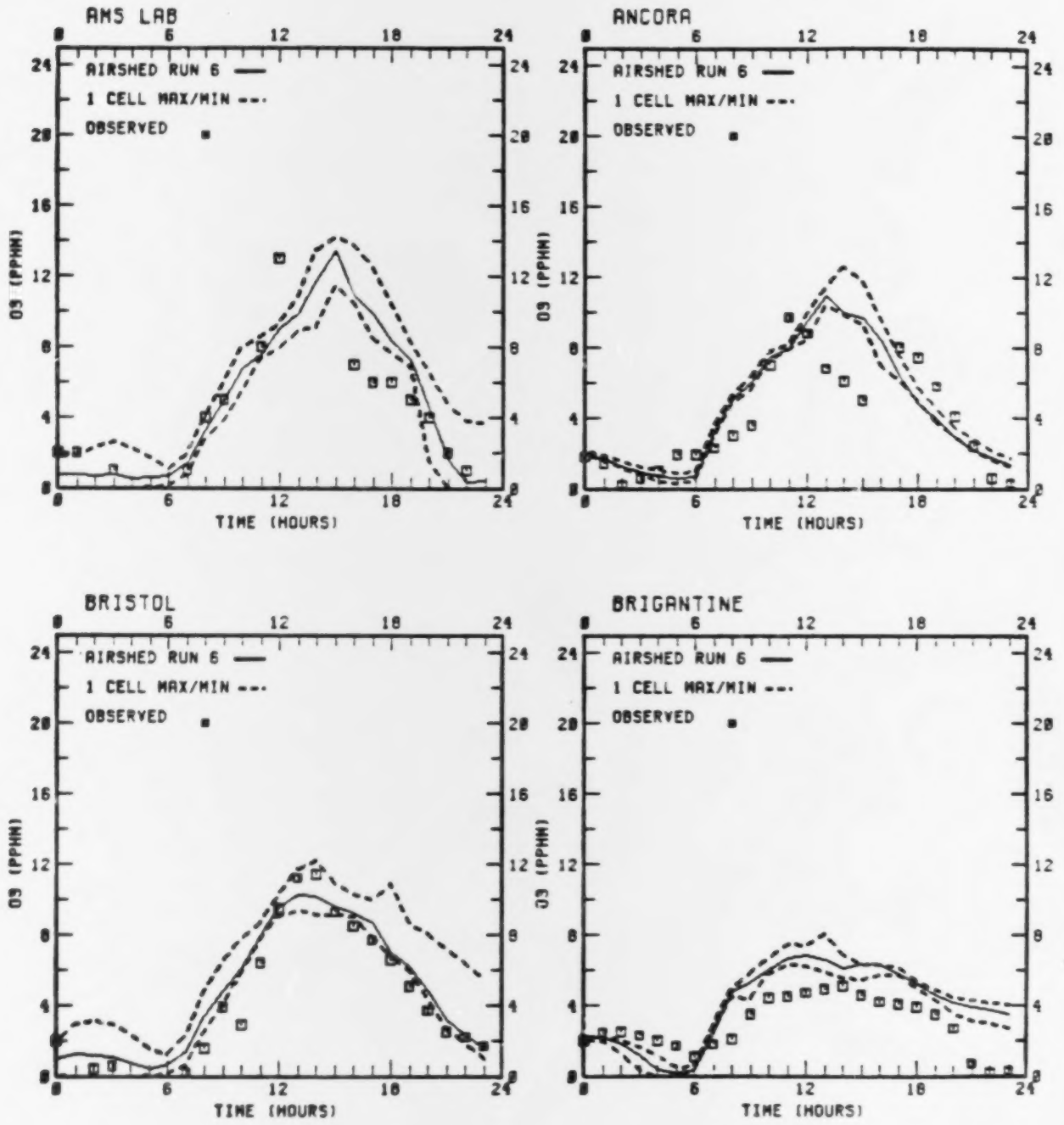

FIGURE B-2. Comparison of Airshed Model predictions and ozone observations for the July 19, 1979 episode, Philadelphia, Pennsylvania.

BEST COPY AVAILABLE

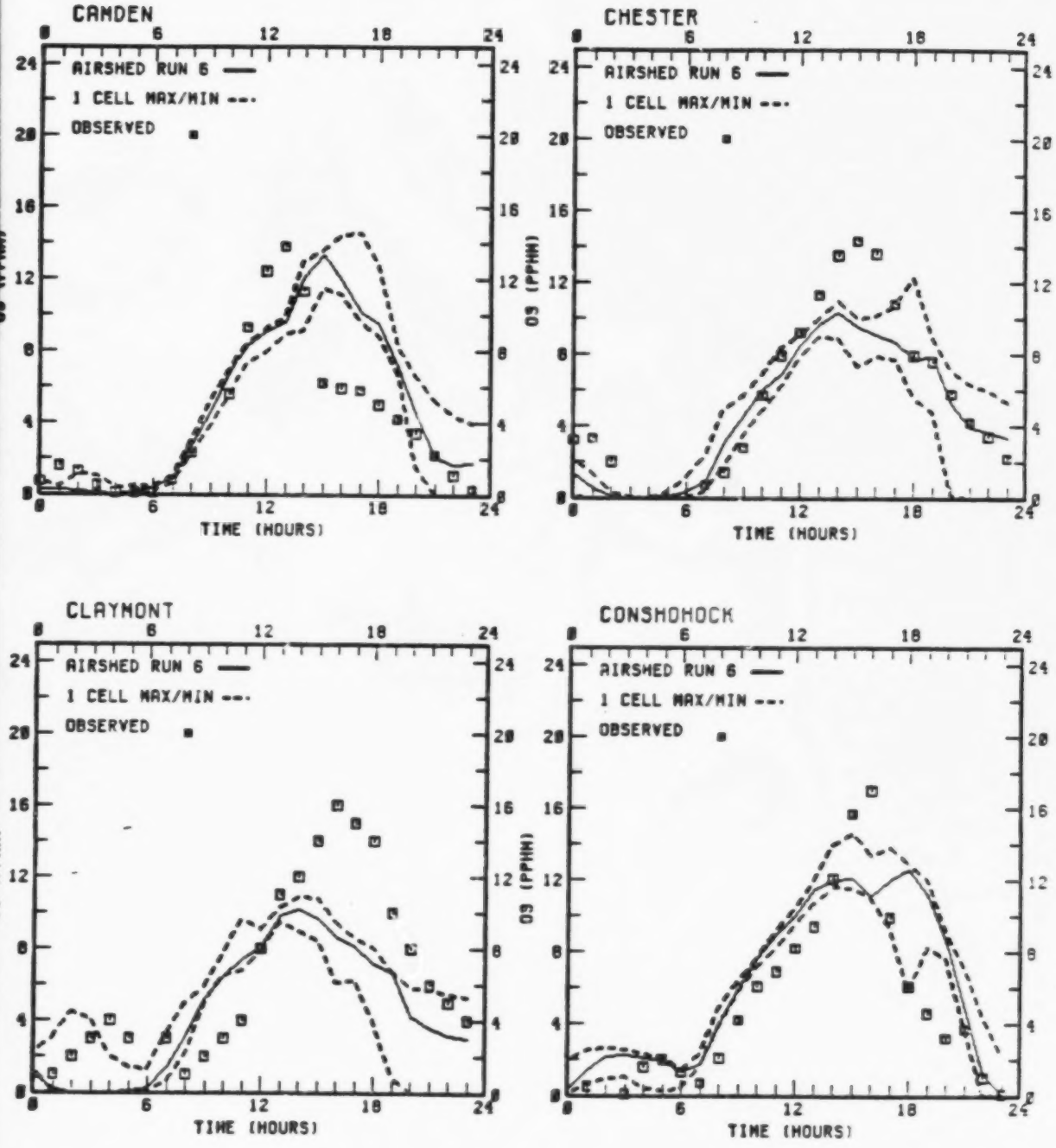

FIGURE B-2 continued.

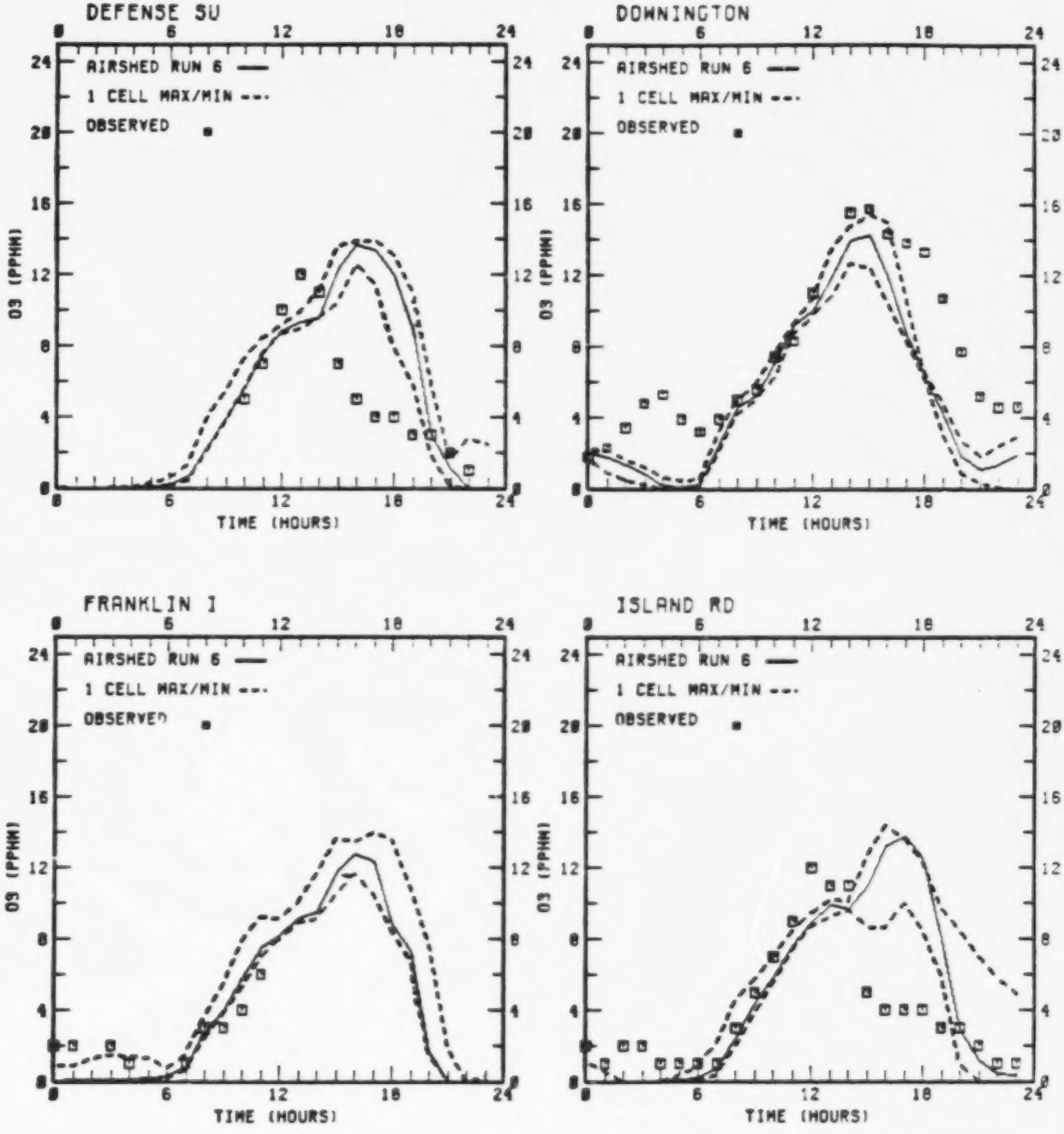

FIGURE B-2 continued.

BEST COPY AVAILABLE

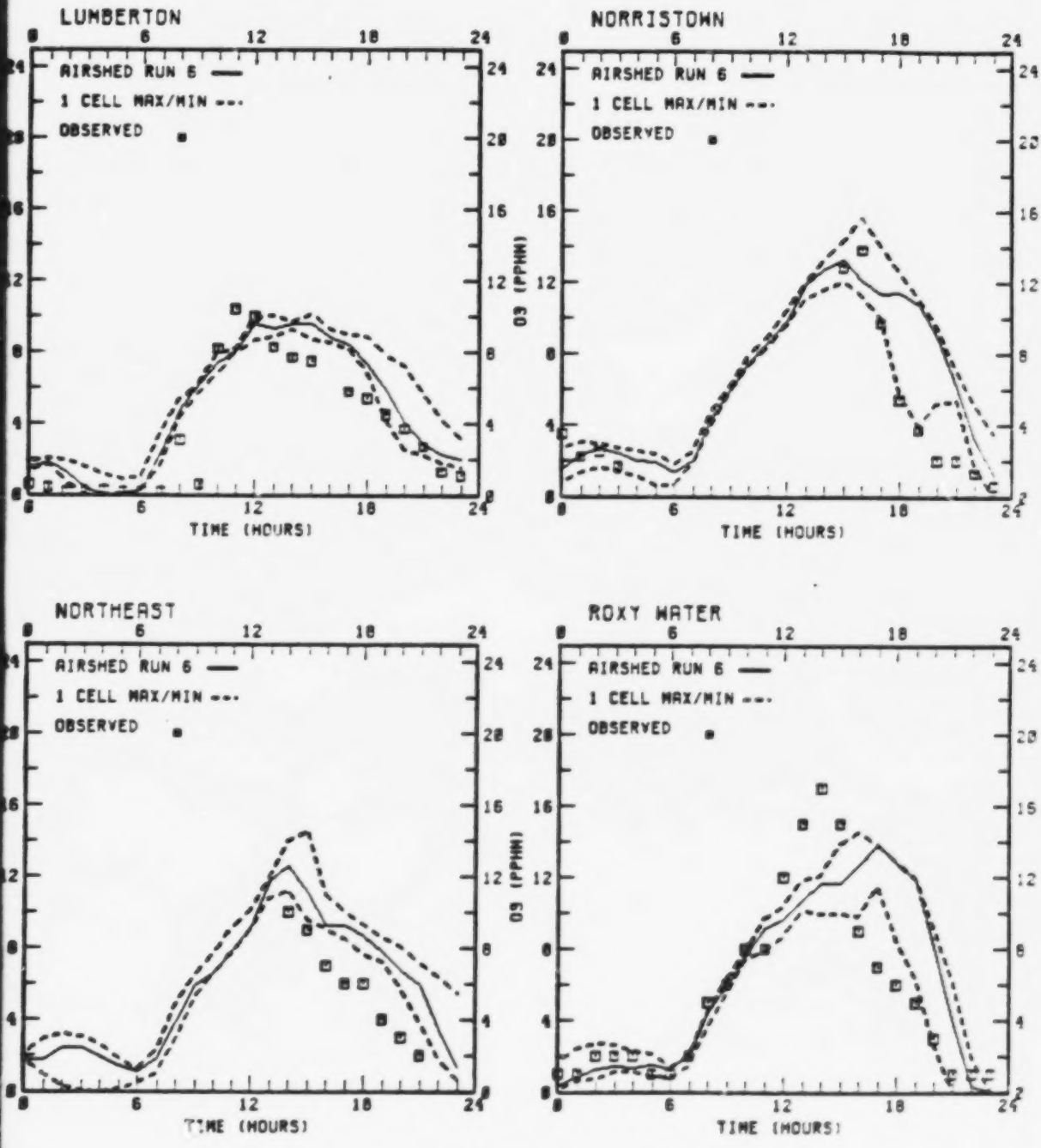

FIGURE B-2 concluded.

TECHNICAL REPORT DATA
(Please read Instructions on the reverse before completing)

1. REPORT NO.	2.	3. RECIPIENT'S ACCESSION NO.
EPA-450/4-85-003		

4. TITLE AND SUBTITLE
Evaluation and Application of the Urban Airshed Model in the Philadelphia Air Quality Control Region

5. REPORT DATE
June 1985

6. PERFORMING ORGANIZATION CODE

7. AUTHOR(S)
T. N. Braverman, EPA; and J. L. Haney, SAI

8. PERFORMING ORGANIZATION REPORT NO.

9. PERFORMING ORGANIZATION NAME AND ADDRESS
Systems Applications, Inc. (SAI)
101 Lucas Valley Road
San Rafael, California 94903

10. PROGRAM ELEMENT NO.

11. CONTRACT/GRANT NO.
68-02-3870

12. SPONSORING AGENCY NAME AND ADDRESS
U.S. Environmental Protection Agency
Office of Air Quality Planning and Standards
Monitoring and Data Analysis Division (MD-14)
Research Triangle Park, NC 27711

13. TYPE OF REPORT AND PERIOD COVERED

14. SPONSORING AGENCY CODE

15. SUPPLEMENTARY NOTES

16. ABSTRACT

The Urban Airshed Photochemical Grid Model has been applied to a data base assembled for the Philadelphia metropolitan area consisting of meteorological and air quality data collected during the EPA 1979 summer field study and a spatially, temporally, and chemically resolved emissions inventory of hydrocarbons and nitrogen oxides. The report presents results of (1) the evaluation of Urban Airshed Model performance on 2 selected model test days, (2) application of the Urban Airshed Model for control strategy planning, and (3) sensitivity tests to determine the response of Urban Airshed Model predictions and control requirements to uncertainty in background concentrations. The model tended to slightly overestimate calculated hourly ozone for both simulation days; but performed well in replicating observed concentrations. Results indicate that urban hydrocarbon emission reductions required to attain the National Ambient Air Quality Standard (NAAQS) for ozone vary widely depending on assumed levels of background hydrocarbons and ozone. Under certain meteorological conditions, fresh precursor emissions may be transported between cities in the Northeast Urban Corridor leading to violations of the ozone standard. Therefore, all large metropolitan areas in the Northeast must cooperate to reduce emissions if region-wide attainment of the ozone standard is to be maintained.

17. KEY WORDS AND DOCUMENT ANALYSIS

a. DESCRIPTORS	b. IDENTIFIERS/OPEN ENDED TERMS	c. COSATI Field/Group
Photochemical models Ozone Hydrocarbon control strategies Background concentrations Interurban transport		

18. DISTRIBUTION STATEMENT	19. SECURITY CLASS *(This Report)*	21. NO. OF PAGES
		239
	20. SECURITY CLASS *(This page)*	22. PRICE

EPA Form 2220-1 (Rev. 4-77) PREVIOUS EDITION IS OBSOLETE

BEST COPY AVAILABLE

United States
Environmental Protection
Agency

Office Of Air And Radiation
Office Of Air Quality Planning And Standards
Research Triangle Park NC 27711

Official Business
Penalty for Private Use
$300

225

If your address is incorrect, please change on the above label, tear off, and return to the above address.
If you do not desire to continue receiving this technical report series, CHECK HERE ☐, tear off label, and return it to the above address.

BEST COPY AVAILABLE